

Synthesis of Modified and Labelled Lipids for Analysis of Enzyme Mechanisms and Membrane Interactions

Dissertation

zur Erlangung

des mathematisch-naturwissenschaftlichen Doktorgrades

“Doctor rerum naturalium”

der Georg-August-Universität Göttingen

im Promotionsprogramm BioMetals, IRTG 1422

der Georg-August University School of Science (GAUSS)

vorgelegt von

Christine Hansen

aus Niebüll

Göttingen, 2017

Thesis Committee Members

Prof. Dr. Ulf Diederichsen *Institut für Organische und Biomolekulare Chemie,*
(Referent) *Georg-August-Universität Göttingen*

Prof. Dr. Ivo Feußner *Albrecht-von-Haller-Institut für Pflanzenwissenschaften,*
(Co-Referent) *Georg-August-Universität Göttingen*

Prof. Dr. Ebbe Nordlander *Chemical Center - Chemical Physics, Lunds Universitet,*
(Co-Referent) *Lund/Schweden*

Further Members of the Examination Board

Prof. Dr. Hartmut Laatsch i. R. *Institut für Organische und Biomolekulare Chemie,*
 Georg-August-Universität Göttingen

Prof. Dr. Manuel Alcarazo *Institut für Organische und Biomolekulare Chemie,*
 Georg-August-Universität Göttingen

Prof. Dr. Konrad Koszinowski *Institut für Organische und Biomolekulare Chemie,*
 Georg-August-Universität Göttingen

Dr. Franziska Thomas *Institut für Organische und Biomolekulare Chemie,*
 Georg-August-Universität Göttingen

Date for Thesis Disputation: 09th October, 2017

This work was supported by the *Deutsche Forschungsgemeinschaft* via the **International Research Training Group 1422 – Metal Sites in Biomolecules – Structures, Regulations and Mechanisms** and has been carried out under the supervision of Prof. Dr. Ulf Diederichsen at the Institut für Organische und Biomolekulare Chemie of the Georg-August-Universität Göttingen between May 2013 and October 2017.

I would like to thank Prof. Diederichsen for giving me the opportunity to work on interesting research topics within his group. Also, I am grateful for his unrestricted support, guidance and high freedom of research.

Table of Contents

| | | |
|-------|--|-----|
| 1 | Introduction and Motivation | 1 |
| 2 | Synthesis of Ca ²⁺ Sensor-Labelled Membrane Components | 3 |
| 2.1 | Introduction | 3 |
| 2.2 | The Role of Calcium in Living Systems | 4 |
| 2.3 | SNARE-mediated Membrane Fusion..... | 7 |
| 2.4 | Fluorescent Ca ²⁺ Sensors | 12 |
| 2.5 | Calcium Sensor-Labelling of Membrane Components | 14 |
| 2.5.1 | Synthesis of Alkyne-Carrying Lipids and Peptides | 14 |
| 2.5.2 | Labelling of Membrane Components via CuAAC (<i>Click</i>) Reaction | 18 |
| 2.6 | Application of Ca ²⁺ Sensor-Labelled Lipids | 32 |
| 2.6.1 | Analysis of SNARE-mediated Membrane Fusion using Labelled Lipids | 32 |
| 3 | Labelling of Lipids via 7-Azaindole | 41 |
| 3.1 | Introduction | 41 |
| 3.2 | Raft Formation in Lipid Membranes..... | 42 |
| 3.3 | 7-Azaindole | 46 |
| 3.4 | Synthesis of 7-Azaindole-3-propionic Acid (25) | 49 |
| 3.5 | Synthesis of Lipid Derivative 27 | 51 |
| 3.6 | Synthesis of 7-Azaindole-3-decanoic Acid (40)..... | 57 |
| 3.7 | Synthesis of Modified Lipid Derivative 55..... | 64 |
| 3.8 | Enzymatic Synthesis of Modified Lipid Derivative 55 | 73 |
| 3.9 | Fluorescence Measurements of 7-Azaindole-Labelled Lipids | 78 |
| 4 | <i>gem</i> -Difluorinated Fatty Acids..... | 83 |
| 4.1 | Introduction | 83 |
| 4.2 | Lipoxygenases..... | 84 |
| 4.3 | Synthesis of 11,11-Difluorolinoleic acid..... | 88 |
| 5 | Summary | 99 |
| 6 | Experimental Part..... | 103 |
| 6.1 | Materials and General Methods | 103 |
| 6.2 | Characterisation..... | 105 |
| 6.3 | Spectroscopic Methods | 106 |

| | | |
|-------|--|-----|
| 6.4 | General Protocols (GP) | 108 |
| 6.4.1 | GP1: Peptide Synthesis | 108 |
| 6.4.2 | GP2: Preparation of Vesicles | 110 |
| 6.5 | Synthesis..... | 112 |
| 6.5.1 | Synthesis of 11,11-Difluorolinoleic acid..... | 112 |
| 6.5.2 | Synthesis of 7-Azaindole Derivatives | 124 |
| 6.5.3 | Synthesis of Phospholipids | 138 |
| 6.5.4 | Synthesis of Ca ²⁺ -sensitive Labelled Membrane Compartments..... | 162 |
| 7 | Abbreviations | 171 |
| 8 | Bibliography | 175 |
| 9 | Appendix | 187 |
| 9.1 | Ceramide 118 | 187 |
| 9.1.1 | Synthesis of Ceramide 118 | 189 |
| 10 | Acknowledgement/Danksagung..... | 191 |
| | Curriculum Vitae | 193 |

1 Introduction and Motivation

Communication is key. The development of language represents a milestone in human evolutionary history. Advancing simple sounds to distinct words and sentences enabled our ancestors not just to share information regarding the richest hunting grounds but to hand on acquired knowledge and skills. Furthermore, the capability to communicate individual emotions and needs facilitated the living in bigger social structures.^[1] Long before verbal communication evolved, other, more essential forms of information transfer, had arisen. The necessity of interaction and transduction of information is omnipresent in living systems. Some plants for example are not just capable of producing defending or toxic substances to protect themselves from herbivores but also to emit hormones to warn neighbouring plants and to attract herbivore predators.^[2,3] On extracellular (i.e. wound healing^[4]) and intracellular (i.e. egg activation for fertilisation^[5]) level, communications take place via messenger compounds, which are classified as extracellular, first messenger and intracellular, second messenger.^[6] Some of the most prominent second messengers are cyclic AMP (cAMP), inositol-1,4,5-trisphosphate (IP₃), diacylglycerin (DAG) and Ca²⁺ ions.^[5,6]

To investigate physiological processes, such as Ca²⁺-triggered neuronal exocytosis, a common procedure is the utilisation of fluorescence spectroscopy. One possibility is the usage of fluorophores, which can be incorporated into cells by stainings.^[7,8] Another approach is the application of sensors. Fluorescent sensors alter their fluorescence behaviour upon environmental changes like shift in pH or alteration of specific metal ion concentration.^[8] A major drawback of many dyeing techniques is the rapid exclusion of the fluorophore out of the cell.^[9] To prevent exclusion or compartmentalisation, coupling to large tags, like dextran, or membrane anchors, like acyl chains, are used methods.

The first chemically designed calcium sensor was described by R. TSIEN in 1980^[10], followed by a variety of broadly applicable sensors.^[11,12] In a previous work performed by J. GRAF, sensors based on fluorescein and rhodamine were modified and equipped with an azide carrying alkyl chain.^[13] This modification enabled coupling with alkyne containing compounds via 1,3-dipolar cycloaddition (HUISGEN or *click* reaction). The first project in this work is concerned with the conjunction of membrane compartments with such functionalised calcium sensors. The selected membrane compartments, like lipids and peptides, were modified to carry an alkyne moiety and subsequently applied to HUISGEN reactions for calcium sensor labelling. Variation of the linker length connecting the lipid or peptide results in different distances between sensor and membrane after incorporation into model or natural membranes. Therefore, changes in

Ca^{2+} concentration can be measured in dependence of membrane distance. A first application of the labelled compounds was tested in SNARE-mediated membrane fusion experiments to follow fusion processes. Furthermore, such labelled molecules are readily available for *in vitro* and *in vivo* experiments for Ca^{2+} -dependent fluorescence measurements.

Other second messenger compounds cannot be taken up from external sources, as it is the case for Ca^{2+} , but have to be generated. The source of the three second messengers phosphatidylinositol-3,4,5-trisphosphate (PIP_3), IP_3 , and DAG is the lipid phosphatidylinositol-4,5-bisphosphate (PIP_2), which is rarely available in plasma membranes.^[14,15] What is more, PIP_2 is thought to play a crucial role in SNARE-mediated neuronal exocytosis by forming domains of increased PIP_2 concentration. These so-called rafts enable the binding of the SNARE proteins, which allows subsequent Ca^{2+} -triggered membrane fusion.^[16,17] Usage of the well studied 7-azaindole enables observation of the environmental character, due to its ability to alter the fluorescence spectrum regarding to polar or non-polar surrounding.^[18-21] Therefore, upon raft formation the locally increased concentration of lipid bound 7-azaindole can be monitored, since the fluorophore tends to form dimers in non-polar, aprotic surrounding, exhibiting a distinct red shift. For this reason, the goal of the second project was the synthesis of labelled lipids using 7-azaindole as fluorophore.

In plants, signalling agents, such as jasmonic acid, are generated by digestion of polyunsaturated fatty acids by specialised enzymes.^[22] The conversion of polyunsaturated acids exhibiting a 1Z,4Z-pentadiene moiety into hydroperoxides is performed by members of the lipoxygenase (LOX) family.^[23] Even though LOXs have been investigated for some decades and are fairly well characterised^[24], the precise mechanism of hydroperoxidation regarding the substrate orientation within the active site is still debated. To disclose this problem, the third project regards the synthesis of 11,11-difluorolinoleic acid. The difluorinated fatty acid mimics the natural substrate linoleic acid and will therefore be bound by the enzyme. Due to the substitution of both hydrogen atoms at C-11 by fluorines no conversion can take place. Co-crystallisation of the formed enzyme-substrate complex should allow to distinguish the exact substrate orientation in the active pocket. Hence, further insight into regio- and stereospecificity would be obtained.

2 Synthesis of Ca²⁺ Sensor-Labelled Membrane Components

2.1 Introduction

Nearly everything we do, how we think and store memories, how we move and even the beginning and end of life, is regulated by Ca²⁺.^[25,26] On the other hand diseases like Alzheimer's or cancer are thought to be connected to intracellular calcium as well. Due to calcium's ubiquitous presence and influence on intracellular and more global processes, the system of Ca²⁺-signalling became a prime target for drug development, aimed at a variety of illnesses such as cancer, heart disease, arthritis or multiple sclerosis.^[5]

To further analyse the role of Ca²⁺ in these diseases and hence optimise treatment, real-time visualisation of Ca²⁺ in living systems might provide crucial information.^[27–29] Especially multicolour imaging, addressing other biomolecules besides Ca²⁺, under utilisation of fluorophores emitting visible light has drawn interest.^[27,28,30,31] A well-established method to observe changes in Ca²⁺ concentrations is the application of chemically engineered fluorescent Ca²⁺ sensors. These indicators bind free Ca²⁺ via a chelating moiety and thereby change their fluorescent properties, manifested in altered fluorescence intensity or shifted excitation or emission wavelength.^[5,9] One example for usage of such a sensor is to measure changes in Ca²⁺ concentration to investigate the Ca²⁺ dependency of synaptic transmission in the brain.^[32] The transduction of neurotransmitter is a Ca²⁺-triggered process, utilising the SNARE protein membrane fusion machinery, whose exact mechanism remains to be discovered.^[33–36]

For this reason a humble contribution to uncover the mechanism of Ca²⁺-dependent membrane fusion shall be presented in the following chapter. Labelling of membrane components with fluorescent Ca²⁺ sensors via 1,3-dipolar cycloaddition (HUISGEN or *click* reaction) enables full-fusion verification in vesicle fusion experiments and allows to study the influence of Ca²⁺ on SNARE-mediated membrane fusion.

2.2 The Role of Calcium in Living Systems

The human body contains an average of 1.4 kg of calcium, which is mainly bound in bones and teeth.^[37] Not even 1 % of the calcium within a human is available outside the skeleton in its ionic form but this small amount occurs to be one the most important signalling agents in living systems.^[37] Every aspect of life, from its beginning to its death, is regulated by Ca²⁺.^[25,38–40] Already in 1883 S. RINGER discovered the significance of Ca²⁺ on the contractibility of heart muscles, when no contraction of hearts took place in distilled water but was observed in London tap water.^[39,41] Following RINGERS finding, a tremendous variety of Ca²⁺-regulated processes was detected, including fertilisation^[39,40,42], cell growth^[43], gene expression^[44], hypertrophy^[45] and apoptosis^[25,38].

Ca²⁺-dependent regulation of processes within cells demands a carefully adjusted equilibrium between uptake of Ca²⁺ into the cytosol and its removal out of the cell or storage in the respective organelles like the endoplasmic reticulum (ER) or mitochondria at all times (Figure 2.1).^[40,46] The efficiency of calcium signalling is based on the enormous gradient between cytosolic ($\sim 10^{-7}$ M) and extracellular ($\sim 10^{-3}$ M) Ca²⁺ concentration. Activation of a cell via a primary stimulus opens Ca²⁺ channels, enabling rapid Ca²⁺ uptake of up to 10^{-6} M within milliseconds.^[5,39,47] For precise concentration control of free Ca²⁺ a multitude of Ca²⁺-binding proteins has evolved, which trigger cell activation by a primary stimulus. These proteins are divisible in two categories: Ca²⁺-buffering and transporting proteins and Ca²⁺ sensors.^[46]

Proteins responsible to transport or buffer Ca²⁺ are generally located in organelles, integrated into membranes or in the cytosol. The soluble cytosolic proteins can store high quantities of Ca²⁺ (i.e. parvalbumin, calsequestrin).^[5,46,48] Proteins located intrinsically to membranes can form channels, pumps or exchangers to transport Ca²⁺ through membranes. These Ca²⁺-transporting proteins regulate the membrane potential and concentration gradients and by modulating the Ca²⁺ concentration in the cytosol lead to signal transduction.

Ca²⁺ channels typically transport Ca²⁺ out of the extracellular space into the cell or enable removal of Ca²⁺ out of the ER or sarcoplasmic reticulum (SR). Channels positioned in the plasma membrane (PM) are triggered to open by extra- or intracellular binding of ligands or voltage change, while channels in the ER/SR regulate Ca²⁺-induced Ca²⁺ release, meaning that Ca²⁺ regulates itself. Still, this kind of control requires further ligands. Two of the best-known ligands are inositol-(1,4,5)-triphosphate (IP₃), that binds to the IP₃ receptor (IP₃R), and cyclic adenosine diphosphoribose (cADP ribose), which activates the Ca²⁺-sensitive ryanodine receptors (RyR).^[38,46,47]

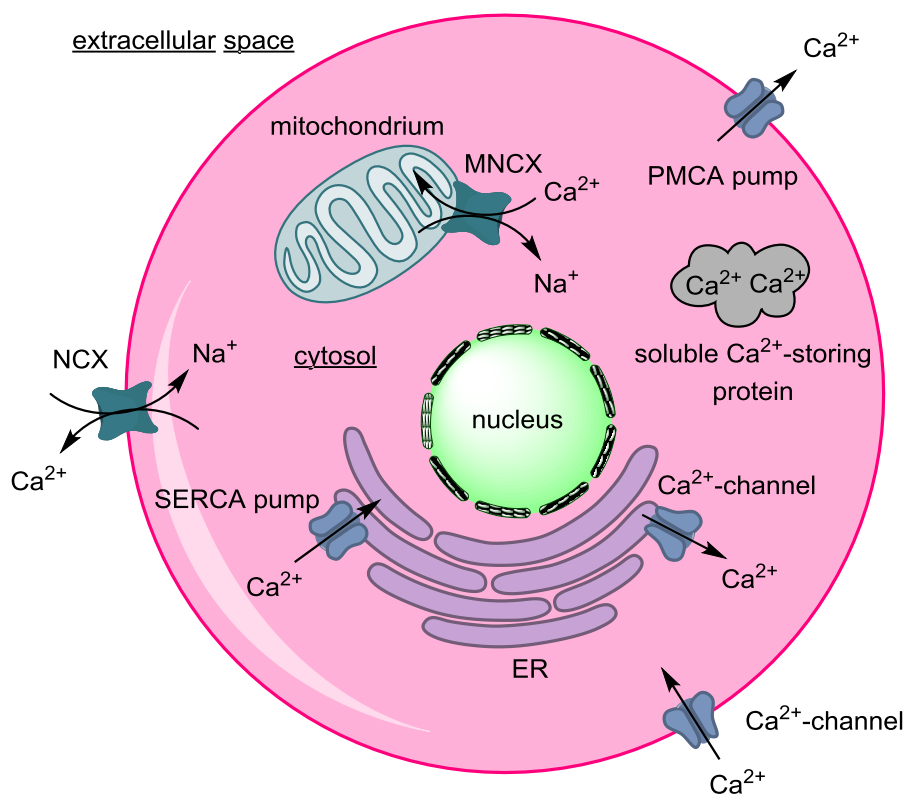


Figure 2.1 Schematic illustration of control proteins in eukaryotic cells depicting Ca^{2+} transport via channels, pumps and exchangers. No differentiation between ligand and voltage gated channels is performed. Picture based on [46].

The second operation mode of membrane-intrinsic proteins is transportation of Ca^{2+} as ion pumps. A commonly discussed pump in eukaryotic cells is the Ca^{2+} ATPase. Within the ER membrane the sarco/endoplasmic reticular Ca^{2+} ATPases (SERCA pumps) convey Ca^{2+} uphill against the gradient into the ER, hydrolysing one ATP molecule to transport two calcium ions. Fulfilling the same task, the ATPase in the plasma membrane, the plasma membrane Ca^{2+} ATPase (PMCA) pump, reduces the cytosolic Ca^{2+} concentration by pumping Ca^{2+} out of the cell. In contrast to SERCA pumps the PMCA pumps consume one ATP molecule per Ca^{2+} .^[46,49,50]

The last type of Ca^{2+} -binding and transporting proteins are the exchangers. Two examples are the $\text{Na}^{+}/\text{Ca}^{2+}$ exchangers in the inner mitochondrial membrane (MNCX) and in the PM (NCX). MNCX removes one Ca^{2+} out of the mitochondrial matrix in exchange for two Na^{+} , resulting in an electrically neutral process. In contrast, NCX substitutes one Ca^{2+} by three Na^{+} , making it responsive towards voltage differences and Na^{+} and Ca^{2+} transmembrane gradients.

The second category of Ca^{2+} -regulating proteins comprises of the Ca^{2+} sensors. The best-characterised sensors are the proteins of the EF-hand protein family. For Ca^{2+} -binding the helix-loop-helix motif is used, in which the on average 12 amino acid short loop binds Ca^{2+} via oxygen-rich side chains like aspartate or glutamate.^[46,51]

Processing of Ca^{2+} signals proceeds via two conformational changes of the EF-hand. Binding of Ca^{2+} induces the first change in conformation while activation of a structural protein or target enzyme, like kinases or phosphatases, by the EF-hand protein causes the second change.^[46,51]

The most frequently mentioned Ca^{2+} sensor exhibiting the EF-hand motif is calmodulin (CaM). The structure of this small (~148 amino acids) pervasive protein is highly conserved and has barely changed over the last 1.5 billion years.^[38,52,53] CaM is formed like a dumbbell featuring a flexible joint in the middle, connecting two roughly balanced domains with two EF-hands each. Containing this motif, CaM exhibits distinct Ca^{2+} affinities ($K_d = 5 \cdot 10^{-7} \text{ M}$ to $5 \cdot 10^{-6} \text{ M}$) with four Ca^{2+} -binding sites, located between the two α -helices of each EF-hand.^[53] The Ca^{2+} -free (apo) CaM is arranged in a closed conformation, shielding the hydrophobic residues from the polar surrounding (Figure 2.2, A). Complexation of Ca^{2+} alters the conformation to an open position, exhibiting hydrophobic areas of each domain (Figure 2.2, B).^[53] The exposed methionine-rich hydrophobic surfaces are now enabled to bind target enzymes by wrapping around their amphipathic domains, i.e. myosin-light-chain kinase (MLCK, Figure 2.2, C).^[38]

Ca^{2+} -bound CaM ($\text{Ca}^{2+}_4\text{-CaM}$) plays a crucial role in activation of a variety of enzymes. One example is the phosphorylase kinase, which is dependent on $\text{Ca}^{2+}_4\text{-CaM}$ to trigger cleavage of glycogen under glucose release.^[54] Furthermore, MLCK is activated by $\text{Ca}^{2+}_4\text{-CaM}$, leading to phosphorylation of the myosin light chain, hence enabling smooth muscle contraction.^[55] As a conclusive example the $\text{Ca}^{2+}_4\text{-CaM}$ -dependent protein kinase II (CaM kinase II) is to be mentioned. This kinase occurs in neurons in high concentrations and is responsible for activating further enzymes like calcineurin (CaN), tyrosine hydroxylase (TYH) and nitric oxide synthases (NOOSs).^[56]

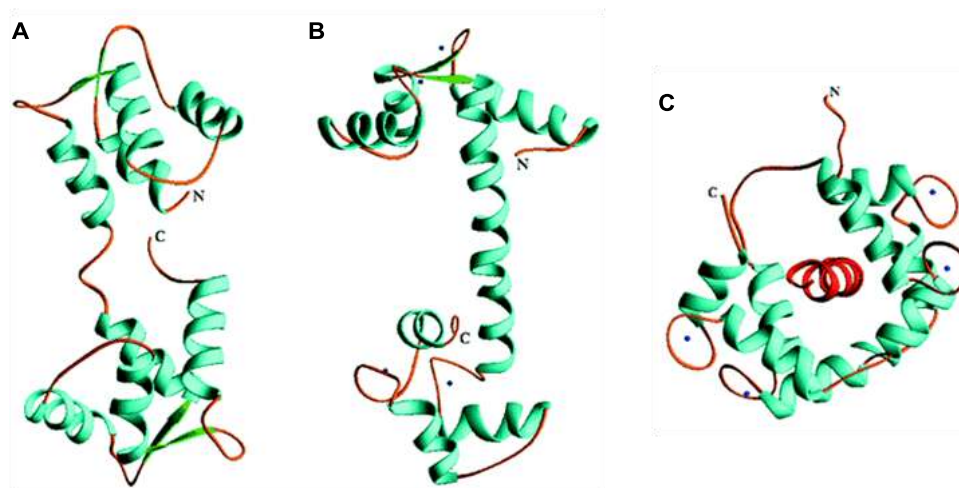


Figure 2.2 CaM in its closed form, with shielded hydrophobic domains (A); $\text{Ca}^{2+}_4\text{-CaM}$ in the open form (B); $\text{Ca}^{2+}_4\text{-CaM}$ complexed a MLCK (red helix) with its hydrophobic binding domain (C). Pictures taken from [57].

2.3 SNARE-mediated Membrane Fusion

As briefly presented in chapter 2.2 the alkaline earth metal calcium is in the ionic form (Ca^{2+}) a highly versatile and important second messenger, triggering a diversity of enzyme driven processes. This finding seems to be true for membrane fusion events as well.^[35] Already in 1967 B. KATZ and R. MILEDI discovered that Ca^{2+} triggers exocytosis of synaptic vesicles, leading to release of neurotransmitters and thereby instigating synaptic transmission.^[36,58] Fusion processes of stable membranes require a driving force to overcome the electrostatic repulsion of the two membranes. Interaction of fusion proteins anchored in the respective membranes enables fusion to proceed.^[59] They participate in steps like protein recognition, hemi-fusion of the respective membranes followed by fusion pore formation.^[60]

The general path of synaptic vesicles in the nerve terminal is depicted in Figure 2.3. During intervals between exocytosis, the synaptic vesicles carrying neurotransmitters are stored in the so-called active zone in the cytoplasm. The active zone, in which a multitude of inimitable multidomain proteins are located, supplies a template for vesicle docking. After stimulation of the cell, the docked and primed vesicles in the active zone fuse with the presynaptic plasma membrane and release their cargo into the synaptic cleft. Clathrin-assisted vesicle recycling via endocytosis provides precursor vesicles for future cycles.^[26,34,61]

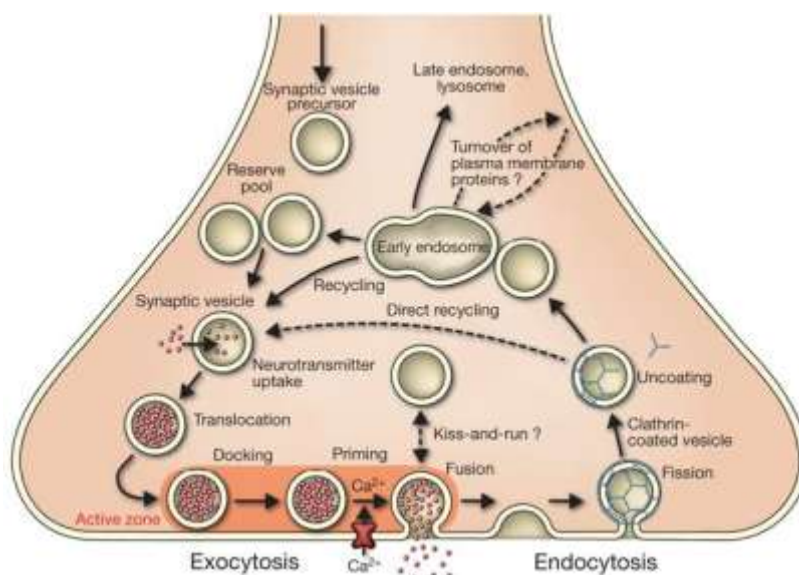


Figure 2.3 Schematic view of synaptic vesicles in the nerve terminal. With neurotransmitter filled vesicles are stored in the cytoplasm. After relocation to the active zone the vesicles are docked to the plasma membrane and release the neurotransmitters into the synaptic cleft upon Ca^{2+} -triggering. Vesicle recycling via endocytosis using clathrin allows cycle repetition. Picture taken from [61].

The key proteins for exocytosis are soluble N-ethylmaleimide-sensitive-factor attachment receptors (SNAREs), Rab proteins, Sec1/Munc18-like (SM) proteins and a protein group named complex associated with tethering containing helical rods (CATCHR).^[61] These proteins form a fusion machinery, which is adapted to specified compartments. One example for these specialisations, which will be focused on in this chapter, is the neuronal exocytosis, utilising the above mentioned SNARE, Rab, SM and CATCHR proteins, and further regulatory proteins like complexins and synaptotagmins (Syt), which serve as Ca²⁺ sensors.^[36,61]

The synaptic SNARE proteins, that participate in the docking and fusion process in neurons, share an extended coiled-coil motif (SNARE motif) and can be divided into Q-SNAREs (Qa, Qb, Qc) and R-SNAREs.^[62] Accordingly, a SNARE fusion complex is composed of three Q-SNAREs and one R-SNARE. Furthermore, most SNARE proteins feature a C-terminal transmembrane domain (TMD), connected to the SNARE motif via a short linker, providing a structure to anchor the SNARE proteins in the respective membrane. Synaptobrevin (Syb, R-SNARE) is positioned in the vesicle membrane while syntaxin 1 (Sx1, Qa) and the 25 kDa synaptosome-associated protein (SNAP-25, Qb and Qc) are located in the target membrane. SNAP-25 lacks a TMD but binds to the membrane utilising palmitoyl side chains.^[63,64] The special feature of Sx1 is an additional N-terminal domain, consisting of a bundle of three antiparallel α -helices, termed Habc domain, whose participation in the fusion process is controversially discussed.^[65]

If the SNARE proteins of vesicle and presynaptic membrane come in contact with each other the proteins assemble in a parallel *trans*-complex of four parallel α -helices. The assembly is thought to start from the N-termini and to proceed towards the C-termini. This 'zippering' mechanism pulls the membranes closer together and has been postulated among others by R. JAHN *et al.* in 1997^[66,67] and verified by D. FASSHAUER *et al.* in 2010 (Figure 2.4).^[68,69]

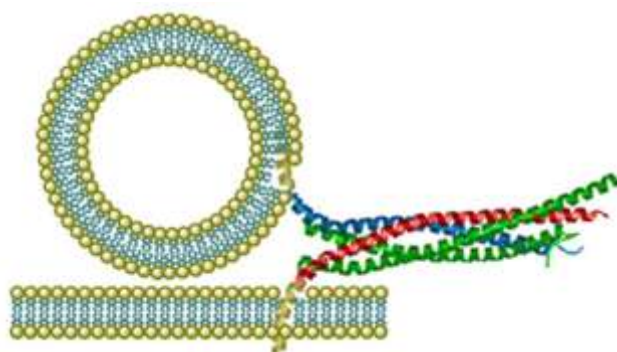


Figure 2.4 The *trans*-SNARE complex (4-helix bundle) brings the membranes into close proximity via 'zippering'. Picture taken from [70].

The exact mechanism of the SNARE-mediated membrane fusion is still debated and further advancement in technologies will be necessary to fully understand the underlying processes. However, one model for fusion and protein recovery developed by R. SCHELLER and R. JAHN in 2006 has been broadly accepted.^[71] In good agreement with this hypothesis T. SÜDHOF postulated a model including the influence of Ca^{2+} as a signalling agent (Figure 2.5).^[72] Starting from the approach of the Syb-containing (also termed VAMP: vesicle-associated membrane protein) vesicle towards the presynaptic membrane, the SNARE complex forms, containing the SM protein Munc18. The loosely formed complex is then activated by complexin to generate a tightly bound SNARE/SM protein complex that brings the vesicle in close proximity to the target membrane. Binding of Ca^{2+} by Syt-1 then triggers the fusion of membranes to form a fusion pore, which expands to complete the fusion process. Under consumption of ATP, binding of *N*-ethylmaleimide-sensitive factor (NSF) and SNAP cofactors disassembles the complex to regenerate the proteins and to provide them for the next fusion cycle.^[26,61,72] The described model is supported by plenty of evidence^[68,69,73] but still many questions remain unanswered.^[61]

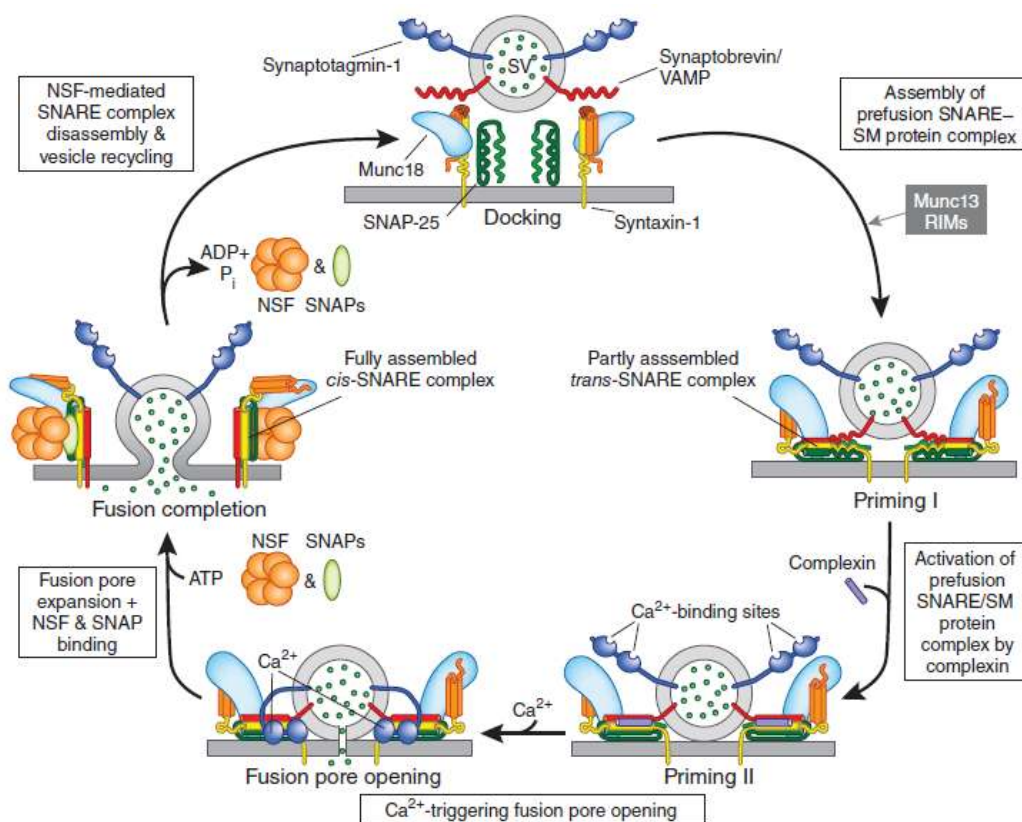


Figure 2.5 Schematic illustration of the SNARE-mediated fusion model under consideration of synaptotagmin and complexin as well as the influence of Ca^{2+} . Picture taken from [72].

2.3.1 Recognition Units in SNARE Analogue Model Systems

Investigations regarding SNARE-mediated fusion have proven to be quite demanding, since the SNARE complex formation is a highly complicated process with a broad variety of proteins involved.^[16,26,61,74] To further unravel the process of membrane fusion with its engaged proteins, model systems of reduced complexity have been developed^[75–78]. Different possibilities to generate and modify simplified model systems are thinkable. Using a bottom-up approach allows synthesising a diversity of SNARE analogues to gain information about influences of specific protein domains.^[75] One possible modification site is the TMD, which is thought to have a great influence on fusion efficiency.^[70,78] Another option is to alter the linker moiety between TMD and recognition unit. As artificial linkers PEG in differing lengths is broadly applied.^[79–81] The focus of this chapter, however, will be on modified recognition units. Prominent examples are boronic acid/*cis*-diol recognition^[82] and DNA-based recognition.^[83–85] In the following, two other recognition motifs shall be briefly introduced: the coiled-coil peptide motif^[80,81,86,87] and the PNA motif.^[70,78,88,89]

The coiled-coil recognition motif describes the interaction of several α -helices (at least two) to wrap around each other forming a bigger, α -helical structure.^[90] To understand the mechanism and specificity of the helix-helix interaction the peptide sequence needs to be taken into account. The majority of coiled-coils exhibits a heptad repeat of seven residues (from 'a' to 'g') to two turns of the helix.^[80] The positions 'a' and 'd' are usually populated by hydrophobic amino acids, facing another peptide for coiled-coil formation. The neighbouring amino acids 'e' and 'g' often feature charged side chains and therefore ensure specific binding of the α -helix (Figure 2.6).^[80,91]

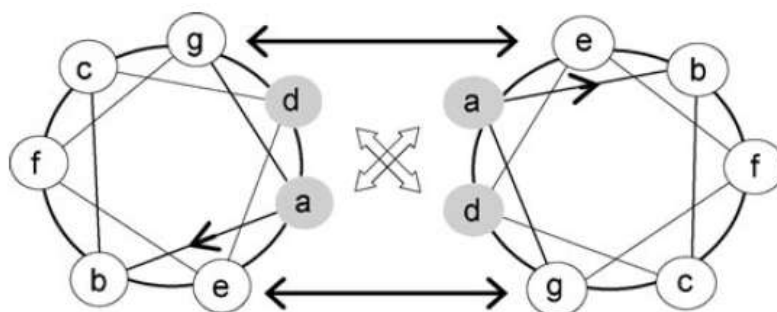


Figure 2.6 Coiled-coil representation of a dimer exhibiting heptad repeat of amino acids. Picture taken and modified from [91].

Another recognition motif utilises peptide nucleic acid (PNA) in form of hybrids between peptidic TMD and PNA, which has been developed in this work group by A. LYGINA.^[78,92] Recognition via WATSON–CRICK base pairing allows to control the orientation of the dimerising recognition motifs. The system of each two different PNA/peptide strands, shown in Figure 2.7, contains three complementary PNA domains, to interact in a parallel (PNA1 and PNA3) or antiparallel (PNA1 and PNA2) manner. Furthermore, the model systems comprise the native TMD and linker sequences of Sx, shown in orange, and Syb, shown in purple. The design of the applied PNA was evolved in 1991 by NIELSEN *et al.*, substituting the negatively charged native deoxyribose phosphate backbone by neutral *N*-(2-aminoethyl)glycine (aeg) units.^[93,94] The uncharged backbone of PNA does not entail electrostatic repulsion like its native template and is stable against nucleases or proteases.^[94]

In summary, both presented motifs of SNARE analoga represent well-suited recognition units. Specific interaction of complementary strands is ensured and recognition properties can easily be altered by modification of the amino acid sequence (coiled-coil) or substitution of specific nucleobases (PNA).

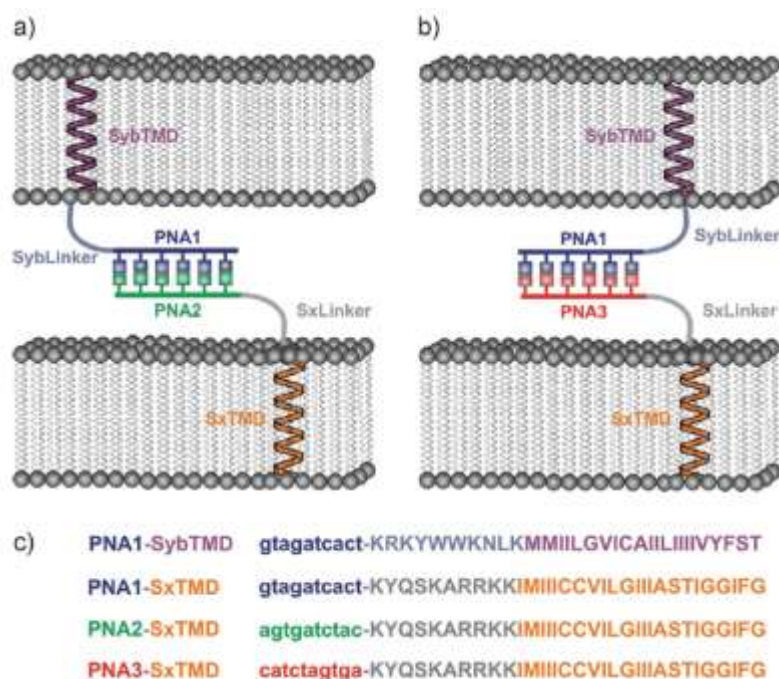


Figure 2.7 Simplified system using PNA/peptide models for vesicle fusion. As TMDs and linker domains native sequences of Syb (purple) and Sx (orange) were applied. Depending on the nucleobase sequences antiparallel (a) or parallel (b) orientation of the interacting SNARE-mimetics can be achieved. Picture taken from [78].

2.4 Fluorescent Ca²⁺ Sensors

After the importance of ionic calcium became apparent in 1883^[41], it took another 60 years for Ca²⁺ as signalling agent to provoke broad interest within the scientific community.^[37] As the diversity of Ca²⁺-dependent processes, like SNARE-mediated membrane fusion to name just one example, was started to be unravelled, the necessity for Ca²⁺ probes like fluorescent Ca²⁺ indicators evolved. To satisfy the demands for fluorescent Ca²⁺ imaging TSIEN *et al.* developed the first chemical fluorescent Ca²⁺ sensor Quin-2 in 1980 (Figure 2.8).^[10,95] Requisites of Ca²⁺ indicators are good selectivity towards Ca²⁺ and altered fluorescence properties after Ca²⁺-binding, like change in emission wavelength or increase in fluorescence intensity.^[9] Quin-2 fulfils the demand of distinct fluorescence increase in presence of free Ca²⁺ and was used for intracellular measurements.^[10,95,96] Drawbacks of Quin-2 are a low quantum yield, a small excitation coefficient and increased photobleaching after Ca²⁺-binding, which is why its usage is rather uncommon these days.^[96]

Since the design of Quin-2 numerous other indicators have been developed, which all have a similar structure.^[9,11,12,28,97-99] Today's most common Ca²⁺ sensors utilise Ca²⁺ chelators like 1,2-bis(*o*-amino-phenoxy)ethane-*N,N,N',N'*-tetraacetic acid (BAPTA) or, more seldom, ethylene glycol-bis(2-aminoethylether)-*N,N,N',N'*-tetraacetic acid (EGTA), which exhibit a one to one stoichiometry for Ca²⁺ and a high binding affinity.^[100] Especially BAPTA is highly selective towards Ca²⁺ over Mg²⁺, less pH dependent in respect to metal chelation and conducts more rapid binding and releasing of Ca²⁺ than EGTA.^[10,11] Introduction of electron-withdrawing groups, like halogen atoms or nitrile moieties, leads to an increase of the *K_D* value while electron-donating groups, like methyl or heteroatoms (O, N), favour a decrease of the *K_D* value. These modifications thus allow to generate low and high affinity Ca²⁺ sensors.^[11]

Chemical sensors build up from two parts, the just discussed Ca²⁺-chelating moiety and a dye, and can be divided into ratiometric and non-ratiometric sensors. The non-ratiometric Ca²⁺ indicators, which mainly utilise BAPTA and dyes like derivatives of Rhodamine or Fluorescein, exhibit a change in fluorescence intensity after Ca²⁺-binding without alteration of the excitation or emission wavelength. The mechanism that forms the basis of changes in the fluorescence intensity, is the photoinduced electron transfer (PET).^[101] Sensors in absence of Ca²⁺ exhibit no or weak fluorescence, since the BAPTA moiety quenches the fluorescence by accepting the excited electron of the fluorophore unit. After Ca²⁺-binding, the PET mechanism becomes energetically unfavoured and the fluorescence increases.^[102]

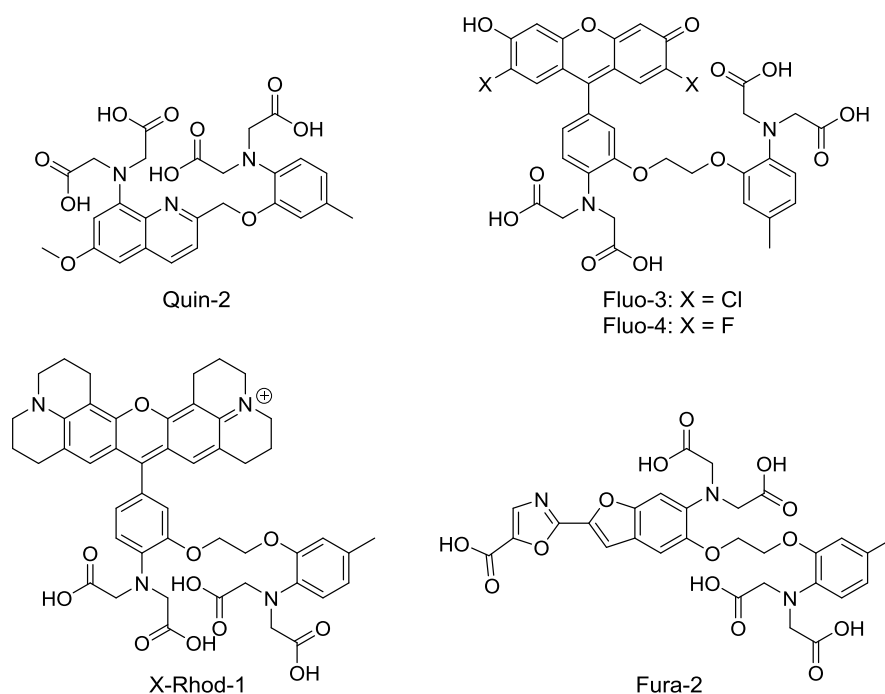


Figure 2.8 Examples for chemical Ca²⁺ indicators with Quin-2 as the archetype and four high affinity Ca²⁺ sensors. Fluo-3, Fluo-4 and X-Rhod-1 belong to the family of non-ratiometric sensors while Fura-2 is a ratiometric indicator.

These sensors, like Fluo-3, Fluo-4 or X-Rhod-1 (Figure 2.8), are excitable with a single wavelength of visible light and feature therefore a reduced phototoxicity.^[27,103]

Ratiometric Ca²⁺ sensors, like Fura-2 (Figure 2.8), experience a shift in their excitation or emission wavelength upon Ca²⁺-binding. This allows a very precise quantification of Ca²⁺ concentration, due to being independent of sensor concentration, equability of the loaded dye or photobleaching, for example. The constraint of ratiometric indicators is the necessity of an enhanced spectral bandwidth, leading to increased phototoxicity.^[9]

2.5 Calcium Sensor-Labelling of Membrane Components

2.5.1 Synthesis of Alkyne-Carrying Lipids and Peptides

Calcium detection in cells is generally performed using one of the many commercially available indicators. A multitude of those sensors is used as acetoxymethyl esters for facilitated cell loading. The ester will, once within the cell, be hydrolysed by an esterase to release the carboxylic acids for calcium binding. The drawback of this method is that the *in vivo* or *in vitro* generated active sensor will not distribute equally within the cell but will accumulate in specific regions and in many cases, will be discharged from the cell. To inhibit discharging of the sensor bulky, nontoxic molecules, like dextrane, are often bound to the sensor.^[43,104,105] The modified sensor will stay within the cell but its distribution is still erratic. To overcome this obstacle, it was thought of to bind a Ca²⁺ sensor to membrane components, which will fixate the sensor in close proximity to the membrane. Since there is a concentration gradient of Ca²⁺ ions in living cells due to opening and closing of ion channels and pumps, placement of the sensor in different distances to the membrane should allow to observe this gradient. Therefore, a variety of potential membrane components were modified with an alkyne moiety for sensor-binding (Figure 2.9).

To bind the sensor close to the membrane phospholipids were chosen. As the best-suited phospholipid to incorporate an alkyne functionality into, a phosphatidylethanolamine (PE) lipid was selected.

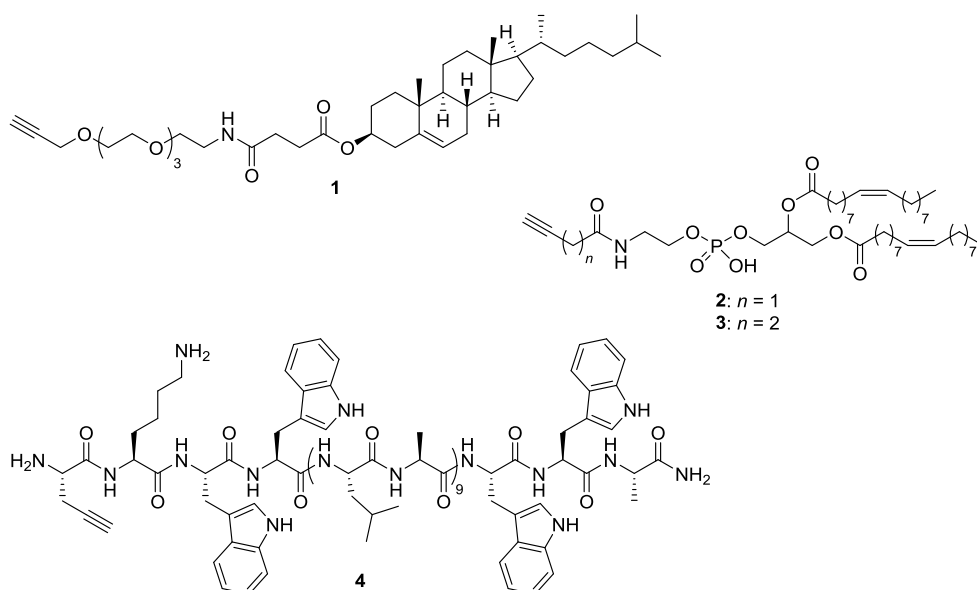


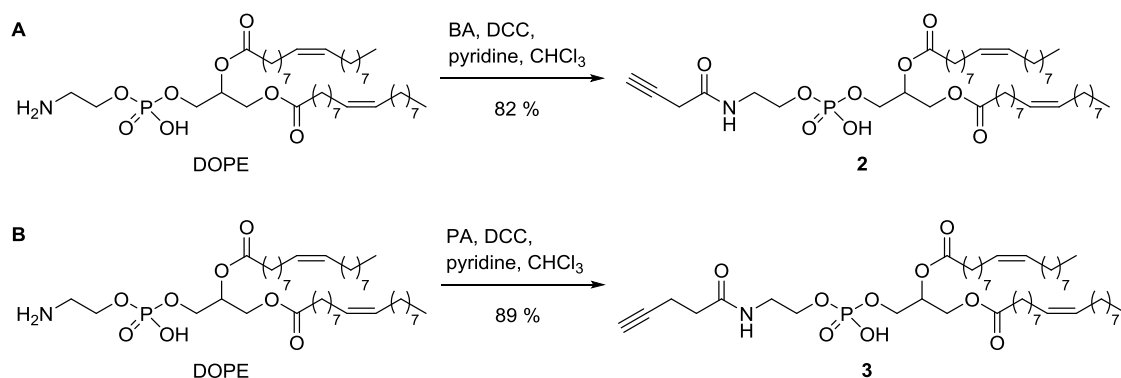
Figure 2.9 With alkyne functionality modified membrane components based on cholesterol (1), DOPE (2,3) and transmembrane WALP peptides (4).

A considerably longer distance between sensor and membrane was supposed to be achieved by modification of cholesterol using a short PEG4 linker. The third employed system was alkyne incorporation into a transmembrane protein. For this work a distance of medium length was chosen, but elongation of the sequence with polar amino acids allows a broad variety in sensor–membrane distances.

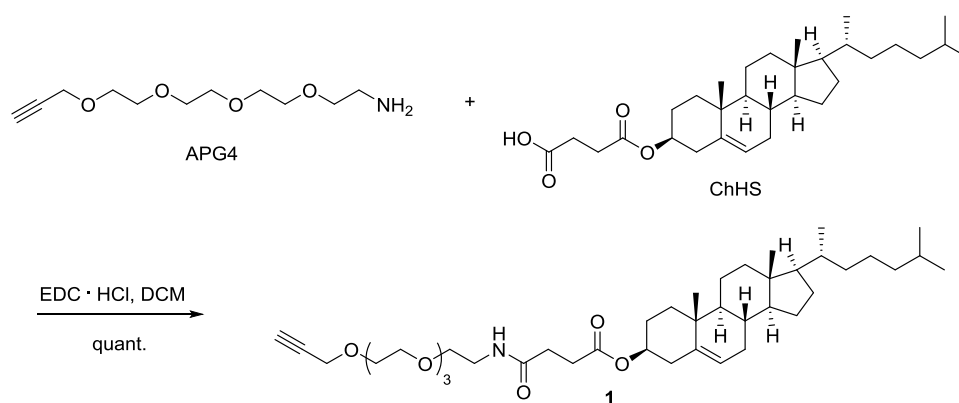
First, the modification of a phospholipid was performed. The amino group of 1,2-dioleoyl-*sn*-glycerol-3-phosphoethanolamine (DOPE) is perfectly applicable for incorporation of an alkyne-carrying carboxylic acid as a linker via amide bond formation (Scheme 2.1, A). As linker 3-butynoic acid (BA) has been coupled by stirring a solution of BA and DCC in chloroform for 4 h, then DOPE and pyridine were added. After heating to 50 °C over 12 h, the formed side product could be filtered off and via RP-FC pure product **2** was obtained in 82 % yield.^[106]

Applying the same conditions as described above but using 4-pentynoic acid (PA), which differs from BA just in one additional methylene unit, the reaction proceeded smoothly to form **3** in 89 % yield (Scheme 2.1, B).

The last lipid to be modified and labelled was cholesterol, which was purchased as cholesteryl hemisuccinate (ChHS). The hemisuccinate unit allowed the incorporation of 3,6,9,12-tetraoxapentadec-14-yn-1-amine (H₂N-PEG4-Alkyne, APG4) via amide bond formation (Scheme 2.2) for subsequent *click* reaction. For coupling a solution of APG4 and ChHS in DCM was treated with 3-(ethyldimethylaminomethyl)carbodiimide-*N,N*-dimethyl-propan-1-amine (EDC · HCl) and stirred at r.t. for two days. After purification via FC pure product **1** was obtained in quantitative yield.



Scheme 2.1 Coupling of BA (**A**) and PA (**B**) to DOPE for subsequent *click* reaction.



Scheme 2.2 Coupling of PEG linker APG4 to the cholesterol derivative ChHS.

Besides these modified lipids, which will be located in one leaflet of the membrane, an alkyne carrying peptide was synthesised. For synthesis of a transmembrane peptide the well-studied WALP peptide class was chosen, since they form stable membrane spanning α -helices. WALP peptides consist of a hydrophobic core region, made of L-alanine (A) and L-leucine (L), as well as L-tryptophan (W) on both ends of the hydrophobic region to anchor the peptide in the membrane. In this work the WALP25 structure **4** (Figure 2.9) was tailored, consisting of a hydrophobic (LA)₉-region, framed by two W on each side. One A was included at the C-terminus. At the N-terminus one L-lysine (K) was incorporated for solubility reasons and terminal the non-natural amino acid propargylglycine was coupled. The designed WALP25 peptide had an approximate length of 37.5 Å as an α -helix with a hydrophobic (LA)₉-domain of about 27 Å.

The synthesis of **4** was conducted via automated solid phase peptide synthesis (SPPS) using **GP1.2** for coupling and **GP1.3** for peptide cleavage. Test cleavage showed no product formation but several truncated sequences. Elongation of coupling times and application of double-coupling steps did not improve the synthetic outcome. To revise whether or not automated synthesis yields the desired peptide if the non-natural amino acid propargylglycine is omitted, a test cleavage was performed after coupling of the 24 natural amino acids (Figure 2.10). Mass spectrometry revealed fairly pure formation of the desired peptide **5** without truncated sequences.

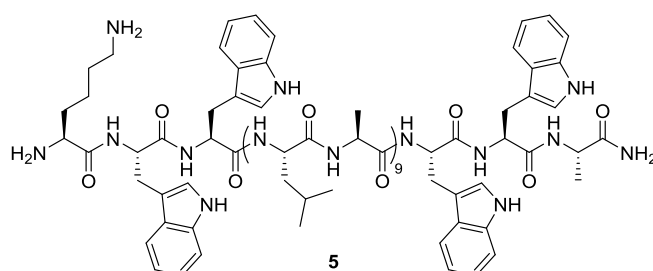


Figure 2.10 Test cleavage of **5** after coupling the 24 natural amino acids, omitting propargyl glycine.

Peptide **5** was transferred into a BD-syringe equipped with a polyethylene filter. Via **GP1.1** the *N*-terminal amino acid was manually coupled using *N,N*-dimethylformamide (DMF) as solvent. After test cleavage formation of small product amounts were observed but the high impurity made HPLC purification unfavourable. For a better yield with fewer side reactions the solvent was changed from DMF to *N*-methyl-2-pyrrolidone (NMP). This led indeed to formidably increased yield while the quantity of impurities was minimised, so that for future WALP syntheses the combination of **GP1.2** in DMF with **GP1.1** in NMP was used.

To verify that peptide **4** will form the desired α -helical structure, circular dichroism (CD-) measurements were conducted. As shown in Figure 2.11, two minima at 208 nm and at 222 nm were observed, displaying a typical curvature of α -helical peptides.

Since the synthesis of WALP peptide **4** is quite resource-demanding, a variety of shorter peptides (Figure 2.12) was prepared as model systems for condition screening for the desired copper(I)-catalysed azide-alkyne cycloaddition (CuAAC). The three short peptides **6**, **7** and **8**, consisting of four to six amino acids, were manually coupled using **GP1.1**. Interestingly, for coupling of propargylglycine to these short peptides no difference was observed between usage of DMF and NMP. The fourth peptide **9** carries no alkyne but is intended for labelling via amide-bond formation.

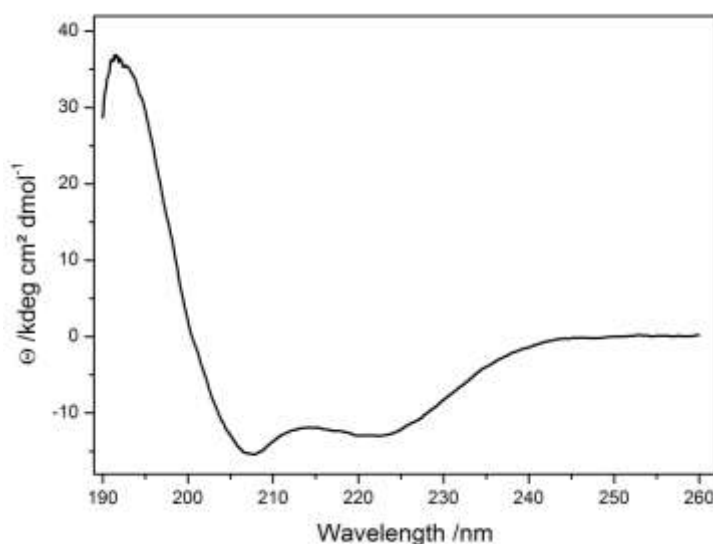


Figure 2.11 CD-spectrum of WALP peptide **4** measured in MeOH.

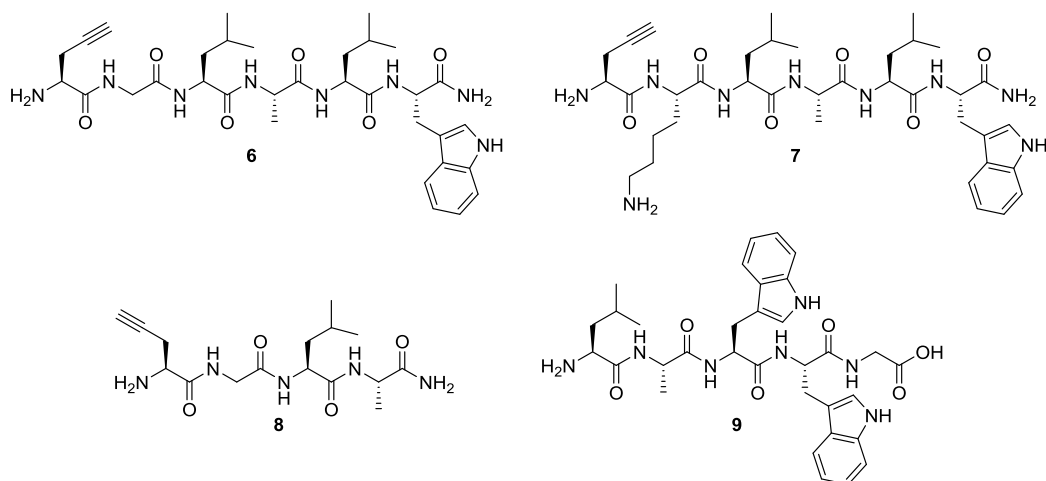


Figure 2.12 Library of shorter peptides designed for condition screening.

2.5.2 Labelling of Membrane Components via CuAAC (*Click*) Reaction

For labelling of various membrane components like lipids and peptides the two different Ca²⁺ sensors X-Rhod-Azide and Fluo-Azide were chosen (Figure 2.13). Both sensor structures, consisting of a fluorophore moiety and a Ca²⁺-chelating BAPTA unit, are based on literature known compounds^[12,27,28,99,107], which are commercially available. They were modified in a previous work^[13] to enable covalent binding without disturbance of the sensor performance, under development of an improved synthetic route. For binding to alkynes a butyl group carrying an azide was incorporated, which allows subsequent copper(I)-catalysed 1,3-dipolar cycloaddition (*click* reaction), forming the five-membered heterocycle triazole. Performance of *click* reaction was carried out under light exclusion to inhibit decomposition of the sensor compounds.

The developed conditions for *click* reactions are highly versatile.^[108–110] At first, WALP25 peptide **4** was supposed to be labelled with sensor X-Rhod-Azide. Due to the small reaction scale of micro- to nanomolar, all compounds were previously prepared as stock solutions in DMF and the reactions were conducted in micro reaction vessels. Sensor and peptide **4** were treated with copper(I) iodide (CuI) and sodium ascorbate (NaAsc) in DMF under argon atmosphere (Scheme 2.3, Table 2.1, A).^[111,112] The reaction mixture was shaken over night and extracted using DCM and water (1:1, v/v). After the organic solvent was removed, analysis of the residue via HPLC and mass spectrometry showed no conversion to the desired product **10**.

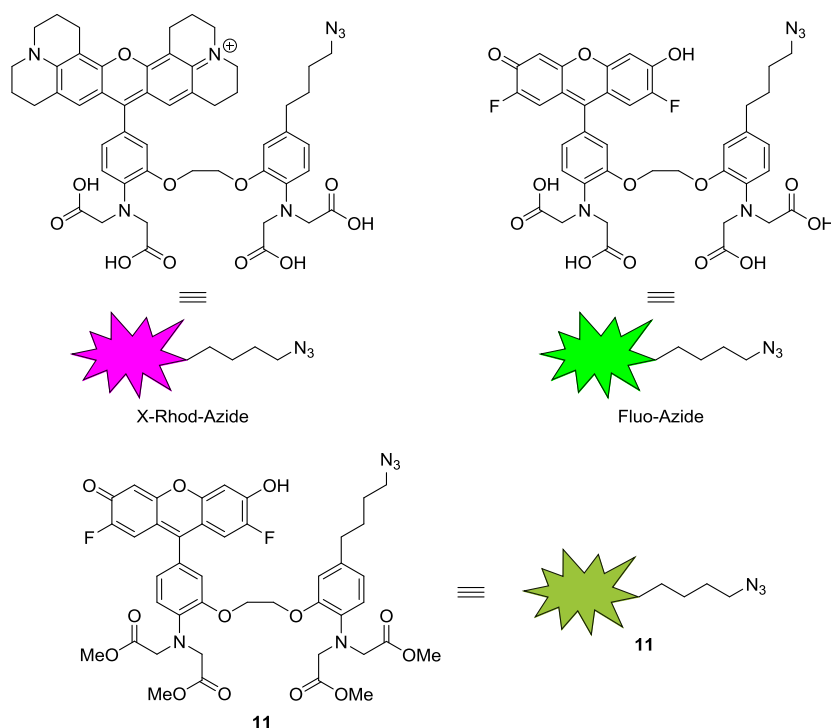
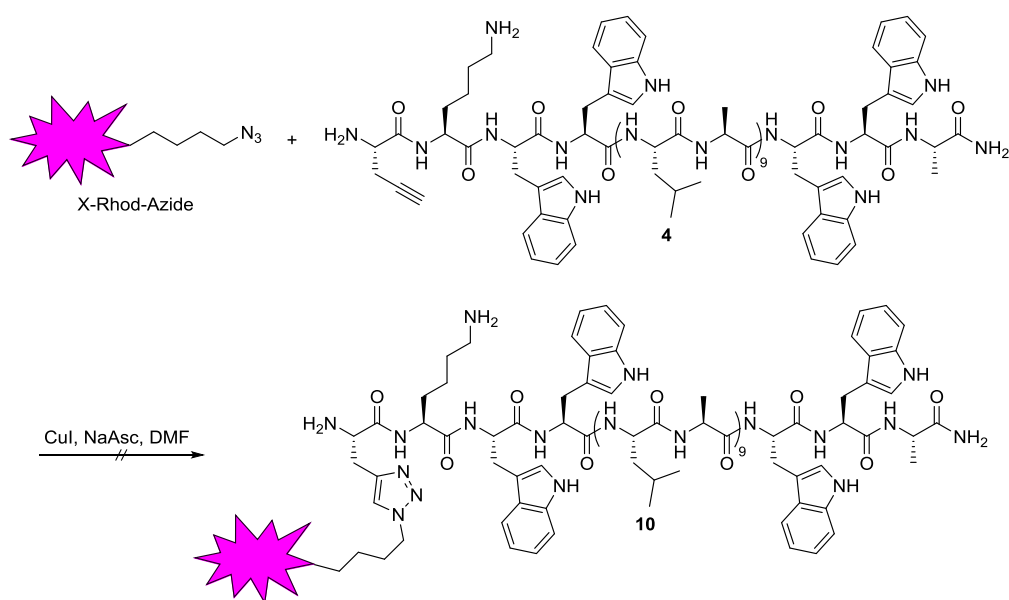
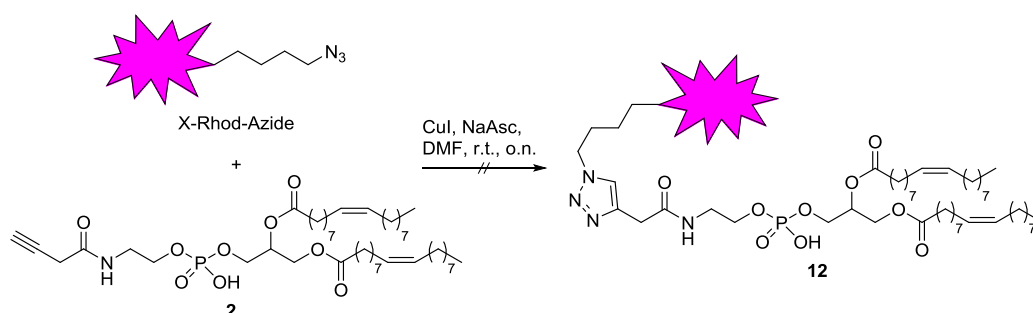


Figure 2.13 Chemical structure of the Ca^{2+} sensors X-Rhod-Azide and Fluo-Azide along with Fluo-Azide precursor 11.



Scheme 2.3 Labelling attempt of WALP25 peptide 4 via HUISGEN cycloaddition.

Since no labelled product was formed, sensor X-Rhod-Azide and lipid **2** were treated with the same conditions as described above (Scheme 2.4), to review whether utilising CuI in DMF is just unfitting for peptide **4** or for a lipid system as well. After workup procedure, again, no product formation was observed. As *click* reaction with **2** and X-Rhod-Azide did not perform, the system itself was changed by substitution of X-Rhod-Azide through Fluo-Azide. The conditions were altered to CuSO₄ · 5H₂O (20.0 eq.) and NaAsc (25.0 eq.) in MeOH and ultrapure water (4:1, v/v).^[113] As reactant the lipids **2** and **3** were tested as well as peptide **4** (Scheme 2.5, Table 2.1, **B**). In all three cases no product was found using mass spectrometry and HPLC showed no conversion.



Scheme 2.4 Testing of *click* conditions for **2** labelling with X-Rhod-Azide (Table 2.1, **A**).

Table 2.1 Selection of tested conditions for labelling via *click* reaction.

| | Azide (eq.) | Alkyne (eq.) | Cu-salt (eq.) | NaAsc (eq.) | Add. | Solvent | Temp. (°C) |
|----------|-------------------|-----------------------------------|---|----------------|-------------------------------|-------------------------------------|---------------|
| A | X-Rhod 1.00 | 2/4 1.20 | CuI 1.50 | 2.00 | – | DMF | 20 |
| B | Fluo 1.00 | 2/3/4 1.00 | CuSO ₄ · 5H ₂ O 20.0 | 25.0 | – | MeOH/H ₂ O, 4:1 | 20 |
| C | Fluo 1.00 | 4 1.00 | CuSO ₄ · 5H ₂ O 20.0 | 25.0 | THPTA 5.00 | MeOH/H ₂ O, 4:1 | 20 |
| D | Fluo 1.00 | 4 1.00 | CuSO ₄ · 5H ₂ O 20.0 | 25.0 | – | MeOH/H ₂ O, 4:1 | 35 |
| E | Fluo 1.00 | 4 1.40 | CuSO ₄ · 5H ₂ O 20.0 | 25.0 | THPTA 13.4 | MeOH/H ₂ O, 4:1 + TFE | 20 → 38 |
| F | Fluo 1.10 | 6 1.00 | CuSO ₄ · 5H ₂ O 0.05 | 0.50 | – | DMF/H ₂ O, 17:1 | 80 (25 W) |
| G | Fluo 1.00 | 4 1.20 | CuSO ₄ · 5H ₂ O 6.70 | 10.0 | THPTA 13.4 | MeOH/H ₂ O, 4:1 | 20 → 35 |
| H | Fluo 1.00 | 4 1.20 | CuSO ₄ · 5H ₂ O 6.70 | 10.0 | THPTA 13.4 | NMP/H ₂ O, 1:1 | 20 → 35 |
| I | Fluo 1.10 | 8 1.00 | CuSO ₄ · 5H ₂ O 6.70 | 10.0 | BTAA 13.4 | DMSO | 20 |
| J | Fluo 1.00 | 6 1.20 | CuSO ₄ · 5H ₂ O 6.70 | 10.0 | THPTA 13.4 | MeOH/PBS, 4:1 | 20 |
| K | Fluo 1.00 | 7 1.50 | CuSO ₄ · 5H ₂ O 6.70 | 10.0 | THPTA 13.4 | MeOH/PBS, 4:1 | 20 |
| L | Fluo 3.00 | 6/7 1.00 | CuSO ₄ · 5H ₂ O 20.0 | 25.0 | THPTA 13.4 | MeOH/PBS, 4:1 | 20 |
| M | BAz 3.00 | 6 1.00 | CuSO ₄ · 5H ₂ O 20.0 | 25.0 | – | MeOH/PBS, 4:1 | 20 |
| N | Fluo 1.10 | 6 1.00 | CuSO ₄ · 5H ₂ O 0.05 | 0.50 | – | MeCN/PBS, 1:1 | 20 |
| O | Fluo 1.50 | 1/3/6 1.00 | CuSO ₄ · 5H ₂ O 6.67 | 10.0 | THPTA 13.4 | MeOH/Gua · HCl, 1:4.3 | 20 |
| P | 11 1.00 | Pra/hPra 1.00 | CuSO ₄ 4.00 | 1.00 | DIPEA 8.00 | MeOH/H ₂ O, 2.8:1 | 20 |
| Q | 11 1.00 | 6/Pra/ hPra 3.00 | CuSO ₄ 6.70 | 10.0 | THPTA 13.4 | MeOH/PBS, 4:1 | 20 |
| R | Fluo 1.10 | 6/8 1.00 | CuSO ₄ · 5H ₂ O 6.70 | 10.0 | BTAA 13.4 | MeOH/PBS, 4:1 | 20 |
| S | Fluo 1.50 | 1/3/ 4/6 1.00 | CuSO ₄ · 5H ₂ O 6.70 | 10.0 | BTAA 13.4 | MeOH/Gua · HCl, 1:4 | 20 |
| T | Fluo 1.50 | 1/3/4 1.00 | CuSO ₄ · 5H ₂ O 6.67 | 10.0 | BTAA 13.4 + PEG 8000 | MeOH/Gua · HCl, 1:4.3 | 20 |

The catalytic active copper species in CuAAC reactions is Cu(I). Since now Cu(II) was added as $\text{CuSO}_4 \cdot 5\text{H}_2\text{O}$ to the reaction, reduction to Cu(I) using NaAsc was necessary. A possible explanation why the *click* reaction would not proceed was, that the active copper species might be too unstable in the given surrounding. Therefore, tris(3-hydroxy-propyltriazolylmethyl)amine (THPTA) was added as ligand (Figure 2.14, left), which binds and thus stabilises Cu(I) to increase product formation.^[108,114,115] While keeping the remaining conditions constant, addition of five equivalents THPTA to the *click* reaction of Fluo-Azide and peptide 4 was tested (Table 2.1, C). Via HPLC analysis a small, new signal was observed with absorption at 488 nm, whereas the main compounds remained Fluo-Azide and 4. After isolation of this compound CD-measurement was conducted, revealing no peptidic character. Then, Ca^{2+} -dependent fluorescence measurements were performed, which exhibited no Ca^{2+} -dependent increase of fluorescence. Hence, the formed substance seemed to be decomposed sensor.

Another reason for the lack of starting material conversion to product might be that the energy barrier of the reaction is too high for the existing system to overcome. If that is the case input of energy in form of elevated in temperature should solve this difficulty. Therefore, peptide 4 and Fluo-Azide were again treated with $\text{CuSO}_4 \cdot 5\text{H}_2\text{O}$ and NaAsc in methanol and water and shaken over night at 35 °C (Table 2.1, D). The HPL-chromatogram of this reaction showed the same outcome as when the ligand THPTA was added, yielding just starting material with small amounts of degraded sensor.

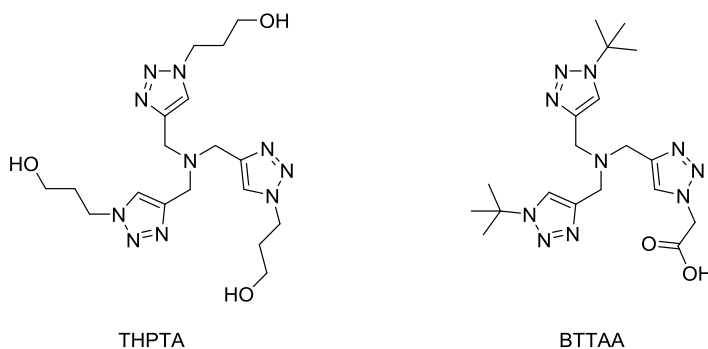
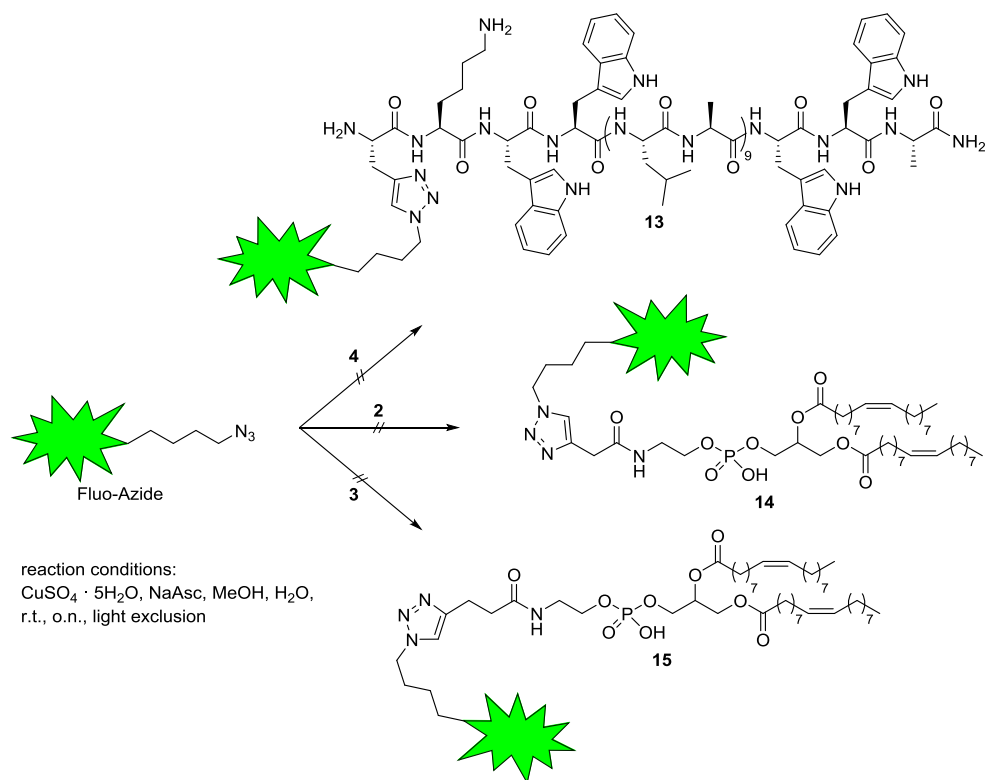


Figure 2.14 Chemical structure of *click* ligands THPTA and BTAA.



Scheme 2.5 Click reaction of 2/3/4 with Ca^{2+} sensor Fluo-Azide using $\text{CuSO}_4 \cdot 5\text{H}_2\text{O}$ and NaAsc.

A combination of heating and admixture of THPTA was tested as well together with a slight excess of peptide 4 (1.40 eq.). At first the reaction with 4 and Fluo-Azide was started at r.t. and without THPTA addition but with admixing of a few drops of trifluoroethanol (TFE) for enhanced solubility of 4 (Table 2.1, E). The reaction was shaken for 24 h and monitored via analytical HPLC. Since after one day no reaction took place, THPTA was added and the reaction mixture heated to 38 °C. After 32 h no conversion was observed and the reaction was stopped.

Another possibility to overcome the energy barrier was the usage of microwave assisted coupling. Fmoc-protected peptide 6 and Fluo-Azide were dissolved in DMF, NaAsc and $\text{CuSO}_4 \cdot 5\text{H}_2\text{O}$ in water were added. The mixture was heated three times over 5 min to 80 °C by applying 25 W (Table 2.1, F). As this approach led to no product formation as well, it could be shown, that the energy barrier is not the limiting factor.

Next, the equivalents were varied. The amount of copper sulphate was reduced by roughly 33 % and NaAsc by about 40 %. Using methanol and water as solvents and shaking at r.t. yielded no product formation. Therefore, the reaction was heated to 35 °C and shaken for further 24 h (Table 2.1, G). HPLC monitoring revealed formation of a new compound with a slightly lower retention time than peptide 4, which and showed absorption at 488 nm (Figure 2.15).

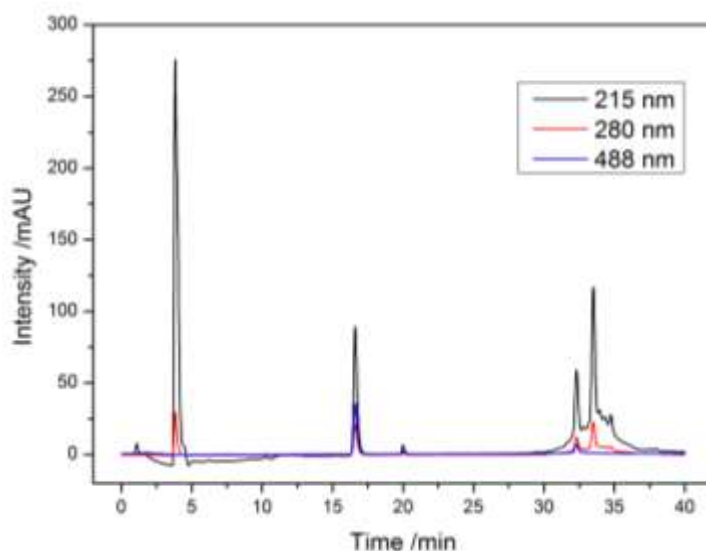
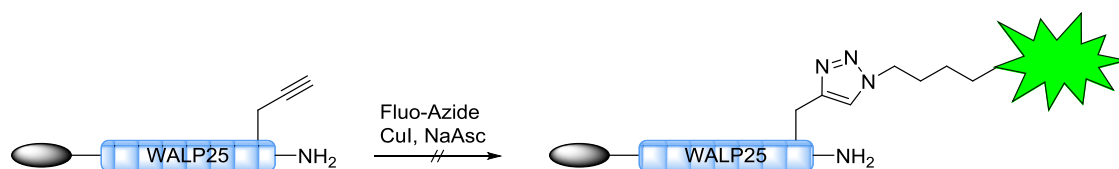


Figure 2.15 HPL-chromatogram of **4** with Fluo-Azide at 38 °C with addition of THPTA after 32 h.

The isolated compound showed no Ca²⁺ dependency, therefore, it can be excluded that the desired product was formed. A possible reason is that some kind of binding between **4** and Fluo-Azide occurred while the ability to bind Ca²⁺ was lost.

To analyse the influence of solvents a mixture of NMP, which proved to be beneficial for coupling of pro-gargyl glycine, and water (1:1, v/v) was tested (Table 2.1, **H**). After 24 h at r.t. no conversion was observed. Therefore, the temperature was increased to 35 °C. The reaction was stopped after 72 h, when no further change was detected via HPLC. Utilising NMP instead of MeOH as organic solvent led to formation of the same new signal, as depicted in Figure 2.15. Another tested solvent was DMSO in combination with another, possibly more potential, ligand. 2-(4-((bis((1-tert-butyltriazol-4-yl)methyl)amino)methyl)triazol-1-yl)acetic acid (BTAA) was found to accelerate CuAAC reactions in comparison to THPTA, increase the Cu^{II}/Cu^I redox potential and reduce potential oxidative side reactions, e.g. on amino acid side chains.^[109,115] Conditions stated in Table 2.1, **I** were applied. Even usage of BTAA and shaking for 24 h could not lead to successful conversion.

Another possibility for *click* reactions with peptides is to conduct the labelling on resin.^[116,117] The coupled peptide is left on a resin instead of been cleaved and isolated. The peptide **4** (1.00 eq.) on resin was swollen in a BD-syringe and treated with Fluo-Azide (1.20 eq.), CuI (5.00 eq.) and NaAsc (5.00 eq.). The mixture was shaken at r.t. over night, followed by washing of the resin, drying under vacuum and subsequent cleavage of the peptide (**GP1.3**). This reaction was performed in DMF and in NMP, but in both cases unreacted peptide **4** was obtained.



Scheme 2.6 Click reaction of WALP25 **4** on resin.

Another *click* attempt on resin was conducted using DMF but using 1.00 eq. of Fluo-Azide, 6.79 eq. of *N*-terminal Fmoc-protected **4** on resin, 7.54 eq. CuI and 9.03 eq. NaAsc. All compounds were placed in a micro reaction vessel, evacuated and flooded with argon. Anhydrous DMF was added and the reaction vessel was carefully shaken for two hours. The resin was thoroughly transferred into a BD-syringe and after washing and drying *in vacuo* the peptide was cleaved via **GP1.3**. HPLC and mass spectrometry revealed no formation of product.

Since no conversion took place, the system was changed back to liquid phase reactions. So far, when the applied solvent system was changed, it was the organic fraction, which was altered. To verify that a specific pH range was maintained, the water fraction was exchanged by different buffer systems. The first buffer tested was a phosphate-buffered saline (PBS), consisting of NaCl (137 mM), KCl (2.7 mM) and phosphate (10 mM) at pH 7.4. The applied conditions are listed in Table 2.1, **J–L**, and reaction time was 24 h for every reaction. The reaction conditions shown in row **L** were used as well to test applicability of an ultrasonic bath over 4 h for 1,3-dipolar cycloaddition. As alkynes the peptides **6** and **7** were used fully deprotected as well as *N*-terminal Fmoc-protected. With these short model peptides potential interfering effects of side chains like lysine or close proximity of tryptophan were supposed to be ruled out. Utilisation of Fmoc-protected peptides additionally masked the *N*-terminus. Copper ions might build complexes via coordination by free amino functionalities and thereby are no longer available anymore for *click* chemistry. Nevertheless, elimination or masking of the respective amino groups did not lead to product formation.

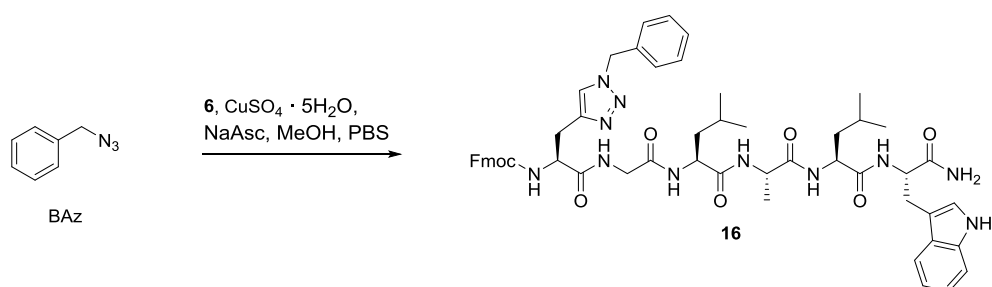
To rule out the possibility that too many copper-ions are available and therefore inhibit the desired reaction^[111,118], reduction of the applied CuSO₄ · 5H₂O to catalytic amount was tested. Peptide **6** was dissolved in MeCN and ultrapure water (1:1, v/v) and degassed with helium over 30 min. CuSO₄ · 5H₂O and NaAsc were dissolved in water, Fluo-Azide in MeCN was added and the reaction vessel shaken over night (Table 2.1, **N**). Monitoring via HPLC showed no conversion of the starting material, hence the copper concentration could successfully be excluded as potential reason for no conversion.

The next step was to revise whether 1,3-dipolar cycloaddition will take place using a simplified system. The sensor was substituted with benzyl azide (BAz) and brought to

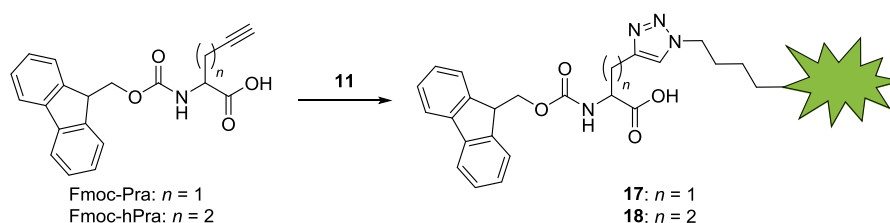
reaction with Fmoc-protected **6** (Scheme 2.7, Table 2.1, **M**). After 24 h the reaction was stopped and analysed via HPLC and mass spectrometry. The obtained HPL-chromatogram showed appearance of a new signal. ESI-MS of the isolated compound revealed that indeed *click* product (**16**) was generated, proving that CuAAC is possible with Fmoc-protected **6**. As *click* reactions using Fluo-Azide in previous work^[13] and the cycloaddition of BAz to **6** were successfully performed, an interaction between Fluo-Azide and the respective peptide seems to inhibit the formation of product.

Since the in Scheme 2.7 depicted conditions yielded no product formation when applied to Fluo-Azide, further screening was necessary. Therefore, another buffer was tested. A guanidine hydrochloride buffer (Gua · HCl) was selected consisting of guanidine hydrochloride (6 M), disodium phosphate (0.2 M) and tris(2-carboxyethyl)phosphine hydrochloride (TCEP · HCl, 30 mM) and used at pH 7.3. Gua · HCl is known to denature proteins and inhibit nucleobases while very hydrophobic proteins remain naturred.^[119] Applying the conditions shown in Table 2.1, **O**, to *click* Fmoc-protected **6** and Fluo-Azide did not lead to triazol formation, which demonstrates that the used buffer does not represent the decisive factor.

To evaluate whether application of *click* chemistry to Fluo-Azide in combination with peptides or amino acids is possible in general, cycloaddition with the Fmoc-protected amino acids propargyl glycine (Fmoc-Pra) and homopropargyl glycine (Fmoc-hPra) was sought of. Simultaneously, potential disturbance by the carboxylic acid groups of the sensor was avoided by utilising the methyl ester carrying sensor precursor **11** (Scheme 2.8). The respective amino acid and Fluo-Azide were treated with CuSO₄ and NaAsc in MeOH and water. DIPEA was added and the reaction vessel shaken for 24 h (Table 2.1, **P**).^[120] Since even cycloaddition with the amino acids did not precede using DIPEA as base, the MeOH/buffer system with ligand as additive was tested. The conditions shown in Table 2.1, **Q** were applied to both amino acids and the reactions shaken for 24 h. No full conversion took place but for both amino acids the desired products **17** and **18** were detected in mass spectrometry and purified via HPLC.



Scheme 2.7 Successful *click* reaction using benzyl azide (BAz) and Fmoc-protected **6**.



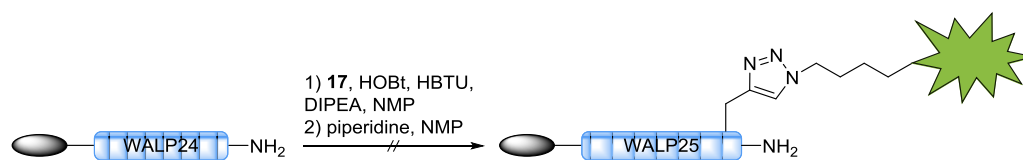
Scheme 2.8 HUISGEN reaction of azide **11** and alkyne Fmoc-Pra or Fmoc-hPra.

After successfully coupling Fmoc-Pra and Fmoc-hPra with sensor precursor **11** via *click* reaction, the same conditions were used to label Fmoc-protected peptide **6**. Despite masking of amines and usage of **11**, containing no free carboxylic acids, the cycloaddition would not proceed.

With the labelled amino acids **17** and **18** in hand but unable to *click* precursor **11** directly to a peptide, incorporation of **17** into a peptide on resin via standard coupling conditions (**GP1.1**) was sought of (Scheme 2.9). This synthetic route was highly unfavourable since the valuable labelled amino acid had to be utilised in excess of five equivalents. Furthermore, after coupling the methyl ester had to be cleaved, which might degrade the peptide, due to the harsh conditions, necessary. Nevertheless, using standard coupling conditions and NMP as solvent **17** was added to WALP24 **5** on swollen resin in a BD-syringe. The reaction vessel was shaken for one hour, *N*-terminal Fmoc removed and the peptide cleaved from resin (**GP1.3**). Analysis of the resulting peptide revealed no product formation, but cleaved WALP24 **5** was not detected either.

Since coupling attempts of **17** were unsuccessful, the strategy was changed again. The new ligand BTAA was tested for peptides **6** and **8** using the conditions shown in Table 2.1, **R**, and conditions **S** for peptides **4** and **6**. Again, no conversion occurred, which is why the focus shifted from peptide labelling towards lipid labelling.

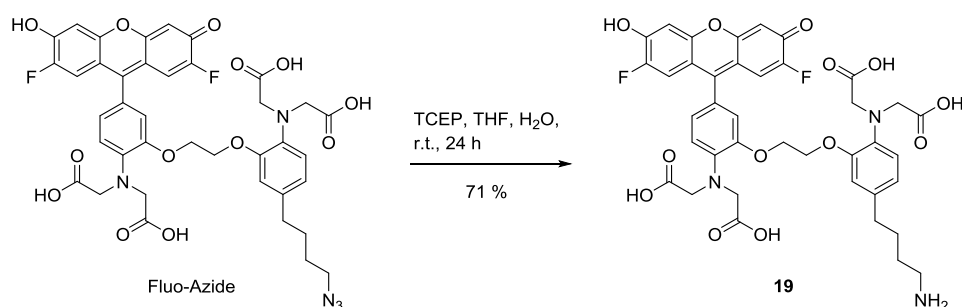
Applying condition **O** (Table 2.1) to cholesteryl derivative **1** and DOPE derivative **3** yielded no product but changing to conditions **S** in the case of **3** a new signal appeared in HPLC. Analysis via Ca²⁺-dependent fluorescence measurements and mass spectrometry revealed no product but degraded Fluo-Azide. Due to the fact that a test reaction of alkyne-modified PEG5000 with Fluo-Azide worked nicely, it was reviewed whether addition of unmodified PEG might be of assistance in this *click* reaction set up (Table 2.1, **T**). However, after addition of PEG5000 no reaction at all had taken place.



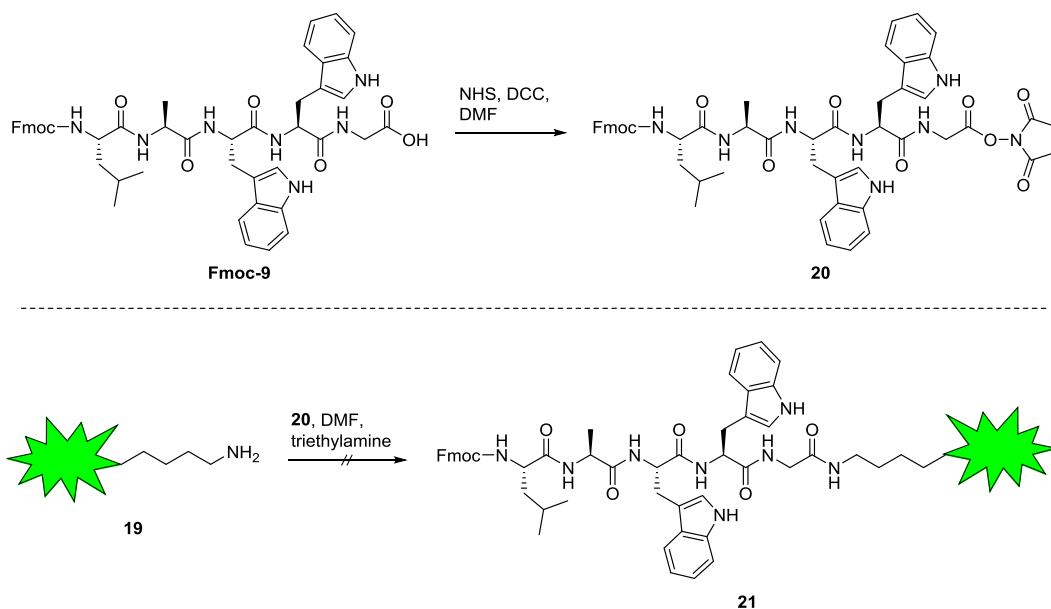
Scheme 2.9 Coupling attempt to incorporate labelled amino acid **17** via standard peptide synthesis.

Another approach to label membrane components instead of CuAAC was sought. The azide moiety of Ca²⁺ sensor Fluo-Azide is readily reducible to generate a primary amine, which can then be coupled via amide-bond formation. For azide reduction Fluo-Azide was treated with TCEP in THF and water and shaken over 24 h. Removal of solvents and isolation using HPLC yielded pure amine **19** (Scheme 2.10). As counterpart for the desired coupling reaction a short peptide (**9**) was synthesized and activated as NHS-ester (Scheme 2.11, top). For coupling **9** and **19** were dissolved in anhydrous DMF and treated with triethylamine for 24 h (Scheme 2.11, bottom). After solvent removal the labelled test-peptide **21** was not obtained.

As this variety of labelling attempts all proved to be unsuccessful, one last effort was conducted. In 2014 SIMERSKA *et al.* published their work on construction of self-adjusting lipopeptides using i.a. CuAAC reactions.^[121] They reported complete conversion after one hour under utilisation of copper wire in DMF. At first these conditions were tested on **4** and **6**. The peptides were dissolved in DMF along with Fluo-Azide in a micro reaction vessel. A piece of copper wire (approximately 0.7 g wire per 0.1 μmol sensor) was formed into a spiral, put inside the reaction vessel, and the reaction was shaken under light exclusion. To begin with, the reaction was conducted at 45 °C with occasional vortexing. Since no reaction was detectable after two hours, the temperature was increased to 50 °C. Even after three days no conversion took place in the case of WALP25 **4**. But using Fmoc-protected **6** a small new signal was observed by HPLC-monitoring after 17 h showing absorption at 488 nm. However, even after three days the newly formed signal would not increase. With these results, no further efforts to label peptides were performed.



Scheme 2.10 Azide reduction using TCEP to obtain amine **19**.



Scheme 2.11 Activation of the test-peptide **9** as NHS-ester (top); Coupling attempt with **19** (bottom).

On the other hand, when these conditions were applied to the modified DOPE **3** and cholesterol **1** full conversion of the sensor was achieved after 17 h at 50 °C (Figure 2.16). Measurement of ESI-MS showed no product but using MALDI as ionisation technique with sinapinic acid as matrix formation of both labelled compounds **15** and **22** was verified.

To control whether the fluorescence and therefore the Ca²⁺-binding performance is still intact after binding the sensor to **1** or **3**, Ca²⁺-dependent fluorescence measurements were conducted (Figure 2.17 and Figure 2.18). For both compounds (**15** and **22**) intact fluorescence compartment via Ca²⁺-binding was observed. These labelled membrane components can now easily be incorporated into model membrane to study membrane interaction, i.e. SNARE mediated membrane fusion.

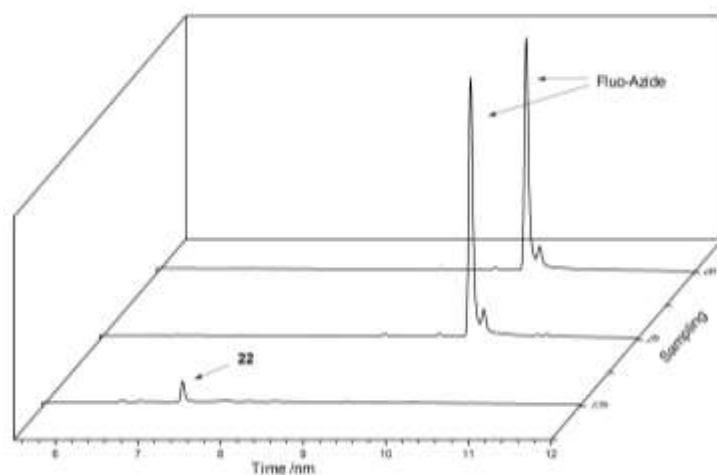


Figure 2.16 Progress of *click* reaction using **1** and Fluo-Azide; HPL-chromatograms of the reaction mixture after 0 h, 2 h and 17 h with normed intensity.

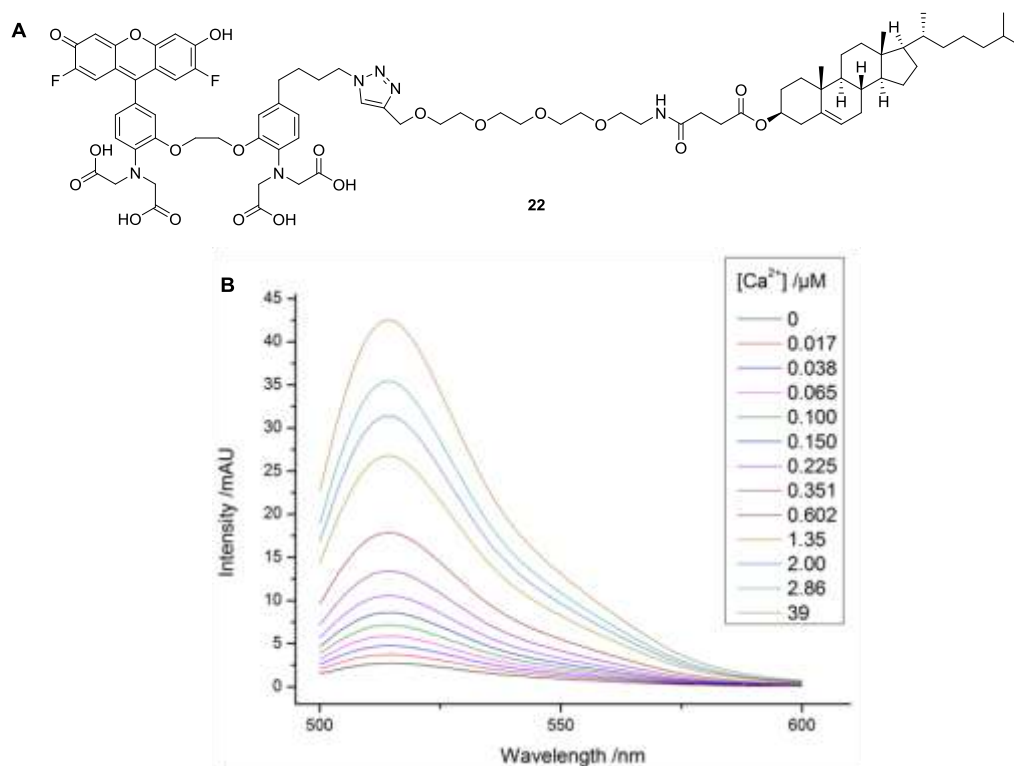


Figure 2.17 Chemical structure of the Fluo-Azide-labelled cholesterol derivative **22** (A); Ca^{2+} -dependent fluorescence measurements of **22** (B).

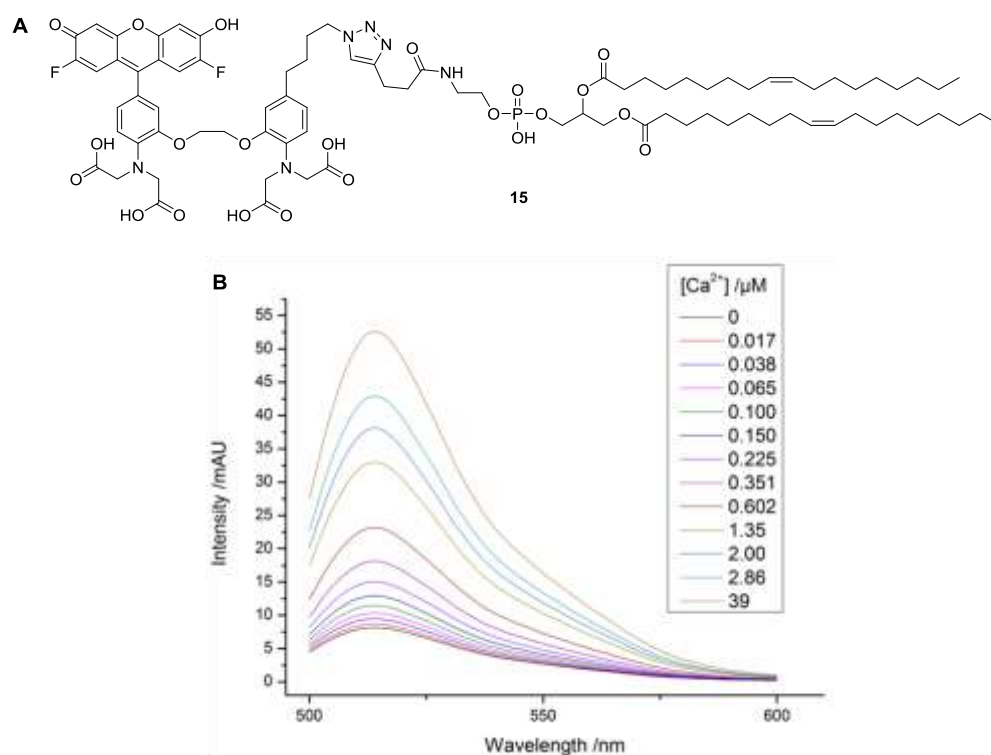


Figure 2.18 Chemical structure of the Fluo-Azide-labelled DOPE derivative **15** (A); Ca^{2+} -dependent fluorescence measurements of **15** (B).

Due to the high sensitivity of Fluo-Azide towards Ca^{2+} , the labelled compounds **15** and **22** are well applicable for systems or cell compartments with low Ca^{2+} concentrations. But when the amount of available Ca^{2+} is too high, all Fluo-Azide molecules are saturated and a further increase in Ca^{2+} quantity cannot be detected. For such systems a sensor with lower Ca^{2+} affinity, like the X-Rhod-Azide, is preferable. Therefore, the X-Rhod-Azide sensor was used for *click* reaction as well. The respective alkyne (**1** or **3**) and X-Rhod-Azide were dissolved in DMF in a micro reaction vessel. A spiral of copper wire was added and the mixture shaken at 50 °C for 17 h. When letting the cholesterol derivative **1** react with the sensor longer reaction times of 24 h were necessary but still complete consumption was not achieved. In case of the lipid derivative **3** the reaction was complete after 17 h. The isolated labelled lipid **23** was used for Ca^{2+} -dependent fluorescence measurements to verify its binding properties (Figure 2.19).

After successful synthesis of the labelled compound **23** it can be used for a variety of Ca^{2+} -dependent measurements, if rather high Ca^{2+} concentrations are present.

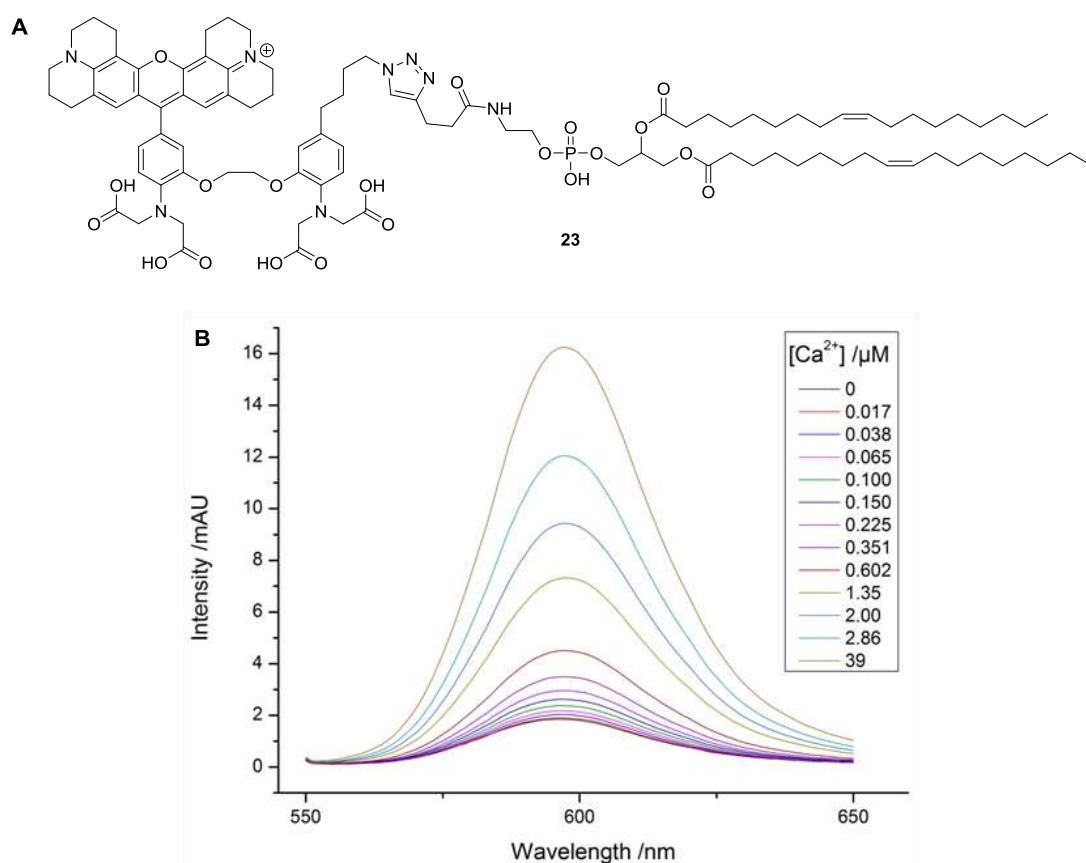


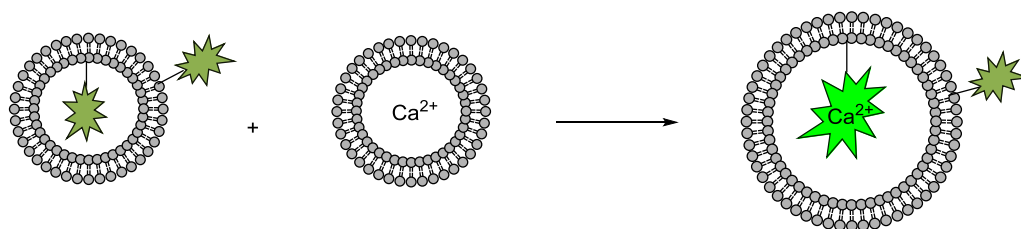
Figure 2.19 Chemical structure of the X-Rhod-Azide-labelled DOPE derivative **23** (A); Ca^{2+} -dependent fluorescence measurements (B).

2.6 Application of Ca^{2+} Sensor-Labelled Lipids

2.6.1 Analysis of SNARE-mediated Membrane Fusion using Labelled Lipids

A problem of many fusion assays is the differentiation of hemi-fusion and full-fusion or even just aggregation. One major aspect of this difficulty is the potential of leakage, which can, depending on the applied fluorescence system, lead to false positive results. Furthermore, dye-loaded vesicles tend to disrupt in case of strongly differing osmolalities of the vesicles interior and the surrounding solution. Since Ca^{2+} is thought to be crucial for membrane fusion in living systems^[26,29,122–124], developing a Ca^{2+} -dependent fluorescence system to detect full-fusion of membranes or vesicles might prove to be useful.

To overcome the obstacles of established assays for detection of membrane fusion while respecting the importance of cellular Ca^{2+} , a new assay was designed. This method uses the Ca^{2+} sensor-labelled cholesterol derivative **22**, due to the high sensitivity of Fluo-Azide towards Ca^{2+} ions. Two species of model membranes in form of large unilamellar vesicles (LUVs) are supposed to be generated, with **22** incorporated into the membrane of one species and Ca^{2+} ions filled in the lumen of the other species (Scheme 2.12). For fusion of the vesicles artificial SNARE analoga are to be applied. To follow the fusion process fluorescence measurements are to be conducted, since only in case of full-fusion, which means that the contents of the vesicles mix, Ca^{2+} ions and the sensor Fluo-Azide come in contact to increase fluorescence. The advantage of this type of content mixing experiment is that it remains unaffected by leakage. In contrast, self-quenching systems yield in fluorescence increase upon vesicle fusion as well as leakage and are therefore sensitive towards false-positive results.



Scheme 2.12 Schematic illustration of the experimental setup, leaving out SNARE proteins and potential further fluorophores.

The lipid system used as the model membrane consisted of 1,2-dioleoyl-*sn*-glycero-3-phosphocholine (DOPC), DOPE and cholesterol (Chol) in the ratio DOPC/DOPE/Chol = 50:25:25, which is the standard lipid system utilised in our work group. Preparation of lipid films and LUVs was conducted following **GP2.1** and **GP2.2**. Before starting with fusion experiments, it was tested whether the labelled compound **22** will show the same Ca^{2+} -dependent fluorescence when incorporated into a model membrane than in solution. Vesicles containing **22** were prepared with a ratio of labelled to unlabelled lipids of 1:75, resulting in a rather high density of the Ca^{2+} sensor. Measuring Ca^{2+} -dependent fluorescence using these labelled vesicles, however, showed no change in fluorescence dependency or emission wavelength (Figure 2.20). Hence, the possibility of self-quenching of the sensor was ruled out.

Since incorporation of labelled cholesterol **22** into a model membrane did not alter the performance of the sensor, vesicle fusion experiments could be performed. The first applied SNARE system for vesicle fusion was developed and synthesised in our work group by B. HUBRICH. The SNARE peptides are modified with a PNA recognition domain. The backbone of the PNA consists of repeating *N*-(2-aminoethyl)-glycine (aeg) units. In this case PNA1s-synaptobrevin and PNA3s-syntaxin were chosen (Figure 2.21). In previous work full-fusion using these SNARE analoga was achieved, while the peptide-containing vesicles seemed to remain stable over hours without aggregation or disintegration observable. Nevertheless, the best results were obtained when the fusion experiments were conducted immediately after extrusion (unpublished results by B. HUBRICH).

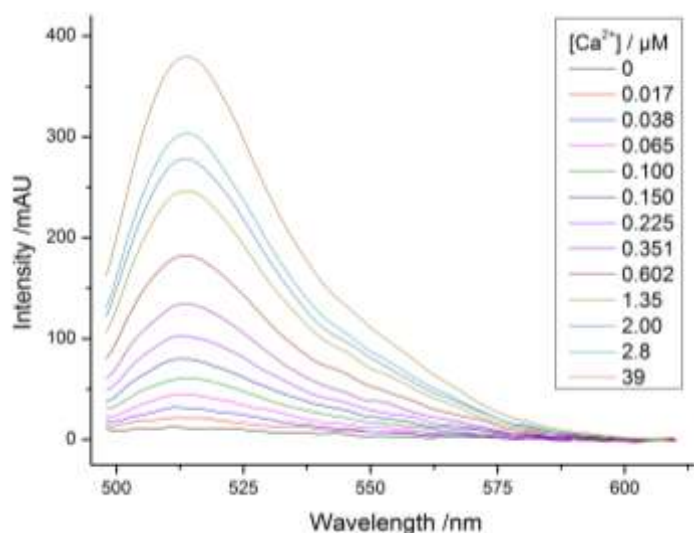


Figure 2.20 Ca^{2+} -dependent fluorescence measurements of labelled vesicles with **22** incorporated.

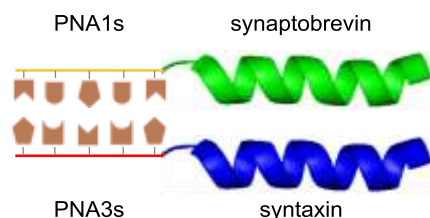


Figure 2.21 Schematic representation of the SNARE-peptides with PNA recognition units. The chemical structure of the PNA-SNARE peptides is not shown due to the unpublished status.

For the first content mixing experiment three different vesicle species were generated, which all had the previously mentioned lipid composition. Vesicle species **A** (**VA**) was labelled with **22** in the **22** to lipid ratio of 1:75 and with sulphorhodamine B-DOPE (0.75 mol-%). As SNARE the peptide PNA1s-synaptobrevin was incorporated in a peptide to lipid ratio of 1:200. Since for Ca^{2+} -dependent fluorescence measurements MOPS-buffers with zero free Ca^{2+} (buffer **A**, 30 mM MOPS, 10 mM EGTA, 100 mM KCl, pH 7.2) and 39 μM free Ca^{2+} (buffer **B**, 30 mM MOPS, 10 mM CaEGTA, 100 mM KCl, pH 7.2) were used (see chapter 2.5.2), these buffers were chosen for monitoring vesicle fusion via fluorescence as well.

Prior to vesicle preparation the osmolality (b_{osm}) of the utilised buffers was measured to ensure vesicle stability. The osmolalities detected were nearly identical for both buffers ($b_{\text{osm}}(\mathbf{A}) = 0.272 \text{ osmol/kg}$; $b_{\text{osm}}(\mathbf{B}) = 0.275 \text{ osmol/kg}$). Hence, a buffer exchange should not lead to disruption of the prepared vesicles.

For extrusion of **VA** buffer **A** was utilised. To inhibit Ca^{2+} -binding by the sensors on the outer membrane leaflet, the vesicles were treated with an aqueous solution of MnCl_2 . Mn^{2+} is bound by the BAPTA moiety with significantly higher affinity than Ca^{2+} , which inhibits binding of Ca^{2+} . Since complexation of Mn^{2+} by BAPTA does not block PET, the fluorescence intensity decreases drastically in comparison to the Ca^{2+} -bound complex. For verification a fluorescence measurement of the vesicles **VA** treated with Mn^{2+} was conducted (Figure 2.22). The vesicles were added to Ca^{2+} -containing buffer **B** and the fluorescence intensity was detected over 60 s. Then, Mn^{2+} was added to check the time needed for Mn^{2+} to quench the fluorescence as well as the amount of fluorescence decrease. After addition of Mn^{2+} an instant drop in fluorescence intensity was observed.

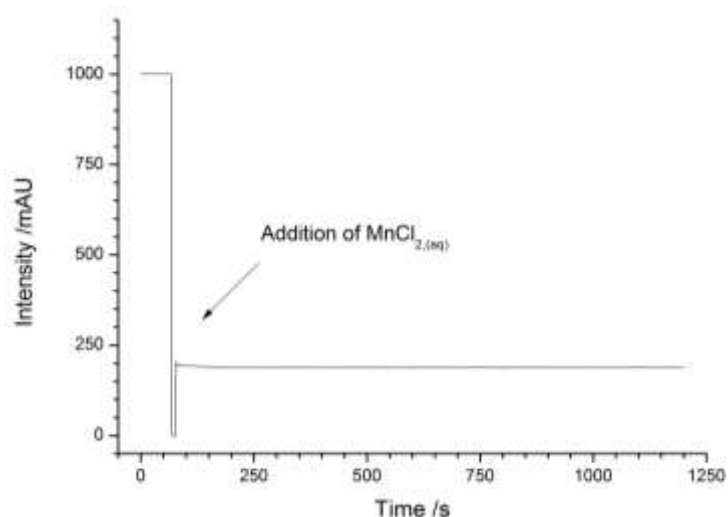


Figure 2.22 Fluorescence measurement of vesicle species **VA** containing labelled cholesterol **22**. Addition of Mn^{2+} after 60 s showed significant decrease in fluorescence intensity.

To remove excessive Mn^{2+} ions from the **VA**-containing solution size-exclusion chromatography using *Sephadex G-50 fine* was conducted, which is why sulphorhodamine B-DOPE was included into the lipid mixture. By means of the pink colour of sulphorhodamine B the movement of the vesicles on the column could be observed. The pure vesicles **VA** were obtained in Ca^{2+} and Mn^{2+} -free buffer **A**. The second vesicle species **VB** was labelled with the same amount of sulphorhodamine B-DOPE as **VA** and as SNARE peptide PNA3s-syntaxin in the peptide to lipid ratio of 1:200 was added. Swelling of the lipid film and extrusion were conducted using buffer **B** to fill the vesicles with Ca^{2+} . To obtain Ca^{2+} -free surroundings a buffer exchange of the vesicles **VB** to buffer **A** was performed by size-exclusion chromatography. The third vesicle species served as control vesicles (**CV**). It was labelled just with sulphorhodamine B-DOPE (0.75 mol-%) and extruded in Ca^{2+} -free buffer **A**. For all three vesicle species the total lipid concentration was adjusted to $0.625\ \mu\text{M}$ prior to extrusion.

To analyse sensor–sulphorhodamine B interactions a solution of 60 nmol Fluo-Azide in 1.3 mL buffer **B** was treated with an aqueous solution of sulphorhodamine B (0.5 mM). As shown in Figure 2.23, at low fluorophore concentrations no disturbance of sensor fluorescence occurred. After further addition of sulphorhodamine B the sensor intensity decreased and a new emission band appeared. When Fluo-Azide was treated with an excess of sulphorhodamine B the sensor band vanished while the sulphorhodamine B band with a maximum at 587 nm increased. From these measurements it was concluded that the influence of sulphorhodamine B on the sensor fluorescence was negligible when low fluorophore concentrations were applied.

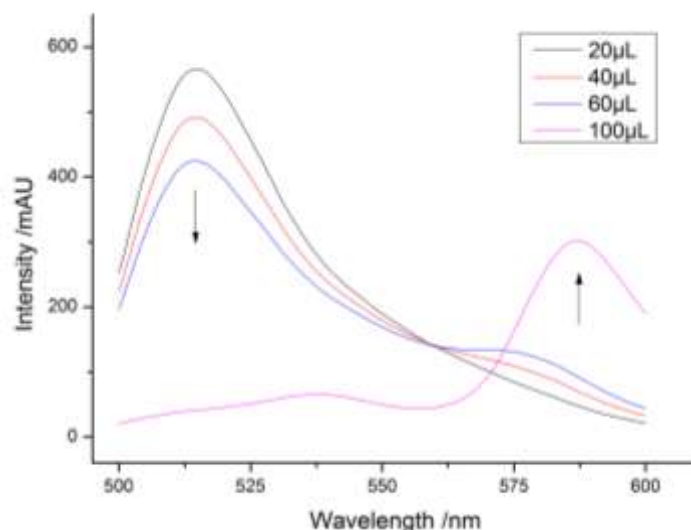


Figure 2.23 Interaction between Fluo-Azide and sulphorhodamine B shown on the basis of Ca^{2+} -dependent fluorescence of Fluo-Azide.

After these preparations and pretests fusion experiments were conducted. Vesicles **VA** (72 μL) and buffer **A** (1.11 mL) were filled into a stirrable fluorescence cuvette and after one minute vesicle species **VB** (169 μL) was added, which equates a **VA/VB**-ratio of 1:4 relating to the vesicle concentrations. As can be seen in Figure 2.24, no increase in fluorescence intensity was detected, meaning that no fusion took place. Since no change occurred, **VA** solution (216 μL) was added after 4.5 min to yield a 1:1-ratio. The fluorescence intensity was observed for another 9 min but still no fusion occurred. Therefore, to destroy the vesicles the solution was treated with Triton X-100 (10 % (v/v) in ultrapure water). This led to a small but steady increase of fluorescence intensity, which did not alter after further addition of Triton X-100. The marginal increase can easily be explained by the fact that the only Ca^{2+} ions available to induce fluorescence were within the **VB** vesicles. After disrupting the vesicles the rather high concentrated (39 μM) Ca^{2+} was diluted in the much bigger Ca^{2+} -free buffer volume, leading to a small fluorescence increase. To gain the maximum possible fluorescence intensity, concentrated aqueous CaCl_2 solution was added to enhance the Ca^{2+} concentration, resulting in a distinct fluorescence increase. A second addition of CaCl_2 yielded a slight decrease in fluorescence, probably due to dilution, and another addition of Triton X-100 led to another minor intensity increase.

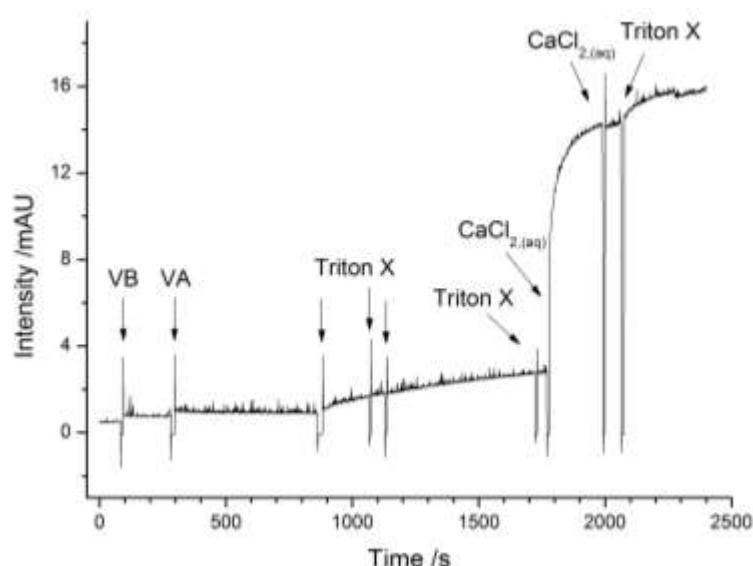


Figure 2.24 Fusion experiment using the SNARE-analoga PNA1s-synaptobrevin and PNA3s-syntaxin with a total lipid concentration of $0.625 \mu\text{M}$. The arrows mark the point of which the indicated reagents were added.

Since the fluorescence intensity was rather low during this first fusion experiment, the total lipid concentration during lipid film preparation was increased to $2.5 \mu\text{M}$. Furthermore, a change in buffer system was performed. Since the previously used MOPS-buffers were utilised for Ca^{2+} -dependent fluorescence measurements, it seemed consequential to test them for fusion experiments, too. The applied standard buffer for fusion assays in our work group was a HEPES-buffer, consisting of 20 mM HEPES, 1 mM EDTA, 100 mM KCl, pH 7.4 (buffer C). For preparation of a Ca^{2+} -containing buffer CaCl_2 was added to the HEPES buffer to adjust the Ca^{2+} concentration to 0.1 mM (buffer D). Again, the osmolality was revised and nearly identical values were obtained ($b_{\text{osm}}(\text{C}) = 0.200 \text{ osmol/kg}$; $b_{\text{osm}}(\text{D}) = 0.203 \text{ osmol/kg}$). Applying these changes the procedure remained otherwise as mentioned before. After extruding the PNA3s-syntaxin-containing vesicles (VB), immediately a white precipitate occurred, indicating aggregation of the vesicles and therefore making them unresponsive towards fusion. Nevertheless, a fusion attempt was performed but no successful fusion occurred. Even though the desired goal was not obtained, important information was reasoned: the influence of sulphorhodamine B on the sensor fluorescence, which was thought to be negligible, seemed to be great enough to disturb the fluorescence intensity. Sulphorhodamine B appeared to form Ca^{2+} complexes, thereby decreasing the amount of sensor- Ca^{2+} complexes and hence the fluorescence intensity as well.

To avoid the obstacles of aggregating vesicles and disturbed data by sulphorhodamine B the system was altered. The total lipid concentration of the stock solution was reduced to $1.25 \mu\text{M}$ and no sulphorhodamine B-DOPE included. Without the fluorophore included no buffer exchange was performed. To avoid interference of fusion by Mn^{2+} , which could not be removed by size exclusion chromatography as

well, the sensor molecules on the outer leaflet remained untreated with MnCl_2 . Leaving the outer sensors active, while no rebuffing of Ca^{2+} -containing vesicles into Ca^{2+} -free buffer is performed, will result in a considerable increase in fluorescence when the sensor-containing vesicles are mixed with the vesicles in Ca^{2+} -including buffer. Still fusion, if occurring, should be detectable since it is a slow process, while the fluorescence increase, caused by Ca^{2+} addition, occurs very fast.

The prepared vesicles **VA**, containing **22** and PNA1s-synaptobrevin, and Ca^{2+} -free HEPES buffer were given into a stirrable fluorescence cuvette and after 100 s treated with Ca^{2+} -containing (1 mM) HEPES buffer to saturate the sensor molecules on the outer membrane leaflet. After stabilisation of the fluorescence intensity, the vesicles **VB**, including PNA3s-syntaxin, were added. A significant fluorescence increase was observed but no fusion detected. The experiment was repeated without previous addition of Ca^{2+} but again, no vesicle fusion was ascertained.

Since no vesicle fusion had been achieved, the utilised SNARE-analoga were exchanged for a possibly more potent SNARE system, shown in Figure 2.25. The K3-/E3-SNARE-peptides are a well studied system and form a coiled-coil bundle to mediate membrane fusion.^[91] The proteins applied in this work were designed and graciously provided by J.-D. WEHLAND. Incorporation of the peptides was conducted likewise as before. Four vesicle species were prepared: **VA** containing **22** and E3-synaptobrevin in Ca^{2+} -free HEPES buffer, **VB** containing K3-syntaxin in 0.1 mM free Ca^{2+} HEPES buffer, **VC** containing **22** in Ca^{2+} -free HEPES buffer and control vesicles **CV** in 0.1 mM free Ca^{2+} HEPES buffer. Since vesicles decorated with K3-syntaxin are prone to aggregation, the **VB** vesicles were extruded last and immediately utilised for fusion experiments.

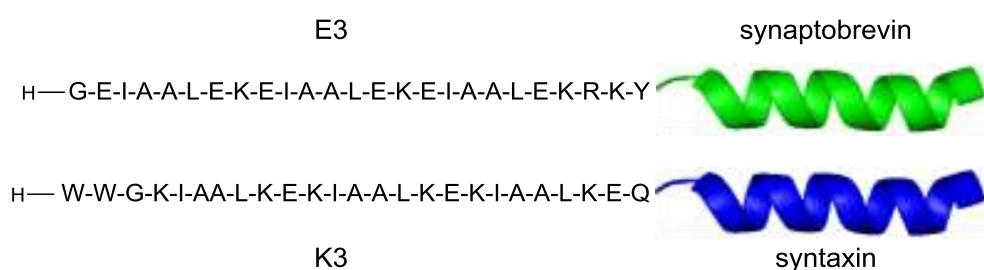


Figure 2.25 Primary structure of the recognition motif of the SNARE-analoga E3-synaptobrevin and K3-syntaxin.

To start the experiment a stirrable fluorescence cuvette was equipped with vesicles **VA** and Ca^{2+} -free buffer. After 145 s **VB** were added to obtain a **VA/VB**-ratio of 1:4. After the immediate and distinct increase of fluorescence intensity, due to addition of Ca^{2+} -containing buffer, a slower and slight fluorescence increase was observed (Figure 2.26, black curve). Addition of 1 mM free Ca^{2+} buffer after 500 s yielded no alteration in intensity, which indicates that all sensor molecules in the outer membrane leaflet are saturated with Ca^{2+} . Further appending of **VA** to gain a 1:1-ratio of **VA** and **VB** after 620 s resulted in a distinct and fast increase in fluorescence intensity due to the enhanced amount. Subsequently a light upward tendency of fluorescence intensity could be observed, which might be accounted by slow fusion processes. As expected, control experiments using **VB** with **VC** (red curve) or **VA** with **CV** (blue curve) showed no fluorescence increase, which could be referred to fusion processes.

Magnifying the curve after addition of **VB** showed a curve progression of restricted growth (Figure 2.27). Due to the very low fluorescence increase of this measurement the experimental outcome has to be treated with caution. It might hint that vesicle fusion occurred but further measurements are needed to confirm these results. Precisely, it is necessary to enhance the overall intensity so that changes in the fluorescence intensity can unequivocally be detected and assigned to fusion processes.

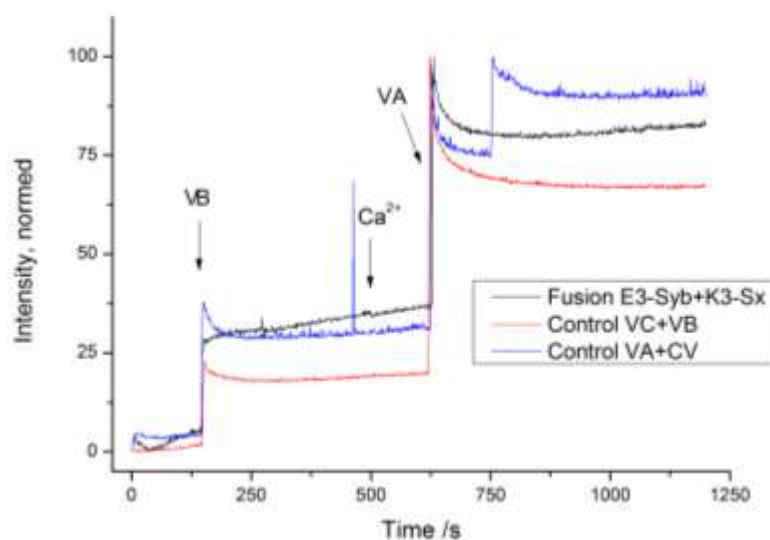


Figure 2.26 Fusion experiment using K3-syntaxin and E3-synaptobrevin (black curve) and control experiments with just one SNARE-species present (red and blue curves). The addition specifications shown refer to the black curve.

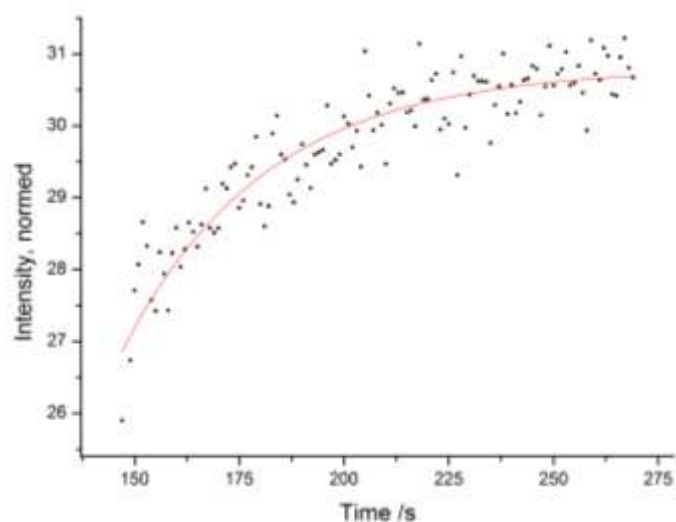


Figure 2.27 Magnified view of probable fusion curve (black curve in Figure 2.26) with fit line (red).

To establish this assay for membrane fusion measurements further enquiries have to be performed, which, unfortunately, could not be done in this work due to time limitations. These first experiments using the E3-synaptobrevin/K3-syntaxin system show promising results. With some refinements this assay will become a very useful and broadly applicable method to follow fusion processes, while taking the respective Ca^{2+} concentration into account.

3 Labelling of Lipids via 7-Azaindole

3.1 Introduction

The phenomenon of membrane fusion is omnipresent in living systems and even though a lot is known about this fundamental process, there is still a tremendous amount to learn regarding the involved molecules and the underlying mechanism.^[125] Via membrane fusion molecules are transported into and out of cells. This translocation is performed by encapsulation of the compounds as cargo and subsequent release by fusion into the target organelle or cell.^[75] For instance, enveloped viruses use the process of membrane fusion to insert their genome into host cells.^[75,125,126] One of the most prominent example for fusion processes is the fertilisation process by fusion of egg cell and sperm in order to create a new organism.^[75,82,105]

The fusion process in natural systems does not occur spontaneously. A highly complex and well-tuned fusion machinery was developed throughout time. In the 1980s, the evolutionary preserved SNARE proteins were discovered, which were identified as key components of this machinery.^[71] Besides these proteins, the composition of the membrane at the fusion site is a crucial factor. A rather rare but significant membrane lipid is phosphatidylinositol-4,5-bisphosphate (PIP₂). PIP₂ is not just a source for essential second messenger compounds^[14] but is required in the plasma membrane for fusion processes.^[16,17] The amount of PIP₂ is increased at the fusion site to form a domain also called raft of altered lipid constitution. To these rafts proteins (i.e. SNAREs) are bound and therefore the rate of vesicle priming is regulated, which includes the rearrangement and modifications of lipids and proteins under usage of ATP prior to fusion. Hence, the presence of PIP₂ is indispensable for active molecule transport, such as Ca²⁺-triggered neuronal exocytosis.^[16,17]

To verify the enrichment of PIP₂ and raft formation at the fusion site and to gain further insight into the fusion process, the ultimate goal of this project is to synthesise a fluorescent probe-labelled PIP₂. In order to develop a synthetic route the sterically and electrically less demanding phosphatidylcholine (PC) was chosen as first synthetic target. As fluorophore the well-studied and environment-sensitive 7-azaindole was selected and chemical modifications of 7-azaindole were performed to enable subsequent incorporation in model lipids for fluorescence measurements in membranes.

3.2 Raft Formation in Lipid Membranes

A basic requirement in biological systems is the separability from the environment. This boundary protects the organism of undesired substances and influences while enabling controlled permeability.^[6,127] Therefore, pH and electrical gradients in eukaryotic cells are maintained and due to membrane proteins the cell can react towards environmental changes or signals of other cells. The main components of membranes are lipids, which can reach a diversity of 500–2000 different lipid species.^[6] Lipids are amphiphilic molecules, containing a polar/hydrophilic head group and usually two non-polar/lipophilic alkyl chains. Via non-covalent interaction lipids form a double layer of approximately 5 nm thickness. In aqueous systems the polar head groups are located facing the environment or cytosol, while the non-polar chains lay within the membrane, protected against the polar solvent.^[6]

The first broadly accepted membrane model was the so-called ‘fluid mosaic’ model, published in 1972 by S. SINGER and G. NICOLSON. They described a homogeneous lipid bilayer for cell-membranes with anchored membrane proteins, that are freely diffusible within the membrane.^[128] Due to research progress, a few important modifications of the model were performed. Some of these findings are limited protein mobility owing to interactions with intra- or extracellular opponents, asymmetrical lipid composition of the bilayer and a drastic increase of protein density on the membrane surface.^[129] Furthermore, dependent on conditions as pressure and temperature a membrane can adopt different states. The solid ordered (S_o or gel) state mainly contains lipids with saturated fatty acids or unsaturated fatty acids in all-*trans* conformation, which increases the VAN DER WAALS interactions and allows a very high degree of order (Figure 3.1, left).^[127] The lateral movement is restricted and membrane rigidity enhanced.^[130–132] Rise in temperature over the lipid’s respective melting temperature (T_m) leads to phase transition from S_o to the liquid disordered (L_d) state (Figure 3.1, middle). In this fluid state the degree of order regarding the acyl chains and head groups is decreased, resulting in an expansion of the membrane (increased area per lipid by 15–30 %^[133]). Lipids and membrane proteins exhibit high lateral mobility in the bilayer. Addition of cholesterol to a bilayer in the L_d state changes the phase properties to generate the liquid ordered (L_o) state (Figure 3.1, right). The rigid and planar cholesterol molecules insert between the acyl chains and therefore impose conformational order comparable to the S_o state while barely restricting lateral mobility.^[130]

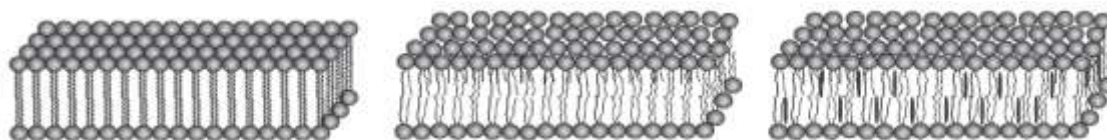


Figure 3.1 Lipid phases of membranes in aqueous medium, showing the solid-ordered (S_o , left), liquid-disordered (L_d , middle) and liquid ordered (L_o , right) state. Picture adapted from [134].

In natural systems the lipid membranes, like the plasma membrane, consist of a diversity of lipids with phospholipids as the dominating species. Further components are sphingolipids, like ceramides, sphingomyelins or glycosphingolipids, and sterols, such as cholesterol or ergosterol.^[132] The concentration ratio of the individual lipids influences the membrane properties as its thickness, curvature or the state of the membrane.^[127,135] Every lipid has a distinct T_m , while lipids with long and saturated hydrocarbon chains reveal high T_m , lipids with shorter or (*cis*-) unsaturated alkyl chains have lower T_m . Lowering the temperature leads to phase transition and separation of lipids with higher T_m to form ordered domains. Present cholesterol is enriched in these ordered domains and inhibits formation of a S_o state under L_o phase generation. Therefore, co-existence of L_o and L_d phases is enabled.^[130]

Over time many proteins were discovered to be functionality-dependent towards membrane composition, and hence, the concept of small domains of micro- or nanoscale was developed.^[129,132] The assembly of specific membrane proteins and lipids with increased acyl chain order was introduced as lipid or membrane rafts.^[127,129] The raft idea was postulated as explanation for lipid sorting *in vivo* and selective self-association of cholesterol and sphingolipids for lateral phase segregation *in vitro*.^[136] Lipid rafts were thought to be stable domains of tightly packed cholesterol and sphingolipids with high concentration of membrane proteins (Figure 3.2).^[129,137,138] Investigation of rafts proved to be difficult due to the lack of suitable methods to observe lipid rafts without disturbing or influencing the system. A popular approach was the use of detergents like Triton-X 100 to dissolve membranes and extract detergent resistant membrane (DRM) fractions at low temperatures, which might be the result of ordered rafts. The thus obtained membrane domains were not just rich in sphingomyelin and cholesterol but in glycosylphosphatidylinositol (GPI)-anchored proteins, as well.^[131,136] Proteins with GPI anchors in the plasma membrane are exclusively positioned in the outer leaflet of the membrane (Figure 3.2). In case of other types of lipids as linker, the protein is to be found just in the inner leaflet.^[139]

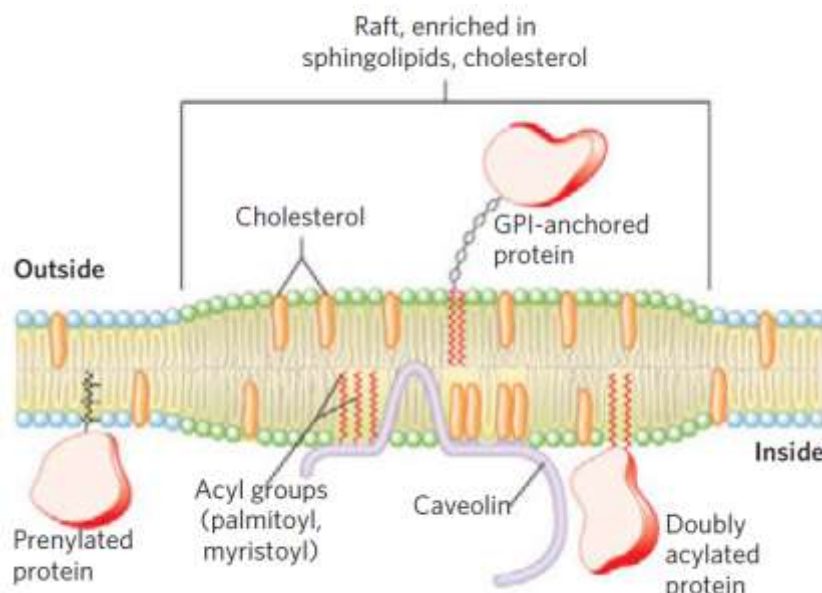


Figure 3.2 Simplified lipid raft model. Sphingolipids and glycerophospholipids with saturated and longer acyl chain form a slightly thicker, cholesterol-enriched raft containing GPI-anchored (outer leaflet) or dually-acylated (inner leaflet) proteins. From: Lehninger Principles of Biochemistry 6e, by David L. Nelson, et al, Copyright 2013 by W.H. Freeman and Company. Used by Permission of the publisher Macmillan Learning.^[139]

Phosphoinositides (PI) are with only 1 % present in the plasma membrane but are not just important to fixate proteins to the membrane.^[14,139] The twice phosphorylated phosphatidylinositol-4,5-bisphosphate (PIP₂) is crucial for a variety of physiological processes, such as ion channel activation, enzyme activation, exocytosis and second messenger production.^[14,16] PIP₂ functions as source for three second messengers via hydrolysis or phosphorylation: inositol-1,4,5-trisphosphate (IP₃), diacylglycerol (DAG) and phosphatidylinositol-1,4,5-trisphosphate (PIP₃).^[15,16] Hydrolysis of PIP₂ to generate IP₃ and DAG is performed by PI-specific phospholipase Cs (PLCs), following the IP₃/DAG-pathway.^[140] The water-soluble IP₃ is emitted into the cytoplasm and induces Ca²⁺ release from internal stores.^[15] DAG stays in the membrane, where it activates the protein kinase C (PKC), which will then phosphorylate various cellular proteins.^[141]

The importance of PIP₂ and its metabolites becomes especially clear when considering egg fertilisation of mammals. During fertilisation, not just genetic material but also PLC- ζ is transported into the egg. The PLC activates the egg by generating a wave of IP₃ and subsequently increased concentration of free Ca²⁺.^[14] Furthermore, presence of PIP₂ in the plasma membrane was found to be a requirement for neuronal exocytosis. During membrane fusion, synaptotagmin binds to PIP₂ in a Ca²⁺-independent manner and is thought to direct and quicken the subsequent Ca²⁺-dependent fusion process.^[17] Using stimulated emission depletion (STED) microscopy, a drastic increase of the PIP₂ concentration to 3–6 % in PC12 cells at fusion site could be verified.^[16]

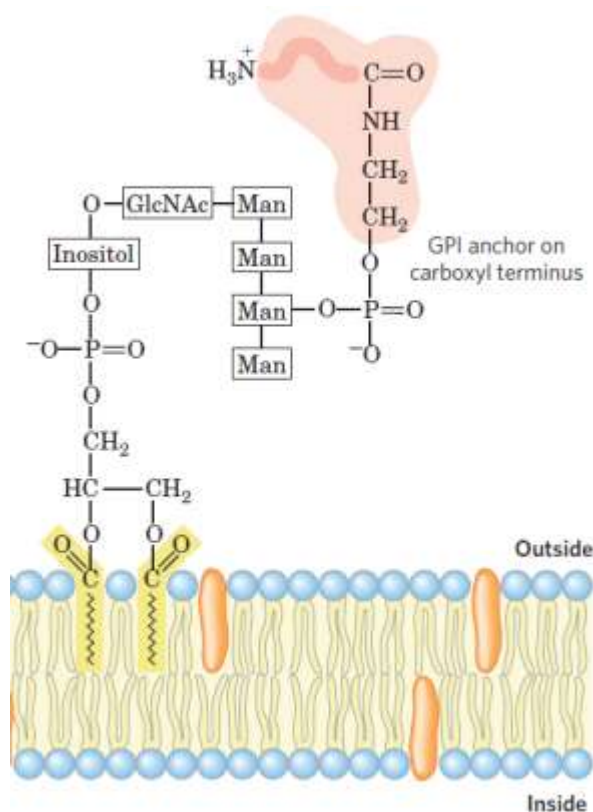


Figure 3.3 Schematic visualisation of a GPI-anchored protein attached to the outer leaflet of a membrane bilayer. A short oligosaccharide consisting of mannose (Man) and *N*-acetylglucosamine (GlcNAc) serves as a linker between lipid and protein. From: Lehninger Principles of Biochemistry 6e, by David L. Nelson, et al, Copyright 2013 by W.H. Freeman and Company. Used by Permission of the publisher Macmillan Learning.^[139]

Although DRM isolation using detergents provided a variety of information regarding raft composition, the temptation to rely on detergent extraction might be deceptive. Other studies reported detergent-induced disruption of membrane raft composition and therefore isolation of non-authentic membrane domains.^[142] Other, probably better suited methods to examine rafts are fluorescence techniques, utilizing fluorescent lipids or proteins, or spin-labelled lipids.^[143] Another very promising approach is the application of super-resolution microscopy techniques like STED microscopy.^[142,144,145]

Due to the general difficulties in raft analysis it is still debated whether rafts in living cells even exist.^[145,146] Nevertheless, an agreement regarding the definition of rafts was obtained: "Membrane rafts are small (10–200 nm), heterogeneous, highly dynamic, sterol- and sphingolipid-enriched domains that compartmentalize cellular processes. Small rafts can sometimes be stabilized to form larger platforms through protein-protein and protein-lipid interactions." (Keystone Symposium of Lipid Rafts and Cell Function 2006).^[138,147] This rather vague definition of lipid or membrane rafts illustrates that, even though quite some information was assembled^[148], further inquiries to unravel existence, formation and functions of raft are inevitable.

3.3 7-Azaindole

Identifying dynamics and structure of proteins is a non-trivial task. To address this problem tryptophan has been used as the most common optical probe.^[21] However, two drawbacks exhibit this approach to be quite unfavourable. First, the fluorescence decay of tryptophan is non-exponential^[149,150], which complicates the interpretation of measurements after the probe has been incorporated into a peptide.^[21,151,152] Second, inartificial proteins usually comprise the natural amino acid tryptophan more than once and therefore, distinguishing of the respective emissions is required.^[21] When searching for a better alternative the unnatural amino acid 7-azatryptophan (7AW, Figure 3.4), using 7-azaindole (7AI) as chromophore, came into focus. Compared to tryptophan, 7AW is a robust probe with specifiable absorption and fluorescence spectra with a red-shifted absorption maximum of 10 nm and fluorescence maximum of 70 nm.^[21] The fluorescence decay in aqueous solutions is single exponential over a broad pH range. Comparison to tryptophan revealed a significantly different distribution of electrons and increased quantum yield.^[153] Due to the non-invasive incorporability of 7AW into peptides via peptide synthesis and bacterial proteins, and the alterability of the fluorescence spectra, a broad field of potential applications is enabled.^[21,154,155]

The shift in fluorescence maxima of 7AW or 7AI is dependent on the environment of the chromophore. This characteristic can be explained by the increased lifetime of the excited state S_1 . Upon excitation the tautomeric form of 7AI is energetically favoured, hence, a hydrogen transfer will take place (Scheme 3.1).^[20] Especially in alcohols such as methanol or ethanol the excited-state tautomerisation proceeds rapidly. Furthermore, the fluorescence intensity is affected by solvents, making 7AI a well applicable probe to analyse water restricted domains as lipid bilayers.^[156]

Upon publication of the DNA model by J. WATSON and F. CRICK the possibility has been suggested that proton transfer tautomerisation might be responsible for mutations.^[157] Due to the structural similarity, the 7AI dimer is used as a model system to analyse mutagenesis of pair structures via photoinduced proton transfer.^[157,158]

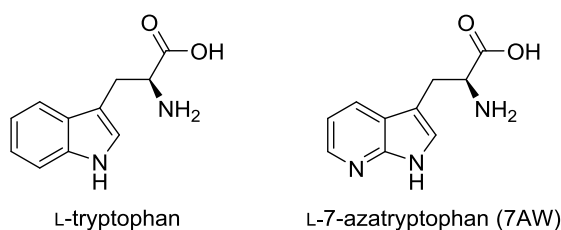


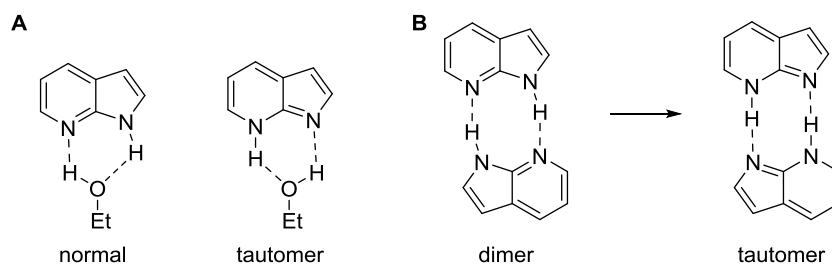
Figure 3.4 Molecular structures of L-tryptophan and 7AW.

In 1969, C. TAYLOR *et al.* proposed the excited-state double proton tautomerisation (ESDPT) of 7AI dimers caused by hydrogen bonds (Scheme 3.1, **B**)^[159] and further studies revealed that a possibly cyclic state of solvation in alcohols enables such a proton transfer in monomers as well (Scheme 3.1, **A**).^[18] Thus, the violet-fluorescing 7AI dimer is converted into the green-fluorescing tautomer.^[158] The monomer dissolved in methanol (comparable spectrum in ethanol shown in Figure 3.5) exhibits two maxima in fluorescence spectra as well with the normal species band of higher energy at 374 nm and the energetically lower tautomeric species at 505 nm.^[18]

Solvation of 7AI in non-polar, aprotic solvents like *n*-hexane or diethyl ether results in two slightly further blue-shifted emission maxima of approximately 490 and 340 nm, as shown in Figure 3.5. In water no emission due to ESDPT is detected, leading to just one signal with an intensity maximum about 390 nm.^[19] The tautomerisation of near 80 % of 7AI is inhibited in water by hydrogen bonds formed between one water molecule and one nitrogen atom, respectively (Figure 3.5).^[18,19] The remaining 20 % capable of ESDPT produce an emission at ~500 nm, which would be visible if the population of tautomerising 7AI in water increases.^[18]

Furthermore, experiments with inversed micelles in *n*-hexane, performed by J. GUHARAY, showed a red-shift of 20 nm and drastic quenching of the fluorescence upon addition of distinct amounts of water.^[156] These results are in good agreement with the findings of 7AI solvated in water.

Another point of interest regarding 7AI as fluorescent probe is whether the double proton transfer proceeds in a concerted or stepwise mechanism. Various measurements, such as fluorescent upconversion and transient conversion techniques^[160], isolated-molecule femtosecond dynamics^[157] and time-resolved fluorescence^[161], and calculations, like density functional theory (DFT)^[162] and Franck-Condon calculations^[158] have been performed. So far, the concertedness or nonconcertedness is still debated with a variety of arguments and indications supporting both possibilities. Therefore, to find the decisive conclusion further investigations are necessary.



Scheme 3.1 Chemical structure of the 7AI monomer in normal and tautomeric coordination of ethanol (**A**) and tautomerisation of the 7AI dimer in apolar solvents (**B**).

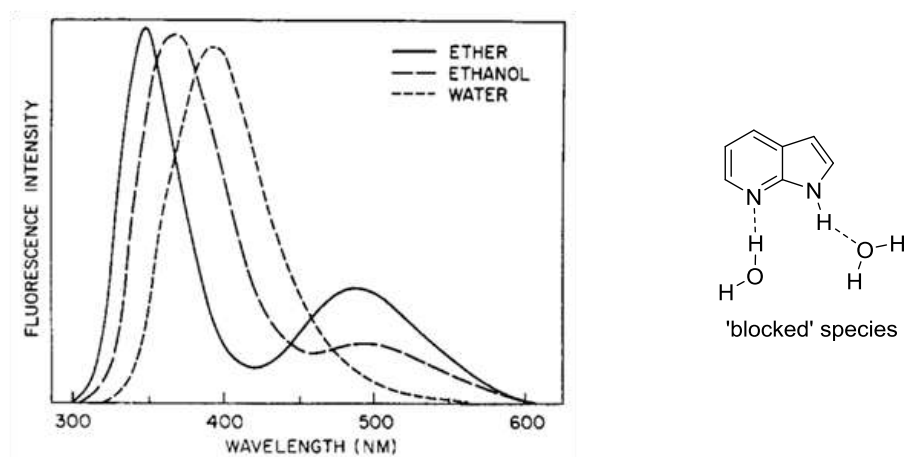


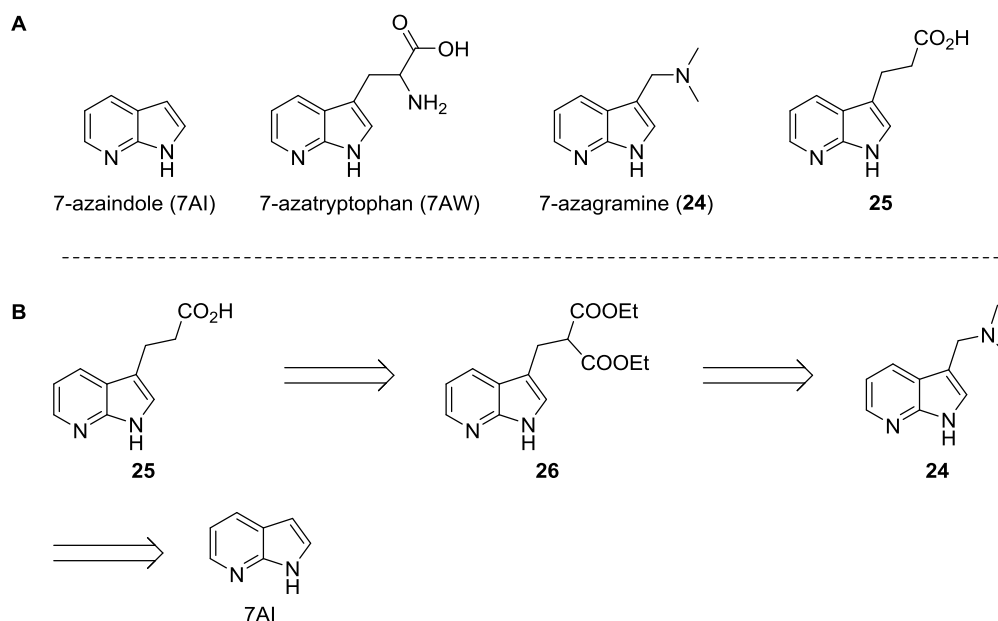
Figure 3.5 Red-shifted fluorescence spectra of 7AI as effect of increased solvent polarity. Picture taken from [19].

3.4 Synthesis of 7-Azaindole-3-propionic Acid (25)

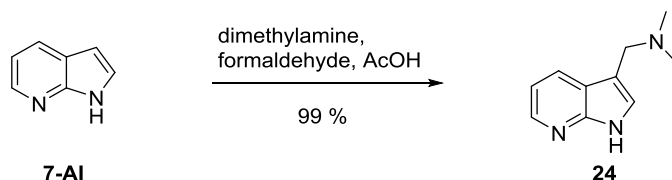
7-Azatryptophan has been identified as an effective tryptophan inhibitor in the eukaryotic unicellular organism *Tetrahymena pyriformis*^[163], and is built from 7-azagranine. Subsequently, in 1956 ROBISON *et al.* published the synthesis of a variety of 3-substituted 7-azaindole derivatives to test their biological activities starting from 7-azagranine (24).^[163]

In this work the synthesis of 24 was previously performed following the procedure stated by PIERCE *et al.* in 2011.^[164] The retrosynthetic analysis for the complete synthesis of 25 is depicted in Scheme 3.2, B, starting with a MANNICH reaction to generate 7-azagranine (24) from 7-azaindole (7AI), followed by alkylation of malonic ester with 24. The last step of this route is the hydrolysis and decarboxylation of the diester 26 to form the desired compound 3-(1*H*-pyrrolo[2,3-*b*]pyridine-3-yl)propanoic acid (25).

For the first step of the synthesis, the conversion of 7AI into 7-azagranine 24, as shown in Scheme 3.3, dimethylamine (33 % (w/v) in ethanol) was dissolved in concentrated acetic acid and water at 0 °C. The mixture was treated dropwise with formaldehyde (37 % (w/v) aq.) and stirred for 30 min. 7-Azaindole in ethanol was added and stirred for 30 min at 0 °C followed by heating to 100 °C over 18 h.^[164] Product 24 was obtained in 99 % yield and further reacted applying the procedure of ROBISON *et al.*^[163]



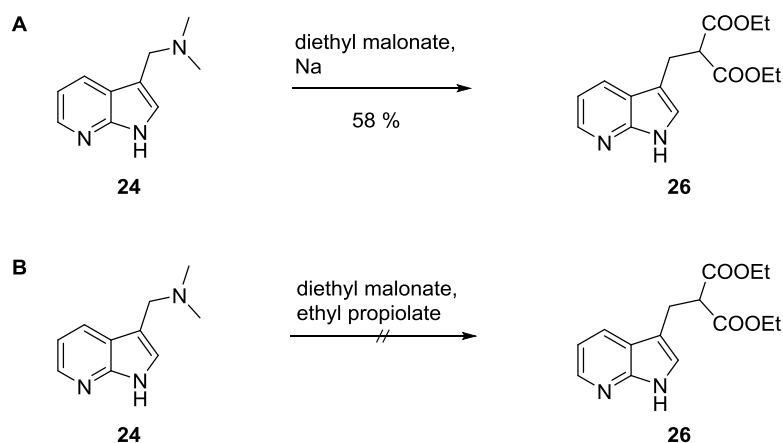
Scheme 3.2 Structures of 7-azaindole, 7-azatryptophan, 7-azagranine and the desired compound 25 (A); Retrosynthetic analysis to synthesise 25 starting from 7-azaindole (B).



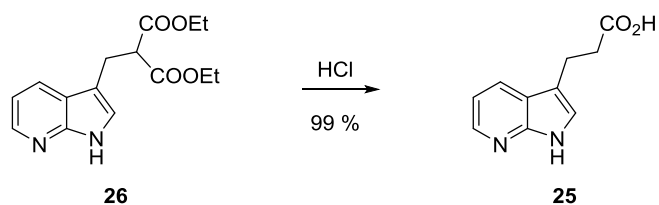
Scheme 3.3 Synthesis of 7-azagamine (**24**) starting from 7-AI.

For the following substitution reaction of the dimethylaminyl moiety by a diethyl malonyl group a mixture of **24** and diethyl malonate was heated to 120 °C and treated with a catalytic amount of elementary sodium. After 6 h of stirring at 120 °C, the reaction was completed and product **26** was isolated with 58 % yield (Scheme 3.4, **A**).^[163] To increase product formation a different procedure known from literature was tested employing milder reaction conditions and shorter reaction time (Scheme 3.4, **B**). A solution of **24** in diethyl ether was treated with diethyl malonate and ethyl propiolate was added at once.^[165] The reaction mixture was stirred at r.t. for 1 h but after standard workup procedure no product could be detected. On this basis the previously stated reaction method was maintained.

After the substitution reaction described above, hydrolysis and decarboxylation were necessary to form **25**. Both reactions were performed in one step by heating **26** in concentrated hydrochlorid acid under reflux for 7 h^[163], yielding the desired product **25** with 99 % isolated yield (Scheme 3.5).



Scheme 3.4 Tested procedures for synthesis of **26** using harsh (**A**) and mild (**B**) conditions.

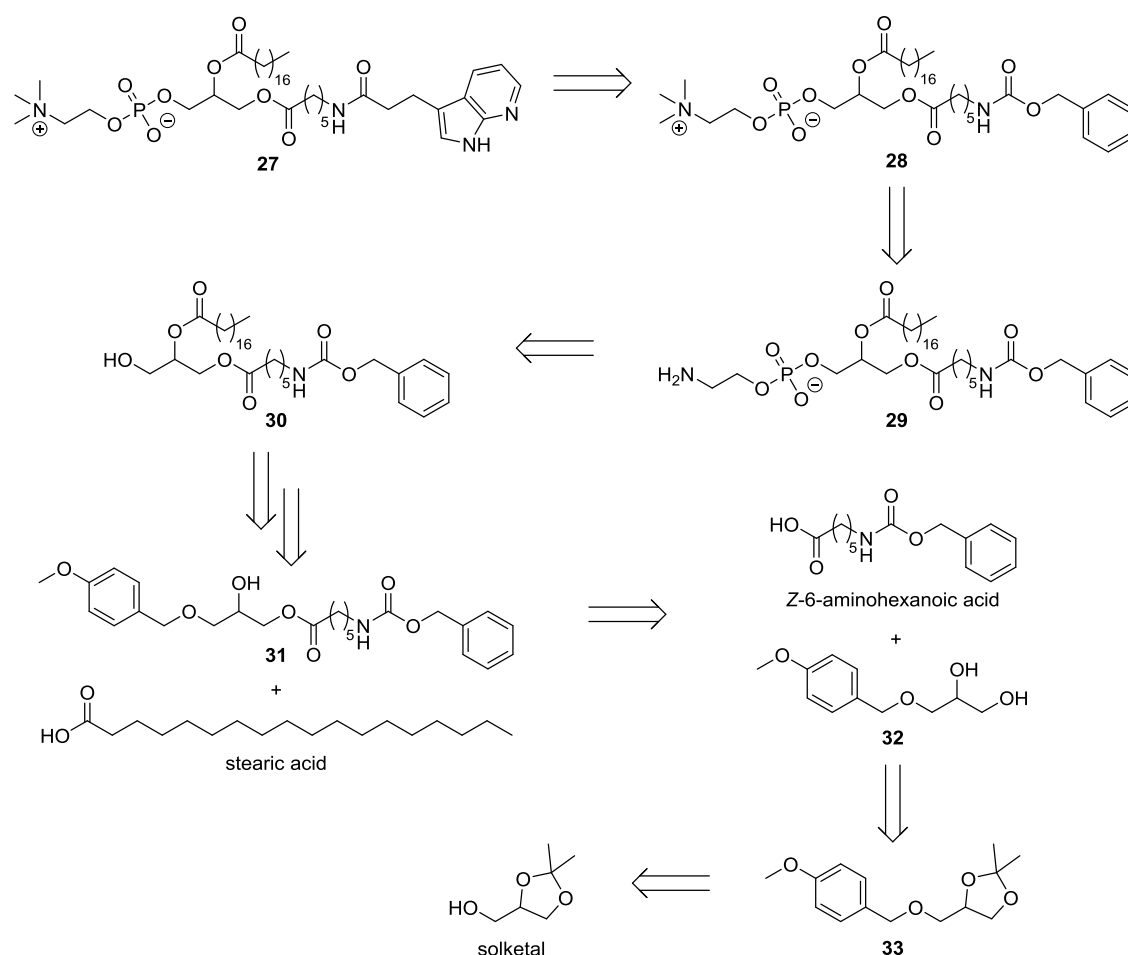


Scheme 3.5 Hydrolysis and decarboxylation of **26** in concentrated hydrochloric acid.

In conclusion, the synthesis of **25** starting from 7AI worked well with an overall yield of 57 % using literature known protocols.

3.5 Synthesis of Lipid Derivative 27

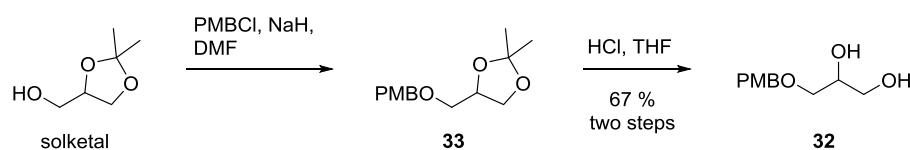
The ultimate goal of this project is the synthesis of a 7AI-labelled phosphatidylinositol-4,5-bisphosphate (PI(4,5)P₂). To develop a synthetic route for fluorescent-labelled lipid synthesis the less sterically hindered and electron dense phosphatidylcholine (PC) presented a good starting point for the synthesis of synthetically labelled lipids. Incorporation of 7AI as fluorescence label was planned via amide bond formation using a six carbon atoms long linker carrying a terminal amino functionality. The retrosynthetic analysis of the planned synthetic route is depicted in Scheme 3.6. At first solketal is protected by a *p*-methoxybenzyl (PMB) group, followed by cleavage of the isopropylidene unit. As linker, *Z*-6-aminohexanoic acid is coupled to the primary alcohol, and consequently a fatty acid to the remaining secondary alcohol. Deprotection by removal of PMB allows subsequent incorporation of the PC-head group over two steps, followed by deprotection of the linker and coupling of the fluorophore **25**.



Scheme 3.6 Retrosynthetic analysis of 27.

The first five steps for lipid backbone synthesis were described in 1996 by CHEN *et al.* beginning with the isopropylidene protected glycerine solketal.^[166] First, the unprotected primary hydroxyl moiety of solketal is protected using *p*-methoxybenzyl chloride (PMBCl) to form a PMB ether by dissolving solketal in DMF and treating the solution with PMBCl and NaH at r.t. for 18 h (Scheme 3.7). Standard workup procedure yielded crude product 33, which was reacted further without previous purification. The subsequent reaction of 33 in THF with HCl (1 M) over 20 h cleaved off the isopropylidene protective group to reveal diol 32.

CHEN *et al.* reported a short reaction time of 1 h each for both reactions. However, TLC monitoring showed that after 1 h barely product has formed.



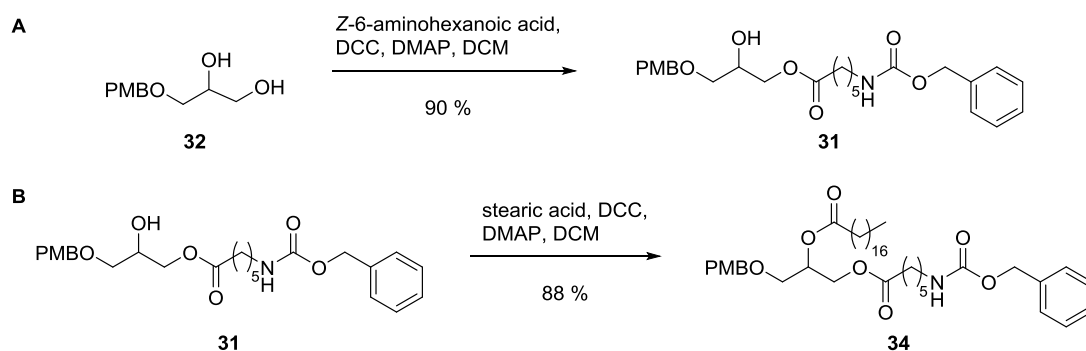
Scheme 3.7 Two step synthesis of 32 via PMB protection followed by isopropylidene deprotection.

Another publication from NÄSER *et al.* stated a reaction time of 20 h under reflux conditions.^[167] Therefore, the reaction period was increased but temperature maintained at r.t. while reaction progress was tracked via TLC. After 18 h the starting material had disappeared and the reaction was stopped. For deprotection of **33** to form diol **32** NÄSER *et al.* mention a longer reaction time than CHEN *et al.* of 6 h but TLC monitoring revealed that a significant amount of starting material still remained. Consequently, the reaction time was prolonged to 20 h, which resulted in complete conversion. Purification via flash column chromatography led to compound **32** in isolated yield of 67 %.

To incorporate the linker unit via ester bond formation the procedure of CHEN *et al.* was applied. A solution of **32** and Z-6-aminohexanoic acid was treated dropwise at 0 °C with a solution of dicyclohexylcarbodiimide (DCC) and 4-dimethylaminopyridine (DMAP) and stirred at 0 °C for 16 h (Scheme 3.8, A). The organic solvent was removed under reduced pressure and the residue redissolved in ethyl acetate. Since dicyclohexylurea (DCU), which is generated from DCC during the reaction, is insoluble in ethyl acetate it could easily be filtered off. The Steglich esterification worked smoothly and after purification **31** was obtained in up to 90 % yield.

The next step was again a Steglich esterification to couple the respective carboxylic acid, in this case stearic acid, to **34**. This was accomplished by treatment of **31** and stearic acid in DCM with a solution of DCC and DMAP at r.t. and stirring for 24 h. The generated product **34** was purified and obtained in 88 % yield as white crystals (Scheme 3.8, B).

At this point of the synthesis two possibilities to proceed are conceivable. One way is to cleave off the carboxybenzyl (Z) protecting group to incorporate the fluorophore **25**, followed by generation of the PC head group. The alternative is to first produce the PC head group and consecutively deprotect the linker and couple **25**.

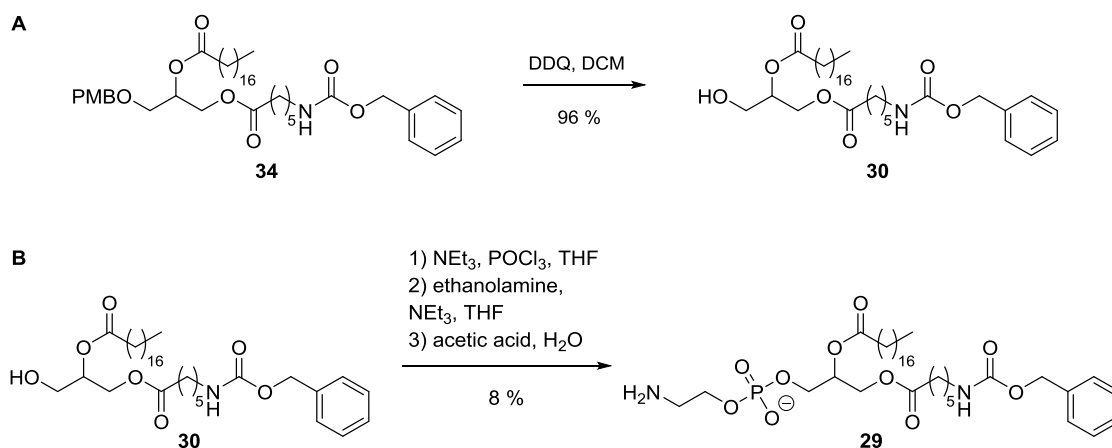


Scheme 3.8 Steglich esterification of **32** with Z-6-aminohexanoic acid (A) and of **31** with stearic acid (B).

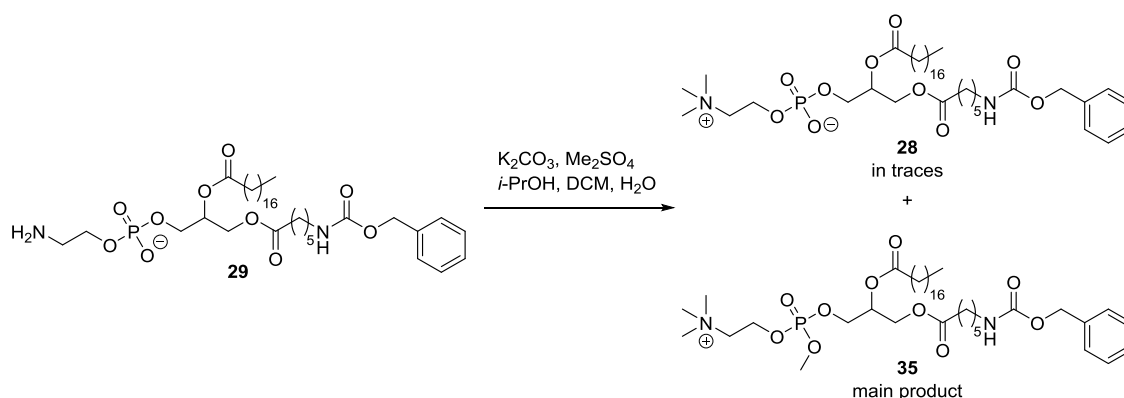
In this case it was preferred to introduce the fluorophore as the very last step, hence the second route was followed. Thus, the next step was to cleave off the PMB group to generate a free primary alcohol. The protected compound **34** was dissolved in DCM and treated with dichlorodicyanobenzoquinone (DDQ) and small amounts of water over 24 h, which deprotected the alcohol following an oxidative mechanism under generation of *p*-methoxybenzaldehyde (Scheme 3.9, A). The isolated product **30** was obtained in 96 % yield.

To introduce the PC head group the deprotected alcohol needed to be phosphorylated and subsequently coupled with ethanolamine. This was conducted in an one-pot reaction starting with deprotonation of **30** using triethylamine. The mixture was added slowly to a solution of phosphoryl chloride in THF at 0 °C, stirred at 0 °C for 10 min followed by stirring at r.t. for 45 min. The reaction mixture was again cooled to 0 °C and treated dropwise with ethanolamine and triethylamine in THF. After stirring for 10 min at 0 °C the mixture was allowed to warm up to r.t. and stirred over night. Filtration and removal of the organic solvent yielded a residue, which was redissolved in concentrated acetic acid and water and heated to 70 °C for 1 h (Scheme 3.9, B).^[168,169] After standard workup procedure compound **29** was obtained with a low yield of 8 %.

For complete head group synthesis the next step was the methylation of the generated phosphoethanolamine derivative **29**. Therefore, a solution of **29** in DCM and 2-propanol was treated with K₂CO₃ in water at 35–40 °C. Dimethyl sulphate in 2-propanol was added slowly and the reaction mixture stirred at 40 °C for 90 min.^[168,169] Using mass spectrometry rather small amounts of formed product were detected, but could not be isolated. Interestingly, methylation of the phosphate group was observed as the dominating reaction (Scheme 3.10). Since the compounds **28** and **35** proved to be inseparable using column chromatography, no yield was determined.



Scheme 3.9 Deprotection of **34** under mild oxidative conditions using DDQ (A). Introduction of the phosphate group and ethanolamine for PC head group formation (B).

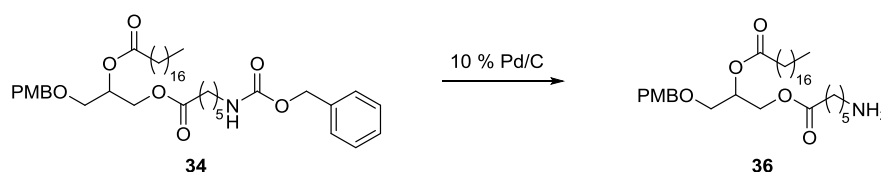


Scheme 3.10 Methylation of **29** yielded the desired compound **28** in traces and the fourfold methylated **35** as main product.

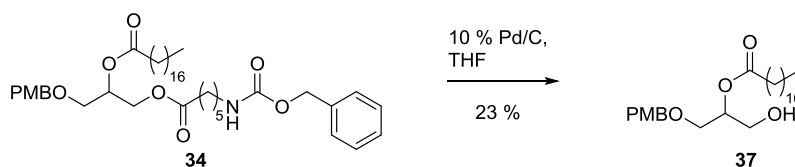
Due to the low yield of the reaction shown in Scheme 3.9, **B** and the undesirable side reaction forming **35**, the strategy was changed, starting after coupling of the fatty acid (Scheme 3.8, **B**, product **34**). Following the modified strategy, first the linker is deprotected to reveal the primary amino functionality (Scheme 3.11), second the fluorophore **25** is incorporated and last the head group is generated. Already the first reaction, cleavage of the Z protecting group (Scheme 3.11), proved to be not as trivial as expected. The tested reaction conditions are summarised in Table 3.1.

To cleave the Z group **34** was given into a pressure vessel along with NaHCO_3 , palladium on charcoal (10 % Pd/C) and a *t*-butanol–water mixture (7:1, v/v). The reaction vessel was attached to a Parr apparatus. A hydrogen atmosphere was generated in the vessel and it was vigorously shaken over 24 h under 3.5 bar hydrogen.^[166,170] The catalyst was then filtrated through Celite®, whereupon it was essential that the catalyst did not dry to avoid flying sparks and inflammation.

Applying the above mentioned reaction conditions only led to product formation in traces, so the reaction conditions were modified by leaving out NaHCO_3 but again no reaction took place. Therefore, reaction conditions described by WADHAVANE *et al.* were tested using dry THF as solvent and increased temperature. The reaction time was decreased to 4 h.^[171] Mass spectrometry revealed no formation of the desired product **36** but cleavage of the linker to form **37** instead (Scheme 3.12).



Scheme 3.11 Deprotection of primary amine of **34** by cleaving the Z protection group via hydrogenation.



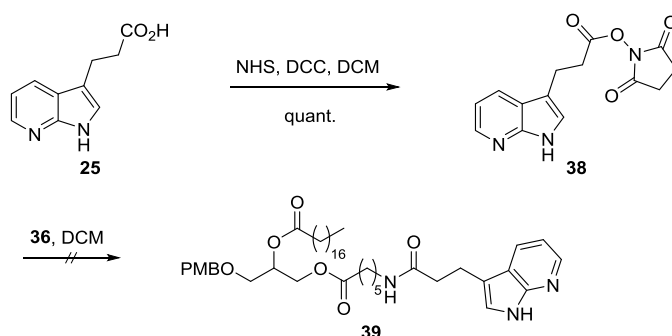
Scheme 3.12 Observed reaction after applying Z deprotection conditions to **34** as described by WADHAVANE *et al.*^[171]

Since the usage of hydrogen atmosphere seemed to be non-applicable for this system, another approach was searched for. A procedure published by BALDOLI *et al.*^[172] was found utilizing ammonium formate and methanol as solvent to generate hydrogen *in situ*. Compound **34** was dissolved in methanol under argon atmosphere and treated with palladium on charcoal and ammonium formate. After reflux for 1 h, filtration and purification pure product **36** in 88 % yield was obtained.

After successful cleavage of the protecting group forming **36**, the next step was the incorporation of the fluorophore. Based on a procedure of JUMA *et al.*^[173] the previously synthesised fluorophore **25** was activated as *N*-hydroxysuccinimide (NHS) ester using NHS and DCC mediation (Scheme 3.13). A solution of **25** in DCM was treated with NHS and DCC at 0 °C and stirred under ice cooling for one hour. After 12 h of stirring at r.t. and filtration of the reaction mixture **36** was added and stirred for additional 2 h. Analysis of the mixture after standard workup procedure revealed that no reaction product was formed but activation of **25** to NHS ester **38** was complete. The compounds **38** and **36** could be isolated.

Table 3.1 Overview over applied reaction conditions for Z cleavage.

| Condition No. | Solvent | Temperature | Time | Admixture | Product |
|---------------|---------------------------------|-------------|------|-------------------------------------|---------|
| 1 | <i>t</i> -BuOH/H ₂ O | r.t. | 24 h | NaHCO ₃ + H ₂ | traces |
| 2 | <i>t</i> -BuOH/H ₂ O | r.t. | 24 h | H ₂ | traces |
| 3 | THF | 50 °C | 4 h | H ₂ | – |
| 4 | MeOH | 75 °C | 1 h | NH ₄ HCO ₂ | ✓ |



Scheme 3.13 Activation of **25** as NHS ester with subsequent coupling to **36**.

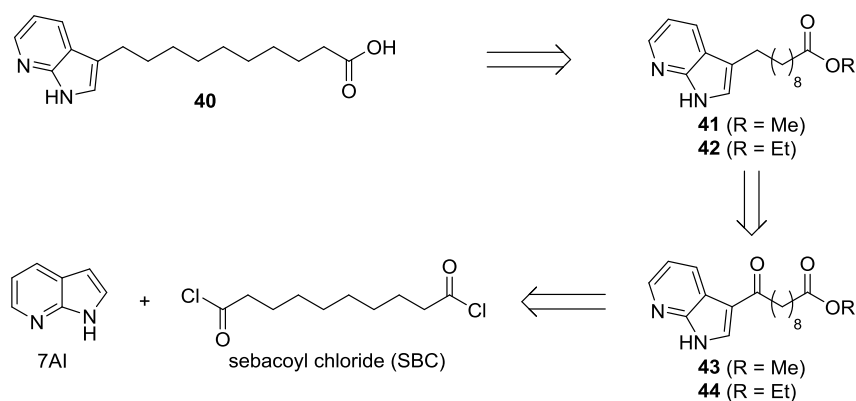
Due to its similar properties but higher alkalinity, DMF was tested as solvent for this reaction instead of DCM. At first no improvement was observed but after addition of triethylamine as supplementary base and washing with citric acid (10 % (w/w) aq.) during workup, traces of product **39** were detected. Isolation of **39** was not possible.

Another attempt to label **36** by coupling with **25** was to vary the base. The lipid derivative **36** was dissolved in 400 μL anhydrous DMF per 1 mmol fluorophore, treated with *N,N*-diisopropylethylamine (DIPEA) and NHS activated **25** was added.^[174] The reaction was allowed to stir over night but after workup again only traces of product formation was observed.

The approaches to synthesise a 7AI-labelled lipid derivative described so far were unsuccessful or showed very low yields. Therefore, a general change in structure of the desired molecule was made, which is presented in the subsequent chapter.

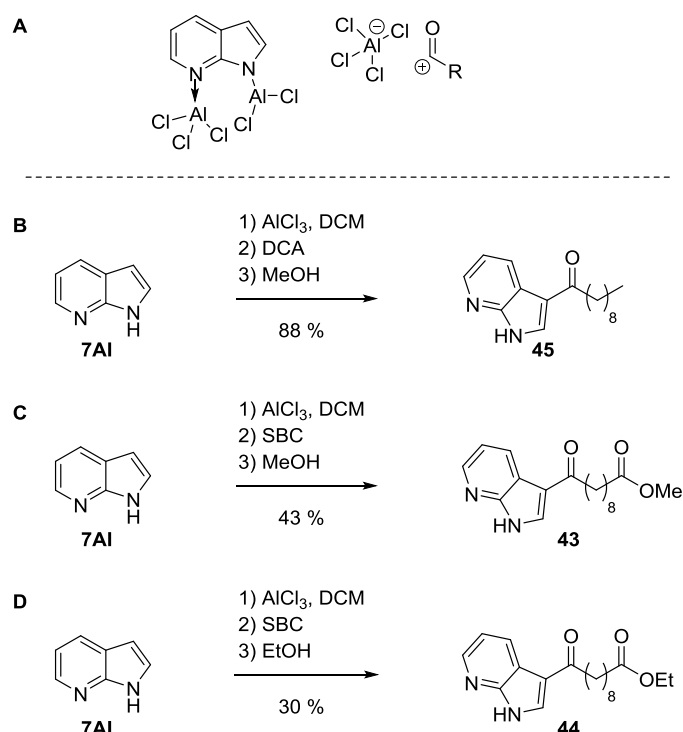
3.6 Synthesis of 7-Azaindole-3-decanoic Acid (**40**)

In order to synthesise a 7AI-labelled lipid derivative the structure of the target compound was altered to exclude the unnatural amide bond, which is generated by fluorophore coupling. Therefore, the design of the fluorophore had to be altered. To avoid amide bond formation the previously used linker to couple the lipid backbone with **25** was omitted. In order to maintain the desired chain length the alkyl chain of the fluorophore needed to be elongated. The retrosynthetic analysis of the newly designed fluorophore **40** is shown in Scheme 3.14, starting with acylation of 7AI using sebacoyl chloride (SBC). After removal of the carbonyl unit by reduction, the ester is hydrolysed to obtain fluorophore **40**.



Scheme 3.14 Retrosynthetic analysis of 7-azaindole decanoic acid (**40**).

The starting material of this synthetic route is, like in synthesis of **25**, 7AI. In a Friedel-Crafts-type reaction 7AI was acylated with SBC.^[175,176] Four equivalents of aluminium chloride were suspended in DCM and 7AI was added. After stirring at r.t. for 1 h, the acid chloride was added dropwise to the suspension and stirred for 18 h. Treatment with MeOH at 0 °C stopped the reaction. To utilise an excess of AlCl₃ of at least three equivalents is crucial in this system, since both nitrogen atoms of 7AI are likely to form complexes with the Lewis acid (Scheme 3.15, **A**).^[175] The reaction conditions described by ZHANG *et al.* were first tested using decanoyl chloride (DCA), which led to pure product **45** of 88 % after purification (Scheme 3.15, **B**). Applying these conditions to the desired system containing sebacyl chloride yielded in formation of **43** with 43 % of pure product (Scheme 3.15, **C**). Stopping the reaction with water instead of methanol to save the ester cleavage step of **41** and **42** (Scheme 3.14) has been tested as well but in this case only sebacyc acid and 7AI could be identified as reaction products. Since cleavage of the methyl ester proved to be occasionally difficult and in need of harsh reaction conditions, EtOH was tested as well to stop the reaction (Scheme 3.15, **D**). The generated ethyl ester **44** demonstrated to be easier to cleave in the last step while stable under the conditions of the acyl reduction reaction (Scheme 3.16).



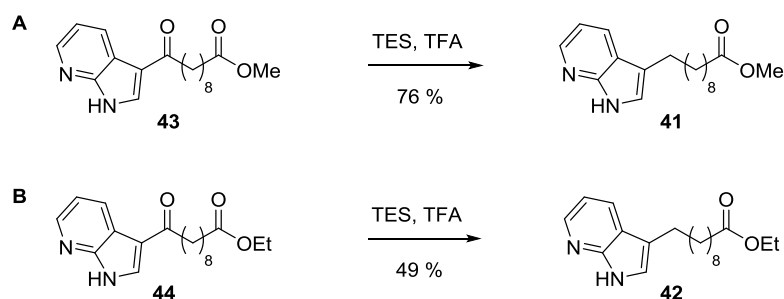
Scheme 3.15 Likely explanation for necessary excess of AlCl₃ are complexes formed during acylation reaction (**A**).^[175] Acylation of 7AI utilizing decanoyl chloride (**B**), sebacyl chloride with MeOH (**C**) and sebacyl chloride with EtOH (**D**).

After just a few repetitions of the reactions shown in Scheme 3.15, **C** and **D**, no conversion would take place anymore. Despite varying equivalents of reagents and reactants as well as amount of solvent and reaction temperature used, the product could not be obtained anymore. Only with exchanging the AlCl_3 by a new batch the reaction would proceed again. But still this reaction remained unreliable.

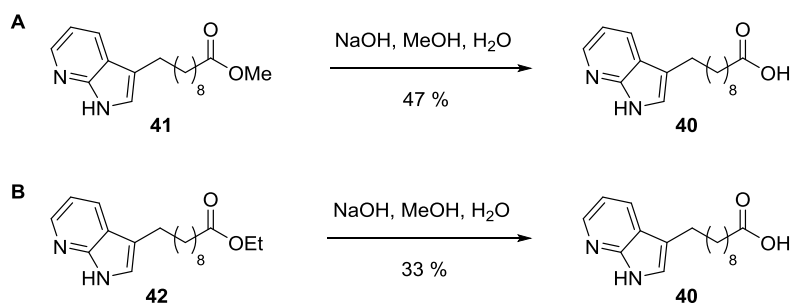
The succeeding step was the reduction of the generated ketone to form a methylen unit using triethylsilane (TES) and trifluoroacetic acid (TFA).^[176] The ketone was dissolved in TFA, treated with TES and stirred at r.t. for 18 h. TFA was removed under reduced pressure and the residue diluted using aqueous potassium hydroxide (2 M). These conditions were applied to both ester compounds **43** and **44** as well as to test molecule **45** and in all cases product was formed in mediocre to good yields (Scheme 3.16). In most cases this reaction was performed utilising the crude product of the previous reaction (Scheme 3.15, **B–D**), since purification of **43** and **44** via flash column chromatography with silica gel seemed to cause degradation of the product, which might explain the rather low yields.

The last step to synthesise the modified fluorophore was the ester cleavage to obtain the carboxylic acid. A solution of the respective ester compound in MeOH and water was prepared along with about two equivalents of sodium hydroxide. After refluxing for 4 h, the corresponding carboxylic acid was supposed to be generated.^[177]

It turned out that employing two to five equivalents of sodium hydroxide and heating to reflux for 2–5 h was mostly sufficient for complete cleavage of the ethyl ester **42** (Scheme 3.16, **B**). In contrast, cleavage of the methyl ester **41** required approximately 20 equivalents sodium hydroxide for complete conversion to **40** (Scheme 3.16, **A**). Elongation of the reaction time led to no increase in yield.



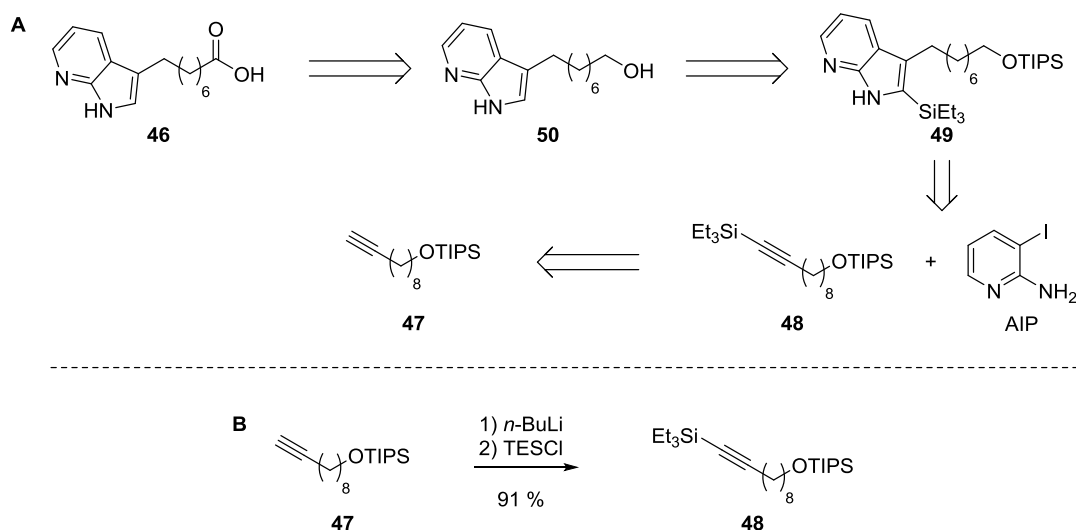
Scheme 3.16 Reduction of the keto-moiety of **43** and **44**.



Scheme 3.17 Ester cleavage of **41** and **42** using sodium hydroxide.

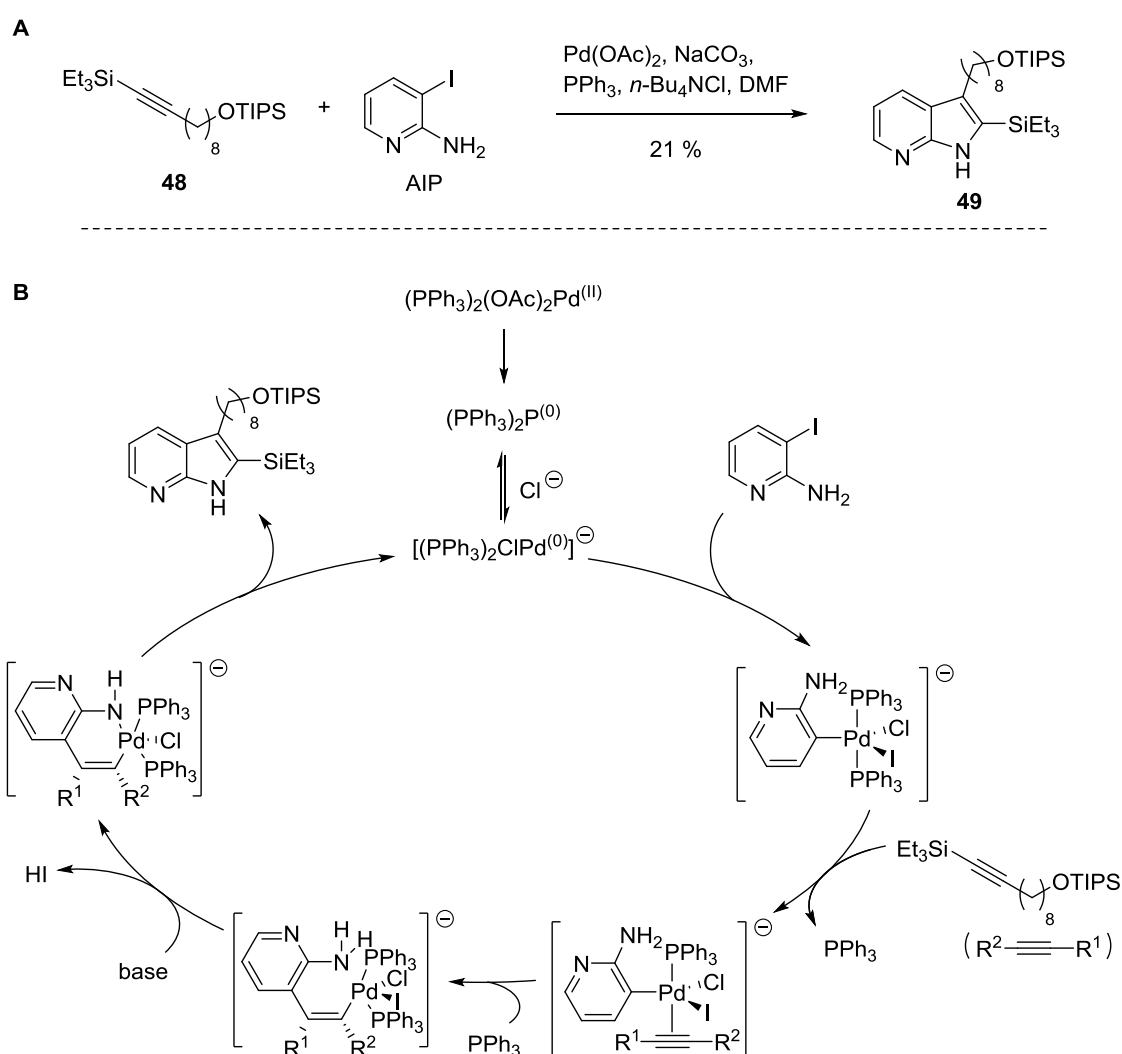
In summary, product **40** was obtained in 5 % overall yield via the ethyl ester route and in 15 % yield over the methyl ester route. The former was more reliable so it became the preferred synthetic approach for **40** synthesis even though it resulted in lower yield. Due to the low yield and the toxicity of sebacoyl chloride, another synthetic approach was tested. In 1991 LAROCK *et al.* published a new palladium-catalysed strategy for the synthesis of indoles starting from *o*-iodoaniline and analogous derivatives.^[178,179] The described procedure was adapted to the system in this work, shown in Scheme 3.18, **A** as retrosynthetic analysis, to prepare the fluorophor with a two carbon atoms shorter linker.

The synthesis of **46** based on LAROCK and NADRES started with insertion of a triethylsilyl (TES) moiety to create a sterically demanding group. Incorporation of TES into **47** is crucial for the regioselectivity of the subsequent reaction since the bulkier group is selectively placed next to nitrogen in position two of the indole or 7AI. A solution of the protected alcohol **47** in THF was treated with *n*-BuLi at -78°C and stirred for 40 min. Dropwise addition of TESCl at -78°C and stirring for 1 h yielded the silylated product **48** with 91 % (Scheme 3.18, **B**).^[179]



Scheme 3.18 Retrosynthetic analysis of **46** based on LAROCK *et al.* and NADRES *et al.* (**A**). Silylation of **47** using TESCl following the protocol of NADRES. (**B**)

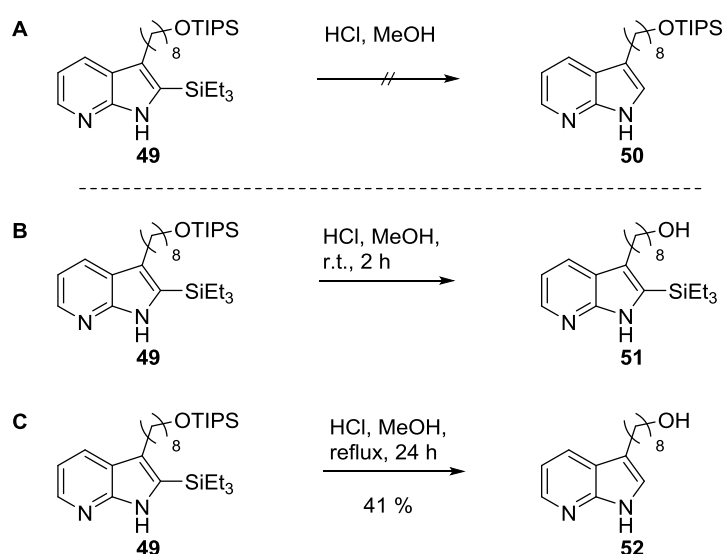
In the following step the 7-azaindole heterobicyclic structure is generated. Palladium(II) acetate, sodium carbonate, tetrabutylammonium chloride, 2-amino-3-iodopyridine (AIP), **48** and triphenylphosphine were dissolved in DMF and heated to 100 °C for 15 h. The product **49** was purified and obtained in 21 % isolated yield. The catalytically active species Pd(0) is generated out of the precatalyst Pd(OAc)₂ by base, coordinates a chloride and is then readily available for oxidative addition by AIP. The alkyne **48** coordinates to the palladium atom, followed by regioselective *syn*-insertion into the previously generated aryl–palladium bond. In the resulting vinylic palladium intermediate the nitrogen replaces the iodide and subsequently palladium undergoes reductive elimination to produce the 7AI derivative while regenerating the Pd(0) species (Scheme 3.19).^[180,181]



Scheme 3.19 Heteroannulation of AIP to form 7-azaindole derivative **49** (A). Mechanism of LAROCK indole synthesis applied to the used system to generate **49** (B).

With **49** in hand, the next step was the cleavage of the TES moiety as described by NADRES *et al.*, to generate compound **50** (Scheme 3.20, A). Compound **49** was treated with concentrated hydrochloric acid and methanol (1:12.3, v/v) and stirred at r.t. for 2 h. After applying these conditions, barely any conversion took place and the little amount of formed product **51** contained the alcohol without protecting group but still carried the TES group (Scheme 3.20, B). Therefore, the conditions were modified to stirring over night and addition of more hydrochloric acid (9.09 eq., HCl/MeOH, 1:2.7, v/v) but still starting material and formation of **51** were observed. In the next attempt the amounts of hydrochloric acid and methanol were increased to 45.5 equivalents HCl (HCl/MeOH, 1:1, v/v). These conditions led to complete conversion of starting material **49** to form the deprotected alcohol **50** as well as small amounts of **52** with both silyl groups cleaved off. Since **52** seemed even more favourable than the beforehand desired compound **50**, the complete cleavage of silyl moieties was now the aim. After dissolving **49** in hydrochloric acid (90.9 eq.) and methanol (HCl/MeOH 1:1, v/v) the solution was heated to reflux and stirred for 24 h. Utilisation of these conditions yielded in full conversion generating only the desired compound **52** (Scheme 3.20, C).

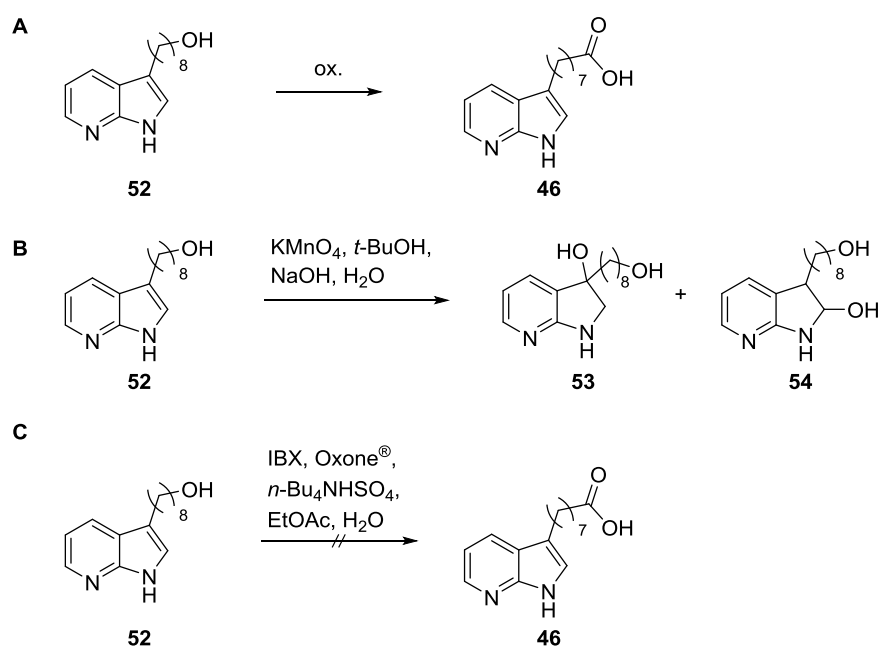
To complete the synthesis of **40**, oxidation of the alcohol **52** needed to be achieved in a final step (Scheme 3.21, A). To accomplish this, a solution of **52** in *t*-butanol was cooled to 0 °C and treated with a mixture of potassium permanganate and sodium hydroxide in water. The mixture was stirred for 1.5 h at 0 °C, warmed up to r.t. and stirred for 24 h. It was again cooled to 0 °C, treated with another portion of KMnO₄ and NaOH in water and stirred for further 24 h.^[182] After quenching of excessive permanganate, the crude product was analysed to reveal no formation of the desired product **40**.



Scheme 3.20 Planned reaction based on NADRES *et al.* to cleave the TES group (A); Actually proceeding reaction deprotecting alcohol **50** (B); Modified reaction conditions to yield cleavage of both silyl groups (C).

Instead addition of water located at the double bond of the five-membered ring took place (Scheme 3.21, **B**). Another approach to oxidise the alcohol was utilising 2-iodoxybenzoic acid (IBX) along with Oxone[®] (Scheme 3.21, **C**).^[183] All solid compounds were dissolved in ethyl acetate and water, and stirred for 4–7 h at 70 °C. After workup no starting material was left but product formation could not be detected.

Since the described route to synthesise the fluorophore carrying an alkyl chain as linker were not as successful as hoped and the yields showed no significant increase compared to the approach via ethyl ester **44**, the attempt to synthesise **46** was dropped. But usage of an oxidation agent like permanganate while applying anhydrous conditions might have enabled production of the desired carboxylic acid.

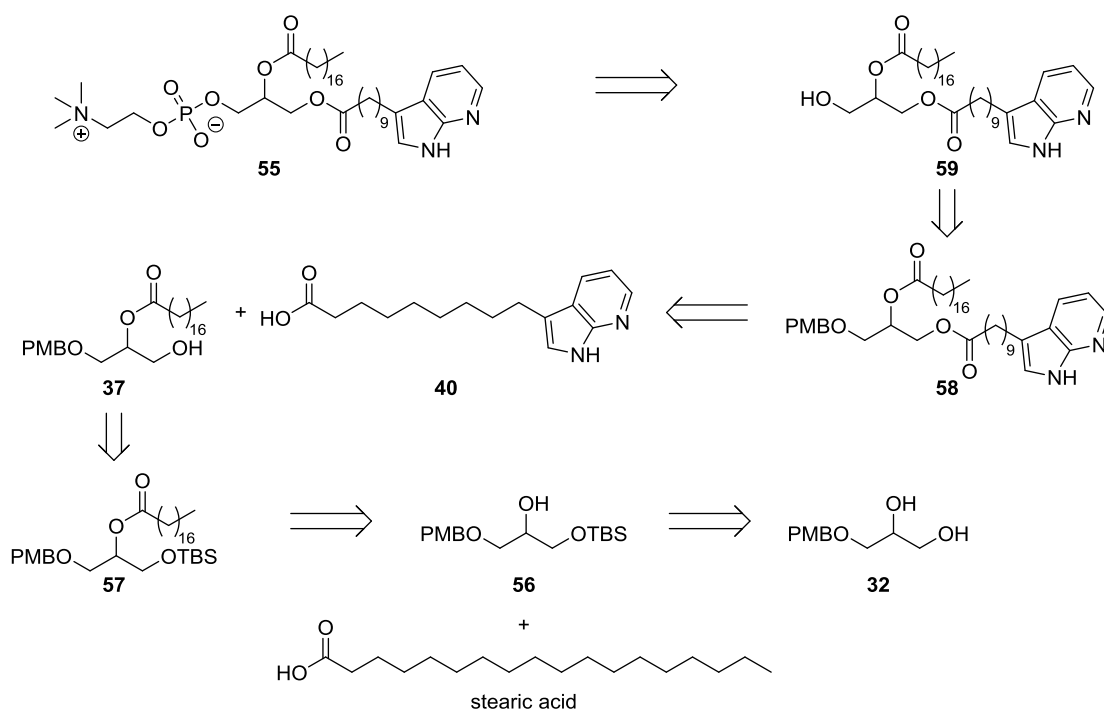


Scheme 3.21 General oxidation reaction to convert alcohol **52** into carboxylic acid **46** (**A**); Oxidation attempt using KMnO_4 with the obtained products **53** and **54** (**B**) and using IBX and Oxone[®] (**C**).

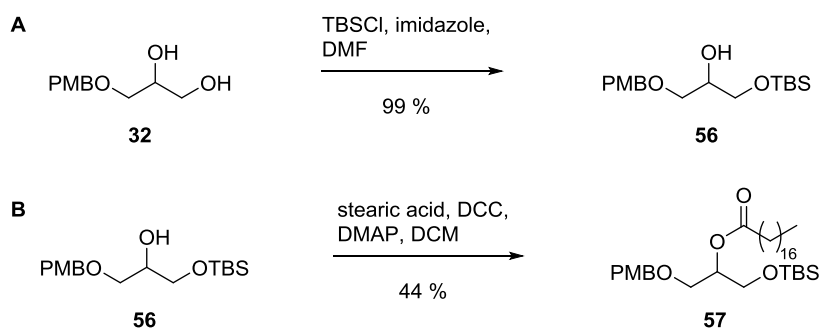
3.7 Synthesis of Modified Lipid Derivative 55

The new target molecule **55** carrying the fluorophore with the modified linker **40** contains no unnatural functionalities besides the fluorophore itself. This increases the probability of smooth integration and arrangement of **55** in membranes. The synthesis started again with PMB protection of the free alcohol of solketal, followed by cleavage of the isopropylidene group to the primary and secondary hydroxyl functionalities. Since these reactions are already shown in Scheme 3.6, they are not depicted in Scheme 3.22, in which the retrosynthetic analysis of compound **55** is illustrated. After deprotection, the primary alcohol is protected again by a *t*-butyldimethylsilyl (TBS) group and subsequently the fatty acid is coupled via ester bond formation. The TBS group is cleaved and fluorophore **40** incorporated. The last two steps of this synthetic route include deprotection by PMB-cleavage and generation of the PC-head group.

The first few steps were performed based on a procedure published by JIANG *et al.* depicting the synthesis of lysobisphosphatic acid and its analogues.^[184] For protection of the primary alcohol a solution of **32** and imidazole in DMF was treated with TBSCl in DMF at 0 °C over a period of 1 h. The reaction mixture was stirred at 4 °C over night and at r.t. for 8 h.^[184] After standard workup procedure and purification **56** was obtained in up to 99 % yield (Scheme 3.23, **A**). Using NMR analysis it was ensured that only the desired product was formed and no protection of the secondary alcohol took place.



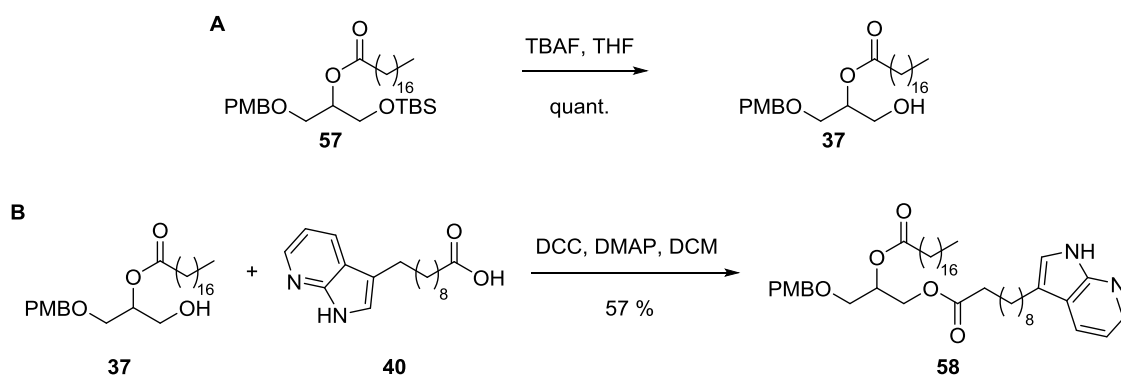
Scheme 3.22 Retrosynthetic analysis of fluorophore **40** labelled lipid **55**.



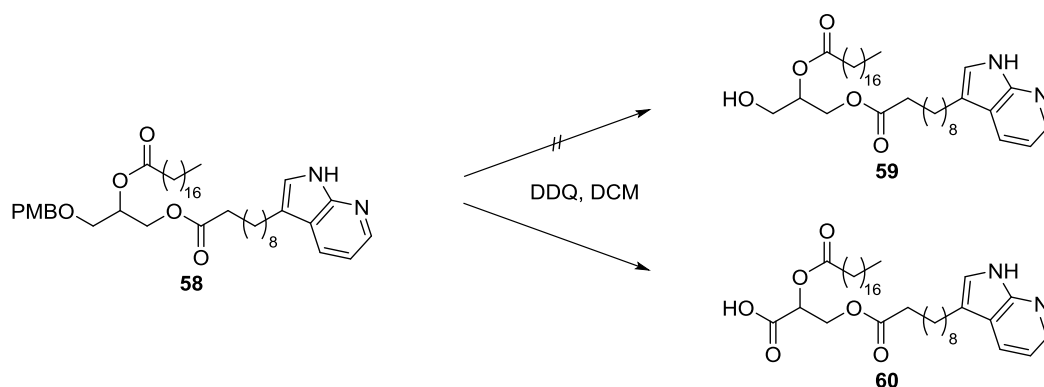
Scheme 3.23 TBS-protection of the primary hydroxy functionality of **32** (A). Acylation of **56** by activation and subsequent coupling of stearic acid (B).

To couple stearic acid to **56** the carboxylic acid was activated by treating a solution of **56** and stearic acid in DCM with a solution of DCC and DMAP in DCM.^[184] After stirring for 24 h at r.t. and purification, pure product **57** was obtained in 44 % yield (Scheme 3.23, B).

Prior to incorporation of the fluorophore, the TBS group was cleaved off. This was performed by treating **57** in THF with tetrabutylammonium fluoride (TBAF, 1 M in THF) at r.t. over night^[184] and gave product **37** in quantitative yield (Scheme 3.24, A). Following the deprotection reaction, fluorophore **40** was coupled (Scheme 3.24, B). Applying the same conditions as for stearic acid, coupling the fluorophore was activated by treatment with DCC and DMAP with the distinction that in this case addition of the reagent mixture was performed at 0 °C. Purification provided product **58** in 57 % yield.



Scheme 3.24 Cleavage of the TBS group of **57** (A) with subsequent fluorophore coupling to yield **58** (B).

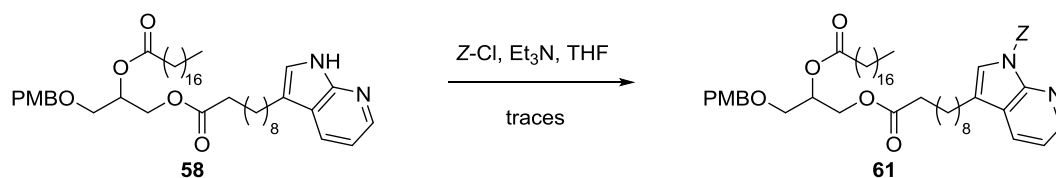


Scheme 3.25 Attempt to cleave off PMB for subsequent head group generation with the desired product **59** (top right) and the actual reaction to form product **60** (bottom right).

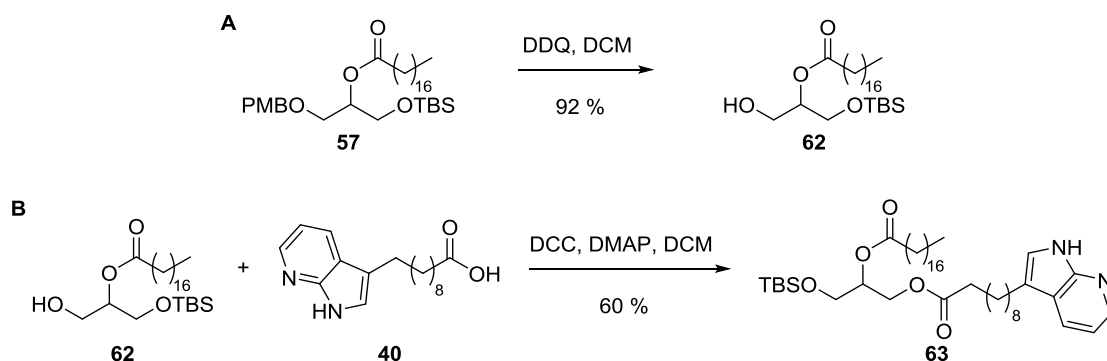
The PMB cleavage worked nicely in first synthetic route (Scheme 3.9) using the Z protecting group bound as carbamate. Since the presence of the fluorophore appeared to be problematic, protection of the secondary amine using the Z group was considered (Scheme 3.26).

To protect the secondary amine a solution of **58** in THF was treated with triethylamine and Z-Cl at 0 °C and stirred at r.t. over night.^[185] Mass spectrometry and TLC revealed that only traces of product **61** were formed, which could not be isolated.

To avoid further protecting attempts as well as the challenge of PMB removal the sequence of deprotection was altered. So far for coupling of the fluorophore the TBS group was cleaved off instead of the PMB group. Exchanging the order and applying the previously stated conditions for PMB removal on compound **57** showed smooth conversion to **62** in good yield (Scheme 3.27, A).



Scheme 3.26 Protection approach of NH using the Z protection group.

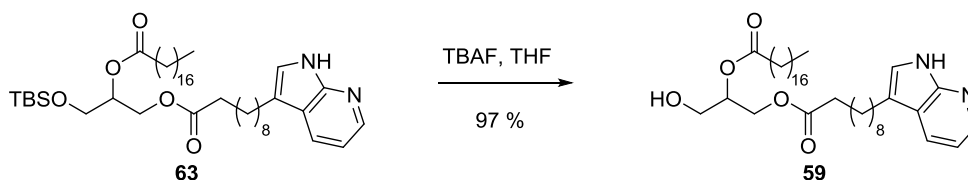


Scheme 3.27 Removal of the PMB group of **57** previous to fluorophore incorporation (**A**); B: Coupling of fluorophore **40** (**B**).

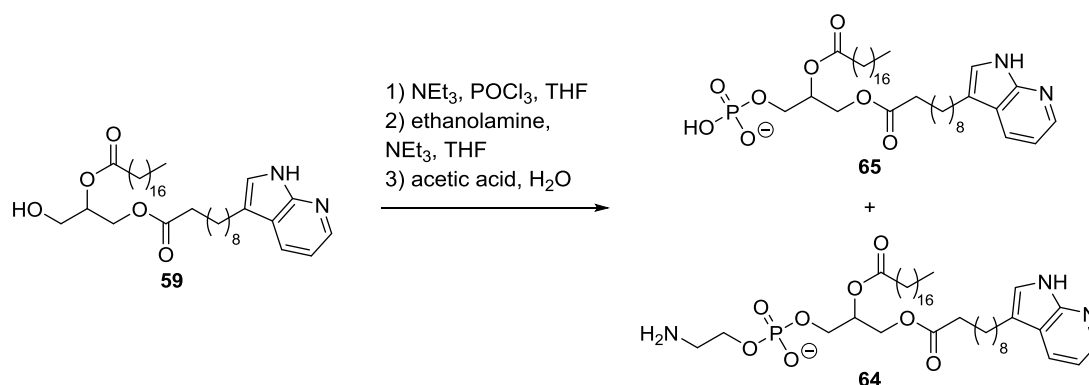
The change in deprotection sequence had one minor drawback. After removal of PMB no UV-active or stainable functionality was left within molecule **62**, which made detection during flash column chromatography (FC) almost impossible. Fortunately, thorough extraction during workup removed nearly all impurities and usually no further purification was necessary. Anyhow, to ensure detectability the whole synthesis was repeated with coupling of oleic acid in place of stearic acid, which is not shown.

Incorporation of fluorophore **40** was carried out analogous to the synthesis of **58**, depicted in Scheme 3.24, **B**. After 16 h at 0 °C and subsequent FC, product **63** was obtained in 60 % yield (Scheme 3.27, **B**). Following the labelling step, cleavage of TBS was conducted. Compound **63** was dissolved in TFA, treated with TBAF (1 M in THF) and stirred over night (Scheme 3.28). The deprotected product **59** was obtained after FC in very good yield of 97 %.

For head group generation the previously described conditions using phosphoryl chloride, triethylamine and ethanolamine were applied (Scheme 3.29). Analysis of the crude product revealed formation of product **64** in traces as well as formation of the intermediate **65** carrying a phosphate group without ethanolamine. Neither of the reaction products could be isolated.



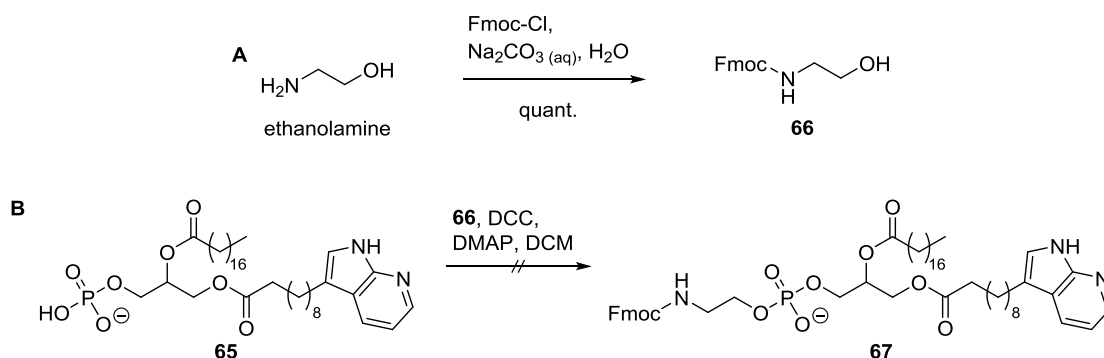
Scheme 3.28 Removal of the TBS group of **63** using TBAF.



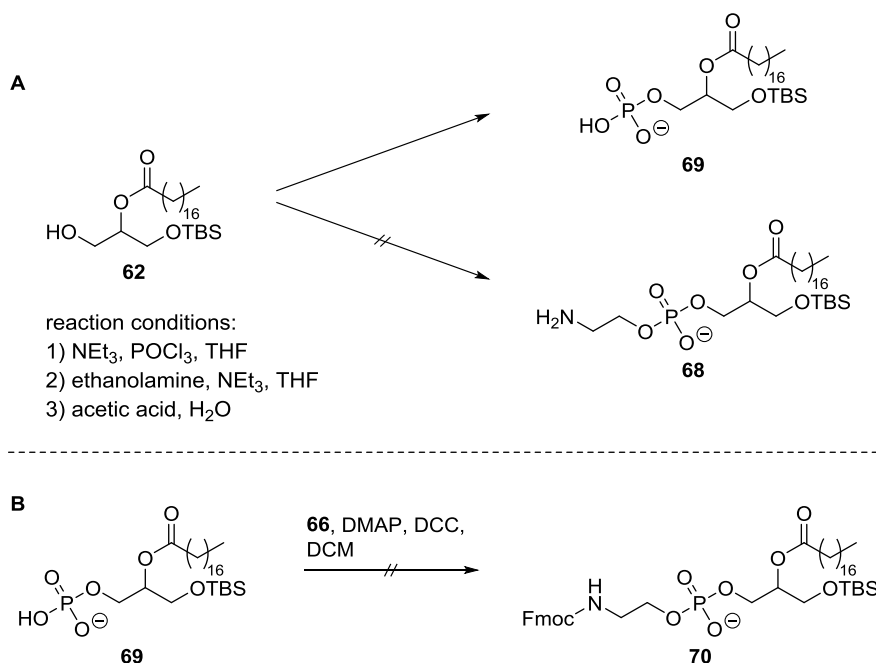
Scheme 3.29 First step of head group generation leading to formation of the desired product **64** and intermediate **65**.

After several attempts using these conditions as well as applying the coupling step of ethanolamine to intermediate **65** separately, no improvement was observed. Since this reaction is known to require dry conditions, the amounts of water traces were further reduced by drying DIPEA and ethanolamine previous to usage over molecular sieve. However, the reaction result stayed the same. Nonetheless, to connect ethanolamine to **65** other conditions were tested. To avoid amide bond formation the amine group of ethanolamine was fluorenylmethoxycarbonyl (Fmoc)-protected using standard conditions (Scheme 3.30, **A**).^[186] *N*-Fmoc-ethanolamine (**66**) was obtained in quantitative yield and then brought to reaction with **65** by addition of DCC and DMAP in DCM (Scheme 3.30, **B**) but no product was formed.

Presumably the early assembly of the fluorophore hindered further reactions, as head group incorporation. On the other hand, previous generation of the charged PC-head group inhibits fluorophore coupling. Therefore, starting from compound **62** a phosphatidylethanolamine (PE) head group was to be generated (Scheme 3.31), followed by fluorophore incorporation with subsequent methylation of the amine for PC-generation.



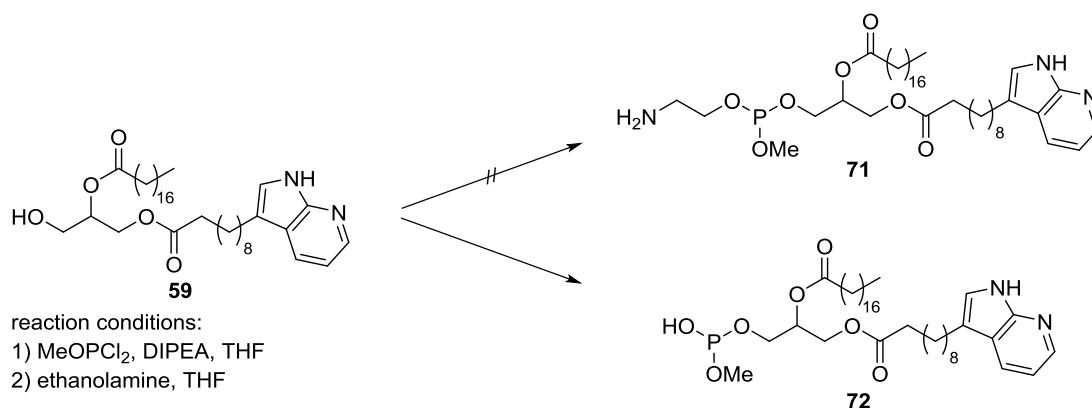
Scheme 3.30 Fmoc-protection of ethanolamine in aqueous Na_2CO_3 solution (**A**); Coupling attempt to connect *N*-Fmoc-ethanolamine (**66**) to **65** (**B**)



Scheme 3.31 PE-head group generation previous to fluorophore coupling for subsequent methylation of 68 (A). Coupling attempt of 69 with *N*-Fmoc-ethanolamine (66) (B).

Following this approach, phosphorylation could be observed but no coupling of ethanolamine took place. To subsequently bind ethanolamine to the phosphate group the conditions depicted in Scheme 3.30, **B** were applied (Scheme 3.31). High resolution mass spectrometry verified that the formed reaction product was not the desired compound 70 and attempts to identify the substance were unsuccessful.

Since the synthesis of target compound 55 following the described routes was not possible, other approaches for head group generation came into focus. Instead of incorporating a phosphor(V) unit, a phosphor(III) compound was used. Treatment of 59 with methyl dichlorophosphite and DIPEA with subsequent addition of ethanolamine was proposed to generate the head group precursor 71 (Scheme 3.32).^[187]

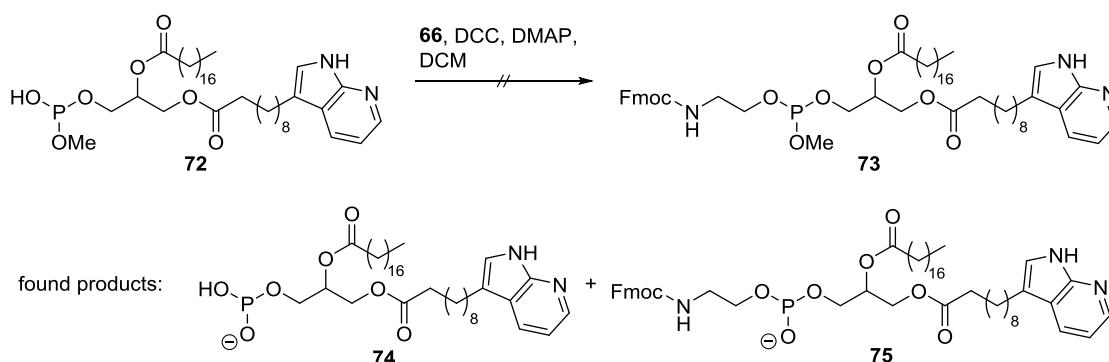


Scheme 3.32 Attempted phosphitylation of 59 using methyl dichlorophosphite.

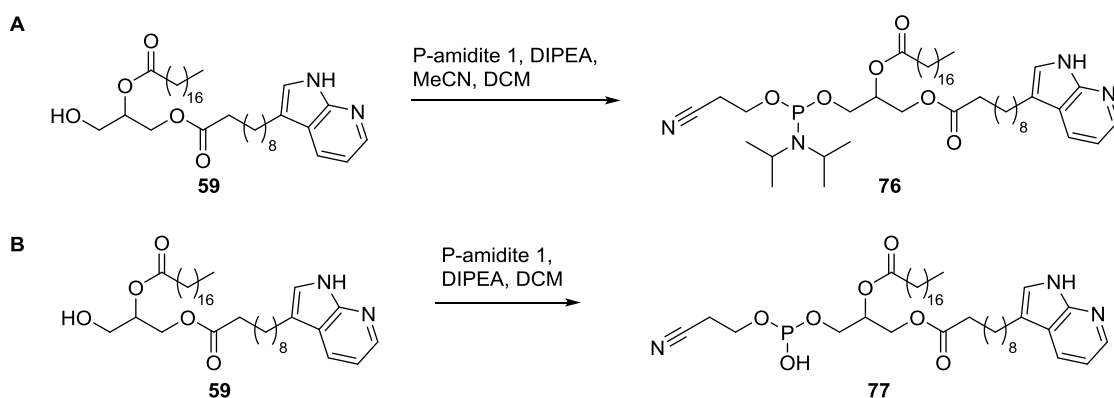
By application of a phosphite instead of phosphoryl chloride no conversion was observed at first. After increasing the amount of phosphite from 1.20 equivalents to 2.40 equivalents small amounts of intermediate product **72** were formed but no product **71**. Increasing reaction times and varying the volume of solvent used did not improve the reaction outcome. To investigate every angle a coupling attempt of **72** with *N*-Fmoc-ethanolamine (**66**) using DCC and DMAP was undertaken (Scheme 3.33). Mass spectrometry revealed that the desired product **73** did not form but starting material (**74**) as well as coupling product (**75**) lacking a methyl group were detected in traces.

A well-known and broadly used procedure to incorporate phosphite units is the application of phosphoramidites. Especially in DNA synthesis phosphoramidites are used for nucleoside building block preparation. Therefore, chloro-(2-cyanoethyl)-*N,N*-diisopropylaminophosphoramidite (P-amidite **1**) was used. A solution of **59** in acetonitrile (MeCN) was treated with DIPEA and P-amidite **1** and stirred at r.t. for 4 h (Scheme 3.34).^[188] To increase solubility 20 % (v/v) of DCM was added in respect to total solvent volume, but applying these conditions led to very low product **76** formation. The reaction time was elongated to achieve better yields and after 24 h no further change in reaction was observed on TLC. Interestingly, with increased reaction time no product formation was observed but small amounts of starting material along with partially deprotected compound **77** (Scheme 3.34, A).

For optimisation MeCN was completely substituted by DCM while keeping the remaining reaction conditions stable. After 4 h barely any starting material was left but no formation of the desired product **76** had occurred. Instead, partially deprotected **77** was formed (Scheme 3.34, B).



Scheme 3.33 Coupling reaction of **72** and **66** resulting in two demethylated species **74** and **75**.



Scheme 3.34 Phosphitylation of **59** using P-amidite 1 (**A**). Change of solvents led to cleavage of the diisopropylamino moiety forming **77** (**B**).

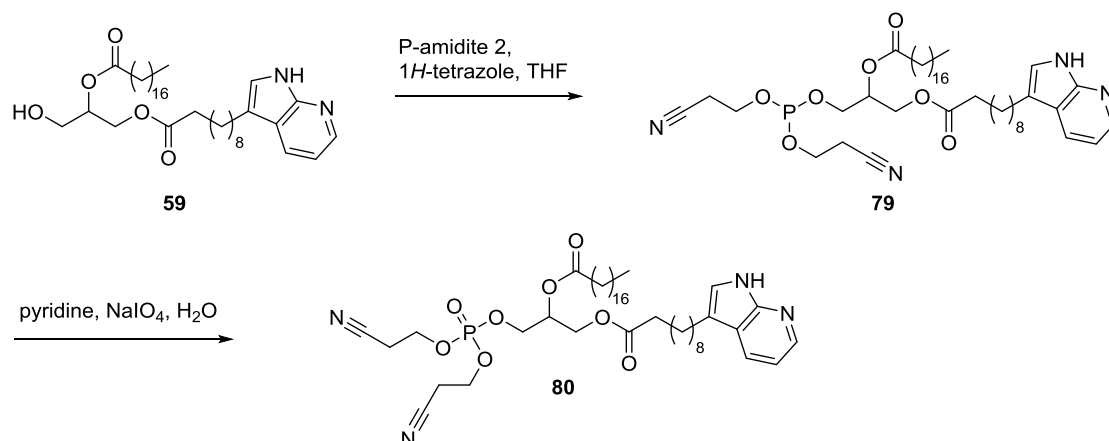
Since changing completely to DCM as solvent proved to be unfeasible, the solvent was changed again in favour of THF. Furthermore, DIPEA dried over molecular sieve was used to assure water-free conditions. Changing the solvent to THF produced the same result as utilization of DCM and yielded in formation of **77**.

Using P-amidite 1 for phosphitylation was additionally tested on the unlabelled compound **62** (Scheme 3.35). After 4 h using MeCN as solvent, conversion of the starting material was complete but just a small amount of product **78** was formed. Attempts to isolate the product were unsuccessful and besides **62** and product **78** just degraded P-amidite 1 could be identified.



Scheme 3.35 Phosphitylation of **62** using P-amidite 1.

To avoid the unwanted cleavage of the diisopropylamino group bis(2-cyanoethyl)-*N,N*-diisopropylphosphoramidite (P-amidite 2) was used for phosphitylation. After the coupling step, the phosphite was directly converted into a phosphate using sodium peroxidate (Scheme 3.36).

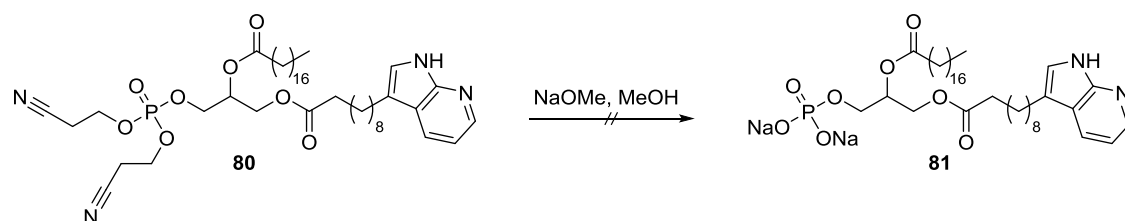


Scheme 3.36 Phosphitylation of **59** using P-amidite 2 followed by oxidation for phosphate generation.

A solution of **59** and P-amidite 2 in THF was cooled to 0 °C, treated with 1H-tetrazole and stirred at r.t. for 1 h. The reaction mixture was cooled again to 0 °C, treated with pyridine and a solution of sodium peroxidate in water and stirred at r.t. for 1 h.^[189] Mass spectrometry of the crude product revealed complete conversion of the starting material **59** under formation of product **80** along with unidentified side products.

Without further purification except extraction during workup the phosphate unit of compound **80** was deprotected using sodium methoxide (1 % (w/w) in methanol) over the period of three days.^[189] Analysis of this reaction showed that conversion of **80** was complete but no product **81** formed.

As already mentioned, all synthetic approaches including stearic acid at the *sn*-2 position have been repeated with oleic acid at this position to ensure detectability of each reaction product and thereby enable purification via FC. Reaction conditions were not altered when using oleic acid instead of stearic acid and the obtained reactions yields were comparable.

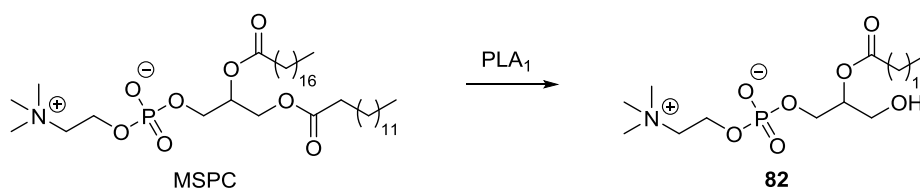


Scheme 3.37 Cleavage of the 2-cyanoethyl protection groups of **80**.

3.8 Enzymatic Synthesis of Modified Lipid Derivative 55

After the purely synthetic route proved to be highly time and energy demanding without promising results, an entirely different strategy was approached. Instead of synthesising modified lipids starting from solketal, an isolated, natural lipid can be modified using an enzyme. The commercially available 1-myristoyl-2-stearoyl-*sn*-glycero-3-phosphocholine (MSPC) was chosen as lipid. For modification the likewise commercially available enzyme phospholipase A₁ (PLA₁) from *Thermomyces lanuginosus* was selected. PLA₁ is known to selectively hydrolyse ester bonds of PC-lipids at *sn*-1 position.^[190] This semi-enzymatic route consists of two steps: In the first step myristic acid is cleaved off to generate a free hydroxy functionality (1-lysoPC, **82**), shown in Scheme 3.38. The second step contains coupling of the fluorophore **40** (Scheme 3.39) to obtain the desired target compound **55**.

For 1-lysoPC **82** generation MSPC was dissolved in Tris buffer with additional 5 % MeOH for solvation purposes. The enzyme was added and the reaction mixture shaken at 37 °C for 30 min. After extraction with diethyl ether, the organic solvent was removed to obtain **82**.^[191,192] To verify the success of this reaction preparative thin layer chromatography (PLC) was used. The crude reaction product, starting material and two standard compounds for reference were applied to the plate and a mixture of chloroform, methanol, acetic acid and water (25:15:4:2) was used as eluent system. Once the PLC was finished and dried, it was treated with aqueous CuSO₄ solution, heated to 120 °C for approximately 30 min. The now charcoaled substances appear as brown stains on the plate. Evaluation of the plate revealed complete conversion of the starting material, a new 1-lysoPC band had appeared as well as two other, unknown bands. Attempts to isolate **82** were unsuccessful but after changing the solvent for extraction from diethyl ether to a chloroform/MeOH mixture (1:1) further purification was no longer necessary. After just a few repetitions of this reaction no product would form anymore without any obvious cause. Various lipid and enzyme concentrations were tested as well as the amount of methanol used for increased solvation. Reaction temperature and time were diversified and different shaking rates reviewed.



Scheme 3.38 Myristic acid hydrolysis at *sn*-1 position to generate lysolipid **82**; buffer system used: Tris (200 mM), pH 7.5.

The activity of the enzyme was tested and showed still high conversion rates with *p*-nitrophenyl palmitate as substrate. Besides Tris buffer (200 mM), Tris-HCl buffer (200 mM) and Bis-Tris propane buffer (20 mM) were tested. All buffer solutions were freshly prepared every four weeks, the pH was measured and readjusted to 7.5, if necessary. The lipid used for hydrolysis was screened for degradation using NMR spectroscopy and mass spectrometry, which both showed no evidence of decomposition. Since the reaction was carried out in reaction tubes made of polypropylene, tubes of different companies were tested to check for cytotoxicity or lability towards specific solvents. None of these variations led to product formation in good or at least moderate yields again.

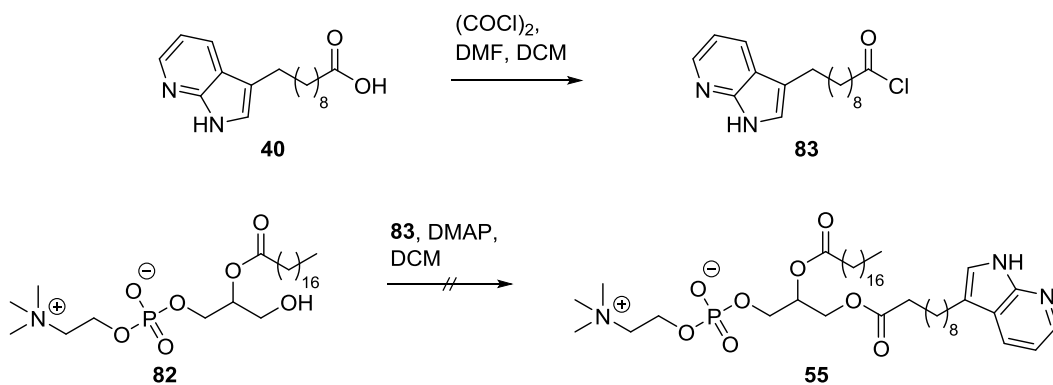
Following another procedure^[193], MSPC was dissolved in diethylether in a snap-cap vial and a solution of enzyme in Bis-Tris propane buffer was added, whereby the ether volume was four-times greater than the buffer volume. The mixture was vigorously shaken for 20 min and extracted using chloroform. With these conditions product formation was obtained but in low yields and purity. Therefore, the organic solvent to buffer ratio was varied to 3:2 and the reaction time decreased to 15 min, which led to a great increase in yield and improved purity. For further optimisation the organic solvent was exchanged from diethyl ether to chloroform. Indeed, applying these changes, complete conversion was achieved with rather pure product **82** in very high up to quantitative yields. The purity was further improved as the volume of solvents was decreased by one-third in total.

After successful hydrolysis of MSPC to generate 1-lysoPC **82**, the next step was to couple fluorophore **40**. For ester bond formation the same coupling conditions as previously described, using DCC and DMAP, were applied (Scheme 3.39). After 24 h the starting material was completely processed but no product was formed. The resulting compounds detected in mass spectrometry could not be identified.

To increase the electrophilic character of the fluorophore, transformation of **40** into an acyl chloride (**83**) was conceived. For conversion a solution of **40** in DCM was cooled to 0 °C and treated with DMF and oxalyl chloride (Scheme 3.40). After stirring for 1.5 h at 0 °C the organic solvent was removed.^[194] Without intermission it was redissolved in DCM and added to a solution of 1-lysoPC **82** and DMAP in DCM at 0 °C and stirred at r.t. for 4 h.^[166]



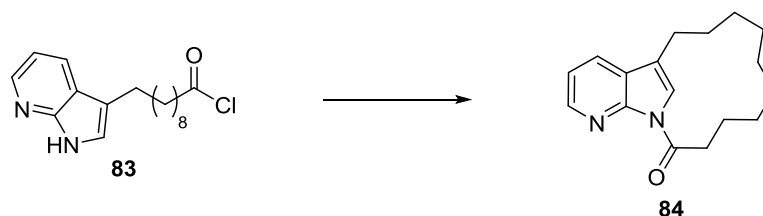
Scheme 3.39 Labelling attempt of 1-lysoPC **82** with fluorophore **40**.



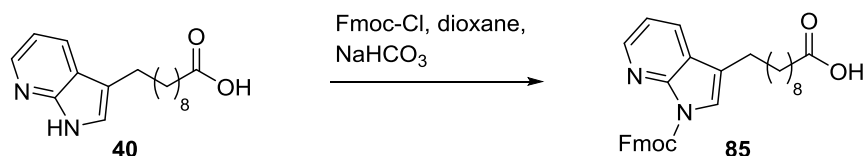
Scheme 3.40 Conversion of fluorophore **40** into an acyl chloride with subsequent coupling attempt to generate **55**.

The coupling reaction yielded no product. One reason might be that the acyl chloride did not form, another possible explanation is that the activated acyl chloride undergoes an immediate ring closing reaction (Scheme 3.41) with the amino functionality of 7-azaindole to build a lactam **84**.

To inhibit the lactam formation the amino functionality had to be protected. The required protecting group needed to fulfil several demands. A suitable protecting group has to bind selectively to the secondary amine without interfering with the carboxylic acid and be acid stable to endure reaction conditions for acyl chloride generation. Furthermore, the labelling reaction of **82** with fluorophore **40** must not be disturbed by the protecting group, while the group itself has to be stable under coupling conditions. Finally, cleavage of the protecting group should take place in a rapid fashion under mild conditions to ensure that no decomposition of the labelled lipid occurs. The chosen protecting group was Fmoc (Scheme 3.42), which is stable under acidic conditions as well as under a broad variety of coupling conditions. It binds amines selectively and cleavage of Fmoc using piperidine is mild enough to not impair the lipid.

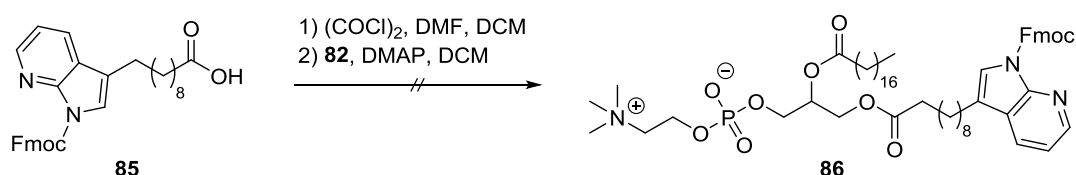


Scheme 3.41 Possible ring closing reaction of **83** to form lactam **84**.



Scheme 3.42 Protection of amine **40** using Fmoc-Cl.

For Fmoc-protection **40** was dissolved in aqueous NaHCO_3 solution (10 % w/w) and treated dropwise with Fmoc-Cl in dioxane with at $0\text{ }^\circ\text{C}$. The reaction mixture was stirred at $0\text{ }^\circ\text{C}$ for 1 h and then at r.t. for 4 h, while the reaction was monitored via TLC. Using this procedure, just traces of product were formed, which is why the reaction time was prolonged and dioxane was substituted by DMF to enhance alkalinity. Applying these conditions no increased product formation was obtained, so the reaction conditions were varied again. The solvent was changed back to dioxane but another base was added. At first DIPEA was used as additional base. When after 24 h no reaction occurred, triethylamine was added as a stronger base. After treatment with triethylamine, a new spot on TLC appeared but mass spectrometry revealed no product formation. Since the first tested conditions provided at least product traces, those were applied again with elongated reaction time to four days. After 4 d approximately 50 % of the starting material was converted into product **85** and with extraction at different pH values as well as varying solvents the unprotected fluorophore and the protected **85** could readily be separated from each other. Attempts to isolate **85** from side products were unsuccessful. To further increase product formation the reaction time was increased to 7 d, after which just small amounts of starting material were left. Since complete purification remained unsuccessful the unpurified product was used for acyl chloride generation. The previously described conditions using oxalyl chloride (Scheme 3.40) were applied with subsequent coupling reaction with lysoPC **82** (Scheme 3.43). Even using the Fmoc-protected fluorophore **85** did not lead to formation of the desired labelled lipid **86**. The most probable reason seemed to be that no acyl chloride was generated. Therefore, instead of oxalyl chloride thionyl chloride was tested (Scheme 3.44).

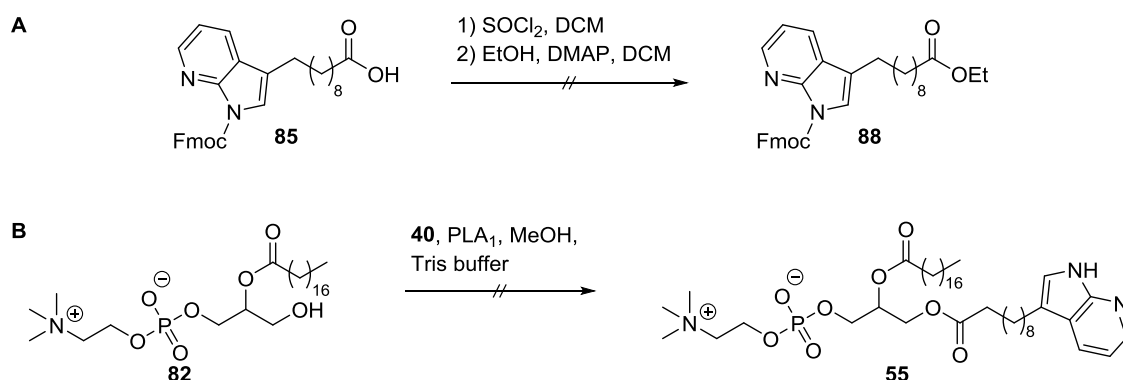


Scheme 3.43 Labelling attempt via conversion of **85** into an acyl chloride followed by coupling with **82**.

To generate acyl chloride **87** a solution of **85** in DCM was heated to 80 °C and treated with thionyl chloride for 30 min. After the mixture had cooled down to r.t., excess of thionyl chloride was removed *in vacuo*^[195] and then brought to reaction with ethanol using the previously described conditions (Scheme 3.44, **A**). Analysis via mass spectrometry revealed that just deprotected fluorophore **40** was obtained.

This semi-enzymatic route yielded the hydrolysed lysoPC **82** after short reaction time and in good purity in quantitative manner but target compound **55** could not be synthesised. Since the enzyme PLA₁ is known to not just cleave the respective fatty acid at *sn*-1 position but to be able to incorporate specific fatty acids as well^[196–198], a full-enzymatic approach was made. To test whether or not fluorophore **40** would be accepted as substrate by PLA₁, lysoPC **82** and fluorophore **40** were brought to reaction with the enzyme (Scheme 3.44, **B**). **40** and **82** were dissolved in MeOH and added to a solution of PLA₁ in Tris buffer at pH 7.5. After incubation under shaking at 37 °C for 30 min, the mixture was extracted using chloroform and the solvent removed under reduced pressure. Analysis of the residue revealed that neither lysoPC nor fluorophore was left, neither could the desired product be detected.

After these tests no further efforts were made to synthesise target compound **55**. Adviceable for further attempts is screening of better suitable protecting groups. One protecting group worth testing is allyloxycarbonyl (Alloc), which is acid stable and can be cleaved via transition metal catalysed cleavage. The purely synthetic route using P-amidite 2 could still lead to formation of the target compound **55**, if the protecting groups were not cleaved after phosphitylation and oxidation to phosphate. Instead direct incorporation of ethanolamine via a substitution reaction should enable formation of compound **55**.



Scheme 3.44 Test reaction to check for acyl chloride generation using **85** and ethanol (**A**). Full-enzymatic attempt for **55** synthesis using enzyme PLA₁ (**B**).

3.9 Fluorescence Measurements of 7-Azaindole-Labelled Lipids

As the synthesis of the 7AI-labelled lipid precursor **59** was successful, incorporation of **59** into membranes was intended. Thereby, the behaviour of **59** in artificial membranes was to be characterised using fluorescence spectroscopy to pave the way for its utilisation in fusion experiments in artificial and possibly natural systems. At first, to determine whether the modification of 7AI to generate **59** altered the fluorescence properties, fluorescence spectroscopy of **59** was performed by applying an excitation wavelength of 288 nm. The first measurements were performed with 2.5 μM **59** in the polar protic solvent methanol, which is known to influence the fluorescence of 7AI. At a wavelength of 390 nm an emission maximum (λ_{max}) was detected along with a broad and shallow shoulder at ~ 480 nm (Figure 3.6). These findings show a red shift of λ_{max} of about 16 nm in comparison to data regarding 7AI in literature.^[18,19] A possible explanation for this shift might be the presence of the neighbouring long alkyl chain, which might locally decrease the polarity of the surrounding of the fluorophore.

Since membrane fusion experiments are usually not performed in methanol, fluorescence measurements were repeated with **59** suspended in an aqueous solution. As solvent a HEPES buffer (20 mM HEPES, 1 mM EDTA, 100 mM KCl, pH 7.4) was used. The labelled compound was suspended in buffer and via ultrasonication a homogeneous solution of 2.5 μM **59** was prepared. The fluorescence spectrum, shown in Figure 3.7, revealed a drastically lowered fluorescence intensity, probably due to water molecules blocking the tautomerisation, and a λ_{max} of 400 nm, which is in good accordance to literature-known data for 7AI.^[155]

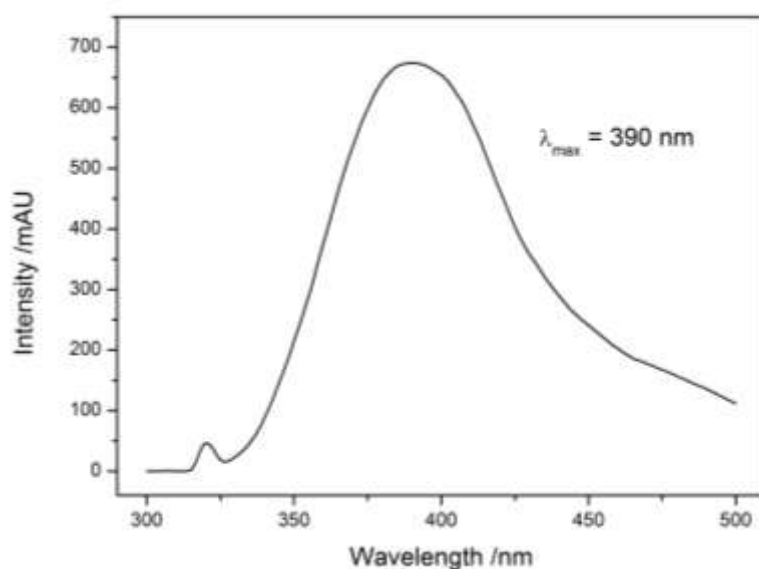


Figure 3.6 Fluorescence spectrum of **59** in MeOH with an excitation wavelength of 288 nm and an emission maximum at 390 nm.

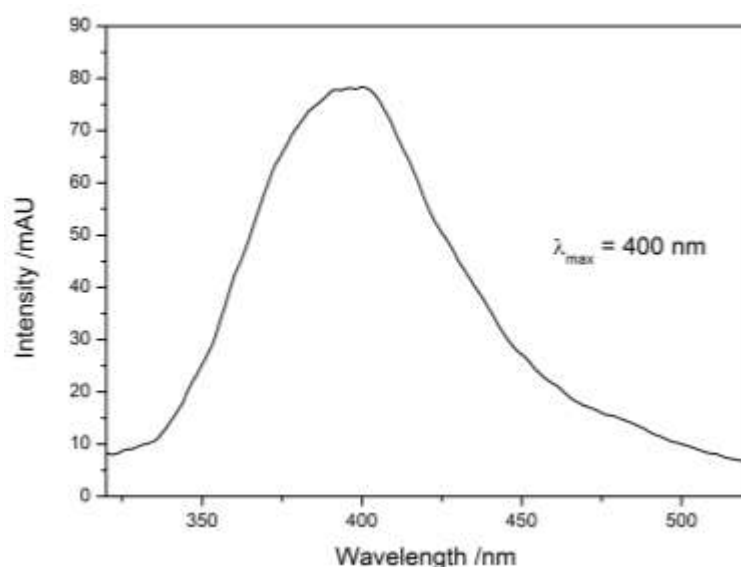


Figure 3.7 Fluorescence spectrum of **59** suspended in HEPES buffer. The emission maximum emerged at 400 nm.

After having obtained the spectra of **59** in aqueous and alcoholic environment, the labelled lipid precursor was incorporated into artificial membranes. Thereto vesicles consisting solely of DOPC and **59** were prepared following GP2.1 and GP2.2 using the previously mentioned HEPES buffer. In total, the amount of substance was 2.5 μmol in a ratio of labelled to unlabelled lipids of 1:1000. The generated vesicles were measured immediately after extrusion and again, an excitation wavelength of 288 nm was applied. Figure 3.8 pictures the obtained fluorescence spectrum with $\lambda_{\text{max}} = 430 \text{ nm}$. Considering former studies regarding 7AI in hydrophobic environment, a different emission maximum was expected. Analysis of 7AI-labelled transmembrane proteins revealed a maximum of $\lambda_{\text{max}} = 372 \text{ nm}$ after incorporation into membranes consisting of 1,2-dimyristoyl-*sn*-glycero-1-phosphocholine (DMPC).^[199] A possible explanation of the obtained spectrum is that the 7AI-modified fatty acid of **59** does not insert into the membrane. Instead, the alkyl chain tilts suchlike that the fluorophore is located in the polar head group region of the membrane. This theory is supported by the fact that tryptophan, which bears the structurally very similar indole moiety in the side chain, is often used as a peptide anchor. It embeds in the head group area and therefore stabilises transmembrane proteins in the membrane.^[200,201]

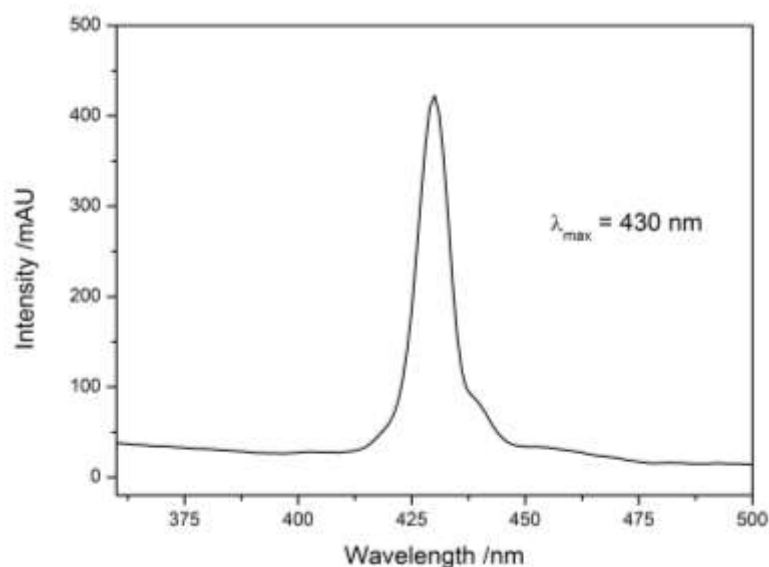


Figure 3.8 Fluorescence spectrum of **59** incorporated into DOPC vesicles in a ratio of 1:1000 showed an emission maximum at 430 nm.

To analyse the influence of **59** concentration in membranes, vesicles with a **59** to DOPC ratio of 1:250 were prepared. Instant fluorescence measurements of this vesicle species yielded the same emission wavelength with slightly decreased intensity (spectrum not shown). The decrease in fluorescence intensity by increased fluorophore concentration was not expected but might be explained by self-quenching or augmented blocking of tautomerisation by water molecules.

Nevertheless, vesicles with a drastically increased **59** to DOPC ratio of 1:20 were established, since lipid rafts at membrane fusion sites are supposed to be greatly enriched in PIP₂. The obtained spectrum still exhibits a local emission maximum (λ_s) at the wavelength of 429 nm but the dominating signal is a maximum (λ_{max}) at 389 nm with an overall explicitly decreased fluorescence intensity (Figure 3.9). The signal at $\lambda_{\text{max}} = 389 \text{ nm}$ cannot be assigned to 7AI in a hydrophobic environment like a membrane core but might be generated by dimer formation of the fluorophore in the polar head group region. This possibility is supported by the nearly identical maximum of **59** obtained in methanol (Figure 3.6) elicited by hydrogen bond formation in a polar environment.

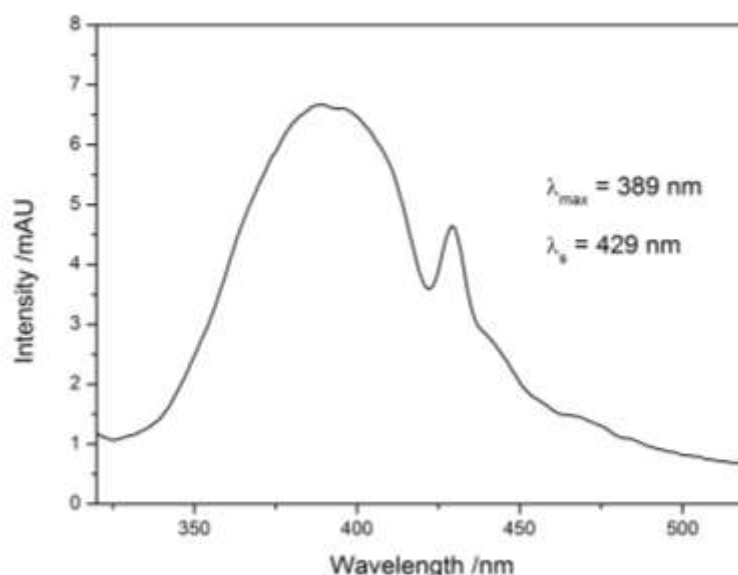


Figure 3.9 Fluorescence spectrum of high **59** concentration in DOPC vesicles in a 1:20 ratio exhibiting a drastically decreased fluorescence with a maximum comparable to **59** in MeOH and a second, smaller maximum at 429 nm.

In conclusion, the synthesis of a 7AI-labelled lipid precursor with no head group was successful. Subsequent incorporation of fluorophore and head group proved to be a difficult task but investigations towards finding a suiting protecting group should enable to complete the synthesis of the labelled DOPC compound **55**. Before performing further attempts to finalise the synthesis of **55**, compound **59** was tested for membrane labelling. Fluorescence spectroscopy revealed that insertion of the fluorophore into the hydrophobic domain of the membrane did not take place. Instead, the 7AI moiety seems to rest on the membrane surface in the polar head group region. For this reason, distinct structural modifications of the target compound **55** are necessary to generate a driving force for fluorophore incorporation into the hydrophobic membrane domain.

4 *gem*-Difluorinated Fatty Acids

4.1 Introduction

One of the most versatile and important second messenger is Ca^{2+} , as discussed in detail in chapter 2, but it is by no means the only one. A tremendous variety of compounds can act as signalling agent. The phytohormone jasmonic acid for example is an essential signal compound in gene expression induced by wounding. Evolution of plants created several chemical defence mechanisms upon wounding, such as the production of toxic compounds or the formation of attractants towards herbivorous insect predators.^[2] In these and other plant responses jasmonic acid plays a key role. It is generated by hydroperoxidation of polyunsaturated fatty acids followed by further processing and hence belongs to the class of oxylipins.^[22]

The insertion of dioxygen into polyunsaturated fatty acids containing a 1*Z*,4*Z*-penta-diene unit to generate the respective hydroperoxidised derivatives is catalysed by the large lipoxygenase family in a regio- and stereoselective manner.^[23,202] Non-enzymatic autoxidation is highly unspecific, yielding a variety of twelve diverging mono-hydroperoxidised derivatives in the case of arachidonic acid. In contrast, dioxygenation catalysed by lipoxygenases generally leads to one specific hydroperoxide enantiomer.^[203]

Lipoxygenases have already been investigated for several decades^[204] and a tremendous amount of knowledge about their incidence, structure and functionality has accumulated.^[24] Still debated is the exact mechanism of substrate conversion, especially the orientation of polyunsaturated fatty acids in the active site. Therefore, this project aims for synthesising the geminal difluorinated substrate analogue 11,11-difluoro-linoleic acid, which shall be bound by the enzyme. By substituting both hydrogen atoms at C-11 by fluorine atoms no digestion of the substrate can take place and co-crystallisation experiments become feasible in order to resolve the substrate orientation in the active pocket.

4.2 Lipxygenases

Fatty acids represent a major part of mammal nutrition and especially polyunsaturated fatty acids (PUFAs) like linoleic acid are essential. The necessity of PUFAs was already discovered in 1929 by G. BURR and M. BURR in fat exclusion experiments on rats.^[205] Since more than half of naturally occurring fatty acids are unsaturated^[206,207], their oxidation constitutes a great portion of lipid metabolism.^[202] One possible reaction pathway is the formation of oxylipins such as hydroperoxy fatty acids.^[3] These are then further metabolised to signalling agents, e.g. jasmonates or leaf aldehydes^[22] in plants and leukotrienes or lipoxins in mammals.^[208]

The digestion of PUFAs is performed by enzymes like lipxygenases (LOXs, linoleate:oxygen oxidoreductases). LOXs belong to a non-heme iron containing enzyme family that performs hydroperoxidase reaction, leukotriene synthase reaction, and most importantly, generates hydroperoxy fatty acids by dioxygenation of PUFAs, containing a (1Z,4Z)-pentadiene unit.^[2,3] LOXs consist of a single polypeptide chain of approximately 75–80 kDa in animals^[209] and 95–100 kDa in plants^[3], featuring two domains (Figure 4.1, left). The bigger C-terminal domain of 55–65 kDa in plant LOXs consists of α -helices and contains the catalytically active centre, while the β -barrel-forming N-terminal domain of 25–30 kDa possibly participates in membrane binding.^[3,210,211]

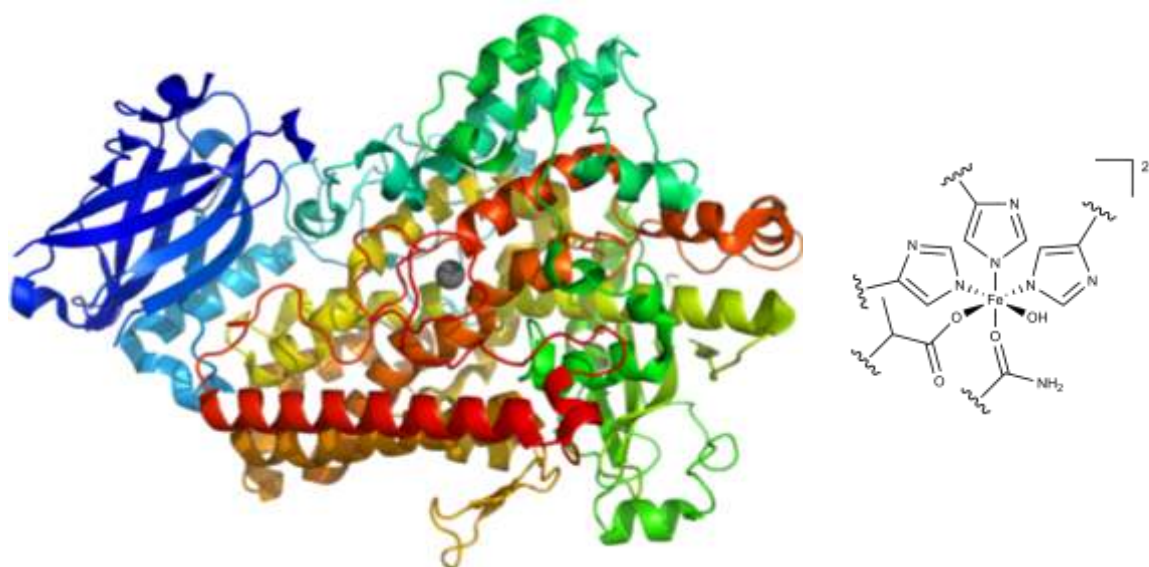


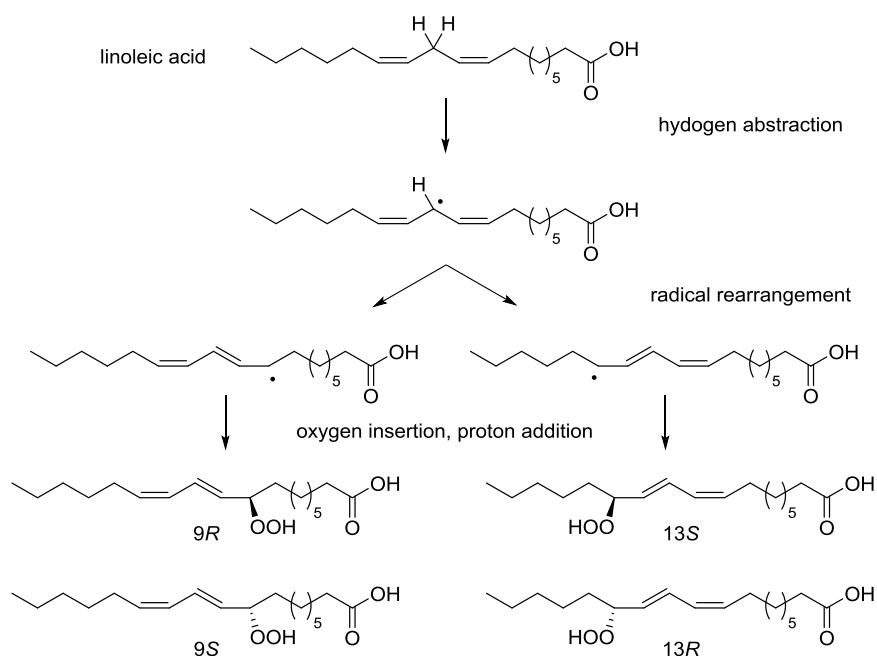
Figure 4.1 Crystal structure of a soybean 13S-LOX with the β -barrel shown in dark blue and the α -helical domain containing the active site with the catalytically active iron ion in grey (left)^[246]; Coordination sphere of the iron ion within the active centre (right).^[3]

The active site contains one iron atom that is, in case of plant LOXs, coordinated by three histidines, one asparagine and the C-terminal isoleucine in an octahedral fashion (Figure 4.1, right).

Historically, two ways to classify plant LOXs have been established and are still commonly used. An earlier categorisation differentiated between type 1-LOXs, that exhibit their activity optimum at alkaline pH, and type 2-LOXs with a neutral pH optimum.^[212] More recently, plant LOXs are classified by their subcellular localisation, meaning plastidial (type 2-LOXs) and extraplastidial (type 1-LOXs) LOXs, or the positional specificity of linoleic acid oxygenation.^[3] Categorisation by positional specificity yields 9-LOXs and 13-LOXs, respective to the carbon atom carrying the hydroperoxide after conversion.^[24] Including stereochemistry a total of four linoleic acid LOX (9*S*, 9*R*, 13*S*, 13*R*) classes arise.

The exact mechanism of the hydroperoxidation reaction is still under investigation but can be divided into three steps (Scheme 4.1). The first reaction step is the stereoselective hydrogen abstraction under generation of a free radical. The hydrogen is cleaved off the methylen carbon of the (1*Z*,4*Z*)-pentadiene unit by Fe³⁺-OH under Fe²⁺-OH₂ formation, allowing delocalisation of the radical over both double bonds.^[213] The rearranged radical then regioselectively binds an oxygen molecule in an antarafacial manner. The antarafacial oxygenation has been verified by experiments using deuterium or tritium labelled fatty acids.^[214,215] Incorporation of O₂ at positions 1 or 5 of the pentadiene unit (respectively position 9 or 13 for linoleic acid) yields a conjugated diene and is therefore thermodynamically favoured over position 3. Reduction of the peroxy radical completes the catalytic cycle under generation of four possible products.^[213]

As the distinct cause for regio- and stereospecificity of individual LOXs is still to be discovered, differing theories have been proposed.^[3,24,213] The space-related model proposes a general tail-first (methyl group first) orientation, in which the depth of the active site dictates the position of lipoygenation.^[216] The substrate orientation hypothesis suggests the orientation of the entering substrate as a key factor. Entering the active site tail-first would lead to dioxygen insertion at C-13, while head-first, penetrating primarily with the carboxylic acid, results in lipoygenation at C-9.^[217]



Scheme 4.1 LOX reaction pathway showing oxygenation of linoleic acid with respect to the regio- and stereospecificity yielding four possible products. Scheme adapted from [3].

Modelling and mutagenesis studies revealed an arginine (R) in the binding pocket of plant 13-LOXs, which might act as a counterpart for the carboxy group in case of head-first substrate orientation and therefore favours dioxygen insertion at C-9. The arginine is usually shielded by sterically demanding amino acid residues like phenylalanine (F) or histidine (H), preferring the tail-first orientation over head-first (Figure 4.2, left). In plant 9-LOX the less bulky amino acid valine (V) substitutes F/H, minimising the shielding effect (Figure 4.2, right).

Besides the regiospecificity the stereospecificity of the enzyme determines the reaction product. Using mutation studies COFFA *et al.* discovered that a single conserved residue is responsible for *R* or *S* stereocontrol. The sterically more demanding alanine (A) was identified in *S*-LOXs and the smaller glycine (G) in *R*-LOXs.^[203] This so-called 'Coffa site' is located in the active site opposite to the complexed iron ion. As it turned out, A/G-exchange of the residue does not just alter the chirality but switches the position of dioxygen insertion as well. Hence, a 9*S*-LOX will be converted after mutation into a 13*R*-LOX.

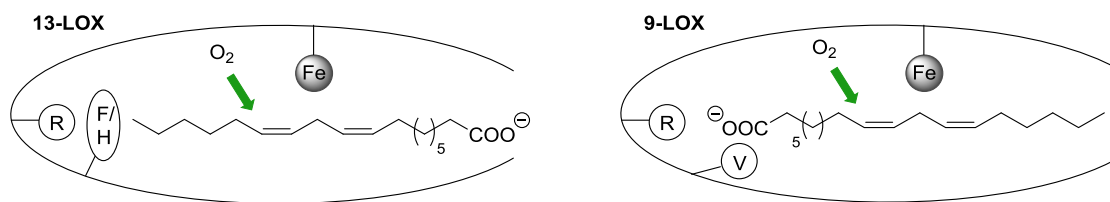


Figure 4.2 Orientation-dependent model depicting linoleic acid in an active site of a 13-LOX in tail-first orientation (left) and of a 9-LOX in head-first orientation (right). Figure adapted from [3].

Assuming that in all LOXs oxygen is furnished from the same side, these findings can be explained by the substrate orientation model.^[3] In case of 13*S*- and 9*R*-LOXs substrate entering of the binding pocket occurs in tail-first manner, leading to a shielded C-9 position in the 13*S*-LOX by the alanine side chain. Since in the 9*R*-LOX enzyme this residue is absent, preferred dioxygen insertion at C-9 can take place, yielding the *R* product (Figure 4.3, top). For 9*S*- and 13*R*-LOXs the substrate penetrates the binding site head-first. In this case the alanine residue blocks C-13 and the respective 9*S*-product is formed. The 13*R*-LOX enzyme is lacking the methyl group, which is why dioxygenation at C-13 in *R*-configuration is favoured (Figure 4.3, bottom).

However, it must be mentioned that exceptions of this model are known. Crystallographic analysis of an inhibitor-bound 13-LOX revealed a U-shaped channel for substrate binding but the exact orientation of substrates within the active site remains elusive.^[218] Therefore, further investigations are required to fully uncover the mechanism of LOX-catalysed fatty acid hydroperoxidation.

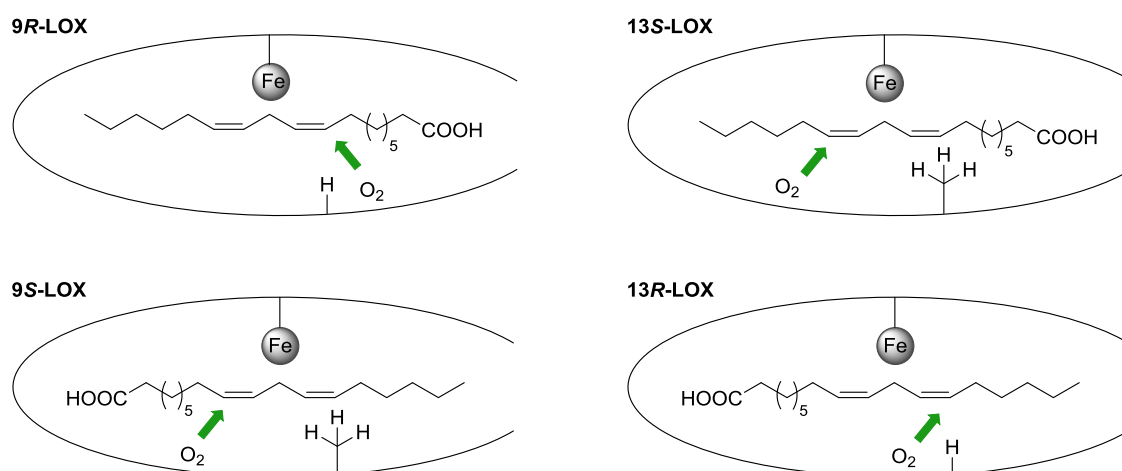
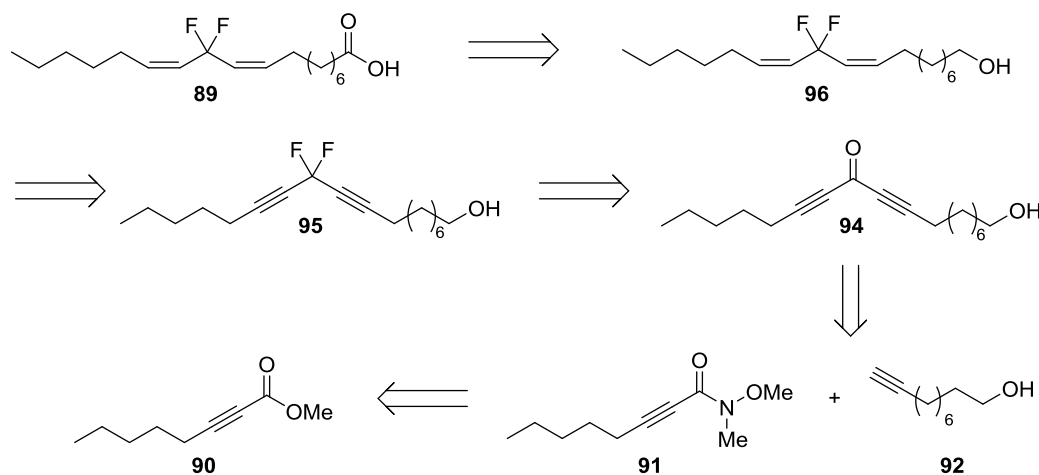


Figure 4.3 Explanation of LOX stereospecificity using the substrate orientation model under assumption that O₂ is inserted from the same side. Figure adapted from [3].

4.3 Synthesis of 11,11-Difluorolinoleic acid

In 2011 PRÉVOST *et al.* published an approach for the total synthesis of the bioactive ceramide symbioramide^[219]. On the basis of this strategy and under consideration of the work done so far on this project by former PhD-students, the decision was made to synthesise 11,11-difluorolinoleic acid (**89**) with the strategy shown in Scheme 4.2. At the beginning, an ester containing an alkynyl moiety on second position will be converted into a Weinreb amide^[220], which will then undergo a reaction with a terminal alkyne to form a ketone. After this step, the final chain length of 18 carbon atoms will already be achieved. Substitution of the keto-moiety by two fluorine atoms should yield the *gem*-difluorodiyne. Hydration of both alkynes using Lindlar catalyst should result in *cis*-alkenes, followed by oxidation of the terminal alcohol to form a carboxylic acid function. During the synthesis, the terminal alcohol has to be protected using a protecting group orthogonal to all employed reaction conditions.

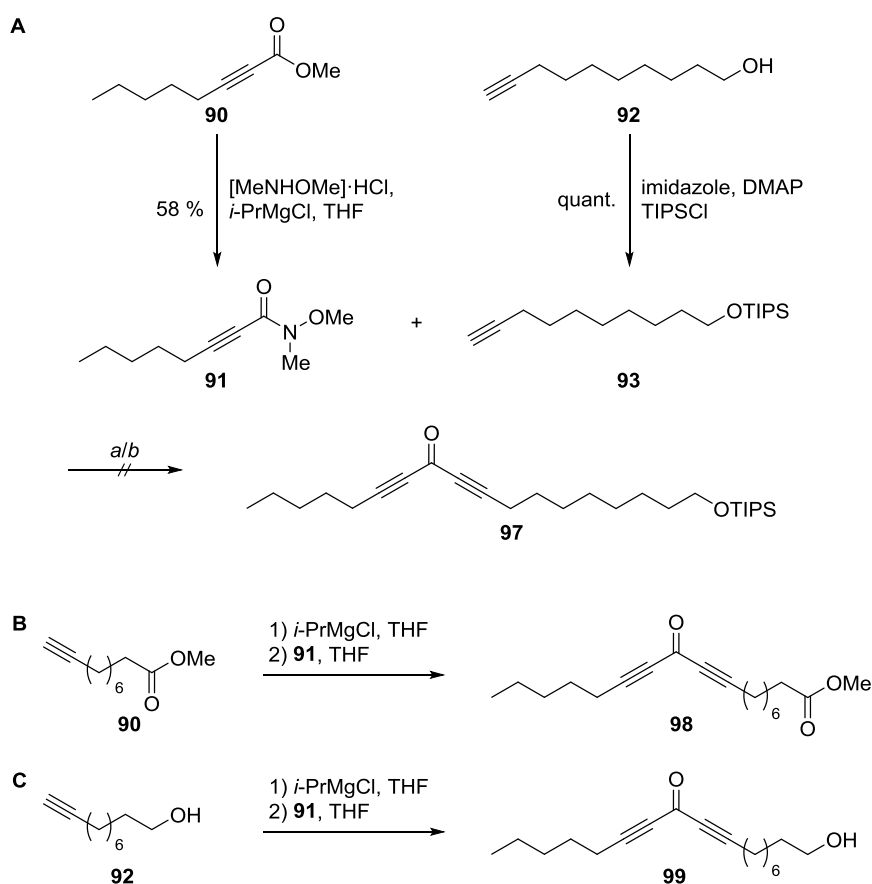
Starting the synthesis of 11,11-difluorolinoleic acid (**89**) based on the work of PRÉVOST *et al.*, methyl 2-octynoate (**90**) was converted into the Weinreb amide **91** using the commercially available *N,O*-dimethylhydroxylamine hydrochloride in combination with the Grignard reagent isopropylmagnesium chloride (*i*-PrMgCl) (Scheme 4.3, A left). After 30 min at r.t. the product **91** was obtained in 58 % purified yield. 9-Decyn-1-ol (**92**) was protected using triisopropylsilyl chloride (TIPSCl) to form a silyl ether (**93**) (Scheme 4.3, A right)^[221], which was received in quantitative yield after flash column chromatography (FC).



Scheme 4.2 Retrosynthetic analysis of 11,11-difluorolinoleic acid.

To undergo the Weinreb-Nahm ketone synthesis, **93** was deprotonated with butyllithium (*n*-BuLi, 2.5 M in *n*-hexane) at $-30\text{ }^{\circ}\text{C}$ for 2 h and coupled with the Weinreb amide **91** at $-78\text{ }^{\circ}\text{C}$ (Scheme 4.3, **A** bottom). This approach led to no product formation but recovery of **93** was possible. Since usage of an organolithium reagent did not show the desired reaction, Grignard reagents were applied. The deprotonation step with 1.3 M or 2.0 M *i*-PrMgCl in THF was conducted at $-10\text{ }^{\circ}\text{C}$ but gave no different results (Scheme 4.3, **A**, bottom). Interestingly, when utilizing methyl dec-9-ynoate or unprotected 9-decyn-1-ol traces of product (**98**, **99**) were detected in mass spectrometry but no isolation attempt was successful (Scheme 4.3, **B** and **C**).

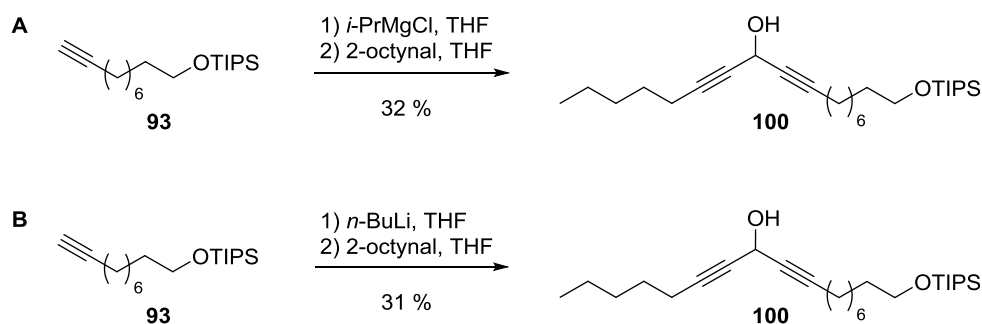
Since the strategy based on the research of PRÉVOST *et al.* gave no promising results, the approach was changed with the introduction of a new starting material. Instead of utilising the Weinreb amide **91** the commercially available 2-octynal was deployed. Applying the same conditions as before, alkyne **93** could be deprotonated with either an organolithium reagent or a Grignard reagent to undergo the subsequent coupling reaction with the aldehyde.^[222]



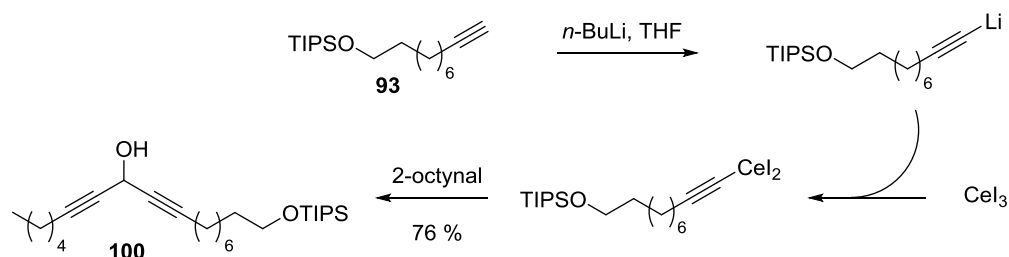
Scheme 4.3 Synthesis of Weinreb amide **91** (**A**, left) and protection of the terminal alcohol of 9-decyn-1-ol (**A**, right) followed by coupling attempts of **91** and **93**; *a*: deprotonation of **93** with *n*-BuLi at $-30\text{ }^{\circ}\text{C}$, stirring for 2 h r.t., addition of **91** in THF at $-78\text{ }^{\circ}\text{C}$, stirring at r.t. for 15 h; *b*: deprotonation of **93** with *i*-PrMgCl, THF, $-10\text{ }^{\circ}\text{C}$, 1 h, addition of **91** in THF at $-10\text{ }^{\circ}\text{C}$, stirring o.n. (**A**, bottom). Coupling of **90** with **91** (**B**). Coupling of **92** with **91** (**C**).

In Scheme 4.4 the reactions to form **100** are displayed utilising the Grignard reagent (**A**) or the organolithium reagent (**B**). In **A** protected alcohol **93** was treated dropwise with *i*-PrMgCl in THF at $-10\text{ }^{\circ}\text{C}$ and stirred for 1 h while keeping the temperature. A solution of 2-octynal in THF was slowly added at $-10\text{ }^{\circ}\text{C}$ and the reaction mixture was stirred at r.t. over night. After standard workup procedure and FC, the pure product was obtained with maximal 32 % in rather low yields. Very similar conditions were applied in **B**. A solution of **93** in THF was slowly treated with *n*-BuLi (2.5 M) at $-30\text{ }^{\circ}\text{C}$ and then stirred at r.t. for 2 h. The mixture was cooled to $-78\text{ }^{\circ}\text{C}$ and carefully treated with a solution of the aldehyde in THF. After stirring at r.t. for 15 h and filtration through silica, the solvent was removed and the product **100** isolated via FC. This approach led with up to 31 % yield to comparable amounts of product **100** as the reaction depicted in **A**.

Since the hitherto stated synthetic routes showed no or insufficient product formation and, especially in the case of organolithium reagent application, high amounts of side products occurred, further strategy investments were required. In 1984 IMAMOTO *et al.* published their studies on carbon-carbon bond formation using elementary cerium or organocerium(III) compounds.^[223] They state that organocerium(III) reagents are less basic than Grignard or organolithium reagents and react fast with carbonyl compounds with few or no side reactions at low temperature (-78 to $-65\text{ }^{\circ}\text{C}$). Even though the reaction set up on systems with alkyne functionalities in one or both of the coupling partners is not shown there, it was applied on the present system (Scheme 4.5). For that purpose the terminal alkyne **93** was deprotonated at $-30\text{ }^{\circ}\text{C}$ using *n*-BuLi. After 2 h at r.t. the mixture was added to a $-65\text{ }^{\circ}\text{C}$ cooled suspension of cerium(III) iodide in THF and stirred for 30 min. 2-Octynal was slowly added and the mixture stirred at $-65\text{ }^{\circ}\text{C}$ for additional 3 h. The reaction was stopped via treatment with saturated ammonium chloride solution and after workup and FC the pure product **100** was obtained in 76 % yield.



Scheme 4.4 Synthesis of **100** with *i*-PrMgCl (**A**) or *n*-BuLi (**B**) as deprotonation agent.



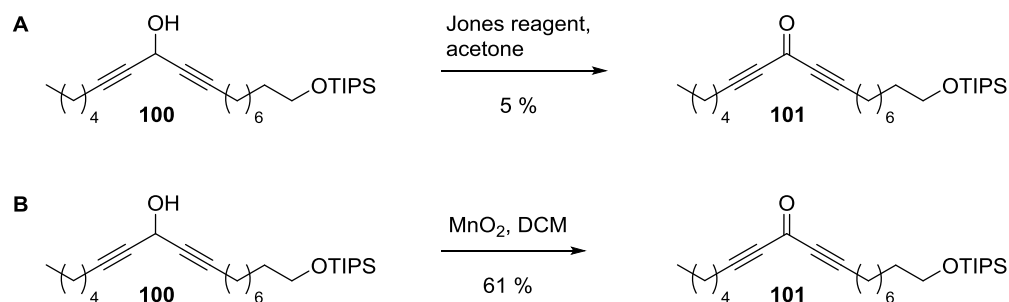
Scheme 4.5 Synthesis of compound **100** via organocerium(III).

This approach using cerium(III) iodide proved to be very beneficial with a smooth reaction showing barely side product formation.

The next synthetic step was the oxidation of the generated secondary alcohol to a keto moiety.^[179,224,225] As oxidising agent Jones reagent was chosen^[222], which was prepared from chromium(VI) trioxide in concentrated sulphuric acid and water. A solution of the secondary alcohol **100** in acetone was treated at 0 °C with the Jones reagent and stirred at r.t. for 1 h (Scheme 4.6, **A**). After standard workup procedure and FC, only 5 % yield of the oxidised compound **101** could be isolated. Due to the low yield and high toxicity of chromium(VI) compounds, manganese(IV) oxide was tested as an alternative (Scheme 4.6, **B**).^[226] MnO_2 is a weak to moderate oxidant and reacts preferably with allylic and benzylic hydroxyl groups to form aldehydes or ketones. Further oxidation to carboxylic acids does not occur.

The secondary alcohol **100** and MnO_2 were dissolved in DCM and stirred at r.t. for 2 h. The mixture was filtrated through Celite® and standard workup procedure was applied. It turned out that the usage of MnO_2 as an oxidising agent had two major advantages: the yield of 61 % was considerably greater utilising MnO_2 than Jones reagent and highly toxic chromium waste was avoided.

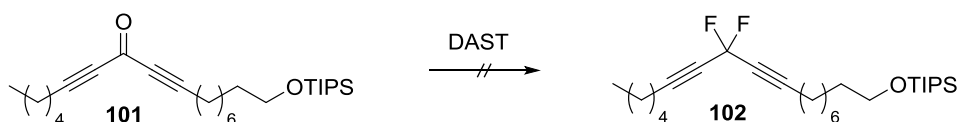
After successful isolation of the keto-moiety bearing compound **101**, the next step included the introduction of two fluorine atoms (Scheme 4.7). As fluorination reagent the aminosulphurane diethylaminosulphur trifluoride (DAST) was chosen and four different reaction conditions were tested (Table 4.1).



Scheme 4.6 Oxidation approaches for the synthesis of **101** using Jones reagent (**A**) and manganese(IV) oxide (**B**).

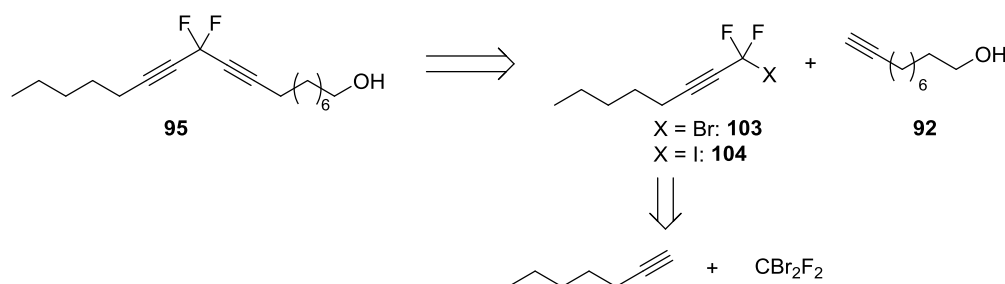
Table 4.1 Overview of tested fluorination condition.

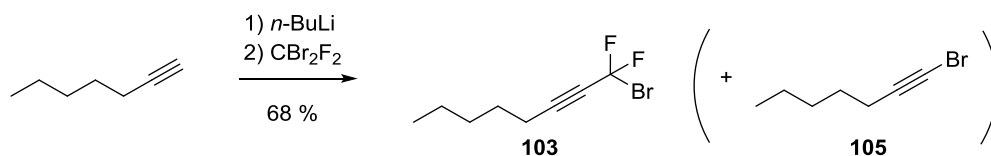
| Condition No. | Temperature | Time Duration | Admixture |
|---------------|-------------|---------------|-----------------|
| 1. [227] | 0 °C - r.t. | over night | – |
| 2. [228] | 45 °C | 6 d | – |
| 3. [229] | 60 °C | 6 h | 2 drops ethanol |
| 4. [230] | r.t. | 8 d | – |

**Scheme 4.7** General fluorination reaction using DAST as fluorination reagent.

None of these conditions led to the formation of the *gem*-fluorinated product **102**. To overcome the obstacle of fluorine insertion a different synthetic approach had to be devised. In 1987 KWOK *et al.* published a strategy for the total synthesis of 7,7-, 10,10- and 13,13-difluoroarachidonic acids^[231], in which incorporation of the fluorine atoms is conducted in an early stage of the synthesis (Scheme 4.8).

The new route was adapted to the system used in this work and started with insertion of the fluorine atoms. KWOK *et al.* used the at r.t. gaseous bromochlorodifluoromethane (CBrClF₂), which needs to be condensed at –78 °C prior usage. This prohibits working with precise stoichiometry, complicates handling and requires special technical setups. To avoid working with this gaseous reagent an alternative was found in dibromodifluoromethane (CBr₂F₂), which is a liquid with a boiling point of 22.8 °C. To incorporate the fluorine carrying moiety, the alkyne 1-heptyne was deprotonated by dropwise addition of *n*-BuLi (2.5 M) at –90 °C. Pre-cooled CBr₂F₂ was slowly added at –110 °C and the reaction mixture stirred for 1 h at –50 °C. Standard workup procedure yielded the pure product **103** without further purification steps with a yield of 68 % (Scheme 4.9). Several publications state the formation of a brominated side product for this reaction^[232–234] but interestingly, no formation of this compound (**105**) could be detected.

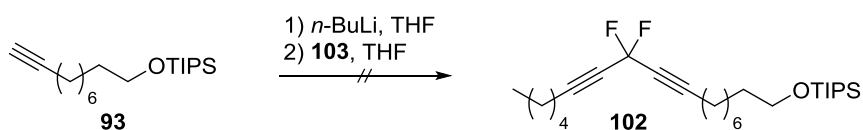
**Scheme 4.8** Retrosynthetic analysis of 11,11-difluorolinoleic acid based on the work of KWOK *et al.*



Scheme 4.9 Incorporation of the fluorine moieties and the literature stated side product **105**.

Another observation was that, when 1-hexyne instead of 1-heptyne was subjected to this reaction condition, no product formation took place but various side reactions could be observed. ¹⁹F-NMR spectroscopy revealed formation of several fluorine containing compounds, which could not be identified.

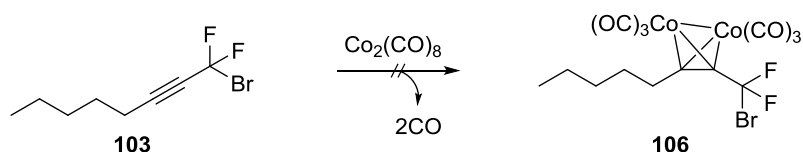
After successful introduction of the fluorine atoms, the next short-term objective was to achieve the desired chain length. For attachment of the second alkynyl moiety, the terminal alkyne of **93** was deprotonated using *n*-BuLi and treated dropwise with a solution **103** in THF at -78 °C (Scheme 4.10).



Scheme 4.10 Attachment of the second alkyne to obtain the desired carbon chain length using the brominated compound **103**.

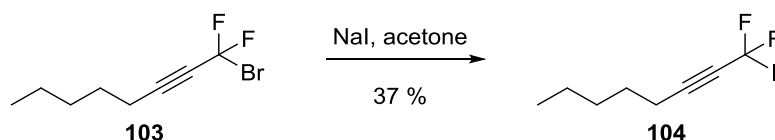
Using these conditions no product was formed. Therefore, a Nicholas-like reaction was tested.^[235–237] Addition of dicobalt octacarbonyl (Co₂(CO)₈) should lead to a complex formation under release of two carbon monoxide molecules (Scheme 4.11). The formed cobalt–alkyne complex should protect the alkynyl moiety and stabilise the generated cation in the following nucleophilic substitution reaction.

The complexation reaction using dicobalt octacarbonyl was tested in DCM and toluene as solvents but in both cases no signal shift in the ¹³C-NMR spectra was observed. A reason that no cobalt–alkyne complex was formed could be the instability of Co₂(CO)₈ to air exposure followed by possible decomposition before the reaction could start.



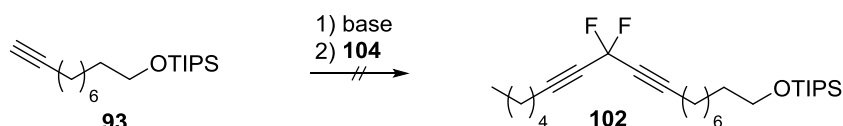
Scheme 4.11 Formation of cobalt–alkyne complex **106**.

Since a Nicholas-like approach was unsuccessful, it was decided to perform a halogen exchange reaction to substitute the bromine of compound **103** with an iodine, which represents a better leaving group.^[231] Heating **103** in acetone in presence of sodium iodide yielded the iodinated compound **104** in equilibrium (Scheme 4.12). The equilibrium was shifted to the product side, because the generated sodium bromide was insoluble in acetone and therefore precipitated.



Scheme 4.12 Substitution of bromine with iodine by halogen exchange reaction.

The reaction conditions depicted in Scheme 4.10 were then applied to the iodised compound **104** (Scheme 4.13). This resulted in formation of product traces, which were detected in mass spectrometry, but could not be isolated. Optimisation attempts by varying *n*-BuLi concentrations (1.6 M or 2.5 M), changing the organolithium reagent to *t*-BuLi (1.7 M) or shifting to another deprotonation agent like NaH or *t*-BuOK showed no increase in product yield. An overview about the tested bases and temperatures for carbon-carbon coupling of **93** and **104** is shown in Table 4.2. Conditions tested for carbon-carbon coupling of **93** and **104**.



Scheme 4.13 Attachment of the second alkyne (**93**) to obtain the desired carbon chain length using the iodised compound **104**.

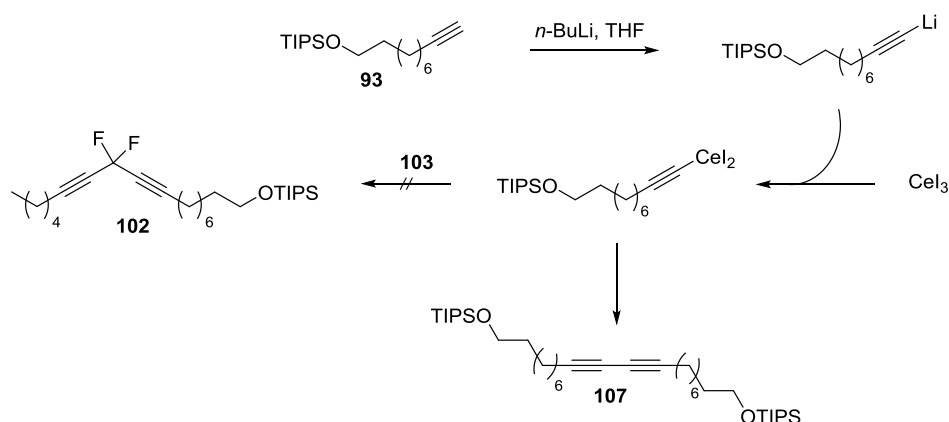
Table 4.2 Conditions tested for carbon-carbon coupling of **93** and **104**.

| Condition No. | Base | Temperature | Product Traces |
|---------------|------------------------|-------------|----------------|
| 1.a | <i>n</i> -BuLi (1.6 M) | -78 °C | – |
| 1.b | <i>n</i> -BuLi (1.6 M) | 0 °C | ✓ |
| 1.c | <i>n</i> -BuLi (1.6 M) | -20 °C | ✓ |
| 2.a | <i>n</i> -BuLi (2.5 M) | -78 °C | – |
| 2.b | <i>n</i> -BuLi (2.5 M) | 0 °C | ✓ |
| 3 | <i>t</i> -BuLi (1.7 M) | -78 °C | ✓ |
| 4 | NaH | -78 °C | – |
| 5 | <i>t</i> -BuOK | -78 °C | – |

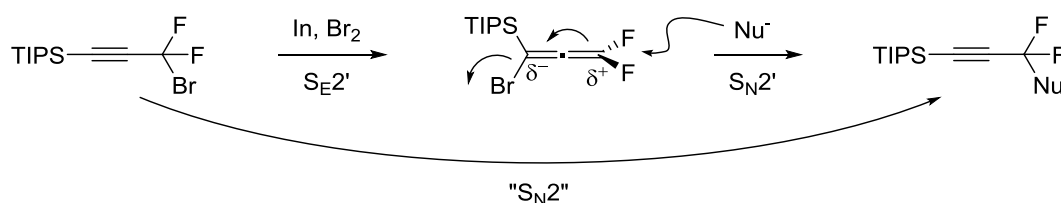
Due to the fact that these efforts led to no constructive route for the synthesis of 11,11-difluorolinoleic acid (**89**), another strategy was necessary. Since the carbon-carbon coupling via organocerium(III) compounds has proven to be a useful synthetic tool (Scheme 4.5), it was applied to the fluorinated alkyne **103** as well. Alkyne **93** was deprotonated using *n*-BuLi and converted into an organocerium(III) compound by treatment with a cerium(III) iodide suspension. Addition of **103** was then supposed to lead to formation of product **102** (Scheme 4.14). The analysis with mass spectrometry revealed no formation of product **102**. The individual components of the reaction mixture were isolated by FC and analysed to reveal that compound **93** was recovered while the *gem*-fluorinated alkyne **103** seemed to be decomposed. A third substance was isolated and identified by HSQC, HMBC and DOSY as a dimerisation product (**107**) of **93**, shown in Scheme 4.14.

It was reported by XU and HAMMOND that the nucleophilic substitution (S_N2) of RCF_2Nu from RCF_2X is a non-trivial challenge due to the carbon atom being shielded by the encircling fluorine atoms.^[238] This hinders nucleophilic substitution reactions, which is why they developed a two-step synthesis consisting of an indium-mediated $Se2'$ bromide substitution followed by a S_N2' reaction (Scheme 4.15).

To test the reported strategy, **103** was treated with ammonium chloride and elementary indium at 5–10 °C for 7 h in an ultrasonic bath. After standard workup procedure, bromine was added to the crude product at –78 °C and stirred for 30 min at –20 °C (Scheme 4.16, A). NMR spectroscopy could not unambiguously show formation of the difluoroallenyl compound **108**. Nevertheless, it was used to try the following nucleophilic substitution reaction. Alkyne **93** was deprotonated by addition of *n*-BuLi at –78 °C and difluoroallene **108** was appended (Scheme 4.16, B).



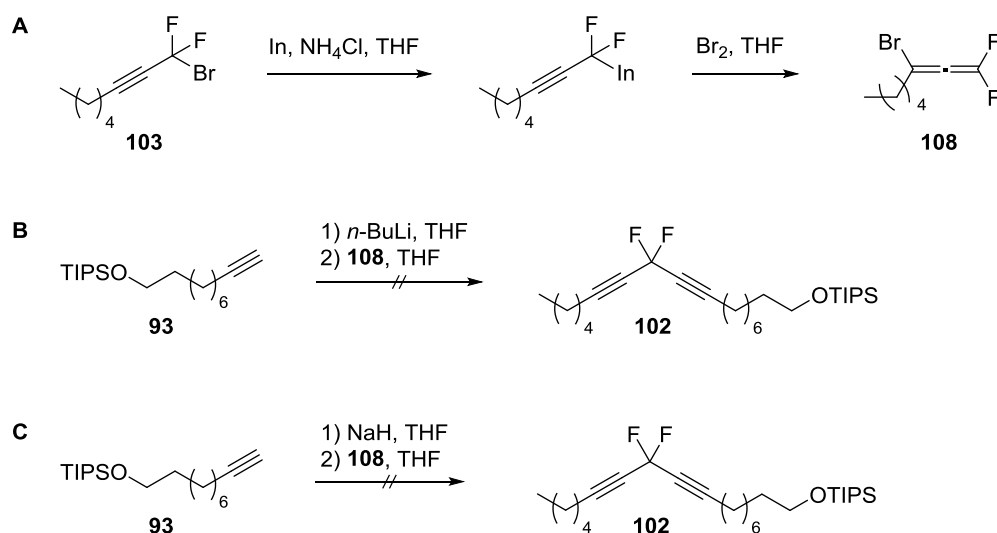
Scheme 4.14 Synthetic route to form **102** using CeI_3 with in lieu thereof observed reaction.



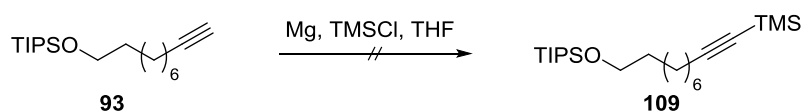
Scheme 4.15 From XU and HAMMOND designed strategy for S_N2 -like substitution.^[238]

Applying these conditions no product formation was detected but the mass spectrum showed unreacted starting material **93**. Therefore, the deprotonation step was varied by addition of NaH at 0 °C instead of *n*-BuLi and the overall reaction time increased (Scheme 4.16, C). Under these conditions no product could be generated, too.

Another attempt to synthesise the desired *gem*-difluorinated fatty acid **89** was to incorporate a better leaving group into **93** by exchanging the terminal hydrogen atom by a TMS group (Scheme 4.17).^[239] A solution of **93** in THF was treated with magnesium swarf and trimethylsilyl chloride (TMSCl) at 0 °C for 30 min but no conversion took place. Since the hydrogen–TMS substitution reaction led to no product formation, the exchange of reactivities of the two alkyne compounds **93** and **103** aimed for and adapted from literature-known procedures for *gem*-difluorinated alkynes.^[239]



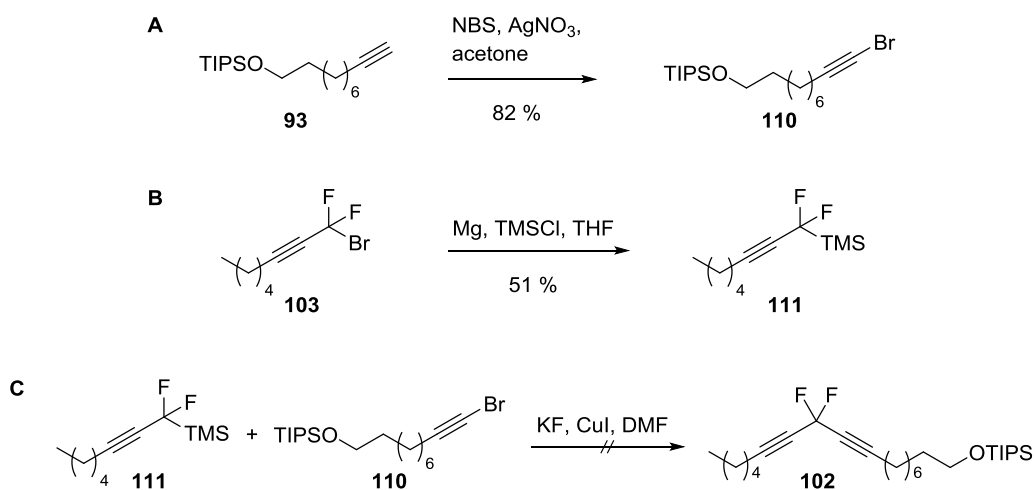
Scheme 4.16 Generation of difluoroallene **108** (A) with subsequent substitution reaction using *n*-BuLi (B) or NaH (C).



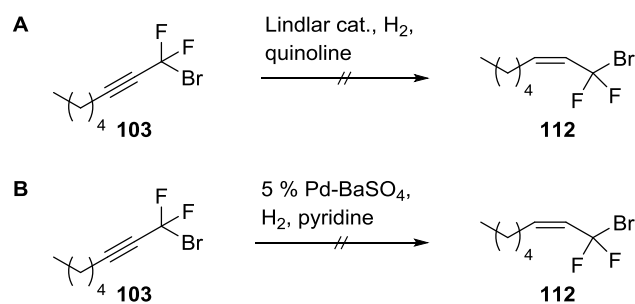
Scheme 4.17 Approach to functionalise alkyne **93** with TMS.

To achieve a reactivity exchange of terminal alkyne **93**, the proton was substituted by a bromine via treatment of **93** with *N*-bromosuccinimide (NBS) and silver nitrate (Scheme 4.18, **A**).^[240] The hydrogen–bromine substitution reacted smoothly to compound **110** within 45 min with a high yield of 82 %. In case of *gem*-fluorinated alkyne **103** the bromine was exchanged by applying the reaction conditions depicted in Scheme 4.18, **B**.^[239] After 30 min at 0 °C the compound **111** was obtained in moderate yield of 51 %. The following reaction using potassium fluoride and copper iodide^[239] to generate a carbon–carbon bond between nucleophilic **111** and electrophilic **110** did not produce the desired molecule **102** (Scheme 4.18, **C**).

Since in the literature no synthesis of a compound with two geminal positioned fluorine atoms along with two geminal stationed alkynyl moieties on the same carbon atom has been described so far, it was considered that the reduction of **103** to the alkene **112** might enable the coupling reaction. It was crucial in this step to ensure the generation of a *cis*-alkene and to stop the reduction on the level of alkene formation. Therefore, compound **103** was treated with a Lindlar catalyst poisoned with quinoline under a hydrogen atmosphere (Scheme 4.19, **A**).^[241] NMR spectroscopy revealed that no reaction took place, and **103** was regained. Another option to generate *cis*-alkenes is the utilisation of palladium on barium sulphate (5 % Pd–BaSO₄), shown in Scheme 4.19, **B**.^[242] This was tested using **103**, which was stirred for 24 h with 5 % Pd–BaSO₄ in pyridine but no product was formed.



Scheme 4.18 Substitution of terminal proton by bromine (**A**); substitution of bromine by TMS-group (**B**); coupling attempt of **110** and **111** (**C**).



Scheme 4.19 Attempts of selective hydration for *cis*-alkene preparation using a Lindlar catalyst poisoned with quinoline (**A**) or 5 % Pd adsorped to BaSO₄ (**B**).

The synthetic approaches performed so far could not lead to the final compound 11,11-difluorolinoleic acid (**89**). Further investigations with other strategies should be tested. Therefore, palladium catalysed coupling conditions could be considered featuring zinc organyles or via organyl cuprates in the case of alkynyl groups.

5 Summary

Communication between cells represents a crucial process, which enables organisms to respond to environmental influences. For interaction of cells with the surrounding or with neighbouring cells, the plasma membrane as a special organelle is necessary. The plasma membrane serves as an active interface by carrying a multitude of receptors and sensors for signal transduction and regulates import and export of a variety of compounds.^[129] To transmit signals, messenger agents are required. One of the most ubiquitous and versatile second messenger is calcium in its ionic form.^[39,67] Typical processes regulated by Ca^{2+} are fertilisation^[42], cell growth^[43], apoptosis^[38] and many more.

Due to the importance of Ca^{2+} as a signalling agent, a high demand for fluorescent Ca^{2+} sensors evolved, which led to the development of a multitude of sensors with diverse fluorescent properties and sensitivities.^[11,12] A major drawback of most commercially available sensors is, however, their unequal distribution within cells and occasionally rapid exclusion from the cell. To overcome this obstacle, several sensors have been modified by incorporation of an azide-carrying alkyl linker to enable the labelling of alkynes via a HUISGEN reaction.^[13] In the first part of this work, two of these modified Ca^{2+} sensors (Fluo-Azide and X-Rhod-Azide) were applied to label membrane compartments. Therefore, the lipid DOPE, a frequently existing lipid in the plasma membrane, and the sterol cholesteryl hemisuccinate were coupled with alkyne-carrying linker compounds. Furthermore, a small library of four peptides with the artificial amino acid propargyl glycine at the *N*-terminus was generated, including a transmembrane WALP25 peptide. After intensive condition screening, HUISGEN reactions were successfully performed using the cholesterol derivative and one of the DOPE derivatives. As products the Fluo-Azide labelled compounds **15** and **22**, as well as the X-Rhod-Azide labelled compound **23** were obtained (Figure 5.1).

Since an increase of fluorescence will occur only if Ca^{2+} is bound by a sensor, the labelled membrane components were thought to serve as a useful system for monitoring membrane fusion. Therefore, fusion experiments were performed using two different systems of SNARE analoga. Fluorescence measurements of fusion experiments utilising modified SNARE peptides with a PNA recognition motif revealed no fusion occurring. Substitution of the fusion proteins by modified SNARE peptides exhibiting a coiled-coil recognition unit resulted in a slight fluorescence increase. Due to the low increase, this result needs to be treated with caution but indicates that vesicle fusion took place.

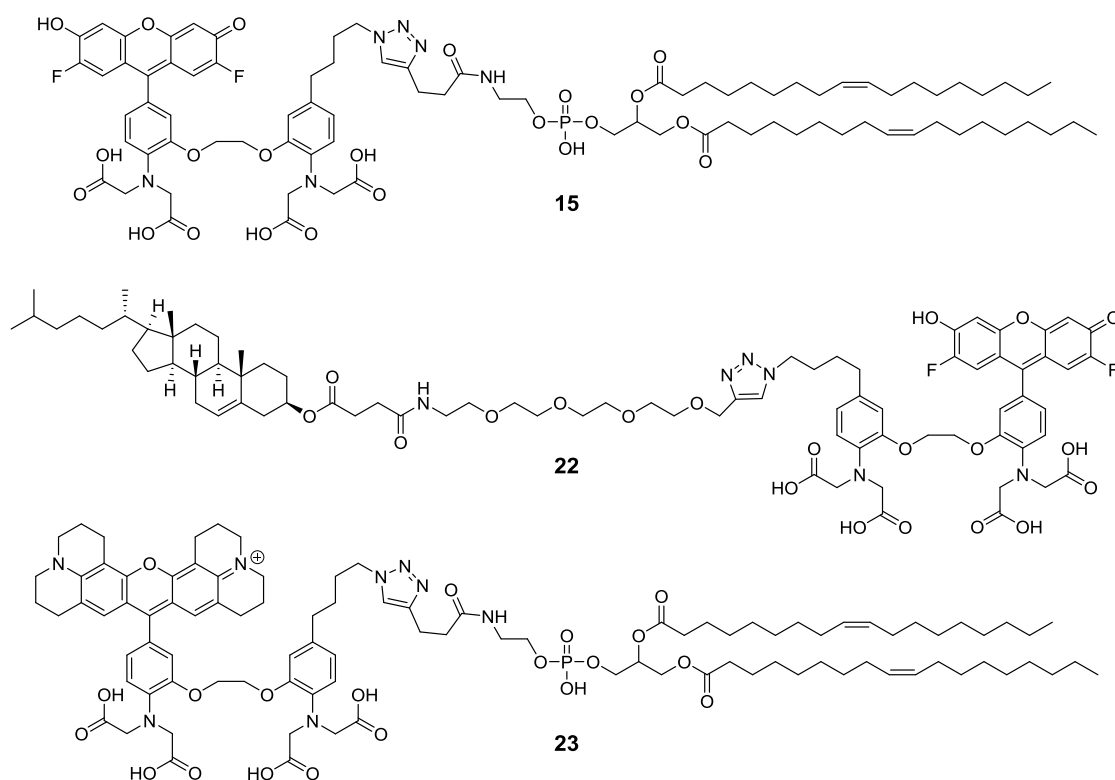


Figure 5.1 Synthesised membrane components **15** and **22** labelled with Fluo-Azide, and **23** labelled with X-Rhod-Azide.

After verification of the outcome via further experiments, the usage of sensor labelled membrane compartments might present a useful system to follow fusion processes, taking the importance of Ca^{2+} for fusion in natural systems into account.

Besides Ca^{2+} other important signalling agents are IP_3 and DAG. The source of both messengers is the rare plasma membrane lipid PIP_2 .^[14] During fusion processes, such as neuronal exocytosis, PIP_2 was found to locally increase its concentration to form PIP_2 and cholesterol enriched domains. These rafts are thought to serve as binding platforms for fusion proteins.^[16,127] The utilisation of a suited fluorophore for the observation of PIP_2 raft formation should enable further insights into the protein mediated membrane fusion. Therefore, the ultimate goal of the second part of this work was to synthesise a labelled PIP_2 derivative. Since the synthesis of the PIP_2 head group requires expensive starting materials, a simplified PC lipid was targeted during the synthesis planning. As fluorophore, 7-azaindole was utilised, which is a well studied and highly environment sensitive labelling compound. The commercially available 7-azaindole was modified by incorporation of two different linkers, which yielded compounds **25** and **40**, to allow subsequent covalent labelling of lipid derivative. Applying several strictly synthetic strategies as well as semi-enzymatic and full-enzymatic approaches to synthesise a 7-azaindole labelled PC lipid, the successful synthesis of a labelled lipid precursor lacking a head group was achieved. Fluorescence measurements of the labelled compound incorporated into model

membranes revealed that the fluorophore does not insert into the membrane but is oriented in the polar head group region of the membrane. For this reason no further experiments were performed.

Lipophilic signalling molecules in plants, like jasmonic acid, are generated by oxidation of polyunsaturated fatty acids, starting with hydroperoxide formation. The enzymatic dioxidation of the fatty acids is mainly performed by LOX enzymes.^[22] So far, many details about the mechanism of hydroperoxidation have been learned but the exact orientation of the substrate within the active site of the enzyme remains to be discovered. As a result, the goal of the third part was to synthesise a substrate-like inhibitor that can be bound by the enzyme but cannot be digested. The target compound was 11,11-difluorolinoleic acid, which mimics the substrate linoleic acid. Substitution of both hydrogen atoms by fluorine atoms at C-11 inhibits the hydrogen abstraction step and no conversion can take place. To synthesise the target compound a multitude of approaches was made but none of them yielded the desired product. Other strategies to generate the target compound, which still have to be tested, are palladium catalysed coupling featuring zinc organyles or application of organyl cuprates.

6 Experimental Part

6.1 Materials and General Methods

Solvents

Technical solvents were distilled before usage. Solvents of “analytical” or “puriss. p. a.” Grade supplied by *Acros Organics*, *Fisher Chemical*, *Merck*, *Sigma-Aldrich* and *VWR* were used without further purification. Anhydrous solvents were purchased as “puriss, absolute, over molecular sieves” from *Acros-Organics*, *Fluka* and *Sigma-Aldrich* and were stored under argon atmosphere. For HPLC purification methanol and acetonitrile in “HPLC grade” were obtained from *Fisher Scientific*, *Sigma-Aldrich* and *VWR*. Demineralised water for HPLC and buffers was purified using as *arium mini* purification system from *Satorius*.

Reagents

All utilised reagents were ordered with the quality “for synthesis” or “analytical grade” and were purchased from *ABCR*, *Acros Organics*, *Alfa Aesar*, *Bachem*, *Carl Roth*, *Fisher Scientific*, *Fluka*, *fluorchem*, *Merck*, *Nova Biochem*, *Sigma-Aldrich*, *TCI* and *VWR*. Resins, amino acids and coupling reagents were obtained from the companies *ABCR*, *Bachem*, *GL Biochem*, *IRIS Biotech* and *Nova Biochem*. Polyethylenglycol (PEG) conjugates were purchased from *Iris Biotech* and fluorescent dyes from *ATTO-TEC*, *Eurogentec* and *Invitrogen*.

Reactions

Air- or moisture-sensitive reactions were carried out under inert atmosphere using anhydrous solvents. Small scale reactions were performed in non-heatable reaction tubes made of polypropylene using a purge and flush procedure. Reactions of larger scale were conducted in under vacuum flame-dried glassware. Addition of solid compounds was performed under counter flow. Light sensitive reactions were carried out under light exclusion.

Lyophilisation

For lyophilisation the compounds dissolved in water or dioxane with minimal amounts of methanol, acetonitrile or DMF were frozen with liquid nitrogen. The frozen solutions were attached to a *Christ-Alpha-2-4plus* lyophiliser connected to a high

vacuum pump from *Vakuubrand*. Freeze-drying of small amounts filled in centrifuge caps were performed using the speed vac *Christ RVC-2-18* linked to the lyophiliser.

Chromatography

- **Thin Layer Chromatography (TLC)**

To follow reactions and as purity control silica gel 60 F₂₅₄ coated aluminium plates with an absorbent layer thickness of 0.25 mm from *Merck* were used. TLC plates with a reverse phase surface were obtained from *Macherey Nagel*. The *Alugram* RP-18 W/UV₂₅₄ plates were pre-coated aluminium sheets with a layer thickness of 0.15 mm of C₁₈ silica gel containing a fluorescent indicator. To detect UV active substances fluorescence elimination at wavelengths 254 and 366 nm were applied, while UV inactive substances were dyed with potassium permanganate solution (2.0 g KMnO₄, 3.3 mL 5 % (w/w) aqueous NaOH, 13.3 g K₂CO₃, 200 mL H₂O) or sulfuric acid solution (20 mL sulfuric acid, 80 mL ethanol).

- **Preparative Thin Layer Chromatography (PLC)**

PLC plates were ordered from *Carl Roth* with glass plates carrying silica gel 60 (thickness: 2 mm, size: 20 cm × 20 cm). For detection the PLC sheet was dipped into an aqueous solution of copper sulphate and then heated to 120 °C for approximately 30 min. This chares the organic substances on the plate and makes them visible. Since the substances are destroyed in this process, the stained PLC plate was used as reference for further PLC.

- **Flash Column Chromatography (FC)**

Silica gel 60 with a particle size of 40–63 µm (230–400 mesh particle size) from *Merck* was used. The silica gel was suspended in the eluent system and filled into the glass column. An excess of silica gel to crude product (50–200 times) was conducted. The crude product was added to the column as a solid adsorbed to silica gel or as a concentrated solution in the employed eluent system. Separation of substances on the column occurred via 0.2–1.0 bar applied pressure.

- **Reverse Phase Chromatography (RPC)**

Purification via RPC was carried out using RP silica gel from YMC (ODS-A, AA06S50, 60 Å, S-50 µm, C18). Substances were dissolved in the respective eluent system and added to the column. Separation of substances occurred without additional pressure.

- **High Performance Liquid Chromatography (HPLC)**

Analytical and semi-preparative HPLC for peptide purification was performed on *Amersham Pharmacia Biotech* devices (*Äkta basic*, high pressure pump module P-900,

variable UV detector UV-900). The isolation of labelled compounds was achieved on a HPLC device from *Jasco* connected to a MD-2010 plus multi wavelength UV detector, a DG-2080-53 degasser, two PU-2080 pumps and a LC-NetII/ADC interface. The runs were executed with a linear gradient of eluent A to eluent B. An overview about utilised eluent systems is shown in Table 6.1. Detection of UV absorption took place at 215, 254 and 280 nm for peptides and at 215 nm, 280 nm and the respective absorption maximum of the fluorophore (488 nm for Fluo-Azide and 580 nm for X-Rhod-Azide) for labelled compounds. Flow rates for analytical columns were 1 mL/min and 3 mL/min for semi-preparative columns. Runs for purely analytical purposes with very small amounts were conducted on a *Dionex UltiMate 3000* device from *Thermo Scientific*, containing a pump type P-3000 and a variable UV detector UV-3000. The flow rate was set to 0.4 mL/min. All samples were dissolved in purified water with minimum amounts of MeCN or MeOH and filtrated prior injection.

Table 6.1 Overview about utilised eluent systems.

| | Eluent A | Eluent B |
|-----------------------|--|--|
| Variant 1 (V1) | ultrapure H ₂ O + 0.1 % TFA | MeOH + 0.1 % TFA |
| Variant 2 (V2) | ultrapure H ₂ O + 0.1 % TFA | MeCN/ultrapure H ₂ O (80:20, v/v) + 0.1 % TFA |
| Variant 3 (V3) | ultrapure H ₂ O + 0.1 % TFA | MeCN + 0.1 % TFA |

6.2 Characterisation

Nuclear Magnetic Resonance Spectroscopy (NMR)

NMR spectra were recorded at *Bruker* (AV401, AV300) and *Varian* instruments (*INOVA500*, *INOVA600* and *Mercury-VX 300*). The chemical shift is stated in ppm (TMS = 0 ppm) while remaining protons of deuterated solvents were used as internal standard. The following abbreviations were used for multiplicities in ¹H-NMR signals: s = singlet, s_b = broad singlet, d = doublet, t = triplet, q = quartet, m = multiplet. Coupling constant *J* is quoted in Hertz [Hz]. ¹³C-NMR spectra were recorded proton-decoupled. Interpretation of signals was carried out using [H,H]-COSY, HSQC and HMBC spectra.

Mass Spectrometry (MS)

Mass spectra were recorded at spectrometer from *Bruker* (*micrOTOF* (ESI-TOF-MS), *maXis* (ESI-QTOF-MS) and *Apex IV* (FT-ICR-MS)) using electron spray ionisation (ESI) as ionisation method. The signals were stated as mass to charge (m/z). Matrix-assisted laser desorption/ionisation (MALDI) spectra were recorded at MALDI-TOF *Autoflex Speed* from *Bruker*.

6.3 Spectroscopic Methods

UV/Vis Spectroscopy

Absorption spectra were recorded at a *Jasco* system *V-650 UV/Vis spectrophotometer* at 20 °C. Absorption spectra of calcium sensor-labelled compounds were measured in a Ca^{2+} -free buffer (30 mM MOPS, 10 mM EGTA, 100 mM KCl, pH 7.2).

Concentrations of peptides were calculated using the law of LAMBERT-BEER via absorption at specific wavelengths (see formula below). The extinction coefficient ε was calculated from of the extinction coefficients of tryptophan, tyrosine and phenylalanine at 280 nm.^[243]

$$\varepsilon = \frac{A}{c \cdot d}$$

A: absorption at specific wavelength,

ε : molar extinction coefficient [$\text{cm}^{-1}\text{M}^{-1}$],

d: layer thickness of the cuvette [cm].

Fluorescence Spectroscopy

Fluorescence measurements were conducted at a *Jasco FP-6200* spectrofluorometer connected to a temperature control unit *Jasco ETC-272T*. For Ca^{2+} -dependent fluorescence measurements a commercially available buffer kit containing a *Zero Free Calcium Buffer* (30 mM MOPS, 10 mM EGTA, 100 mM KCl, pH 7.2, buffer **A**) and a *39 μM Free Calcium Buffer* (30 mM MOPS, 10 mM CaEGTA, 100 mM KCl, pH 7.2, buffer **B**) from *Invitrogen* was used. By mixing defined volumes of the buffer specific Ca^{2+} concentrations can be adjusted varying from 0 to 39 μM . All measurements for the various concentrations were repeated four times while keeping pH, temperature and

sensor concentration constant. Employed parameters for fluorescence measurements are listed in Table 6.2.

Table 6.2 Parameters applied for Ca^{2+} -dependent fluorescence measurements.

| | $\lambda_{\text{Ex}} / \text{nm}$ | Measuring range /nm | Measurement Mode |
|--------------|-----------------------------------|---------------------|------------------|
| Fluo-Azide | 488 | 500–600 | Emission |
| X-Rhod-Azide | 540 | 550–650 | Emission |

The employed procedure for Ca^{2+} -dependent fluorescence measurements was based on the protocol stated by *Invitrogen*:

1. The sensor-labelled compounds were dissolved as stock solution in DMF or MeOH with a resulting concentration of 0.2–1 mM.
2. One part of the respective stock solution was added to 2 mL of buffer **A** to obtain a **15/22/23** concentration of 2 μM (mixture **C**).
3. Three parts of the stock solution was added to 6 mL of buffer **B** to gain the same concentration (2 μM , mixture **D**).
4. 1.3 mL of mixture **C** was transferred to a fluorescence cuvette to detect the fluorescence spectrum of the labelled compound in absence of free Ca^{2+} -ions.
5. The following fluorescence measurements at varying Ca^{2+} -concentration were performed by substitution of specific volumes of the mixture in the cuvette through the same volumes of mixture **D** (Table 6.3) while keeping the concentration of the sensor-labelled compound constant.

Table 6.3 Serial dilution with resulting concentrations for Ca^{2+} -dependent fluorescence measurements.

| $c(\text{CaEGTA}) / \text{mM}$ | $c(\text{Ca}^{2+}) / \mu\text{M}$ | Replaced Volume* / μL |
|--------------------------------|-----------------------------------|----------------------------------|
| 0 | 0 | - |
| 1.0 | 0.017 | 130 |
| 2.0 | 0.038 | 144 |
| 3.0 | 0.065 | 163 |
| 4.0 | 0.100 | 186 |
| 5.0 | 0.150 | 217 |
| 6.0 | 0.225 | 260 |
| 7.0 | 0.351 | 325 |
| 8.0 | 0.602 | 433 |
| 9.0 | 1.35 | 650 |
| 9.3 | 2.00 | 390 |
| 9.5 | 2.86 | 371 |
| 10 | 39 | Mixture D |

* When using 1.3 mL of mixture **C**.

Circular Dichroism Spectroscopy (CD)

CD measurements were performed at a *Jasco* J-810A spectropolarimeter connected to a PTC-423S Peltier element. To prevent ozone formation the sample chamber was flushed with nitrogen. The following parameters were adjusted during measurements: *data mode*: CD and absorption, *band width*: 1.0 nm, *response*: 2 s, *datapitch*: 0.1 nm, *scanning speed*: 50 nm/min, *accumulations*: 10. The spectra were corrected by sample concentration and layer thickness of the cuvette (0.1 cm). The curves were filtered following SAVITZKY-GOLAY. The molar ellipticity was calculated using the measured values (see formula below).

$$\Theta_{\text{molar}} = 100 \cdot \frac{CD}{c \cdot d}$$

Θ_{molar} : molar ellipticity [deg·cm²/dmol],

CD: measured ellipticity [mdeg],

c: sample concentration [mol/cm³],

d: layer thickness of the cuvette [cm].

6.4 General Protocols (GP)

6.4.1 GP1: Peptide Synthesis

GP1.1: Manual Solid Phase Peptide Synthesis (SPPS)

In this work the synthesis of peptides was achieved by applying SPPS with the standard Fmoc-protocol. For manual peptide coupling on solid support acid- and base-resistant *Becton Dickinson Discardit* (BD)-syringes provided with a polyethylene filter were used. The Fmoc-loaded Rink-Amide MBHA resin (loading density 0.76 mmol/g) was swollen in DMF (~10 mL/g resin) for a minimum of 1 h. The batch size was varied for each peptide synthesis. The protocol stated below refers to 0.05 mmol (65.8 mg resin) in a 2 mL BD syringe.

1. Deprotection: Removal of the Fmoc group was carried out by treatment with piperidine (20 % v/v) in DMF (2 × 1.5 mL) for 10 min each. Afterwards, the resin was washed with DMF (10 × 2 mL).
2. Coupling: The respective amino acid (5.0 eq.), HBTU (4.5 eq.) and HOBT (5.0 eq.) were dissolved in DMF (1.5 mL). After addition of DIPEA (10.0 eq.) the coupling mixture was immediately transferred to the resin and agitated for

30 min. For double coupling the resin was treated with the coupling mixture a second time. After coupling the resin was washed with DCM/DMF (1:1, 3 × 2 mL), DCM (2 × 2 mL), DCM/DMF (1:1, 3 × 2 mL) and DMF (2 × 2 mL).

3. Repetition: The steps 1 and 2 were repeated as often as required to obtain the desired sequence. In case of longer intermission during synthesis the resin was washed with DCM (10 × 2 mL) after step 2, dried and stored *in vacuo*.

GP1.2: Automated Solid Phase Peptide Synthesis

Automated solid phase peptide synthesis was performed using standard Fmoc-protocol. The synthesis was conducted on a CEM (Kamp-Lintfort) microwave-supported *LibertyBlue* peptide synthesiser. The *Discover* microwave was equipped with a reaction cavity connected to the *LibertyBlue* unit with all required reagents and solvents. Besides the positions for the 20 natural amino acids up to seven non-natural amino acids could be attached on the available external positions. The used amino acids were prepared as 2 M solutions in DMF. Standard reagents were used for coupling (0.5 M DIC in DMF, 1.0 M Oxyma in DMF), for deprotection (20 % (v/v) piperidine in DMF) and for washing (DMF). All reactions were carried out microwave-assisted and under nitrogen. A standard cycle with a batch size of 0.1 mmol using double coupling on high-swelling resins was performed, which consisted of two deprotection steps (1. 15 s, 75 °C, 155 W; 2. 50 s, 90 °C, 35 W), two coupling steps (1. 15 s, 75 °C, 170 W; 2. 110 s, 90 °C, 30 W) and washing with DMF between deprotection and coupling steps. After finishing the synthesis the resin was transferred from the reaction vessel into a 10 mL BD-syringe, washed with DCM (10 × 6 mL) and dried *in vacuo*.

GP1.3: Cleavage from Solid-Support

To cleave synthesised peptides from solid support the dry resin was treated with a solution of TFA, TIS and H₂O (95:2.5:2.5, v/v/v, ~10 mL/g) and agitated for 2 h. The cleavage solution was collected and the resin washed with TFA (2 × 10 mL/g). The solvents were removed by a gentle nitrogen stream and the peptide precipitated with cold Et₂O (4–10 mL). The suspension was vortexed and centrifuged (9000 rpm, -10 °C, 20 min). The solvent was decanted and the precipitation repeated twice. The crude peptide was dried under reduced pressure and purified by HPLC.

6.4.2 GP2: Preparation of Vesicles

GP2.1: Preparation of Lipid Films

The lipids used in this work for vesicle preparation were 1,2-dioleoyl-*sn*-glycero-3-phosphocholine (DOPC), 1,2-dioleoyl-*sn*-glycero-3-phosphoethanol-amine (DOPE) and cholesterol in the relation of DOPC/DOPE/cholesterol 50:25:25. The total lipid concentration was varied between 0.625 – 2.50 μM . For lipid film preparation stock solution of each lipid in chloroform (20 mg/mL) was assembled, which were stored at -20 °C. For each desired vesicle population one small reagent tube was provided. A specific volume of chloroform was added to the tubes that contained up to 500 μL after addition of lipid solution for vesicles without peptides and 250 μL for vesicles with peptides. Examples for both systems are shown in Table 6.4. The calculated amount of lipid stock solutions was pipetted into the prepared tubes. For vesicles containing peptides, a specific amount TFE was added, which is again supposed to sum up to 250 μL after addition of peptide solution. The in TFE dissolved peptides were added to yield a peptide to lipid ratio varying from 1:200 to 1:750. The solutions were warmed up to r.t. and vortexed for 5 s each. The tubes were heated to 50 °C and after 5 min vortexed again. The solvents were slowly removed at 50 °C by nitrogen stream to obtain even lipid films. These films were further dried over night in a vacuum oven at 45 °C. If the lipid films were not used on the next day they were stored under argon at -20 °C.

Table 6.4 Exemplary composition of four different lipid films: **VA** and **VC** containing the Ca^{2+} sensor-labelled **22**. **VB** and **CV** do not comprise a sensor, while **VA** and **VB** hold SNARE fusion proteins E3-Syb and K3-Sx.

| [μL] | VA | VB | VC | CV |
|-------------------|-----------|-----------|-----------|-----------|
| DOPC | 24.24 | 24.24 | 24.24 | 24.24 |
| DOPE | 17.21 | 17.21 | 17.21 | 17.21 |
| cholesterol | 26.62 | 28.12 | 26.62 | 28.12 |
| 22 | 14.28 | - | 14.28 | - |
| E3-Syb | 2.13 | - | - | - |
| K3-Sx | - | 2.92 | - | - |
| CHCl_3 | 167.65 | 180.43 | 417.65 | 430.43 |
| TFE | 247.87 | 247.08 | - | - |

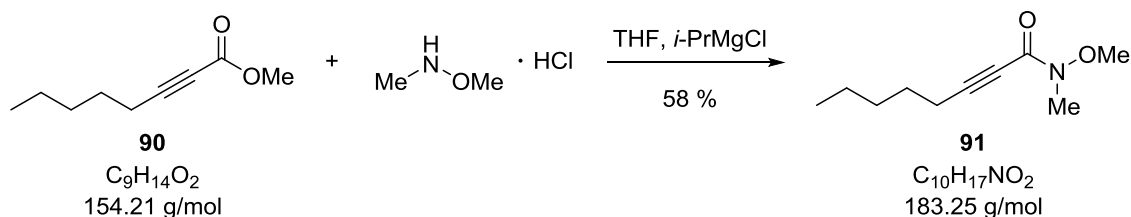
GP2.2 Preparation of Large Unilamellar Vesicles (LUVs)

For preparation of large unilamellar vesicles the prepared lipid films were incubated with 0.5 mL buffer, MOPS (30 mM MOPS, 10 mM CaEGTA/10 mM EGTA, 100 mM KCl, pH 7.2) or HEPES (20 mM HEPES, 1 mM EDTA, 100 mM KCl, pH = 7.4), at 40 °C for at least 2 h. To improve dissolution of the lipid films from the glass wall three small glass beads were given into each reaction tube. The tubes were closed with *Parafilm* and shaken at approximately 150 rpm. To produce LUVs the extrusion method^[244] was used. In this method a multilamellar vesicle suspension is forced 31 times through a polycarbonate membrane from *Avestin* with a pore diameter of 100 nm. The employed extruder was a *LiposoFast* type from *Avestin*. Using this method vesicles with an average size of 80 nm were prepared.^[244] The obtained vesicles were used immediately after extrusion for fluorescence spectroscopy. Vesicles containing the head labelled *N*-(lyssamine rhodamine B sulfonyl)-1,2-dioleoyl-*sn*-3-phosphatidylethanol-amine (Rhod-DOPE) were purified using *Sephadex* G-50 fine and used for measurements right away.

6.5 Synthesis

6.5.1 Synthesis of 11,11-Difluorolinoleic acid

N-Methoxy-*N*-methyloct-2-ynamide (**91**)



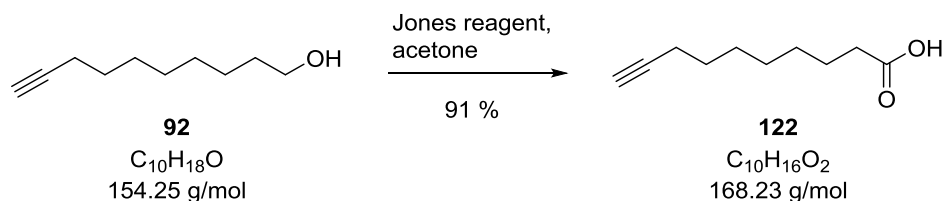
To a solution of **90** (300 mg, 330 μ L, 1.95 mmol, 1.00 eq.) and *N,O*-dimethylhydroxylamine hydrochloride (470 mg, 4.86 mmol, 2.50 eq.) in THF (3.5 mL) isopropylmagnesium chloride (2 M in THF, 2.43 mL, 4.86 mmol, 2.50 eq.) was added dropwise under argon atmosphere. The mixture was stirred for 30 min and treated with aqueous NH_4Cl -solution (200 μ L). The mixture was diluted with MTBE (1.2 mL) and filtrated through celite. The solvent was evaporated and the crude product purified via flash column chromatography (*n*-pentane/ethyl acetate, 4:1). The isolated product **91** (210 mg, 1.13 mmol, 58 %) was obtained as colourless oil.

TLC (*n*-pentane/ethyl acetate, 4:1): R_f = 0.43.

1H -NMR (300 MHz, $CDCl_3$): δ [ppm] = 0.88 (t, J = 7.1 Hz, 3H, CH_3), 1.28–1.40 (m, 4H, $2 \times CH_2$), 1.53–1.64 (m, 2H, CH_2), 2.35 (t, J = 7.0 Hz, 2H, CH_2), 3.15–3.28 (m, 3H, NCH_3), 3.74 (s, 3H, OCH_3).

^{13}C -NMR (125 MHz, $CDCl_3$): δ [ppm] = 13.75 (C-8), 18.79 (C-4), 21.91 (C-7), 27.27 (C-5), 30.80 (C-6), 32.19 (NCH_3), 61.77 (OCH_3), 72.99 (C-2), 93.38 (C-3), 125.69 (C=O).

ESI-MS m/z : 184.1 $[M+H]^+$, 206.1 $[M+Na]^+$, 367.3 $[2M+H]^+$, 389.2 $[2M+Na]^+$.

Dec-9-ynoic acid (122**)**

Dec-9-ynol (**92**, 1.50 g, 1.70 mL, 9.72 mmol, 1.00 eq.) was dissolved in acetone (70 mL), cooled to 0 °C and treated dropwise with Jones reagent (5.00 mL, 10.0 mmol, 1.14 eq.). The mixture was stirred for 2 h at 0 °C. The solvent was removed under reduced pressure and the residue dissolved in diethyl ether (250 mL), washed with saturated aqueous sodium chloride solution (200 mL) and dried over MgSO₄. Evaporation of the solvent and purification via flash column chromatography (*n*-pentane/ethyl acetate, 3:2) yielded **122** (1.49 g, 8.85 mmol, 91 %) as colourless oil.

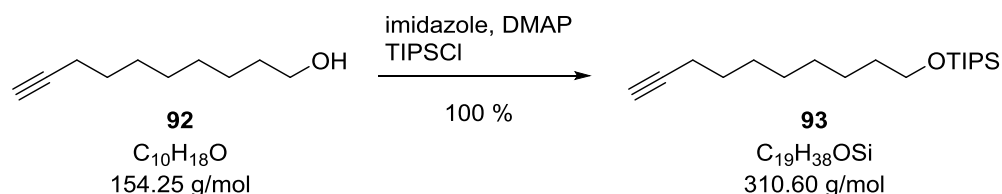
TLC (*n*-pentane/ethyl acetate, 3:2): *R*_f = 0.63.

¹H-NMR (300 MHz, CDCl₃): δ [ppm] = 1.25–1.37 (m, 6H, 4-CH₂, 5-CH₂, 6-CH₂), 1.41–1.50 (m, 2H, 7-CH₂), 1.57 (dt, *J* = 14.8, 7.2 Hz, 2H, 3-CH₂), 1.87 (t, *J* = 2.6 Hz, 1H, 10-CH), 2.11 (td, *J* = 6.9, 2.6 Hz, 2H, 8-CH₂), 2.28 (t, *J* = 7.5 Hz, 2H, 2-CH₂), 9.54–9.75 (m, 1H, COOH).

¹³C-NMR (125 MHz, CDCl₃): δ [ppm] = 18.33 (C-8), 24.58, 28.34, 28.47, 28.68, 28.87 (C-3, C-4, C-5, C-6, C-7), 33.91 (C-2), 68.13 (C-10), 84.60 (C-9), 179.53 (C-1).

ESI-MS *m/z*: 169.1 [M+H]⁺, 191.1 [M+Na]⁺, 359.2 [2M+Na]⁺, 167.1 [M-H]⁻, 335.2 [2M-H]⁻.

HR-MS (ESI): calculated for [C₁₀H₁₇O₂] ([M+H]⁺): 169.1223, found: 169.1220; calculated for [C₁₀H₁₆O₂Na] ([M+Na]⁺): 191.1043, found: 191.1042; calculated for [C₁₀H₁₅O₂] ([M-H]⁻): 167.1078, found: 167.1078.

(Dec-9-yn-1-yloxy)triisopropylsilane (93)

To a solution of dec-9-ynol (**92**, 1.31 g, 1.50 mL, 8.46 mmol, 1.00 eq.) in DCM (60 mL) imidazole (1.73 g, 25.4 mmol, 3.00 eq.), DMAP (41.3 mg, 338 μmol , 4 mol-%) and TIPSCl (1.63 g, 1.81 mL, 8.46 mmol, 1.00 eq.) was added. The reaction mixture was stirred at r.t. for 16 h. The solvent was evaporated, the residue dissolved in diethyl ether (30 mL) and washed with hydrochloric acid (1 M, 30 mL). The mixture was dried over MgSO_4 , the solvent was evaporated. After flash column chromatography (*n*-pentane/ethyl acetate, 8:1) the product (**93**, 2.63 g, 8.46 mmol, 100 %) was obtained as colourless oil.

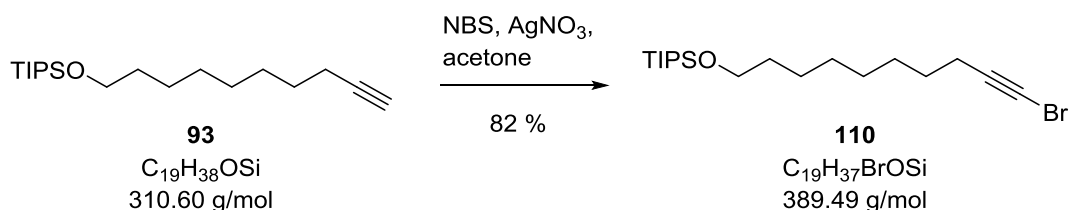
TLC (*n*-pentane/ethyl acetate, 6:1): $R_f = 0.90$.

$^1\text{H-NMR}$ (300 MHz, CDCl_3): δ [ppm] = 1.01–1.06 (m, 21H, $6\times\text{CH}_3_{\text{TIPS}}$, $3\times\text{CH}_{\text{TIPS}}$), 1.25–1.39 (m, 8H), 1.45–1.55 (m, 4H), 1.90 (t, $J = 2.6$ Hz, 1H, 10-CH), 2.15 (td, $J = 7.0$, 2.6 Hz, 2H, 8- CH_2), 3.64 (t, $J = 6.6$ Hz, 2H, 1- CH_2).

$^{13}\text{C-NMR}$ (125 MHz, CDCl_3): δ [ppm] = 12.02 ($3\times\text{CH}_{\text{TIPS}}$), 18.01 ($6\times\text{CH}_3_{\text{TIPS}}$), 18.38 (C-8), 25.77, 28.48, 28.69, 29.09, 29.31 (C-3, C-4, C-5, C-6, C-7), 33.00 (C-2), 63.45 ($\text{H}_2\text{C-OTIPS}$), 68.00 (C-10), 84.69 (C-9).

ESI-MS m/z : 311.3 $[\text{M}+\text{H}]^+$, 333.3 $[\text{M}+\text{Na}]^+$.

HR-MS (ESI): calculated for $[\text{C}_{19}\text{H}_{39}\text{OSi}]$ ($[\text{M}+\text{H}]^+$): 311.2765, found: 311.2762; calculated for $[\text{C}_{19}\text{H}_{38}\text{OSiNa}]$ ($[\text{M}+\text{Na}]^+$): 333.2584, found: 333.2582.

((10-Bromodec-9-yn-1-yl)oxy)triisopropylsilane (110)

To a solution of **93** (1.38 g, 4.43 mmol, 1.00 eq.) in acetone (25 mL) NBS (920 mg, 5.17 mmol, 1.17 eq.) and AgNO_3 (75.2 mg, 440 μmol , 0.10 eq.) was added at r.t.. The mixture was stirred for 45 min, poured onto ice water and the resulting precipitate was filtered off. The precipitate was dissolved in ethyl acetate (20 mL) and washed with water (2×15 mL). The organic layer was dried over MgSO_4 and the solvent was removed under reduced pressure. After flash column chromatography (*n*-pentane/ethyl acetate, 10:1) the desired compound **110** (1.42 g, 3.64 mmol, 82 %) was obtained as brown oil.

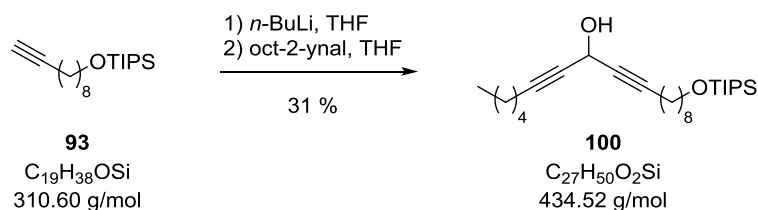
TLC (*n*-pentane): $R_f = 0.76$.

^1H -NMR (400 MHz, CDCl_3): δ [ppm] = 1.02–1.05 (m, 18H, $6 \times \text{CH}_3$,TIPS), 1.25–1.39 (m, 9H, $3 \times \text{CH}_2$,TIPS, $3 \times \text{CH}_2$), 1.43–1.56 (m, 6H, $3 \times \text{CH}_2$), 2.17 (t, $J = 7.1$ Hz, 2H, $\text{Br}-\text{C}\equiv\text{C}-\underline{\text{CH}_2}$), 3.65 (t, $J = 6.6$ Hz, $\text{CH}_2\text{-OTIPS}$).

^{13}C -NMR (125 MHz, CDCl_3): δ [ppm] = 12.01 ($3 \times \text{CH}_2$,TIPS), 18.02 ($6 \times \text{CH}_3$,TIPS), 19.66 (C-8), 25.76, 28.27, 28.72, 29.06, 29.29, 32.99 (C-2), 37.40 ($\text{HC}\equiv\text{C}$), 63.45 (C-1), 80.44 ($\text{Br}-\text{C}\equiv\text{C}$).

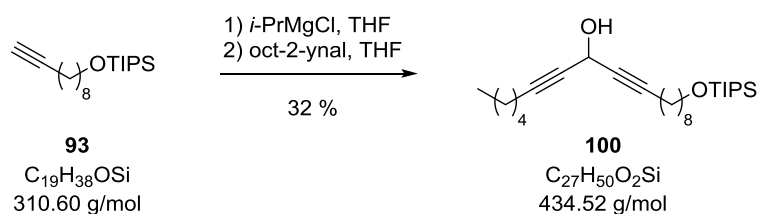
ESI-MS m/z : 389.2 $[\text{M}+\text{H}]^+$, 411.2 $[\text{M}+\text{Na}]^+$, 427.3 $[\text{M}+\text{K}]^+$.

HR-MS (ESI): calculated for $[\text{C}_{19}\text{H}_{37}\text{OSiBrNa}]$ ($[\text{M}+\text{Na}]^+$): 411.1689, found: 411.1669.

18-((Triisopropylsilyl)oxy)octadeca-6,9-diyn-8-ol (**100**) — 1. Variant

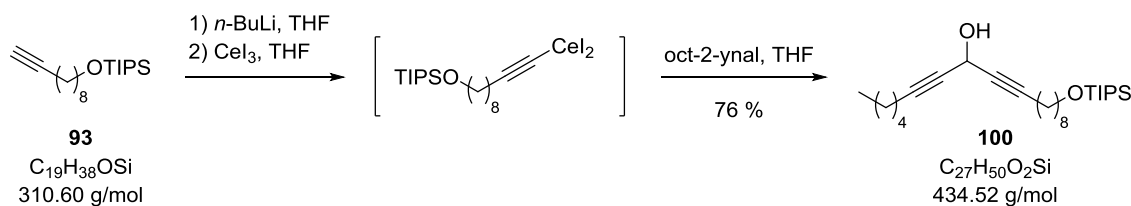
To a solution of **93** (1.00 g, 3.22 mmol, 1.25 eq.) in THF (6 mL) *n*-BuLi (2.5 M, 1.26 mL, 3.14 mmol, 1.22 eq.) was added at $-30\text{ }^{\circ}\text{C}$ under dry conditions. The mixture was stirred at r.t. for 2 h. Oct-2-ynal (370 μL , 330 mg, 2.58 mmol, 1.00 eq.) was dissolved in THF (4 mL) and added dropwise to the prepared mixture at $-78\text{ }^{\circ}\text{C}$. The reaction mixture was allowed to warm up slowly to r.t. and stirred for 15 h. The mixture was filtered through silica and the solvent was removed under reduced pressure. The product **100** (440 mg, 1.01 mmol, 31 %) was obtained after flash column chromatography (*n*-pentane) as brown oil.

2. Variant



To a solution of **93** (800 mg, 2.58 mmol, 1.05 eq.) in THF (5 mL) *i*-PrMgCl (2.0 M, 1.41 mL, 2.81 mmol, 1.15 eq.) was added dropwise at $-10\text{ }^{\circ}\text{C}$ under dry conditions. The reaction mixture was stirred at $-10\text{ }^{\circ}\text{C}$ for 1 h. Oct-2-ynal (350 μL , 300 mg, 2.45 mmol, 1.00 eq.) was dissolved in THF (5 mL), added dropwise to the mixture at $-10\text{ }^{\circ}\text{C}$ and then stirred at r.t. over night. The reaction was stopped by addition of water (20 mL) and washed with ethyl acetate ($3 \times 10\text{ mL}$) and saturated aqueous sodium chloride solution (20 mL). The combined organic layers were dried over MgSO_4 and concentrated under reduced pressure. The crude product was purified by flash column chromatography (*n*-pentane/ethyl acetate, 6:1) to yield the pure **100** (360 mg, 840 μmol , 32 %) as brown oil.

3. Variant



Compound **93** (660 mg, 2.13 mmol, 2.20 eq.) was dissolved in THF (4.5 mL) under dry conditions, cooled to $-30\text{ }^\circ\text{C}$ and treated dropwise with $n\text{-BuLi}$ (2.5 M, 850 μL , 2.13 mmol, 2.20 eq.). The reaction mixture was stirred at r.t. for 2 h. In a second reaction vessel cerium (III) triiodide (1.01 g, 1.93 mmol, 2.00 eq.) was suspended in THF (6 mL) and cooled to $-65\text{ }^\circ\text{C}$. The mixture of the first reaction vessel was added dropwise to the suspension and after stirring at $-65\text{ }^\circ\text{C}$ oct-2-ynal (170 μL , 120 mg, 970 μmol , 1.00 eq.) was added. The suspension was stirred for 3 h at $-65\text{ }^\circ\text{C}$. The reaction mixture was allowed to warm up to r.t., quenched with saturated aqueous ammonium chloride solution (10 mL) and extracted with chloroform ($3 \times 15\text{ mL}$). The combined organic extracts were dried over MgSO_4 and the solvent was evaporated. After flash column chromatography ($n\text{-pentane/ethyl acetate}$, 6:1) the pure product **100** (320 mg, 730 μmol , 76 %) was obtained.

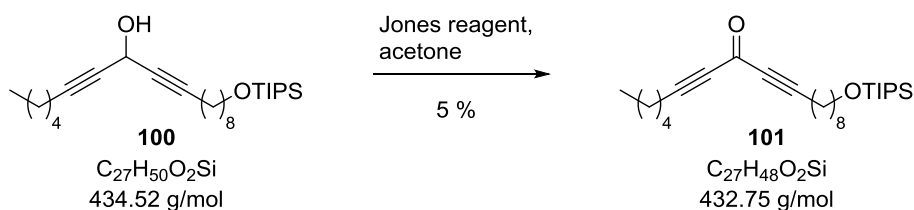
TLC ($n\text{-pentane/ethyl acetate}$, 6:1): $R_f = 0.49$.

$^1\text{H-NMR}$ (300 MHz, CDCl_3): δ [ppm] = 0.82–0.89 (m, 6H, CH_3 , $3 \times \text{CH}_{\text{TIPS}}$), 1.02 (t, $J = 3.6\text{ Hz}$, 18H, $6 \times \text{CH}_3_{\text{TIPS}}$), 1.36–1.21 (m, 12H, $6 \times \text{CH}_2$), 1.47 (dd, $J = 8.9, 3.0\text{ Hz}$, 6H, $3 \times \text{CH}_2$), 2.18 (ddd, $J = 7.1, 4.7, 2.1\text{ Hz}$, 4H, $2 \times \text{C}\equiv\text{C}-\text{CH}_2$), 3.63 (t, $J = 6.6\text{ Hz}$, 2H, $\text{CH}_2\text{-OTIPS}$), 5.05 (dt, $J = 4.0, 2.0\text{ Hz}$, 1H CH-OH).

$^{13}\text{C-NMR}$ (125 MHz, CDCl_3): δ [ppm] = 11.97 ($3 \times \text{CH}_{\text{TIPS}}$), 13.87 (C-1), 17.96 ($6 \times \text{CH}_3_{\text{TIPS}}$), 18.63, 18.65 (C-5, C-11), 22.12 (C-2), 25.72, 28.02, 28.31, 28.76, 29.04, 29.26, 30.98, 32.94 (C-17), 52.43 (C-8), 63.43 (C-18), 78.07 (C-7, C-9), 84.94, 84.95 (C-6, C-10).

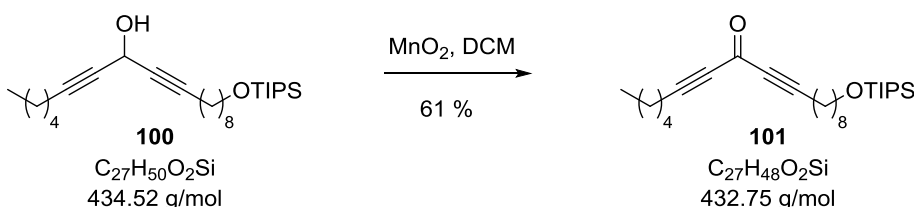
ESI-MS m/z : 435.4 $[\text{M}+\text{H}]^+$, 457.4 $[\text{M}+\text{Na}]^+$, 433.4 $[\text{M}-\text{H}]^-$.

HR-MS (ESI): calculated for $[\text{C}_{27}\text{H}_{50}\text{O}_2\text{SiNa}]$ ($[\text{M}+\text{Na}]^+$): 457.3572, found: 457.3573; calculated for $[\text{C}_{27}\text{H}_{49}\text{O}_2\text{Si}]$ ($[\text{M}-\text{H}]^-$): 433.3507, found: 433.3494.

18-((Triisopropylsilyl)oxy)octadeca-6,9-diyn-8-one (**101**) – 1. Variant

To a solution of **100** (200 mg, 460 μmol , 1.00 eq.) in acetone (5 mL) Jones reagent (1.5 M, 340 μL , 510 μmol , 1.10 eq.) was added dropwise at 0 °C. The reaction mixture was stirred at r.t. for 1 h. After quenching the reaction by addition of 2-propanol (3 mL) the organic solvents were removed under reduced pressure and the concentrated solution was extracted with ethyl acetate (3 \times 5 mL). The combined organic layers were washed with saturated aqueous sodium chloride solution (10 mL) and dried over MgSO_4 . The organic solvent was removed *in vacuo* and the purification via flash column chromatography (*n*-pentane/ethyl acetate, 8:1) yielded the desired compound **101** (9.30 mg, 21.5 μmol , 5 %) as brown oil.

2. Variant



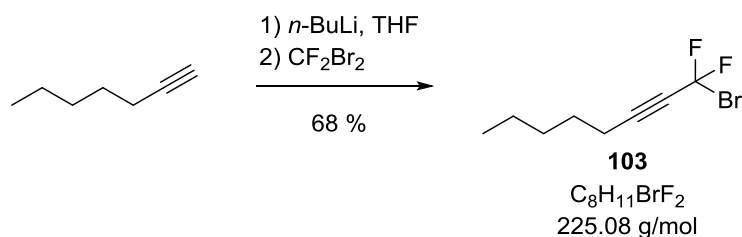
Compound **100** (100 mg, 230 μmol , 1.00 eq.) and MnO_2 (440 mg, 5.09 mmol, 22.1 eq.) were dissolved in anhydrous DCM (4.5 mL). The reaction mixture was stirred at r.t. for 2 h and then filtrated through celite. The celite was washed with DCM (5 \times 5 mL), the combined organic layers were dried over MgSO_4 and concentrated under reduced pressure. Flash column chromatography (*n*-pentane/ethyl acetate, 8:1) led to the pure product **101** (60.9 mg, 140 μmol , 61 %) as brown oil.

TLC (*n*-pentane/ethyl acetate, 8:1): R_f = 0.75.

$^1\text{H-NMR}$ (300 MHz, CDCl_3): δ [ppm] = 0.79–0.89 (m, 6H, CH_3 , 3 \times CH_{TIPS}), 1.21–1.43 (m, 28 H, 6 \times $\text{CH}_{3,\text{TIPS}}$, 5 \times CH_2), 1.46–1.76 (m, 8H, 4 \times CH_2), 2.26 (t, J = 7.1 Hz, 4H, 2 \times $\text{C}\equiv\text{C-CH}_2$), 4.32 (td, J = 6.1, 2.0 Hz, 2H, $\text{CH}_2\text{-OTIPS}$).

ESI-MS m/z : 433.4 [$\text{M}+\text{H}$] $^+$, 455.3 [$\text{M}+\text{Na}$] $^+$, 887.7 [$2\text{M}+\text{Na}$] $^+$.

HR-MS (ESI): calculated for $[\text{C}_{27}\text{H}_{49}\text{O}_2\text{Si}]$ ($[\text{M}+\text{H}]^+$): 433.3496, found: 433.3497; calculated for $[\text{C}_{27}\text{H}_{48}\text{O}_2\text{SiNa}]$ ($[\text{M}+\text{Na}]^+$): 455.3316, found: 455.3318; calculated for $[\text{C}_{54}\text{H}_{96}\text{O}_4\text{Si}_2\text{Na}]$ ($[\text{M}+\text{Na}]^+$): 887.6739, found: 887.6734.

1-Bromo-1,1-difluorohept-2-yne (103)

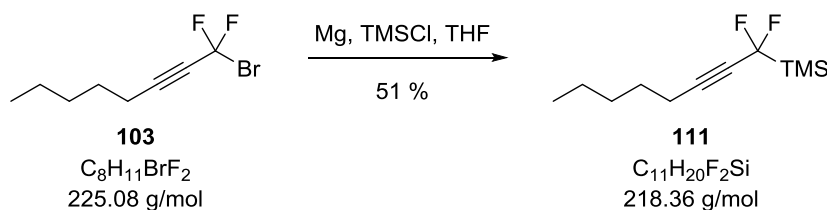
1-Heptyne (680 μL , 500 mg, 5.20 mmol, 1.00 eq.) was dissolved in dry THF (25 mL) and cooled to $-90\text{ }^\circ\text{C}$. To the solution $n\text{-BuLi}$ (2.08 mL, 2.5 M, 5.20 mmol, 1.00 eq.) was added dropwise. The mixture was stirred at $-90\text{ }^\circ\text{C}$ for 30 min and then cooled to $-110\text{ }^\circ\text{C}$. $-78\text{ }^\circ\text{C}$ cold dibromodifluoromethane (570 μL , 1.31 g, 6.24 mmol, 1.20 eq.) was slowly added and the mixture allowed to warm up to $-50\text{ }^\circ\text{C}$. After stirring for 1 h at $-50\text{ }^\circ\text{C}$ the reaction mixture was warmed up to r.t. and quenched with saturated aqueous ammonium chloride solution (5 mL). Diethyl ether (20 mL) was added and the mixture extracted with water ($2 \times 20\text{ mL}$). The organic layer was dried over MgSO_4 and concentrated under reduced pressure. Without further purification the pure product (790 mg, 3.52 mmol, 68 %) was obtained as brown oil.

^1H -NMR (300 MHz, CDCl_3): δ [ppm] = 0.87–0.94 (m, 3H, CH_3), 1.27–1.41 (m, 4H, 6- CH_2 , 7- CH_2), 1.52–1.61 (m, 2H, 5- CH_2), 2.29–2.36 (m, 2H, 4- CH_2).

^{13}C -NMR (101 MHz, CDCl_3): δ [ppm] = 13.83 (CH_3), 18.47 (t, $J = 1.9\text{ Hz}$, C-4), 22.03 (s, C-7), 26.94 (t, $J = 1.5\text{ Hz}$, C-5), 30.88 (s, C-6), 73.95 (t, $J = 37.7\text{ Hz}$, C-2), 93.20 (t, $J = 5.7\text{ Hz}$, C-3), 101.47 (t, $J = 288.6\text{ Hz}$, CBrF_2).

^{19}F -NMR (376 MHz, CDCl_3): δ [ppm] = -29.97 (t, $J = 4.7\text{ Hz}$, 2F).

EI-MS m/z : 226.0 $[\text{M}+\text{H}]^+$, 147.1 $[\text{M}-\text{Br}+2\text{H}]^+$.

(1,1-Difluorooct-2-yn-1-yl)trimethylsilane (111)

Magnesium cuttings (430 mg, 17.8 mmol, 8.00 eq.) and TMSCl (1.12 mL, 970 mg, 8.89 mmol, 4.00 eq.) were suspended in dry THF (22 mL). The suspension was cooled to 0 °C and **103** (500 mg, 2.22 mmol, 1.00 eq.) was added dropwise. After stirring at 0 °C for 30 min the suspension was decanted, the filtrate washed with water (10 mL) and the aqueous layer extracted with *n*-pentane (3 × 12 mL). The combined organic layers were dried over MgSO_4 and the organic solvents removed under reduced pressure. After flash column chromatography (*n*-pentane) compound **111** (250 mg, 1.13 mmol, 51 %) was obtained as brown oil.

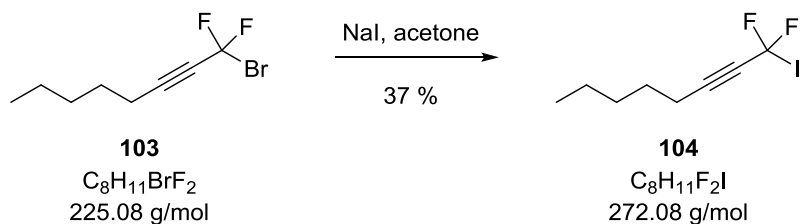
TLC (*n*-pentane): $R_f = 0.74$.

^1H -NMR (300 MHz, CDCl_3): δ [ppm] = 0.18–0.21 (m, 6H, $3 \times \text{CH}_3, \text{TMS}$), 0.84–0.92 (m, 3H, CH_3), 1.23–1.46 (m, 4H, 6- CH_2 , 7- CH_2), 1.46–1.59 (m, 2H, 5- CH_2), 2.23–2.34 (m, 2H, 4- CH_2).

^{13}C -NMR (101 MHz, CDCl_3): δ [ppm] = -2.09 (s, $3 \times \text{CH}_3, \text{TMS}$), 13.98 (s, C-8, CH_3), 18.72 (t, $J = 3.4$ Hz, C-4), 22.16 (s, C-7), 27.79 (t, $J = 3.0$ Hz, C-5), 30.98 (s, C-6), 74.41 (t, $J = 31.0$ Hz, C-2), 93.01 (t, $J = 9.2$ Hz, C-3), 120.34 (t, $J = 251.7$ Hz, CF_2TMS).

^{19}F -NMR (376 MHz, CDCl_3): δ [ppm] = -103.02 (t, $J = 6.9$ Hz, 2F).

EI-MS m/z : 219.2 $[\text{M}+\text{H}]^+$.

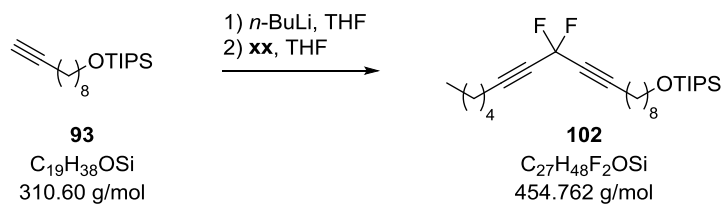
1,1-Difluoro-1-iodohept-2-yne (104)

Compound **103** (850 mg, 3.77 mmol, 1.00 eq.) was dissolved in NaI in acetone (1 M, 21 mL, 3.21 g, 21.4 mmol, 5.68 eq.) and heated to reflux for 2 h. After cooling down to r.t. the reaction mixture was added to a mixture of *n*-pentane and water (20 mL, 1:1). After extraction with *n*-pentane (2×10 mL) the organic solvent was removed under reduced pressure. The product **104** (380 mg, 1.41 mmol, 37 %) was obtained as brown oil.

$^1\text{H-NMR}$ (300 MHz, CDCl_3): δ [ppm] = 0.84–0.95 (m, 3H, CH_3), 1.25–1.43 (m, 4H, 6- CH_2 , 7- CH_2), 1.57 (dt, $J = 14.1, 7.0$ Hz, 2H, 5- CH_2), 2.27–2.38 (m, 2H, 4- CH_2).

$^{13}\text{C-NMR}$ (126 MHz, CDCl_3): δ [ppm] = 13.92 (s, CH_3), 18.56 (t, $J = 1.9$ Hz, C-4), 22.11 (s, C-7), 27.01 (t, $J = 1.8$ Hz, C-5), 30.95 (s, C-6), 73.95 (t, $J = 38.0$ Hz, C-2), 93.17 (t, $J = 5.9$ Hz, C-3), 101.43 (t, $J = 288.1$ Hz, C-1).

$^{19}\text{F-NMR}$ (282 MHz, CDCl_3): δ [ppm] = -24.94 (t, $J = 5.3$ Hz, 2F).

((11,11-Difluorooctadeca-9,12-diyn-1-yl)oxy)triisopropylsilane (102)

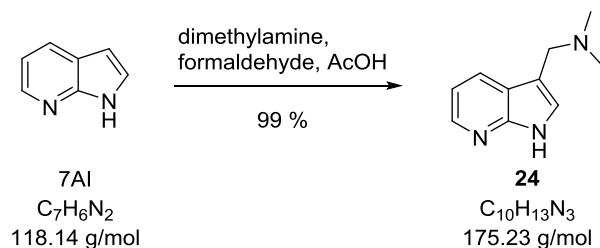
To a solution of **93** (750 mg, 1.40 mmol, 2.00 eq.) in THF (16 mL) *n*-BuLi (2.5 M, 960 μL , 2.40 mmol, 2.00 eq.) was added dropwise at 0 °C under argon atmosphere. The mixture was allowed to warm up to r.t. and stirred for 1 h. After cooling the reaction mixture to –15 °C **104** (330 mg, 1.20 mmol, 1.00 eq.) in THF (4 mL) was added and the mixture was stirred for 2 h. Water (20 mL) was added and the mixture extracted with pentane (3x15 mL). The combined organic layers were dried over MgSO_4 and solvents were removed under reduced pressure. Mass spectrometry revealed that product traces were formed, which could not be isolated.

ESI-MS m/z : 455.3 $[\text{M}+\text{H}]^+$, 477.4 $[\text{M}+\text{Na}]^+$, 453.3 $[\text{M}-\text{H}]^-$.

HR-MS (ESI): calculated for $[\text{C}_{27}\text{H}_{47}\text{OSiF}_2]$ ($[\text{M}-\text{H}]^-$): 453.3370, found: 453.3375.

6.5.2 Synthesis of 7-Azaindole Derivatives

7-Azagramine (**24**)



To a mixture of dimethylamine in ethanol (33 wt-%, 9.80 mL, 55.0 mmol, 1.30 eq.), concentrated acetic acid (2.70 mL, 47.8 mmol, 1.13 eq.) and water (10 mL) formaldehyde (3.60 mL, 47.8 mmol, 1.13 eq.) was added at 0 °C. The mixture was stirred for 30 min and then treated with 7-azaindole (5.00 g, 42.3 mmol, 1.00 eq.) in ethanol (20 mL). After further stirring at 0 °C for 30 min the reaction mixture was heated to 100 °C for 18–20 h. The mixture was allowed to cool to r.t. and treated with water (40 mL). Before extraction with DCM (3 × 30 mL) a pH of 11 was adjusted using aqueous sodium hydroxide solution (50 wt-%). The combined organic extracts were dried over MgSO_4 and concentrated under reduced pressure. The product **24** (7.33 g, 41.8 mmol, 99 %) was obtained as yellow solid.

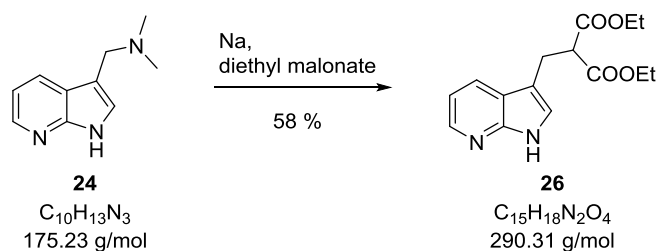
TLC (ethyl acetate/MeOH, 4:1): R_f = 0.26.

$^1\text{H-NMR}$ (301 MHz, CDCl_3): δ [ppm] = 2.26 (s, 6 H, $2\times\text{CH}_3$), 2.61 (s, 2H CH_2), 7.06 (dd, J = 7.8, 4.8 Hz, 1H, 5-CH), 7.27 (s, 1H, 2-CH), 8.03 (dd, J = 7.9, 1.6 Hz, 1H, 6-CH), 8.30 (dd, J = 4.8, 1.5 Hz, 1H, 4-CH), 11.41 (s, 1H, NH).

$^{13}\text{C-NMR}$ (76 MHz, CDCl_3): δ [ppm] = 45.16 ($2\times\text{CH}_3$), 54.72 (CH_2), 111.38 (C-3), 115.42 (C-5), 120.57 (C-9), 124.44 (C-2), 127.89 (C-4), 142.35 (C-6), 149.07 (C-8).

ESI-MS m/z : 176.1 $[\text{M}+\text{H}]^+$, 174.1 $[\text{M}-\text{H}]^-$.

HR-MS (ESI): calculated for $[\text{C}_{10}\text{H}_{14}\text{N}_3]$ ($[\text{M}+\text{H}]^+$): 176.1182, found: 176.1183; calculated for $[\text{C}_{10}\text{H}_{12}\text{N}_3]$ ($[\text{M}-\text{H}]^-$): 174.1037, found: 174.1037.

Diethyl 2-((1*H*-pyrrolo[2,3-*b*]pyridin-3-yl)methyl)malonate (**26**)

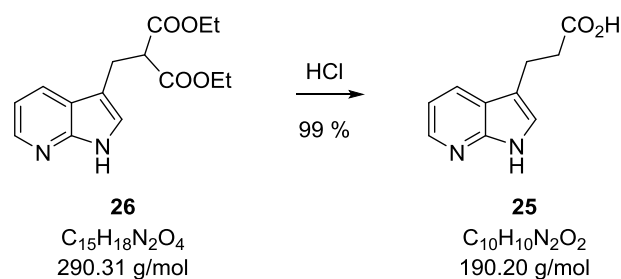
Compound **24** (200 mg, 1.14 mmol, 1.00 eq.) was dissolved in diethyl malonate (520 μL , 550 mg, 3.42 mmol, 3.00 eq.) under dry conditions and heated to 120 $^{\circ}\text{C}$. A catalytically amount of sodium was added to the reaction mixture and then stirred for 6 h at 120 $^{\circ}\text{C}$. The mixture was cooled to r.t., treated with hydrochloric acid (5 *v/v*-%, 2 mL) and extracted with diethyl ether (2 \times 10 mL). After basification with sodium carbonate the aqueous layer was extracted with diethyl ether (2 \times 10 mL), dried over MgSO_4 and concentrated under reduced pressure. The pure product (2.88 g, 9.92 mmol, 58 %) was obtained as yellow solid.

$^1\text{H-NMR}$ (400 MHz, CDCl_3): δ [ppm] = 1.16 (t, J = 7.1 Hz, 6H, 2 \times CH₃), 3.36 (d, J = 7.7 Hz, 2H, CH₂), 3.71 (t, J = 7.7 Hz, 1H, CH-(COOEt)₂), 4.04–4.19 (m, 4H, 2 \times CH₂), 7.07 (dd, J = 7.8, 4.8 Hz, 5-CH), 7.95 (dd, J = 7.8, 1.0 Hz, 1H, 6-CH), 8.29 (d, J = 4.2 Hz, 1H, 4-CH), 11.44 (s_{br}, 1H, NH).

$^{13}\text{C-NMR}$ (101 MHz, CDCl_3): δ [ppm] = 13.99 (2 \times CH₃), 24.57 (CH₂), 53.11 (CH-(COOEt)₂), 61.25 (2 \times CH₂), 110.46 (C-3), 115.31 (C-5), 120.19 (C-9), 123.74 (C-2), 127.53 (C-4), 142.11 (C-6), 148.63 (C-8), 169.12 (2 \times C(O)OEt).

ESI-MS (m/z): 291.1 $[\text{M}+\text{H}]^+$, 313.1 $[\text{M}+\text{Na}]^+$, 329.1 $[\text{M}+\text{K}]^+$.

HR-MS (ESI): calculated for $[\text{C}_{15}\text{H}_{19}\text{N}_2\text{O}_4]$ ($[\text{M}+\text{H}]^+$): 291.1339, found: 291.1341; calculated for $[\text{C}_{15}\text{H}_{18}\text{N}_2\text{O}_4\text{Na}]$ ($[\text{M}+\text{Na}]^+$): 313.1159, found: 313.1155; calculated for $[\text{C}_{15}\text{H}_{17}\text{N}_2\text{O}_4]$ ($[\text{M}-\text{H}]^-$): 289.1194, found: 289.1193.

3-(1H-Pyrrolo[2,3-*b*]pyridin-3-yl)propanoic acid (**25**)

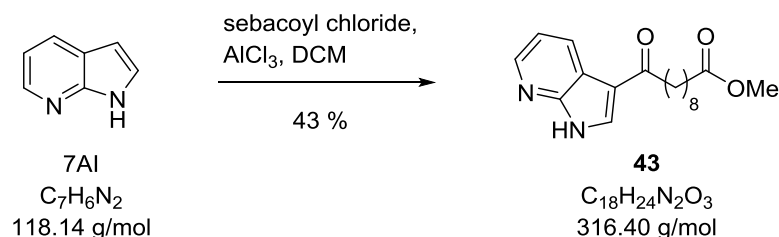
Compound **26** (1.90 g, 6.55 mmol, 1.00 eq.) was dissolved in hydrochloric acid (37 %, 28.2 mL) and heated to reflux for 7 h. The mixture was concentrated *in vacuo* to dryness. A few milliliters of water were added to the solid and a pH of 7 was adjusted by treating with aqueous Na_2CO_3 -solution (5 wt-%). The solvent was removed under reduced pressure and recrystallisation from water yielded the pure product **25** (1.23 g, 6.48 mmol, 99 %) as yellow solid.

1H -NMR (500 MHz, DMSO): δ [ppm] = 2.60 (t, J = 7.4 Hz, 2H, \underline{CH}_2 -COOH), 2.93 (t, J = 7.5 Hz, 2H, \underline{CH}_2 -C_{Ar}), 7.01 (dd, J = 7.5, 4.6 Hz, 1H, 5-CH), 7.22 (s, 1H, 2-CH), 7.94 (d, J = 7.6 Hz, 1H, 6-CH), 8.17 (d, J = 3.4 Hz, 1H, 4-CH), 11.28 (s, 1H, NH), 12.06 (s_{br}, 1H, COOH).

^{13}C -NMR (126 MHz, DMSO): δ [ppm] = 20.28 (\underline{CH}_2 -C_{Ar}), 34.43 (\underline{CH}_2 -COOH), 112.23 (C-3), 114.48 (C-5), 118.98 (C-9), 122.55 (C-2), 126.28 (C-4), 142.13 (C-6), 148.35 (C-8), 173.79 (COOH).

ESI-MS (m/z): 191.1 [M+H]⁺, 189.1 [M-H]⁻.

HR-MS (ESI): calculated for [C₁₀H₁₁N₂O₂] ([M+H]⁺): 191.0815, found: 191.0819; calculated for [C₁₀H₉N₂O₂] ([M-H]⁻): 189.0670, found: 189.0670.

Methyl 10-oxo-10-(1*H*-pyrrolo[2,3-*b*]pyridin-3-yl)decanoate (43**)**

Aluminium chloride (2.26 g, 16.9 mmol, 4.00 eq.) was suspended in anhydrous DCM (35 mL), 7AI (500 mg, 4.23 mmol, 1.00 eq.) was added and the suspension was stirred at r.t. for 1 h. Sebacoyl chloride (3.61 mL, 4.05 g, 19.9 mmol, 4.00 eq.) was added dropwise and the reaction mixture was stirred for 18 h. The suspension was cooled to 0 °C and treated dropwise with methanol (30 mL). After stirring for 1 h solid components were filtered off and the organic solvent was removed under reduced pressure. Flash column chromatography (ethyl acetate/*n*-pentane, 3:1) yielded the pure product **43** (570 mg, 1.80 mmol, 43 %) as yellow solid.

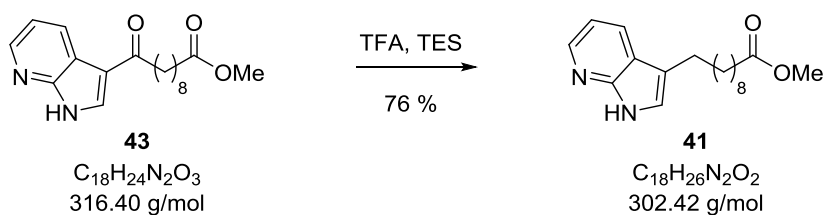
TLC (ethyl acetate/*n*-pentane 3:1): $R_f = 0.51$.

$^1\text{H-NMR}$ (400 MHz, CHCl_3): δ [ppm] = 1.17–1.45 (m, 12 H, 6 \times CH₂), 1.48–1.67 (m, 2H, 3-CH₂), 1.69–1.85 (m, 2H, 8-CH₂), 2.21–2.34 (m, 2H, 2-CH₂), 2.81–2.93 (m, 2H, 9-CH₂), 3.61 (s, 3H, OCH₃), 7.32 (dd, $J = 7.9, 5.0$ Hz, 1H, 5'-CH), 8.08 (s, 1H, 2'-CH), 8.39 (dd, $J = 5.0, 1.2$ Hz, 6'-CH), 8.80 (dd, $J = 7.9, 1.5$ Hz, 4'-CH).

$^{13}\text{C-NMR}$ (101 MHz, CDCl_3): δ [ppm] = 24.92 (C-3), 28.98 (C-8), 29.05 (C-4, C-5, C-6, C-7), 34.07 (C-2), 39.45 (C-9), 51.44 (OCH₃), 101.37 (C-3'), 116.40 (C-5'), 126.80 (C-9'), 132.03 (C-4'), 132.18 (C-2'), 142.92 (C-6'), 148.52 (C-8'), 173.89 (C-1), 196.42 (C-10).

ESI-MS (m/z): 317.2 $[\text{M}+\text{H}]^+$, 339.2 $[\text{M}+\text{Na}]^+$, 355.2 $[\text{M}+\text{K}]^+$, 315.2 $[\text{M}-\text{H}]^-$.

HR-MS (ESI): calculated for $[\text{C}_{18}\text{H}_{25}\text{N}_2\text{O}_3]$ ($[\text{M}+\text{H}]^+$): 317.1860, found: 317.1863; calculated for $[\text{C}_{18}\text{H}_{24}\text{N}_2\text{O}_3\text{Na}]$ ($[\text{M}+\text{Na}]^+$): 339.1679, found: 339.1680; calculated for $[\text{C}_{18}\text{H}_{23}\text{N}_2\text{O}_3]$ ($[\text{M}-\text{H}]^-$): 315.1714, found: 315.1717.

Methyl 10-(1*H*-pyrrolo[2,3-*b*]pyridin-3-yl)decanoate (41**)**

To a solution of **43** (150 mg, 476 μ mol, 1.00 eq.) in TFA (1.7 mL) TES (470 μ L, 350 mg, 2.97 mmol, 6.25 eq.) was added. The reaction mixture was stirred at r.t. for 18 h. TFA was removed under reduced pressure and the residue was diluted with aqueous KOH (2 M, 3 mL). The mixture was extracted with DCM (3 \times 5 mL) and the combined organic extracts were dried over $MgSO_4$. After filtration the organic solvent was removed *in vacuo* and purification via flash column chromatography (ethyl acetate/*n*-pentane, 3:1) yielded the pure product **41** (110 mg, 363 μ mol, 76 %) as yellow solid.

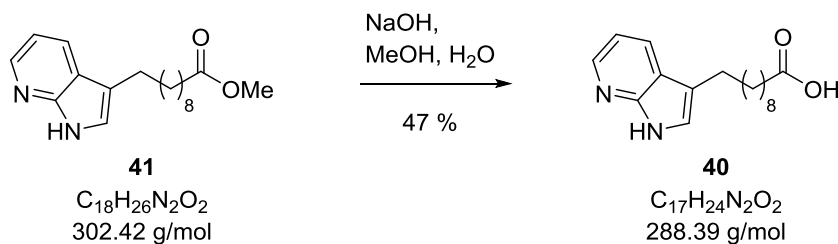
TLC (ethyl acetate/*n*-pentane, 3:1): R_f = 0.50.

1H -NMR (400 MHz, $CHCl_3$): δ [ppm] = 1.24–1.36 (m, 10H, 5 \times CH₂), 1.58 (d, J = 7.1 Hz, 2H, 9-CH₂), 1.75 (d, J = 7.5 Hz, 2H, 3-CH₂), 2.26 (dd, J = 14.4, 7.1 Hz, 2H, 2-CH₂), 2.82–2.88 (m, 2H, 10-CH₂), 3.62 (s, 3H, CH₃), 7.94–8.00 (m, 1H, 5'-CH), 8.05 (s, 1H, 2'-CH), 8.34–8.42 (m, 1H, 6'-CH), 8.70 (dd, J = 7.9, 1.5 Hz, 1H, 4'-CH).

^{13}C -NMR (101 MHz, $CDCl_3$): δ [ppm] = 25.02 (C-3), 29.09, 29.12, 29.31, 29.35, 29.45 (C-4, C-5, C-6, C-7, C-8), 34.36 (C-9), 39.47 (C-2), 45.79 (C-10), 49.89 (OCH₃), 100.81 (C-3'), 116.41 (C-5'), 118.35 (C-9'), 125.57 (C-2'), 129.66 (C-4'), 143.51 (C-6'), 149.18 (C-8'), 173.92 (C-1').

ESI-MS (m/z): 303.2 [M+H]⁺, 325.2 [M+Na]⁺.

HR-MS (ESI): calculated for [C₁₈H₂₇N₂O₂] ([M+H]⁺): 303.2067, found: 303.2073; calculated for [C₁₈H₂₆N₂O₂Na] ([M+Na]⁺): 325.1886, found: 325.1875.

10-(1*H*-Pyrrolo[2,3-*b*]pyridin-3-yl)decanoic acid (**40**)

To a solution of **41** (110 mg, 363 μ mol, 1.00 eq.) in methanol (300 μ L) water (500 μ L) and NaOH (28.0 mg, 697 μ mol, 1.92 eq.) were added. The mixture was heated to reflux for 4 h. After cooling down to r.t. the mixture was neutralised using 2 M hydrochloric acid and extracted with DCM (3 \times 2 mL). The combined organic extracts were dried over $MgSO_4$ and solvents were removed under reduced pressure. Flash column chromatography yielded the pure product (49.0 mg, 170 μ mol, 47 %) as yellow solid.

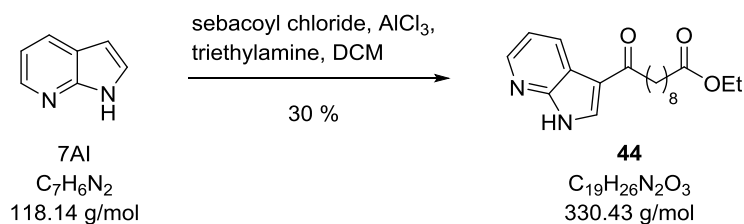
TLC (ethyl acetate/*n*-pentane, 3:1): R_f = 0.49.

1H -NMR (400 MHz, $CHCl_3$): δ [ppm] = 1.15–1.38 (m, 10H, 5 \times CH $_2$), 1.59 (d, J = 4.8 Hz, 4H, 3-CH $_2$, 9-CH $_2$), 2.29 (t, J = 7.5 Hz, 2H, 2-CH $_2$), 2.64 (t, J = 7.5 Hz, 2H, 10-CH $_2$), 6.53 (d, J = 3.5 Hz, 1H, 2'-CH), 7.39 (d, J = 3.5 Hz, 1H, 5'-CH), 8.04 (dt, J = 7.8, 1.5 Hz, 1H, 6'-CH), 8.24–8.29 (m, 1H, 4'-CH), 11.13 (s_{br}, COOH).

^{13}C -NMR (76 MHz, $CDCl_3$): δ [ppm] = 24.90 (C-3), 28.95, 29.11, 29.22, 29.91 (C-4, C-5, C-6, C-7, C-8), 34.60 (C-9), 39.24 (C-2), 45.49 (C-10), 101.11 (C-3'), 115.70 (C-5'), 121.56 (C-9'), 125.99 (C-2'), 130.50 (C-4'), 140.40 (C-6'), 147.04 (C-8'), 179.13 (C-1).

ESI-MS (m/z): 289.2 $[M+H]^+$, 287.2 $[M-H]^-$.

HR-MS (ESI): calculated for $[C_{17}H_{25}N_2O_2]$ ($[M+H]^+$): 289.1911, found: 289.1905.

Ethyl 10-oxo-10-(1*H*-pyrrolo[2,3-*b*]pyridin-3-yl)decanoate (44**)**

Aluminium chloride (2.26 g, 16.9 mmol, 4.00 eq.) was suspended in anhydrous DCM (35 mL), 7AI (500 mg, 4.23 mmol, 1.00 eq.) and triethylamine (290 μL , 210 mg, 2.12 mmol, 0.50 eq.) were added and the suspension was stirred at r.t. for 1 h. Sebacoyl chloride (3.61 mL, 4.05 g, 19.9 mmol, 4.00 eq.) was added dropwise and the reaction mixture was stirred for 18 h. The suspension was cooled to 0 °C and treated dropwise with ethanol (30 mL). After stirring for 1 h solid components were filtered off and the organic solvent was removed under reduced pressure. Flash column chromatography (ethyl acetate/*n*-pentane, 3:1) yielded the pure product **44** (420 mg, 1.26 mmol, 30 %) as yellow solid.

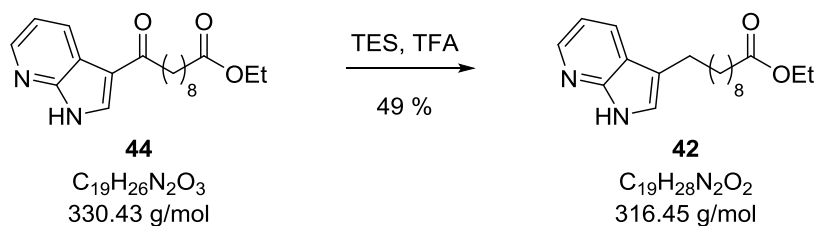
TLC (ethyl acetate/*n*-pentane, 3:1): $R_f = 0.44$.

$^1\text{H-NMR}$ (400 MHz, CHCl_3): δ [ppm] = 1.20–1.42 (m, 15H, $6\times\text{CH}_2$, CH_3), 1.51–1.65 (m, 2H, CH_2), 1.71–1.82 (m, 2H, CH_2), 2.22–2.32 (m, 2H, CH_2), 2.82–2.92 (m, 2H, CH_2), 4.06–4.19 (m, 2H, OCH_2CH_3), 7.32 (dd, $J = 7.9, 5.0 \text{ Hz}$, 1H, 5'-CH), 8.08 (s, 1H, 2'-CH), 8.39 (dd, $J = 5.0, 1.2 \text{ Hz}$, 1H, 6'-CH), 8.80 (dd, $J = 7.9, 1.5 \text{ Hz}$, 1H, 4'-CH).

$^{13}\text{C-NMR}$ (101 MHz, CDCl_3): δ [ppm] = 14.25 (CH_3), 24.95 (C-3), 29.09, 29.12, 29.31, 29.45 (C-4, C-5, C-6, C-7, C-8), 34.36 (C-2), 60.17 (OCH_2CH_3), 100.81 (C-3'), 116.40 (C-5'), 118.35 (C-9'), 131.35 (C-4'), 131.80 (C-2'), 143.51 (C-6'), 149.18 (C-8'), 173.92 (C-1'), 196.43 (C-10).

ESI-MS (m/z): 331.2 $[\text{M}+\text{H}]^+$, 329.2 $[\text{M}-\text{H}]^-$.

HR-MS (ESI): calculated for $[\text{C}_{19}\text{H}_{27}\text{N}_2\text{O}_3]$ ($[\text{M}+\text{H}]^+$): 331.2016, found: 331.2020; calculated for $[\text{C}_{19}\text{H}_{25}\text{N}_2\text{O}_3]$ ($[\text{M}-\text{H}]^-$): 329.1871, found: 329.1856.

Ethyl 10-(1*H*-pyrrolo[2,3-*b*]pyridin-3-yl)decanoate (**42**)

To a solution of **44** (200 mg, 605 μ mol, 1.00 eq.) in TFA (2 mL) TES (610 μ L, 440 mg, 3.78 mmol, 6.25 eq.) was added. The reaction mixture was stirred at r.t. for 18 h. TFA was removed under reduced pressure and the residue was diluted with aqueous KOH (2 M, 3 mL). The mixture was extracted with DCM (3 \times 5 mL) and the combined organic extracts were dried over $MgSO_4$. After filtration the organic solvent was removed *in vacuo* and purification via flash column chromatography (ethyl acetate/*n*-pentane, 3:1) yielded the pure product **42** (93.8 mg, 296 μ mol, 49 %) as yellow solid.

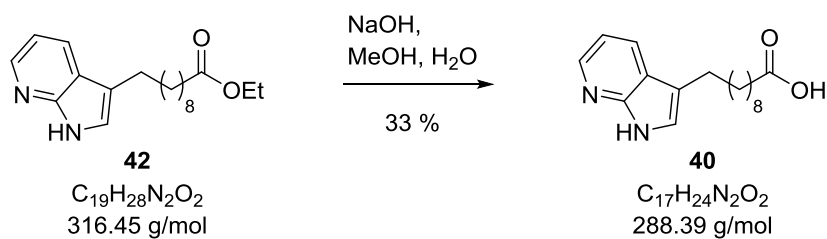
TLC (ethyl acetate/*n*-pentane, 2:1): R_f = 0.41.

1H -NMR (400 MHz, $CHCl_3$): δ [ppm] = 1.22 (t, J = 7.1 Hz, 3H, CH_3), 1.24–1.36 (m, 10H, $5 \times CH_2$), 1.58 (d, J = 7.1 Hz, 2H, 9- CH_2), 1.75 (d, J = 7.5 Hz, 2H, 3- CH_2), 2.26 (dd, J = 14.4, 7.1 Hz, 2H, 2- CH_2), 2.82–2.88 (m, 2H, 10- CH_2), 4.09 (q, J = 7.1 Hz, 2H, OCH_2CH_3), 7.94–8.00 (m, 1H, 5'-CH), 8.05 (s, 1H, 2'-CH), 8.34–8.42 (m, 1H, 6'-CH), 8.70 (dd, J = 7.9, 1.5 Hz, 1H, 4'-CH).

^{13}C -NMR (101 MHz, $CDCl_3$): δ [ppm] = 14.25 (CH_3), 25.02 (C-3), 29.09, 29.12, 29.31, 29.35, 29.45 (C-4, C-5, C-6, C-7, C-8), 34.36 (C-9), 39.47 (C-2), 45.79 (C-10), 60.17 (OCH_2CH_3), 100.81 (C-3'), 116.41 (C-5'), 118.35 (C-9'), 125.57 (C-2'), 129.66 (C-4'), 143.51 (C-6'), 149.18 (C-8'), 173.92 (C-1).

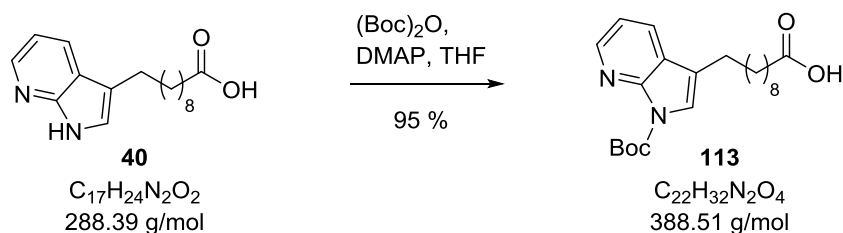
ESI-MS (m/z): 317.2 $[M+H]^+$.

HR-MS (ESI): calculated for $[C_{19}H_{29}N_2O_2]$ ($[M+H]^+$): 317.2224, found: 317.2223.

10-(1*H*-Pyrrolo[2,3-*b*]pyridin-3-yl)decanoic acid (40**)**

To a solution of **42** (700 mg, 2.21 mmol, 1.00 eq.) in methanol (1.8 mL) water (2.7 mL) and NaOH (1.77 g, 44.1 mmol, 20.0 eq.) were added. The mixture was heated to reflux for 4 h. After cooling down to r.t. the mixture was neutralised using 2 M hydrochloric acid and extracted with DCM (3 × 10 mL). The combined organic extracts were dried over MgSO₄ and solvents were removed under reduced pressure. Flash column chromatography yielded the pure product **40** (270 mg, 717 μmol, 33 %) as yellow solid.

Analytical data see page 123.

10-(1-(*tert*-Butoxycarbonyl)-1*H*-pyrrolo[2,3-*b*]pyridin-3-yl)decanoic acid (**113**)

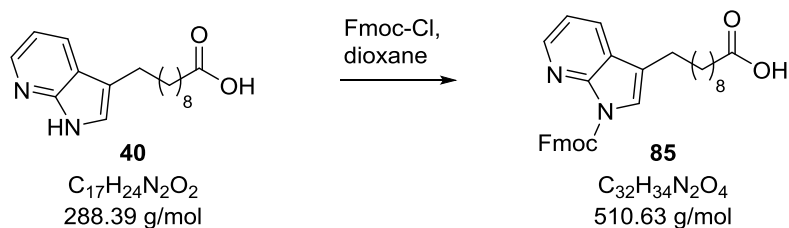
To a solution of **40** (100 mg, 347 μ mol, 1.00 eq.) in THF (500 μ L) DMAP (400 μ g, 3.46 μ mol, 0.01 eq.) and Boc anhydride (80.0 mg, 375 μ mol, 1.08 eq.) were added. The mixture was stirred at r.t. for 1 h and treated with a second portion of Boc anhydride (8.00 mg, 37.5 μ mol, 0.11 eq.). After stirring for another hour water (8 μ L) was added and the mixture was stirred for 30 min. The mixture was concentrated under reduced pressure and coevaporated with toluene (2×1 mL). Purification via flash column chromatography (DCM/MeOH, 98:2) yielded the product **113** (128 mg, 330 μ mol, 95 %) as yellow solid.

TLC (DCM/MeOH, 98:2): R_f = 0.49.

1H -NMR (400 MHz, $CHCl_3$): δ [ppm] = 1.20–1.37 (m, 14H, $7 \times CH_2$), 1.61 (s, 9H, $3 \times CH_3$,_{Boc}), 2.32 (t, J = 7.5 Hz, 2H, CH_2), 2.66 (t, J = 7.4 Hz, 2H, CH_2), 7.05 (s, 1H, 2'-CH), 7.29–7.33 (m, 1H, 5'-CH), 8.11 (d, J = 3.6 Hz, 1H, 6'-CH), 8.46 (d, J = 5.1 Hz, 1H, 4'-CH).

ESI-MS (m/z): 389.2 $[M+H]^+$, 411.2 $[M+Na]^+$, 387.3 $[M-H]^-$.

HR-MS (ESI): calculated for $[C_{22}H_{31}N_2O_4]$ ($[M-H]^-$): 387.2289, found: 387.2279.

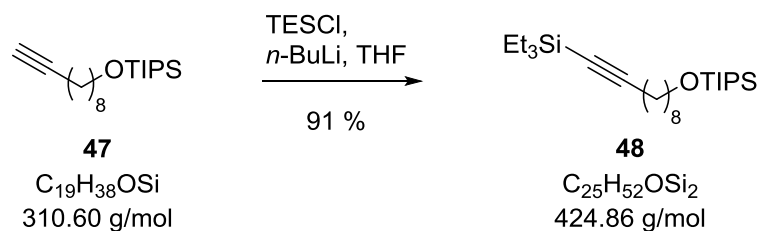
10-(1-(((9H-Fluoren-9-yl)methoxy)carbonyl)-1H-pyrrolo[2,3-b]pyridin-3-yl) decanoic acid (85)

Compound **40** (100 mg, 347 μ mol, 1.00 eq.) was dissolved in aqueous $NaHCO_3$ -solution (10 w/w-%, 1 mL). The solution was cooled down to 0 °C and treated dropwise with Fmoc-Cl (110 mg, 409 μ mol, 1.18 eq.) in dioxane (1 mL). The mixture was stirred at 0 °C for 1 h, warmed up to r.t. and stirred for 7 d. After dilution with water (10 mL) the mixture was extracted with diethyl ether (2×10 mL). The combined organic extracts were dried over $MgSO_4$ and concentrated under reduced pressure. The obtained yellow solid was a mixture of Fmoc-protected **85** and **40**. Attempts to purify the crude were unsuccessful.

TLC (*n*-pentane/ethyl acetate, 3:1): R_f = 0.40.

ESI-MS (m/z): 533.2 $[M+Na]^+$.

HR-MS (ESI): calculated for $[C_{32}H_{34}N_2O_4Na]$ ($[M+Na]^+$): 533.2411, found: 533.2400.

Triethyl(10-((triisopropylsilyl)oxy)dec-1-yn-1-yl)silane **48**

A solution of **47** (2.00 g, 6.44 mmol, 1.00 eq.) in anhydrous THF (20 mL) was cooled to $-78\text{ }^{\circ}\text{C}$, treated dropwise with *n*-BuLi (2.5 M, 2.78 mL, 6.95 mmol, 1.08 eq.) and stirred for 30–40 min. TESCl (1.17 mL, 1.05 g, 6.95 mmol, 1.08 eq.) was slowly added and the reaction mixture stirred at $-78\text{ }^{\circ}\text{C}$ stirred for 60 min. The mixture was warmed up to r.t. and diluted with aqueous NaHCO₃-solution (5 w/w-%, 15 mL). After extraction with *n*-pentane (3 \times 20 mL) the combined organic extracts were washed with water (2 \times 45 mL), dried over MgSO₄ and concentrated *in vacuo*. Purification via flash column chromatography (*n*-pentane/ethyl acetate, 6:1) yielded the pure product **48** (2.48 g, 5.84 mmol, 91 %) as colourless oil.

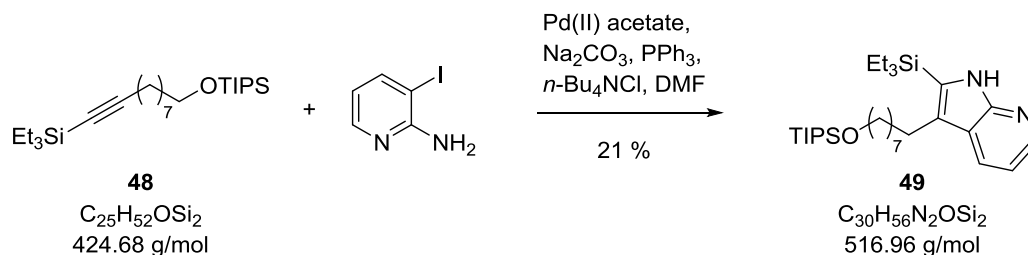
TLC (*n*-pentane/ethyl acetate 6:1): $R_f = 0.92$.

¹H-NMR (400 MHz, CHCl₃): δ [ppm] = 0.55 (q, $J = 8.1\text{ Hz}$, 6H, 3 \times CH_{2,TES}), 0.96 (t, $J = 7.9\text{ Hz}$, 9H, 3 \times CH_{3,TES}), 1.02–1.07 (m, 18H, 6 \times CH_{3,TIPS}), 1.24–1.42 (m, 10H, 5 \times CH₂), 1.45–1.55 (m, 5H, 3 \times CH_{TIPS}, 9-CH₂), 2.21 (t, $J = 7.0\text{ Hz}$, 2H, 3-CH₂), 3.64 (t, $J = 6.6\text{ Hz}$, 2H, 10-CH₂).

¹³C-NMR (101 MHz, CDCl₃): δ [ppm] = 4.58 (3 \times CH_{2,TES}), 7.45 (3 \times CH_{3,TES}), 18.02 (6 \times CH_{3,TIPS}), 19.85 (C-3), 25.77 (3 \times CH_{TIPS}), 28.69, 28.76, 29.08, 29.35 (C-4, C-5, C-6, C-7, C-8), 33.02 (C-9), 63.48 (C-10), 81.33 (C-2), 108.82 (C-1).

ESI-MS (m/z): 425.4 [M+H]⁺, 447.4 [M+Na]⁺.

HR-MS (ESI): calculated for [C₂₅H₅₂OSiNa] ([M+Na]⁺): 447.3449, found: 447.3441.

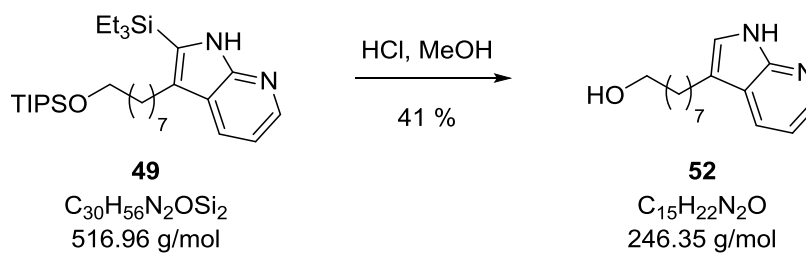
2-(Triethylsilyl)-3-(8-((triisopropylsilyl)oxy)octyl)-1H-pyrrolo[2,3-b] pyridine 49

A Schlenk flask was furnished with palladium(II) acetate (10.2 mg, 45.5 μmol , 0.05 eq.), Na_2CO_3 (480 mg, 4.55 mmol, 5.00 eq.), 2-amino-3-iodopyridine (200 mg, 909 μmol , 1.00 eq.) and **48** (500 mg, 1.18 mmol, 1.30 eq.). Triphenylphosphine (11.9 mg, 45.5 μmol , 0.05 eq.) and tetra-*n*-butylammonium chloride (250 mg, 909 μmol , 1.00 eq.) were added. The solids were dissolved in anhydrous DMF (20 mL) and the flask was provided with a reflux condenser. The reaction mixture was stirred at 100 $^\circ\text{C}$ for 15 h. The mixture was allowed to cool down to r.t., diluted with water (30 mL) and extracted with DCM (3×20 mL). The combined organic layers were dried over MgSO_4 and the solvent was removed under reduced pressure. Flash column chromatography (*n*-pentane/ethyl acetate, 5:1) provided the product **49** (200 mg, 386 μmol , 21 %) as brown oil.

TLC (*n*-pentane/ethyl acetate, 5:1): $R_f = 0.41$.

ESI-MS (m/z): 517.4 $[\text{M}+\text{H}]^+$, 1033.9 $[2\text{M}+\text{H}]^+$, 515.4 $[\text{M}-\text{H}]^-$.

HR-MS (ESI): calculated for $[\text{C}_{30}\text{H}_{57}\text{N}_2\text{OSi}_2]$ ($[\text{M}+\text{H}]^+$): 517.4004, found: 517.4003; calculated for $[\text{C}_{30}\text{H}_{55}\text{N}_2\text{OSi}_2]^-$ ($[\text{M}-\text{H}]^-$): 515.3858, found: 515.3849.

8-(1*H*-Pyrrolo[2,3-*b*]pyridin-3-yl)octan-1-ol (**52**)

To a solution of **49** (170 mg, 320 μmol , 1.00 eq.) in concentrated hydrochloric acid (2.4 mL) methanol (2.4 mL) was added and stirred under reflux for 24 h. The reaction mixture was diluted with isopropyl acetate (6.4 mL) and water (1.1 mL). The layers were separated and the organic layer was concentrated under reduced pressure. Purification via flash column chromatography (*n*-pentane/ethyl acetate, 3:1) yielded the product **52** (32.4 mg, 132 μmol , 41 %) as yellow solid.

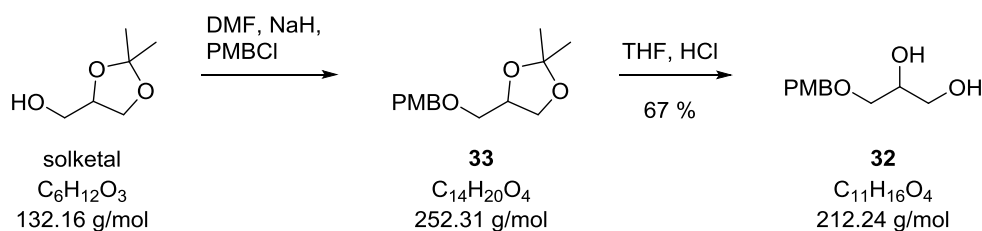
TLC (*n*-pentane/ethyl acetate 3:1): R_f = 0.46.

ESI-MS (m/z): 247.2 $[\text{M}+\text{H}]^+$, 245.2 $[\text{M}-\text{H}]^-$.

HR-MS (ESI): calculated for $[\text{C}_{15}\text{H}_{23}\text{N}_2\text{O}]$ ($[\text{M}+\text{H}]^+$): 247.1805, found: 247.1805; calculated for $[\text{C}_{15}\text{H}_{21}\text{N}_2\text{O}]$ ($[\text{M}-\text{H}]^-$): 245.1659, found: 245.1654.

6.5.3 Synthesis of Phospholipids

3-((4-Methoxybenzyl)oxy)propane-1,2-diol (**32**)



To a solution of solketal (2.34 mL, 2.50 g, 18.9 mmol, 1.00 eq.) in dry DMF (250 mL) sodium hydride (60 %, 1.14 g, 28.4 mmol, 1.50 eq.) and *p*-methoxybenzyl chloride (3.08 mL, 3.56 g, 22.7 mmol, 1.20 eq.) were added. The reaction mixture was stirred under inert gas at r.t. for 18 h. Excess of sodium hydride was quenched by addition of methanol. The mixture was extracted with DCM (3 × 200 mL), and the combined organic extracts were washed with water and brine. After drying over MgSO_4 the solvent was removed under reduced pressure.

The obtained oil was dissolved in THF (50 mL), hydrochloric acid (1 M, 50 mL) was added and the mixture was stirred at r.t. for 20 h. The mixture was neutralised using saturated aqueous sodium hydrogen carbonate solution. The organic solvent was removed *in vacuo* and the aqueous layer was extracted with ethyl acetate (3 × 40 mL) added. The mixture was dried over MgSO_4 and concentrated under reduced pressure. Flash column chromatography (ethyl acetate/*n*-pentane, 3:1) yielded the product **32** (2.70 g, 12.7 mmol, 67 %) as white solid.

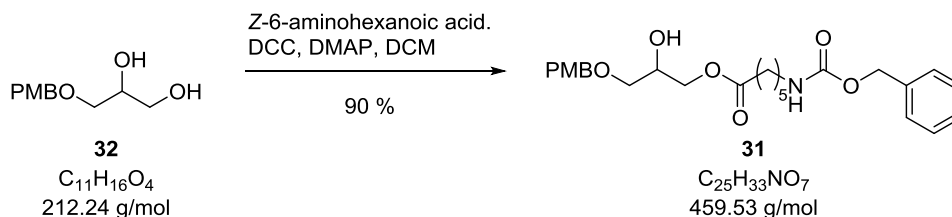
TLC (ethyl acetate): $R_f = 0.49$.

$^1\text{H-NMR}$ (300 MHz, CDCl_3): δ [ppm] = 3.39–3.60 (m, 2H, 1- CH_2), 3.72 (d, $J = 4.6$ Hz, 2H, 3- CH_2), 3.74 (s, 3H, OCH_3), 3.80 (dd, $J = 6.3, 2.5$ Hz, 1H, 2-CH), 4.41 (s, 2H, $\text{CH}_2\text{-C}_{\text{Ar}}$), 6.80–6.86 (m, 2H, $2 \times \text{CH}_{\text{Ar}}$), 7.17–7.23 (m, 2H, CH_{Ar}).

$^{13}\text{C-NMR}$ (126 MHz, CDCl_3): δ [ppm] = 55.06 (OCH_3), 63.81 (C-1), 70.69 (C-2), 71.14 (C-3), 72.93 ($\text{CH}_2\text{-C}_{\text{Ar}}$), 113.66 ($2 \times \text{CH}_{\text{Ar}}$), 129.28 ($2 \times \text{CH}_{\text{Ar}}$), 129.69 ($\text{C}_{\text{Ar}}\text{-CH}_2$), 159.12 ($\text{C}_{\text{Ar}}\text{-OCH}_3$).

ESI-MS (m/z): 235.1 $[\text{M}+\text{Na}]^+$, 251.1 $[\text{M}+\text{K}]^+$, 211.1 $[\text{M}-\text{H}]^-$.

HR-MS (ESI): calculated for $[\text{C}_{11}\text{H}_{16}\text{O}_4\text{Na}]$ ($[\text{M}+\text{Na}]^+$): 235.0941, found: 235.0943; calculated for $[\text{C}_{11}\text{H}_{15}\text{O}_4]$ ($[\text{M}-\text{H}]^-$): 211.0976, found: 211.0979.

2-Hydroxy-3-((4-methoxybenzyl)oxy)propyl hexanoate (31)**6-(((benzyloxy)carbonyl)amino)**

A solution of **32** (4.82 g, 22.7 mmol, 1.04 eq.) and Z-6-aminohexanoic acid (5.79 g, 21.8 mmol, 1.00 eq.) in DCM (200 mL) was treated dropwise at 0 °C with a solution of DCC (5.40 g, 26.2 mmol, 1.20 eq.) and DMAP (3.20 g, 26.2 mmol, 1.20 eq.) in DCM (50 mL) under dry conditions. The reaction mixture was stirred at 0 °C for 16 h, concentrated under reduced pressure and redissolved in ethyl acetate (100 mL). The resulting solid was filtered off and the filtrate was concentrated *in vacuo*. The pure product **31** (9.41 g, 20.5 mmol, 90 %) was obtained after flash column chromatography (DCM/ethyl acetate, 3:1).

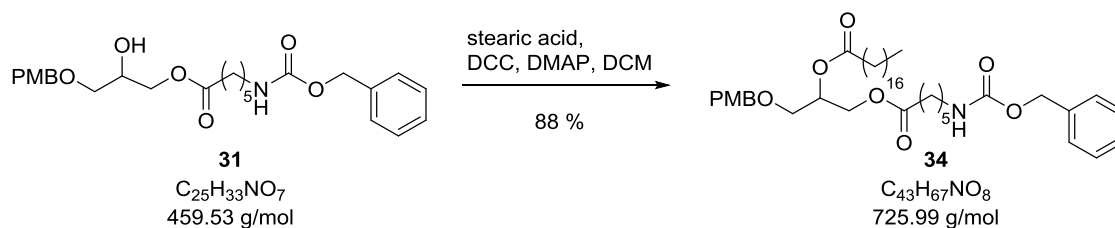
TLC (DCM/ethyl acetate, 3:1): $R_f = 0.41$.

$^1\text{H-NMR}$ (301 MHz, CDCl_3): δ [ppm] = 1.46 (dd, $J = 14.3, 7.2$ Hz, 2H, 4'- CH_2), 1.58 (dt, $J = 15.4, 7.9$ Hz, 4H, 3'- CH_2 , 5'- CH_2), 2.29 (t, $J = 6.2$ Hz, 2H, 2'- CH_2), 3.15 (dd, $J = 13.0, 6.7$ Hz, 2H, 6'- CH_2), 3.49–3.55 (m, 2H, 3- CH_2), 3.76 (s, 3H, OCH_3), 4.09–4.18 (m, 1H, 2-CH), 4.31 (dd, $J = 11.9, 3.8$ Hz, 2H, 1- CH_2), 4.37–4.49 (m, 2H, $\text{CH}_2\text{-C}_{\text{PMB}}$), 4.89 (s, 1H NH), 5.06 (s, $\text{CH}_{2,\text{Z}}$), 6.81–6.87 (m, 2H, $2\times\text{CH}_{\text{PMB}}$), 7.17–7.23 (m, 2H, $2\times\text{CH}_{\text{PMB}}$), 7.31 (s, 5H, $5\times\text{CH}_2$).

$^{13}\text{C-NMR}$ (125 MHz, CDCl_3): δ [ppm] = 24.52 (C-3'), 26.18 (C-4'), 29.62 (C-5'), 33.89 (C-2'), 40.83 (C-6'), 55.26 (OCH_3), 62.76 (C-2), 66.53 ($\text{CH}_{2,\text{Z}}$), 67.82 (C-3), 70.09 (C-1), 72.89 ($\text{CH}_2\text{-C}_{\text{PMB}}$), 113.72 ($2\times\text{CH}_{\text{PMB}}$), 127.93 ($2\times\text{CH}_Z$), 127.96 (CH_Z), 128.36 ($2\times\text{CH}_Z$), 129.20 ($2\times\text{CH}_{\text{PMB}}$), 129.58 ($\text{C}_{\text{PMB}}\text{-CH}_2$), 136.51 ($\text{C}_Z\text{-CH}_2$), 156.24 (N-C(O)OZ), 159.14 ($\text{C}_{\text{PMB}}\text{-OCH}_3$), 172.88 (C-1').

ESI-MS (m/z): 460.2 $[\text{M}+\text{H}]^+$, 477.3 $[\text{M}+\text{NH}_4]^+$, 482.2 $[\text{M}+\text{Na}]^+$.

HR-MS (ESI): calculated for $[\text{C}_{25}\text{H}_{34}\text{NO}_7]$ ($[\text{M}+\text{H}]^+$): 460.2330, found: 460.232; calculated for $[\text{C}_{25}\text{H}_{33}\text{NO}_7\text{Na}]$ ($[\text{M}+\text{Na}]^+$): 482.2149, found: 482.2150.

16-(4-Methoxyphenyl)-3,10-dioxo-1-phenyl-2,11,15-trioxa-4-azahexadecan-13-yl stearate (34)


To a solution of **31** (1.20 g, 2.61 mmol, 1.00 eq.) and stearic acid (950 μL , 890 mg, 3.13 mmol, 1.20 eq.) in anhydrous DCM (14.4 mL) a solution of DCC (650 mg, 3.13 mmol, 1.20 eq.) and DMAP (180 mg, 1.44 mmol, 0.55 eq.) in anhydrous DCM (7.2 mL) was added dropwise. The reaction mixture was stirred for 24 h at r.t.. After reducing the mixture under reduced pressure the residue was dissolved in ethyl acetate (12 mL), filtrated and concentrated again under reduced pressure. The crude product was purified via flash column chromatography (*n*-pentane/ethyl acetate, 4:1) to yield the pure product **34** (1.66 g, 2.29 mmol, 88 %) as white crystals.

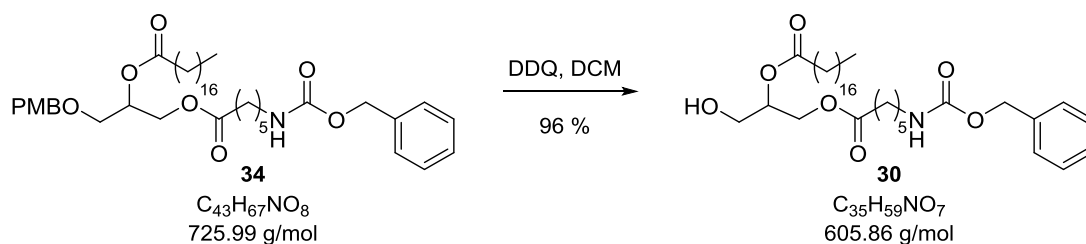
TLC (*n*-pentane/ethyl acetate, 4:1): 0.55.

$^1\text{H-NMR}$ (300 MHz, CDCl_3): δ [ppm] = 0.86 (t, J = 6.7 Hz, 3H, CH_3), 1.23 (s, 30H, $15\times\text{CH}_2$), 1.46 (dd, J = 14.3, 7.2 Hz, 2H, CH_2), 1.52–1.66 (m, 4H, $2\times\text{CH}_2$), 2.27 (dt, J = 12.0, 7.4 Hz, 4H, $2'\text{-CH}_2$, $2''\text{-CH}_2$), 3.15 (dd, J = 13.0, 6.7 Hz, 2H, $6'\text{-CH}_2$), 3.52 (dd, J = 5.1, 2.1 Hz, 2H, 3-CH_2), 3.76 (s, 3H, OCH_3), 4.13 (dd, J = 11.9, 6.5 Hz, 1H, $1\text{-CH}_{2,a}$), 4.31 (dd, J = 11.9, 3.8 Hz, 1H, $1\text{-CH}_{2,b}$), 4.36–4.50 (m, 2H, $\text{C-CH}_2\text{PMB}$), 4.89 (sbr, 1H, NH), 5.06 (s, 2H, CH_2,z), 5.15–5.26 (m, 1H, 2-CH), 6.81–6.88 (m, 2H, $2\times\text{CH}_{\text{PMB}}$), 7.16–7.23 (m, 2H, $2\times\text{CH}_{\text{PMB}}$), 7.26–7.34 (m, 5H, $5\times\text{CH}_2$).

$^{13}\text{C-NMR}$ (126 MHz, CDCl_3): δ [ppm] = 14.02 (C-18''), 22.59 (C-17''), 24.30, 24.85, 26.05, 28.98, 29.19, 29.26, 29.39, 29.53, 29.56, 29.60, 31.82, 33.75, 34.21, 40.72 (C-6'), 55.13 (OCH_3), 62.72 (C-2), 66.43 ($\text{CH}_{2,z}$), 67.78 (C-3), 69.91 (C-1), 72.84 ($\text{CH}_2\text{-C}_{\text{PMB}}$), 113.71 ($2\times\text{CH}_{\text{PMB}}$), 127.93 ($2\times\text{CH}_z$), 127.96 (CH_z), 128.37 ($2\times\text{CH}_z$), 129.18 ($2\times\text{CH}_{\text{PMB}}$), 129.65 ($\text{C}_{\text{PMB}}\text{-CH}_2$), 136.58 ($\text{C}_z\text{-CH}_2$), 156.28 (N-C(O)OZ), 159.21 ($\text{C}_{\text{PMB}}\text{-OCH}_3$), 172.94 (C(O)O), 173.00 (C(O)O).

ESI-MS (m/z): 726.5 $[\text{M}+\text{H}]^+$, 743.5 $[\text{M}+\text{NH}_4]^+$, 748.5 $[\text{M}+\text{Na}]^+$, 724.5 $[\text{M}-\text{H}]^-$.

HR-MS (ESI): calculated for $[\text{C}_{43}\text{H}_{68}\text{NO}_8]$ ($[\text{M}+\text{H}]^+$): 726.4939, found: 726.4918; calculated for $[\text{C}_{43}\text{H}_{67}\text{NO}_8\text{Na}]$ ($[\text{M}+\text{Na}]^+$): 748.4759, found: 748.4765; calculated for $[\text{C}_{43}\text{H}_{71}\text{N}_2\text{O}_8]$ ($[\text{M}+\text{NH}_4]^+$): 743.5205, found: 743.5204; calculated for $[\text{C}_{43}\text{H}_{66}\text{NO}_8]$ ($[\text{M}-\text{H}]^+$): 724.4794, found: 724.4808.

1-((6-(((Benzyloxy)carbonyl)amino)hexanoyl)oxy)-3-hydroxypropan-2-yl stearate (30)

A solution of **34** (1.10 g, 1.52 mmol, 1.00 eq.) in DCM (50 mL) was treated with DDQ (720 mg, 3.17 mmol, 2.09 eq.) and stirred at r.t. for 24 h. The mixture was diluted with DCM (20 mL), washed with aqueous NaHCO_3 solution (10 w/w-%, 60 mL) and dried over MgSO_4 . After removal of the organic solvent under reduced pressure the product was purified using flash column chromatography (*n*-pentane/ethyl acetate, 7:3). The pure product (880 mg, 1.45 mmol, 96 %) was obtained as white crystals.

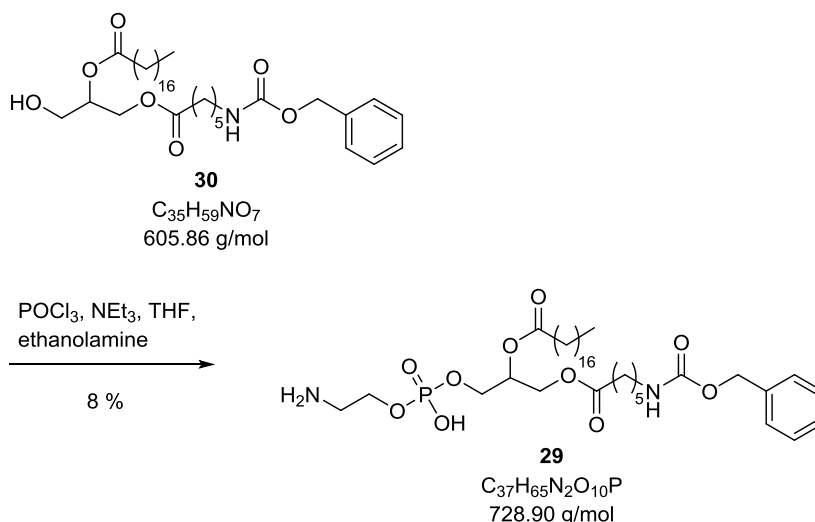
TLC (*n*-pentane/ethyl acetate, 7:3): $R_f = 0.73$.

$^1\text{H-NMR}$ (300 MHz, CDCl_3): δ [ppm] = 0.86 (t, $J = 6.7$ Hz, 3H, 18'- CH_3), 1.23 (s, 30H, 15 \times CH_2), 1.43–1.65 (m, 6H, 3 \times CH_2), 2.22–2.39 (m, 4H, 2'- CH_2 , 2''- CH_2), 3.16 (dt, $J = 11.7$, 5.8 Hz, 2H, 6''- CH_2), 3.53–3.72 (m, 2H, 3- CH_2), 4.14–4.35 (m, 2H, 1- CH_2), 5.02–5.10 (m, 1H, 2-CH), 5.21 (s, 2H, $\text{CH}_{2,Z}$), 6.82 (s_{br}, 1H, NH), 7.29–7.39 (m, 5H, CH_Z).

ESI-MS (m/z): 606.4 $[\text{M}+\text{H}]^+$, 623.5 $[\text{M}+\text{NH}_4]^+$, 628.4 $[\text{M}+\text{Na}]^+$.

HR-MS (ESI): calculated for $[\text{C}_{35}\text{H}_{60}\text{NO}_7]$ ($[\text{M}+\text{H}]^+$): 606.4364, found: 606.4353; calculated for $[\text{C}_{35}\text{H}_{59}\text{NO}_7\text{Na}]$ ($[\text{M}+\text{Na}]^+$): 628.4184, found: 628.4183.

1-(((2-Aminoethoxy)(hydroxy)phosphoryl)oxy)-3-(((6-(((benzyloxy)carbonyl)amino)hexanoyl)oxy)propan-2-yl stearate (29)



To a solution of phosphoryl trichloride (270 μ L, 450 mg, 2.93 mmol, 3.09 eq.) in anhydrous THF (3.3 mL) a mixture of **30** (580 mg, 958 μ mol, 1.00 eq.) and triethylamine (410 μ L, 300 mg, 2.92 mmol, 3.05 eq.) in anhydrous THF (5 mL) was added over 15 min at 0 °C. The reaction mixture was stirred at 0 °C for 10 min and for 45 min at r.t.. The mixture was cooled down again to 0 °C and treated with a mixture of ethanolamine (180 μ L, 180 mg, 2.93 mmol, 3.06 eq.) and triethylamine (810 μ L, 590 mg, 5.84 mmol, 6.10 eq.) in THF (8.5 mL) dropwise over 15 min. After stirring for 10 min at 0 °C the reaction mixture was stirred at r.t. over night. The mixture was filtered and the filtrate concentrated under reduced pressure. The residue was dissolved in a mixture of acetic acid (8.3 mL) and water (3.5 mL) and heated to 70 °C for 1 h. After extraction with chloroform (3 \times 15 mL) the combined organic extracts were washed with water (2 \times 20 mL) and concentrated under reduced pressure. Flash column chromatography (*n*-pentane/ethyl acetate, 7:3) yielded the pure product **29** (56.0 mg, 77.2 μ mol, 8 %) as yellow solid.

TLC (*n*-pentane/ethyl acetate, 7:3): *R*_f = 0.81.

¹H-NMR (400 MHz, CDCl₃): δ [ppm] = 0.86 (t, *J* = 6.8 Hz, 3H, 18'-CH₃), 1.23 (s, 30H, 15 \times CH₂), 1.44–1.68 (m, 6H, 3 \times CH₂), 2.25–2.36 (m, 4H, 2'-CH₂, 2''-CH₂), 3.14–3.21 (m, 2H, 6'-CH₂), 3.56–3.68 (m, 2H, 2'''-CH₂), 3.70–3.75 (m, 2H, 1'''-CH₂), 3.86 (s, 2H, NH₂), 4.01–4.34 (m, 4H, 1-CH₂, 3-CH₂), 4.78 (s_{br}, 1H, OH), 5.08 (s, 2H, CH₂z), 5.16–.24 (m, 1H, 2-CH), 6.76 (s, 1H, NH) 7.33 (s, 5H, 5 \times CH₂).

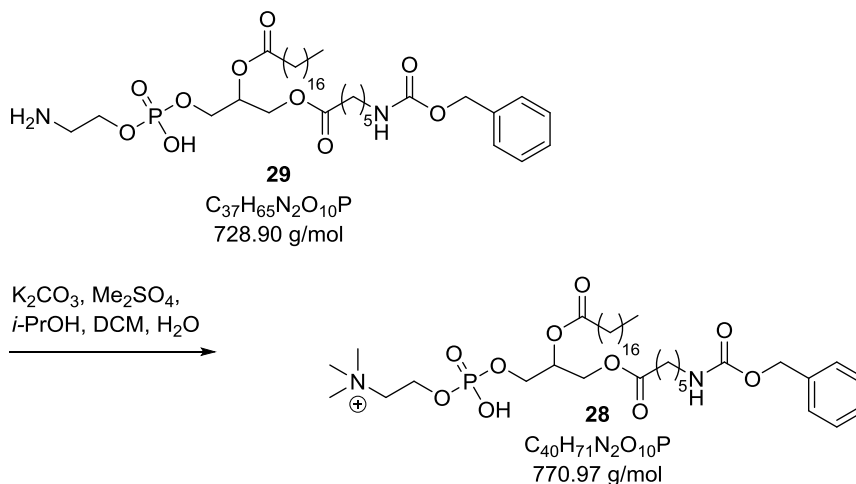
¹³C-NMR (101 MHz, CDCl₃): δ [ppm] = 14.12 (C-18''), 22.69 (C-17''), 24.44, 24.89 (C-3', C-3''), 25.61, 26.14, 29.06, 29.25, 29.36, 29.47, 29.61, 29.66, 29.70, 31.93 (C-16''), 33.80 (C-2'), 34.17 (C-2''), 40.82 (C-6'), 42.28 (C-2'''), 62.16 (C-1'''), 62.39 (C-2), 66.65 (CH₂z),

67.97 (C-3), 70.17 (C-1), 128.11 (CH₂), 128.52 (2×CH₂), 132.02 (C_Z-CH₂), 132.33 (2×CH₂), 164.00 (N-C(O)OZ), 172.87, 172.93 (C-1', C-1'').

ESI-MS (*m/z*): 729.5 [M+H]⁺, 751.4 [M+Na]⁺, 727.4 [M-H]⁻.

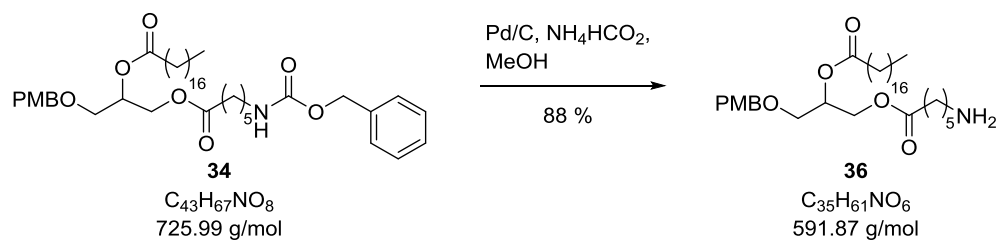
HR-MS (ESI): calculated for [C₃₇H₆₆N₂O₁₀P] ([M+H]⁺): 729.4450, found: 729.4440; calculated for [C₃₇H₆₅N₂O₁₀PNa] ([M+Na]⁺): 751.4269, found: 751.4256.

3-(((6-(((Benzyloxy)carbonyl)amino)hexanoyl)oxy)-2-(stearoyloxy)propyl (trimethylammonio)ethyl) phosphate (28) (2-



Compound **29** (300 mg, 412 μ mol, 1.00 eq.) was dissolved in 2-propanol (7 mL) and DCM (2.4 mL) and heated afterwards to 35–40 °C. The mixture was treated dropwise with K_2CO_3 (280 mg, 2.06 mmol, 5.00 eq.) in water (1.4 mL) over 5 min. A solution of dimethylsulfate (200 μ L, 270 mg, 2.10 mmol, 5.11 eq.) in 2-propanol (1.4 mL) was added over 10 min at 40 °C. The reaction mixture was stirred at 40 °C for 90 min, diluted with water (5 mL) and extracted with chloroform (2 \times 10 mL). The combined organic extracts were washed with water (20 mL) and the organic solvent was removed under reduced pressure. Product traces were found in mass spectrometry, but isolation of the pure product **28** was unsuccessful. Furthermore, the mass spectrum showed formation of a methylphosphate ester (**35**).

ESI-MS (m/z): 769.5 $[M-H]^-$, 785.5 $[MeM]^+$.

1-((6-Aminohexanoyl)oxy)-3-((4-methoxybenzyl)oxy)propan-2-yl stearate (36)

To a solution of **34** (500 mg, 689 μmol , 1.00 eq.) in anhydrous methanol (20 mL) Pd/C (10 %, 140 mg) and ammonium formate (220 mg, 3.45 mmol, 5.00 eq.) were added. The mixture was heated to reflux for 2.5 h, cooled down to r.t. and solid components were filtered off. The filtrate was concentrated under reduced pressure. Without further purification the pure product **36** (360 mg, 603 μmol , 88 %) was yielded as yellow solid.

TLC (DCM/MeOH, 9:1): R_f = 0.62.

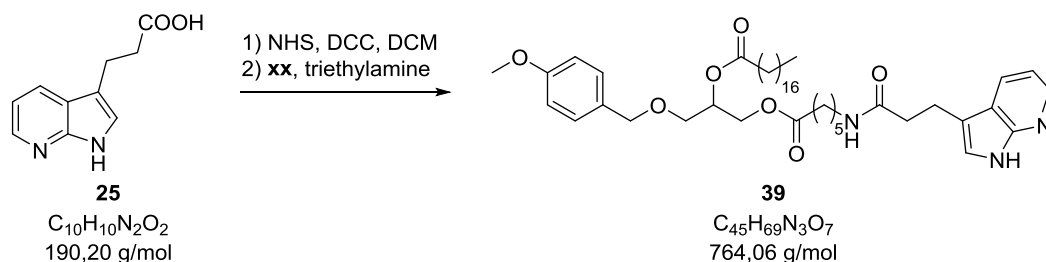
$^1\text{H-NMR}$ (301 MHz, CHCl_3): δ [ppm] = 0.85 (t, J = 6.7 Hz, 3 H, CH_3), 1.22 (s, 30 H, $15 \times \text{CH}_2$), 1.53–1.77 (m, 6H, $3 \times \text{CH}_2$), 2.22–2.46 (m, 4H, $2'\text{-CH}_2$, $2''\text{-CH}_2$), 3.19 (dd, J = 11.7, 5.7 Hz, 2H, $6'\text{-CH}_2$), 3.39–3.59 (m, 2H, 3-CH_2), 3.77 (s, 3H, OCH_3), 4.04–4.17 (m, 2H, 1-CH_2), 4.45 (s, 2H, $\text{C-CH}_2\text{PMB}$), 5.14–5.24 (m, 1H, 2-CH), 6.85 (dt, J = 4.9, 2.9 Hz, 2H, $2 \times \text{CH}_{\text{PMB}}$), 7.17–7.24 (m, 2H, $2 \times \text{CH}_{\text{PMB}}$).

$^{13}\text{C-NMR}$ (76 MHz, CDCl_3): δ [ppm] = 14.07 ($\text{CH}_{3,\text{FA}}$), 22.64 (C-17''), 24.86, 26.33, 29.09, 29.21, 29.31, 29.41, 29.56, 29.61, 29.64, 30.52, 30.86, 31.87, 32.77, 33.85, 34.11, 36.53, 42.86 (C-6'), 55.21 (OCH_3), 63.37 (C-2), 68.82 (C-3), 70.20 (C-1), 73.11 ($\text{CH}_2\text{-C}_{\text{PMB}}$), 113.80 ($2 \times \text{CH}_{\text{PMB}}$), 129.37 ($2 \times \text{CH}_{\text{PMB}}$), 129.40 ($\text{C}_{\text{PMB}}\text{-CH}$), 159.31 ($\text{C}_{\text{PMB}}\text{-OCH}_3$), 173.92 (C(O)O), 174.20 (C(O)O).

ESI-MS (m/z): 592.4 $[\text{M}+\text{H}]^+$, 1183.9 $[2\text{M}+\text{H}]^+$.

HR-MS (ESI): calculated for $[\text{C}_{35}\text{H}_{62}\text{NO}_6]$ ($[\text{M}+\text{H}]^+$): 592.4572, found: 592.4575.

1-((6-(3-(1*H*-Pyrrolo[2,3-*b*]pyridin-3-yl)propanamido)hexanoyl)oxy)-3-((4-methoxybenzyl)oxy)propan-2-yl stearate (39)

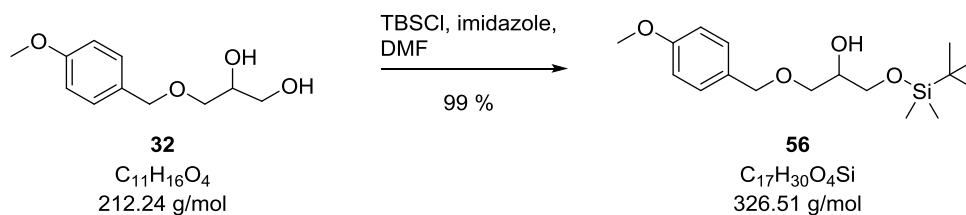


A solution of **25** (60.0 mg, 318 μ mol, 1.00 eq.) in anhydrous DCM (10 mL) was treated with NHS (36.0 mg, 312 μ mol, 0.98 eq.) and DCC (66.0 mg, 318 μ mol, 1.00 eq.) and stirred for 1 h at 0 °C. The mixture was allowed to warm up to r.t. and stirred for additional 12 h. The resulting solid was filtered off, **36** (200 mg, 338 μ mol, 1.06 eq.) and triethylamine (154 μ L, 112 mg, 3.49 eq.) were added to the filtrate and the mixture was stirred for 1 h. The mixture was diluted with ethyl acetate (5 mL) and washed with aqueous citric acid (10 w/w-%, 3 \times 5 mL). The organic extract was washed with water (1 \times 5 mL), saturated aqueous sodium hydrogen carbonate solution (3 \times 4 mL) and saturated aqueous sodium chloride solution (1 \times 5 mL). The organic layer was dried over $MgSO_4$ and concentrated under reduced pressure. Traces of product **39** were observed in mass spectrometry but isolation attempts were unsuccessful.

TLC (*n*-pentane/ethyl acetate, 3:1): R_f = 0.53.

ESI-MS (m/z): 764.5 $[M+H]^+$.

HR-MS (ESI): calculated for $[C_{45}H_{70}N_3O_7]$ ($[M+H]^+$): 764.5208, found: 764.5186.

1-((*tert*-Butyldimethylsilyl)oxy)-3-((4-methoxybenzyl)oxy)propan-2-ol (**56**)

Compound **32** (1.50 g, 7.07 mmol, 1.00 eq.) and imidazole (1.07 g, 15.7 mmol, 2.22 eq.) were dissolved in anhydrous DMF (5 mL) and the mixture was cooled to 0 °C. In a second flask TBSCl (1.24 g, 8.20 mmol, 1.16 eq.) was dissolved in anhydrous DMF (3.5 mL) and added to the previously prepared mixture dropwise over a period of 1 h. The reaction mixture was stirred at 4 °C over night followed by stirring at r.t. for additional 8 h. The reaction was stopped by addition of water (5 mL). After extraction with *n*-pentane/ethyl acetate (4:1, 5 mL) and diethyl ether (5 mL) the combined organic layers were washed with hydrochloric acid (0.5 M, 10 mL), saturated aqueous NaHCO₃-solution and saturated aqueous sodium chloride solution (10 mL). The pure product **56** (2.29 g, 6.98 mmol, 99 %) was obtained after flash column chromatography (*n*-pentane/ethyl acetate, 5:1) as white solid.

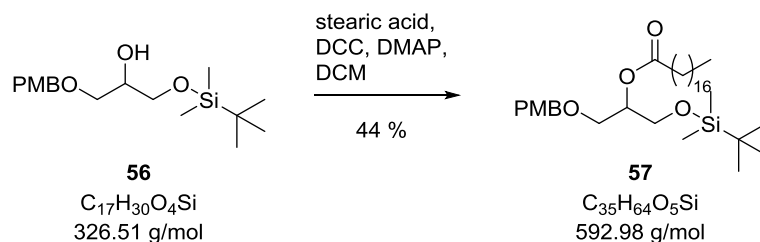
TLC (*n*-pentane/ethyl acetate, 5:1): R_f = 0.21.

¹H-NMR (400 MHz, CHCl₃): δ [ppm] = 0.04 (s, 6H, 2×CH₃), 0.87 (s, 9H, 3×CH₃,*t*-Bu), 3.42–3.51 (m, 2H, 1-CH₂), 3.58–3.66 (m, 2H, 3-CH₂), 3.78 (s, 3H, OCH₃), 3.79–3.83 (m, 1H, 2-CH), 4.46 (s, 2H, CH₂,_{PMB}), 6.84–6.88 (m, 2H, 2×CH_{PMB}), 7.21–7.25 (m, 2H, 2×CH_{PMB}).

¹³C-NMR (101 MHz, CDCl₃): δ [ppm] = -5.41 (2×CH₃), 18.29 (C_q,*t*-Bu), 25.88 (3×CH₃,*t*-Bu), 55.26 (OCH₃), 64.06 (C-1), 70.70 (C-2, CH₂-C_{PMB}), 73.10 (C-3), 113.83 (2×CH_{PMB}), 129.38 (2×CH_{PMB}), 130.19 (C_{PMB}-CH₂), 159.28 (C_{PMB}-OCH₃).

ESI-MS (m/z): 349.2 [M+Na]⁺, 365.2 [M+K]⁺.

HR-MS (ESI): calculated for [C₁₇H₃₀O₄SiNa] ([M+Na]⁺): 349.1806, found: 349.1809; calculated for [C₁₇H₃₀O₄SiK] ([M+K]⁺): 365.1545, found: 365.1540.

1-((*tert*-Butyldimethylsilyl)oxy)-3-((4-methoxybenzyl)oxy)propan-2-yl stearate (**57**)

Stearic acid (92.8 mg, 326 μ mol, 1.21 eq.) and **56** (88.6 mg, 270 μ mol, 1.00 eq.) were dissolved in anhydrous DCM (500 μ L). In a second flask DCC (71.8 mg, 348 μ mol, 1.29 eq.) and DMAP (42.5 mg, 348 μ mol, 1.29 eq.) were dissolved in anhydrous DCM (2 mL) and added to the first flask. The reaction mixture was stirred at r.t. for 24 h, solid components were filtered off and the organic solvent was removed under reduced pressure. The pure product **57** (70.6 mg, 119 μ mol, 44 %) was obtained after flash column chromatography (*n*-pentane/ethyl acetate, 50:1) as white solid.

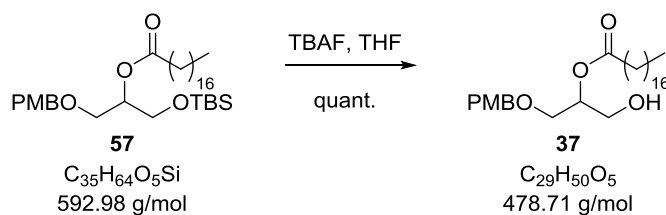
TLC (*n*-pentane/ethyl acetate, 50:1): R_f = 0.25.

1H -NMR (400 MHz, $CHCl_3$): δ [ppm] = 0.01 (s, 6H, 2 \times SiCH₃), 0.84 (s, 9H, 3 \times CH₃,*t*-Bu), 0.85 (t, J = 1.6 Hz, 3H, 18'-CH₃), 1.21–1.28 (m, 28H, 4'-17'-CH₂), 1.53–1.63 (m, 2H, 3'-CH₂), 2.25–2.31 (m, 2H, 2'-CH₂), 3.52–3.60 (m, 2H, 1-CH₂), 3.70 (dd, J = 5.3, 1.7 Hz, 2H, 3-CH₂), 3.78 (s, 3H, OCH₃), 4.40–4.48 (m, 2H, CH₂,PMB), 4.98–5.04 (m, 1H, 2-CH), 6.50 (dd, J = 5.2, 1.6 Hz, 2H, 2 \times CH_{PMB}), 6.82–6.86 (m, 2H, 2 \times CH_{PMB}).

^{13}C -NMR (101 MHz, $CDCl_3$): δ [ppm] = -5.45 (SiCH₃), -5.42 (SiCH₃), 14.11 (C-18'), 18.21 (C_q,*t*-Bu), 22.69 (C-17'), 25.00 (C-3'), 25.79 (3 \times CH₃,*t*-Bu), 29.14, 29.30, 29.36, 29.47, 29.56, 29.63, 29.66, 29.70 (C-4', C-5', C-6', C-7', C-8', C-9', C-10', C-11', C-12', C-13', C-14', C-15'), 31.92 (C-16'), 34.48 (C-2'), 55.26 (OCH₃), 61.69 (C-1), 68.11 (C-3), 72.87 (CH₂-C_{PMB}), 72.96 (C-2), 113.76 (2 \times CH_{PMB}), 129.24 (2 \times CH_{PMB}), 130.19 (C_{PMB}-CH₂), 159.21 (C_{PMB}-OCH₃), 173.36 (C-1').

ESI-MS (m/z): 593.5 [M+H]⁺, 610.5 [M+NH₄]⁺, 615.5 [M+Na]⁺, 631.5 [M+K]⁺, 1223.9 [2M+K]⁺.

HR-MS (ESI): calculated for [C₃₅H₆₈O₅SiN] ([M+NH₄]⁺): 610.4861, found: 610.4856; calculated for [C₃₅H₆₄O₅SiNa] ([M+Na]⁺): 615.4415, found: 615.4396; calculated for [C₃₅H₆₄O₅SiK] ([M+K]⁺): 631.4155, found: 631.4151.

1-Hydroxy-3-((4-methoxybenzyl)oxy)propan-2-yl stearate (37)

To a solution of **57** (100 mg, 169 μmol , 1.00 eq.) in anhydrous THF (30 mL) TBAF (1 M, 340 μL , 88.2 mg, 337 μmol , 2.00 eq.) was added. The reaction mixture was stirred at r.t. over night and concentrated under reduced pressure. The product **37** (80.7 mg, 169 μmol , quant.) was obtained as yellow solid.

TLC (*n*-pentane/ethyl acetate, 3:1): $R_f = 0.91$.

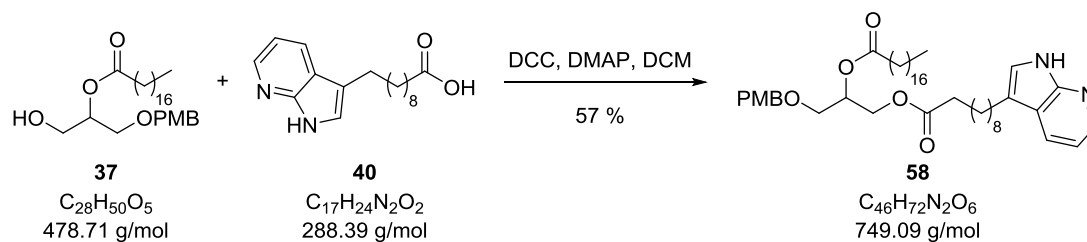
$^1\text{H-NMR}$ (400 MHz, CHCl_3): δ [ppm] = 0.83 (s, 3H, 18'-CH₃), 1.21 (s, 26H, 13 \times CH₂), 1.39 (s, 2H, 4'-CH₂), 1.51–1.70 (m, 2H, 3'-CH₂), 2.18–2.31 (m, 2H, 2'-CH₂), 3.24–3.37 (m, 2H, 3-CH₂), 3.40–3.54 (m, 1H, 1-CH_{2,a}), 3.76 (s, 3H, OCH₃), 4.04–4.18 (m, 1H, 1-CH_{2,b}), 4.44 (s, 2H, CH_{2,PMB}), 6.44 (d, $J = 5.8$ Hz, 1H, CH_{PMB}), 6.84 (d, $J = 8.4$ Hz, 1H, CH_{PMB}), 7.21 (d, $J = 8.1$ Hz, 1H, CH_{PMB}), 8.17 (d, $J = 5.5$ Hz, 1H, CH_{PMB}).

$^{13}\text{C-NMR}$ (101 MHz, CDCl_3): δ [ppm] = 14.10 (C-18'), 22.67 (C-17'), 24.91 (C-3'), 29.13, 29.26, 29.35, 29.46, 29.60, 29.64, 29.68, 30.31 (C-4', C-5', C-6', C-7', C-8', C-9', C-10', C-11', C-12', C-13', C-14', C-15'), 31.91 (C-16'), 34.17 (C-2'), 55.25 (OCH₃), 65.49 (C-1), 68.72 (C-3), 70.71 (CH₂-C_{PMB}), 73.13 (C-2), 113.83 (2 \times CH_{PMB}), 129.28 (CH_{PMB}), 129.38 (CH_{PMB}), 129.90 (C_{PMB}-CH₂), 159.33 (C_{PMB}-OCH₃), 173.93 (C-1').

ESI-MS (m/z): 496.4 [$\text{M}+\text{NH}_4$]⁺, 501.4 [$\text{M}+\text{Na}$]⁺, 517.4 [$\text{M}+\text{K}$]⁺, 477.4 [$\text{M}-\text{H}$]⁻.

HR-MS (ESI): calculated for [$\text{C}_{29}\text{H}_{50}\text{O}_5\text{Na}$] ($[\text{M}+\text{Na}]^+$): 501.3550, found: 501.3521.

1-((10-(1H-Pyrrolo[2,3-b]pyridin-3-yl)decanoyl)oxy)-3-((4-methoxybenzyl)oxy)propan-2-yl stearate (58)

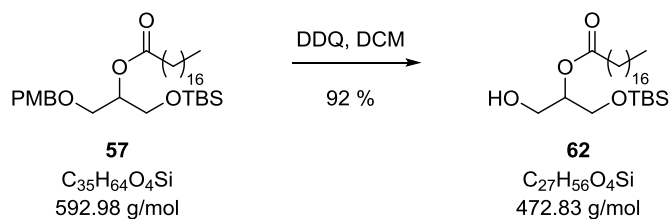


The compounds **37** (30.7 mg, 64.1 μ mol, 1.04 eq.) and **40** (17.8 mg, 61.7 μ mol, 1.00 eq.) were dissolved in anhydrous DCM (800 μ L) and cooled to 0 °C. The mixture was treated dropwise with a mixture of DCC (15.3 mg, 74.0 μ mol, 1.20 eq.) and DMAP (9.04 mg, 74.0 μ mol, 1.20 eq.) in anhydrous DCM (200 μ L) and stirred at 0 °C for 16 h. Under reduced pressure the solvent was removed and the residue was redissolved in ethyl acetate (2 mL). Solid components were filtered off and the filtrate was concentrated *in vacuo*. After flash column chromatography (*n*-pentane/ethyl acetate, 1:1) the pure product **58** (26.4 mg, 35.3 μ mol, 57 %) was obtained as yellow solid.

TLC (*n*-pentane/ethyl acetate, 1:1): R_f = 0.38.

ESI-MS (m/z): 749.6 $[M+H]^+$, 787.5 $[M+K]^+$, 747.5 $[M-H]^-$.

HR-MS (ESI): calculated for $[C_{46}H_{73}N_2O_6]$ ($[M+H]^+$): 749.5463, found: 749.5456.

1-((*tert*-Butyldimethylsilyl)oxy)-3-hydroxypropan-2-yl stearate (**62**)

To a solution of **57** (1.36 g, 2.30 mmol, 1.00 eq.) in wet DCM (50 mL) DDQ (1.09 g, 4.81 mmol, 2.09 eq.) was added. The mixture was stirred at r.t. for 24 h, diluted with DCM (20 mL) and washed with aqueous NaHCO_3 -solution (10 w/w-%, 60 mL). The organic extract was dried over MgSO_4 and concentrated under reduced pressure. After purification using flash column chromatography (*n*-pentane/ethyl acetate, 3:1) the pure product **62** (1.01 g, 2.13 mmol, 92 %) was obtained as white solid.

TLC (*n*-pentane/ethyl acetate, 3:1): $R_f = 0.90$.

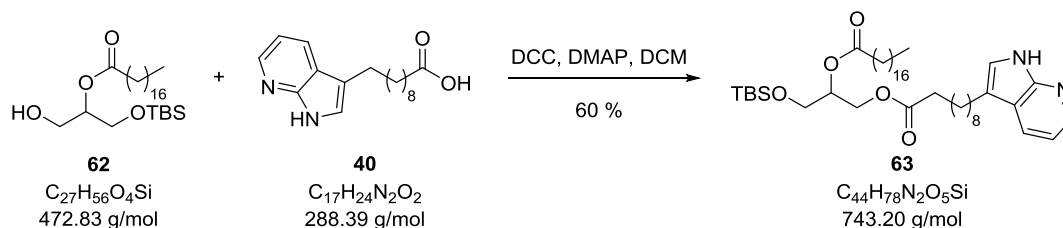
$^1\text{H-NMR}$ (400 MHz, CHCl_3): δ [ppm] = 0.05 (s, 6H, $2 \times \text{SiCH}_3$), 0.85–0.89 (m, 12H, $3 \times \text{CH}_{3,t\text{-Bu}}$, 18'-CH₃), 1.22–1.27 (m, 28H, $14 \times \text{CH}_2$), 1.56–1.65 (m, 2H, 3'-CH₂), 2.28–2.34 (m, 2H, 2'-CH₂), 3.72–3.84 (m, 4H, 1-CH₂, 3-CH₂), 4.83–4.89 (m, 1H, 2-CH).

$^{13}\text{C-NMR}$ (101 MHz, CDCl_3): δ [ppm] = -5.52 ($2 \times \text{SiCH}_3$), 14.11 (C-18'), 18.20 ($\text{C}_{q,t\text{-Bu}}$), 22.69 (C-17'), 24.97 (C-3'), 25.77 ($3 \times \text{CH}_{3,t\text{-Bu}}$), 29.13, 29.46, 29.61, 29.66, 29.70 (C-4', C-5', C-6', C-7', C-8', C-9', C-10', C-11', C-12', C-13', C-14', C-15'), 31.93 (C-16'), 34.41 (C-2'), 62.54 (C-3), 62.85 (C-1), 74.28 (C-2), 173.71 (C-1').

ESI-MS (m/z): 473.4 $[\text{M}+\text{H}]^+$, 495.4 $[\text{M}+\text{Na}]^+$, 511.4 $[\text{M}+\text{K}]^+$, 967.8 $[2\text{M}+\text{Na}]^+$.

HR-MS (ESI): calculated for $[\text{C}_{27}\text{H}_{57}\text{O}_4\text{Si}]$ ($[\text{M}+\text{H}]^+$): 473.4021, found: 473.4001; calculated for $[\text{C}_{27}\text{H}_{56}\text{O}_4\text{SiNa}]$ ($[\text{M}+\text{Na}]^+$): 495.3840, found: 495.3820; calculated for $[\text{C}_{27}\text{H}_{56}\text{O}_4\text{SiK}]$ ($[\text{M}+\text{K}]^+$): 511.3579, found: 511.3571.

1-((10-(1H-Pyrrolo[2,3-b]pyridin-3-yl)decanoyl)oxy)-3-((tert-butyldimethyl-silyl)oxy)propan-2-yl stearate (63)



Compounds **62** (330 mg, 701 μ mol, 1.04 eq.) and **40** (194 mg, 674 μ mol, 1.00 eq.) were dissolved in anhydrous DCM (9 mL). The mixture was cooled to 0 °C and treated dropwise with a mixture of DCC (167 mg, 809 μ mol, 1.20 eq.) and DMAP (99.0 mg, 809 μ mol, 1.20 eq.) in anhydrous DCM (3 mL). The reaction mixture was stirred for 24 h at 0 °C and concentrated under reduced pressure. The residue was dissolved in ethyl acetate (50 mL), the precipitate was filtered off and the filtrate was concentrated *in vacuo*. After flash column chromatography (*n*-pentane/ethyl acetate, 3:1) the pure product **63** (311 mg, 418 μ mol, 60 %) was obtained as yellow solid.

TLC (*n*-pentane/ethyl acetate, 3:1): R_f = 0.26.

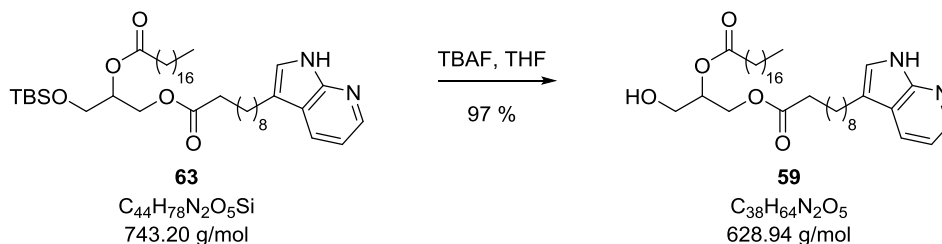
1H -NMR (400 MHz, $CHCl_3$): δ [ppm] = 0.03 (s, 6H, 2 \times SiCH₃), 0.83–0.87 (m, 12H, 3 \times CH₃,*t*-Bu, 18'-CH₃), 1.19–1.27 (m, 38H, 19 \times CH₂), 1.49–1.62 (m, 2H, 9''-CH₂), 1.66–1.74 (m, 4H, 3'-CH₂, 3''-CH₂), 1.84–1.92 (m, 4H, 2'-CH₂, 2''-CH₂), 2.26–2.32 (m, 2H, 10''-CH₂), 3.73–3.80 (m, 3H, 1-CH_{2,a}, 3-CH₂), 4.04–4.13 (m, 1H, 1-CH_{2,b}), 4.84–4.90 (m, 1H, 2-CH), 6.46–6.51 (m, 1H, 2'''-CH), 7.03–7.07 (m, 1H, 5'''-CH), 8.18 (dd, J = 5.2, 1.5 Hz, 6'''-CH), 8.23–8.29 (m, 1H, 4'''-CH).

^{13}C -NMR (101 MHz, $CDCl_3$): δ [ppm] = -5.47 (2 \times SiCH₃), 14.11 (C-18'), 18.20 (C_{q,t}-Bu), 22.68 (C-17'), 24.69 (C-3''), 24.97 (C-3'), 25.45 (C-9''), 25.77 (3 \times CH₃,*t*-Bu), 29.12, 29.26, 29.35, 29.45, 29.65, 29.69 (C-4', C-5', C-6', C-7', C-8', C-9', C-10', C-11', C-12', C-13', C-14', C-15', C-4'', C-5'', C-6'', C-7'', C-8''), 31.92 (C-16'), 34.42 (C-2''), 34.92 (C-2'), 39.19 (C-10''), 55.75 (C-1), 62.45 (C-3), 74.50 (C-2), 100.81 (C-3'''), 106.57 (C-9'''), 115.89 (C-5'''), 124.99 (C-2'''), 128.89 (C-4'''), 142.79 (C-6'''), 147.93 (C-8'''), 173.73 (C-1', C-1'').

ESI-MS (m/z): 743.6 [M+H]⁺.

HR-MS (ESI): calculated for [C₄₄H₇₉N₂O₅Si] ([M+H]⁺): 743.5753, found: 743.5755; calculated for [C₄₄H₇₈N₂O₅SiNa] ([M+Na]⁺): 765.5572, found: 765.5558.

1-((10-(1*H*-Pyrrolo[2,3-*b*]pyridin-3-yl)decanoyl)oxy)-3-hydroxypropan-2-yl stearate (59)



To a solution of **63** (1.00 g, 1.35 mmol, 1.00 eq.) in anhydrous THF (220 mL) TBAF (1 M, 2.70 mL, 2.69 mmol, 2.00 eq.) was added. The reaction mixture was stirred at r.t. over night and concentrated under reduced pressure. Flash column chromatography (DCM/ethyl acetate, 1:1) provided the pure product **59** (817 mg, 1.30 mmol, 97 %) as yellow solid.

TLC (DCM/ethyl acetate, 1:1): R_f = 0.36.

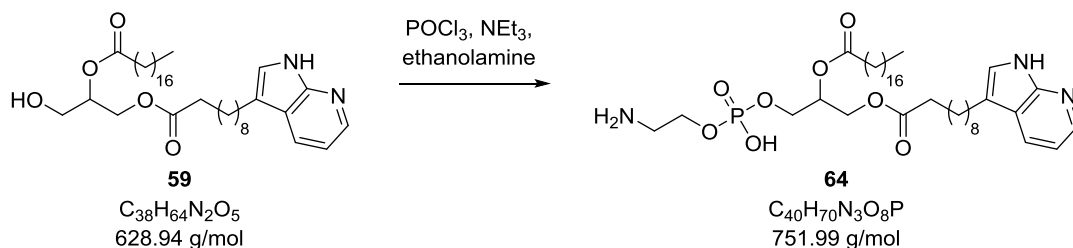
¹H-NMR (400 MHz, CHCl₃): δ [ppm] = 0.85 (t, J = 7.1 Hz, 3H, 18'-CH₃), 1.15–1.38 (m, 38H, 19×CH₂), 1.53–1.70 (m, 6H, 3'-CH₂, 3''-CH₂, 9''-CH₂), 2.23–2.34 (m, 4H, 2'-CH₂, 2''-CH₂), 2.71 (t, J = 7.1 Hz, 2H, 10''-CH₂), 3.63–3.65 (m, 1H, 1-CH_{2,a}), 4.06–4.20 (m, 3H, 1-CH_{2,b}, 3-CH₂), 6.51 (d, J = 3.5 Hz, 1H, 2'''-CH), 7.07–7.14 (m, 1H, 5'''-CH), 7.99 (ddd, J = 7.8, 2.2, 1.3 Hz, 1H, 6'''-CH), 8.26 (dd, J = 18.7, 4.4 Hz, 1H, 4'''-CH).

¹³C-NMR (101 MHz, CDCl₃): δ [ppm] = 14.11 (C-18'), 22.69 (C-17'), 24.78 (C-3''), 25.00 (C-3'), 28.92, 29.11, 29.13, 29.25, 29.36, 29.45, 29.60, 29.65, 29.69, 29.82 (C-4', C-5', C-6', C-7', C-8', C-9', C-10', C-11', C-12', C-13', C-14', C-15', C-4'', C-5'', C-6'', C-7'', C-8'', C-9''), 31.92 (C-16'), 34.01 (C-2''), 34.13 (C-2'), 39.47 (C-10''), 51.44 (C-1), 63.35 (C-3), 70.28 (C-2), 101.08 (C-3'''), 115.87 (C-5'''), 122.61 (C-9'''), 125.43 (C-2'''), 129.07 (C-4'''), 140.03 (C-6'''), 141.62 (C-8'''), 173.88, 173.94 (C-1', C-1'').

ESI-MS (m/z): 629.5 [M+H]⁺, 651.5 [M+Na]⁺, 627.5 [M-H]⁻.

HR-MS (ESI): calculated for [C₃₈H₆₅N₂O₅] ([M+H]⁺): 629.4888, found: 629.4882; calculated for [C₃₈H₆₃N₂O₅] ([M-H]⁻): 627.4742, found: 627.4739.

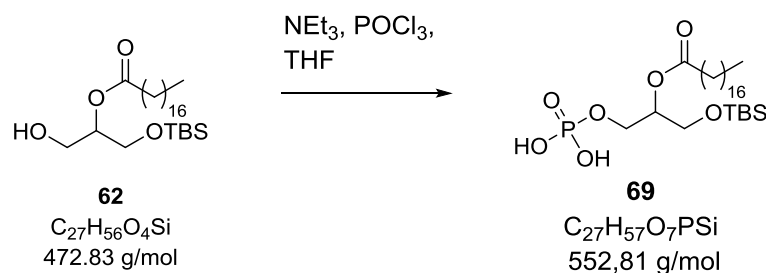
1-((10-(1*H*-Pyrrolo[2,3-*b*]pyridin-3-yl)decanoyl)oxy)-3-(((2-aminoethoxy) (hydroxy) phosphoryl)oxy)propan-2-yl stearate (64)



Compound **59** (31.0 mg, 49.3 μmol , 1.00 eq.) was dissolved in anhydrous THF (300 μL) together with triethylamine (20.0 μL , 15.2 mg, 150 μmol , 3.05 eq.). The mixture was added dropwise to a solution of phosphoryl chloride (14.0 μL , 23.4 mg, 153 μmol , 3.09 eq.) in anhydrous THF (200 μL) at 0 °C. The mixture was stirred at 0 °C for 10 min followed by stirring at r.t. for 45 min. The reaction mixture was again cooled to 0 °C and treated dropwise over 15 min with ethanolamine (9.00 μL , 9.28 mg, 152 μmol , 3.06 eq.) and triethylamine (42.0 μL , 30.4 mg, 301 μmol , 6.10 eq.) and anhydrous THF (500 μL). After stirring at 0 °C for 10 min the reaction mixture was stirred at r.t. over night. Formed precipitate was filtered off and the filtrate concentrated under reduced pressure. The residue was redissolved in acetic acid/water (2.4:1, 20 mL) and heated to 70 °C for 1 h. After cooling down the mixture was extracted using chloroform (3 \times 15 mL). The combined organic extracts were washed with water (2 \times 20 mL) and concentrated under reduced pressure. Mass spectrometry showed formation of product **64** as well as phosphorylated intermediate product carrying no ethanolamine (**65**). Attempts to isolate the substances was not successful.

ESI-MS (m/z): 752.5 $[\text{M}+\text{H}]^+$.

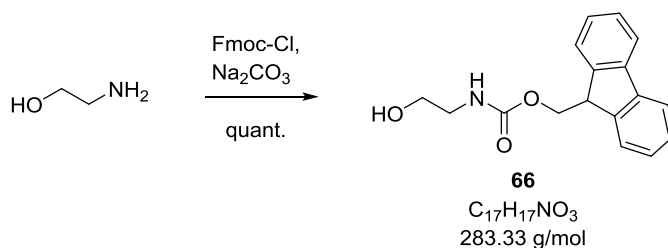
HR-MS (ESI): calculated for $[\text{C}_{40}\text{H}_{71}\text{N}_3\text{O}_8\text{P}]$ ($[\text{M}+\text{H}]^+$): 752.4973, found: 752.4973.

1-((*tert*-Butyldimethylsilyl)oxy)-3-(phosphonooxy)propan-2-yl stearate (**69**)

Triethylamine (180 μL , 130 mg, 1.29 mmol, 3.05 eq.) and **62** (200 mg, 423 μmol , 1.00 eq.) were dissolved in anhydrous THF (4 mL). The mixture was cooled to 0 °C and treated dropwise over 15 min with a prepared solution of phosphoryl chloride (120 μL , 200 mg, 1.31 mmol, 3.09 eq.) in THF (2.9 mL). The reaction mixture was stirred at r.t. for 45 min. After addition of water (10 mL) the mixture was extracted with chloroform (3×10 mL). The combined organic extracts were washed with water (30 mL) and concentrated *in vacuo*. The product **69** was confirmed by ESI-MS. Attempts to isolate the formed product were not successful.

ESI-MS (m/z): 551.4 [M-H]⁻.

HR-MS (ESI): calculated for [$\text{C}_{27}\text{H}_{56}\text{O}_7\text{PSi}$] ([M-H]⁻): 551.3538, found: 551.3525.

(9H-Fluoren-9-yl)methyl (2-hydroxyethyl)carbamate (66**)**

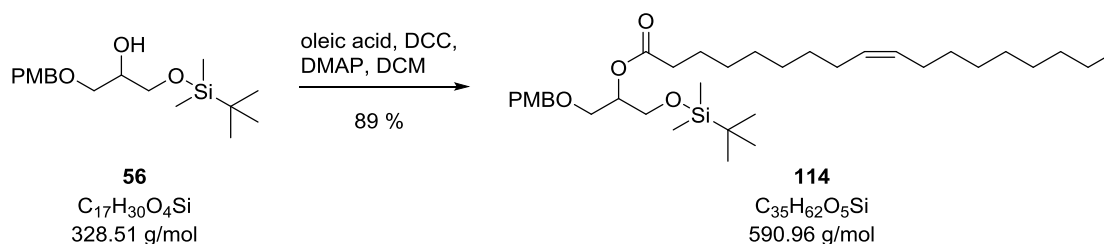
Ethanolamine (990 μ L, 1.00 g, 16.4 mmol, 1.00 eq.) was dissolved in aqueous sodium carbonate (10 w/w-%, 150 mL) and treated with 9-fluorenylmethoxy-carbonyl chloride (4.71 g, 18.2 mmol, 1.11 eq.). The reaction mixture was stirred at r.t. for 2 h and extracted with ethyl acetate (2 \times 100 mL). The combined organic extracts were washed with hydrochloric acid (1 M, 2 \times 150 mL) and saturated aqueous sodium chloride solution (1 \times 200 mL). The organic layer was dried over MgSO₄ and concentrated under reduced pressure. Without further purification the pure product **66** (4.64 g, 16.4 mmol, quant.) was obtained as white solid.

¹H-NMR (400 MHz, CHCl₃): δ [ppm] = 3.28–3.36 (m, 2H, 1-CH₂), 3.64–3.74 (m, 2H, 2-CH₂), 4.20 (t, J = 6.7 Hz, 1H, CH_{Fmoc}), 4.42 (d, J = 6.7 Hz, 2H, CH_{2,Fmoc}), 5.17 (s, 1H, NH), 7.31 (dtd, J = 8.6, 7.5, 1.2 Hz, 2H, 2 \times CH_{Fmoc}), 7.36–7.45 (m, 2H, 2 \times CH_{Fmoc}), 7.55–7.60 (m, 2H, 2 \times CH_{Fmoc}), 7.76 (t, J = 7.9 Hz, 2H, 2 \times CH_{Fmoc}).

¹³C-NMR (126 MHz, CDCl₃): δ [ppm] = 43.50 (C-1), 46.20 (CH_{Fmoc}), 62.30 (C-2), 66.78 (CH_{2,Fmoc}), 120.27 (2 \times CH_{Fmoc}), 125.01 (2 \times CH_{Fmoc}), 127.39 (2 \times CH_{Fmoc}), 128.26 (2 \times CH_{Fmoc}), 142.43 (2 \times C_{q,Fmoc}), 143.89 (2 \times C_{q,Fmoc}), 157.17 (NCOO).

ESI-MS (m/z): 306.1 [M+Na]⁺, 589.3 [2M+Na]⁺.

HR-MS (ESI): calculated for [C₁₇H₁₇NO₃] ([M+Na]⁺): 306.1101, found: 306.1106.

1-((*tert*-Butyldimethylsilyl)oxy)-3-((4-methoxybenzyl)oxy)propan-2-yl oleate (114)


Oleic acid (1.74 mL, 1.56 g, 5.53 mmol, 1.21 eq.) and **56** (1.50 g, 4.57 mmol, 1.00 eq.) were dissolved in anhydrous DCM (7.5 mL) and treated with DCC (1.22 g, 5.89 mmol, 1.29 eq.) and DMAP (720 mg, 5.89 mmol, 1.29 eq.) in anhydrous DCM (28 mL). The reaction mixture was stirred at r.t. for 24 h, the precipitate was filtered off and the filtrate was concentrated under reduced pressure. Flash column chromatography (*n*-pentane/ethyl acetate, 20:1) yielded the pure product **114** (2.40 g, 4.06 mmol, 89 %) as white solid.

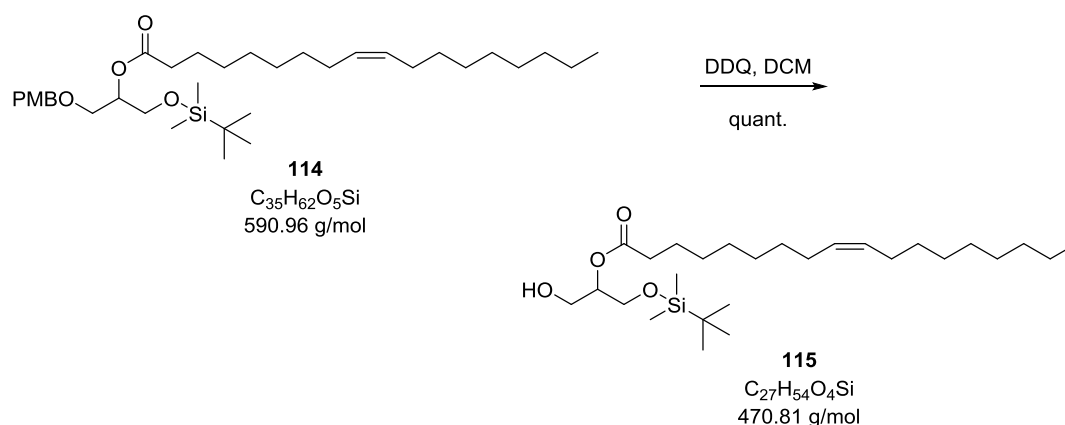
TLC (*n*-pentane/ethyl acetate, 20:1): $R_f = 0.49$.

1H -NMR (300 MHz, $CHCl_3$): δ [ppm] = 0.03 (s, $J = 3.1$ Hz, 6H, $2 \times SiCH_3$), 0.82–0.90 (m, 12H, $3 \times CH_{3,t-Bu}$, $18'$ - CH_3), 1.23–1.35 (m, 20H, $10 \times CH_2$), 1.54–1.65 (m, 2H, $3'$ - CH_2), 1.99 (dd, $J = 12.2, 6.5$ Hz, $8'$ - CH_2 , $11'$ - CH_2), 2.26–2.34 (m, 2H, $2'$ - CH_2), 3.57 (dd, $J = 5.0, 2.6$ Hz, 2H, 3 - CH_2), 3.72 (dd, $J = 5.3, 0.9$ Hz, 2H, 1 - CH_2), 3.78 (s, 3H, OCH_3), 4.45 (d, $J = 2.6$ Hz, 2H, $CH_{2,PMB}$), 4.98–5.07 (m, 1H, 2 -CH), 5.33 (ddd, $J = 5.6, 3.6, 1.9$ Hz, 2H, $HC=CH$), 6.82–6.87 (m, 2H, $2 \times CH_{PMB}$), 7.22 (dd, $J = 8.1, 1.4$ Hz, 2H, CH_{PMB}).

^{13}C -NMR (126 MHz, $CDCl_3$): δ [ppm] = -5.48 ($SiCH_3$), -5.45 ($SiCH_3$), 14.08 (C- $18'$), 18.18 (C- $q,t-Bu$), 22.65 (C- $17'$), 24.95 (C- $3'$), 25.76 ($3 \times CH_{3,t-Bu}$), 27.15, 27.19 (C- $8'$, C- $11'$), 29.07, 29.08, 29.17, 29.28, 29.29, 29.49, 29.69, 29.74 ($8 \times CH_2$), 31.87 (C- $16'$), 34.42 (C- $2'$), 55.19 (OCH_3), 61.65 (C-1), 68.06 (C-3), 72.84 ($\underline{CH_2}$ - C_{PMB}), 72.93 (C-2), 113.72 ($2 \times CH_{PMB}$), 129.17, 129.19 (C- $9'$, C- $10'$), 129.71, 129.93 ($2 \times CH_{PMB}$), 130.14 ($\underline{C_{PMB}}\text{-}CH_2$), 159.17 ($\underline{C_{PMB}}\text{-}OCH_2$), 173.24 (C- $1'$).

ESI-MS (m/z): 591.5 $[M+H]^+$, 608.5 $[M+NH_4]^+$, 613.4 $[M+Na]^+$, 629.4 $[M+K]^+$.

HR-MS (ESI): calculated for $[C_{35}H_{66}NO_5Si]$ ($[M+NH_4]^+$): 608.4705, found: 608.4676; calculated for $[C_{35}H_{62}O_5SiNa]$ ($[M+Na]^+$): 613.4259, found: 613.4229; calculated for $[C_{35}H_{62}O_5SiK]$ ($[M+K]^+$): 629.3998, found: 629.3986.

1-((*tert*-Butyldimethylsilyl)oxy)-3-hydroxypropan-2-yl oleate (115**)**

To a solution of **114** (500 mg, 846 μ mol, 1.00 eq.) in wet DCM (26 mL) DDQ (400 mg, 1.77 mmol, 2.09 eq.) was added and the mixture stirred at r.t. for 24 h. The reaction mixture was diluted with DCM (10 mL) and washed with aqueous NaHCO₃ solution (10 w/w-%, 30 mL). The organic extract was dried over MgSO₄ and concentrated under reduced pressure. After purification via flash column chromatography (*n*-pentane/ethyl acetate, 3:1) the pure product **115** (400 mg, 844 μ mol, quant.) was obtained as brown oil.

TLC (*n*-pentane/ethyl acetate, 3:1): *R*_f = 0.77.

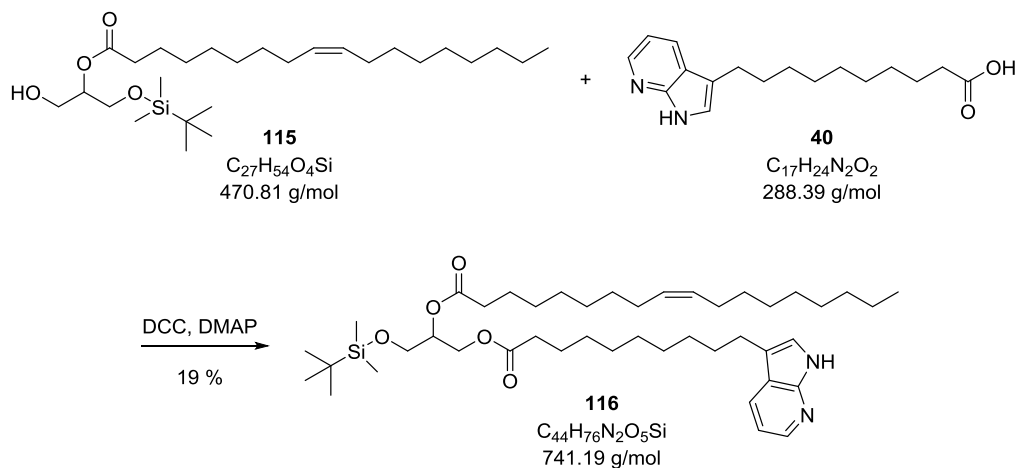
¹H-NMR (300 MHz, CHCl₃): δ [ppm] = 0.04 (s, *J* = 2.1 Hz, 6H, 2×SiCH₃), 0.83–0.89 (m, 12H, 3×CH₃,*t*-Bu, 18'-CH₃), 1.18–1.34 (m, 20H, 10×CH₂), 1.53–1.65 (m, 2H, 3'-CH₂), 1.98 (dd, *J* = 12.2, 6.5 Hz, 4H, 8'-CH₂, 11'-CH₂), 2.23–2.34 (m, 2H, 2'-CH₂), 3.77 (ddd, *J* = 8.5, 4.8, 3.1 Hz, 4H, 1-CH₂, 3-CH₂), 4.86 (dt, *J* = 9.6, 4.8 Hz, 1H, 2-CH), 5.31 (ddd, *J* = 5.7, 3.5, 22 Hz, 2H, HC=CH).

¹³C-NMR (126 MHz, CDCl₃): δ [ppm] = -5.53 (2×SiCH₃), 14.05 (C-18'), 18.14 (C_q,*t*-Bu), 22.62 (C-17'), 24.90 (C-3'), 25.71 (3×CH₃,*t*-Bu), 27.11, 27.16 (C-8', C-11'), 29.04, 29.12, 29.26, 29.27, 29.46, 29.64, 29.71, 29.74 (8×CH₂), 31.85 (C-16'), 34.33 (C-2'), 62.42 (C-1), 62.66 (C-3), 74.30 (C-2), 129.66, 129.94 (C-9', C-10'), 173.24 (C-1').

ESI-MS (*m/z*): 471.4 [M+H]⁺, 493.4 [M+Na]⁺, 509.4 [M+K]⁺, 469.4 [M-H]⁻.

HR-MS (ESI): calculated for [C₂₇H₅₅O₄Si] ([M+H]⁺): 471.3864, found: 471.3858; calculated for [C₂₇H₅₄O₄Si] ([M+Na]⁺): 493.3684, found: 493.3685; calculated for [C₂₇H₅₄O₄SiK] ([M+K]⁺): 509.3423, found: 509.3428; calculated for [C₂₇H₅₃O₄Si] ([M-H]⁻): 469.3719, found: 469.3712.

1-((10-(1*H*-Pyrrolo[2,3-*b*]pyridin-3-yl)decanoyl)oxy)-3-((*tert*-butyldimethylsilyl)oxy)propan-2-yl oleate (116**)**



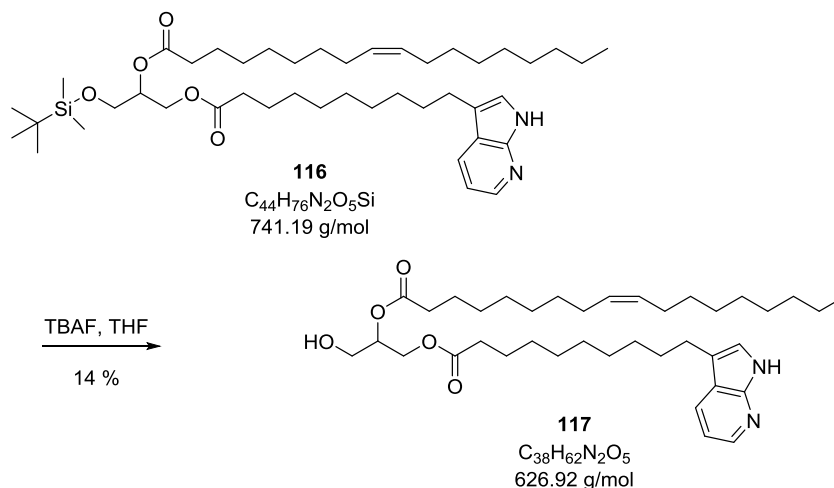
The compounds **115** (160 mg, 330 μ mol, 1.04 eq.) and **49** (91.6 mg, 318 μ mol, 1.00 eq.) were dissolved in anhydrous DCM (4 mL), cooled to 0 °C and treated dropwise with a mixture of DCC (78.6 mg, 381 μ mol, 1.20 eq.) and DMAP (46.6 mg, 381 μ mol, 1.20 eq.) in anhydrous DCM (1.3 mL). The reaction mixture was stirred at 0 °C for 24 h and then concentrated under reduced pressure. The residue was redissolved in ethyl acetate (2.5 mL) and filtered. The filtrate was concentrated under reduced pressure. The product **116** (45.1 mg, 60.8 μ mol, 19 %) was isolated via flash column chromatography (*n*-pentane/ethyl acetate 3:1) and obtained as yellow solid.

TLC (*n*-pentane/ethyl acetate, 3:1): R_f = 0.36.

ESI-MS (m/z): 741.6 $[M+H]^+$, 739.6 $[M-H]^-$.

HR-MS (ESI): calculated for $[C_{44}H_{77}N_2O_5Si]$ ($[M+H]^+$): 741.5596, found: 741.5606.

1-((10-(1*H*-Pyrrolo[2,3-*b*]pyridin-3-yl)decanoyl)oxy)-3-hydroxypropan-2-yl oleate (117)



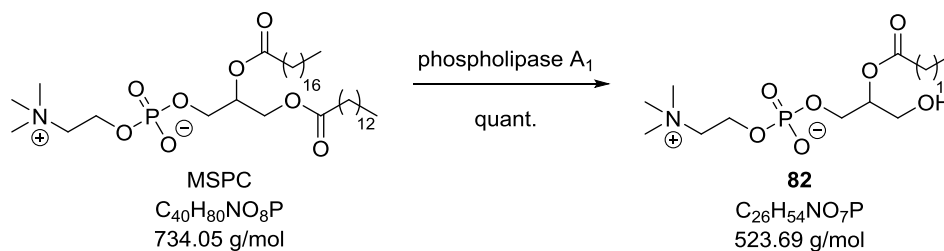
Compound **116** (130 mg, 175 μ mol, 1.00 eq.) was dissolved in anhydrous THF (38 mL) and treated with TBAF (1 M, 350 μ L, 351 μ mol, 2.00 eq.). The reaction mixture was stirred at r.t. over night followed by removal of solvent under reduced pressure. After flash column chromatography (DCM/ethyl acetate, 1:1) the pure product **117** (15.9 mg, 25.3 μ mol, 14 %) was obtained as yellow solid.

TLC (DCM/ethyl acetate, 1:1): R_f = 0.34.

ESI-MS (m/z): 627.5 [M+H]⁺, 625.5 [M-H]⁻.

HR-MS (ESI): calculated for [C₃₈H₆₃N₂O₅] ([M+H]⁺): 627.4731, found: 627.4731; calculated for [C₃₈H₆₂N₂O₅Na] ([M+Na]⁺): 649.4551, found: 649.4544; calculated for [C₃₈H₆₁N₂O₅] ([M-H]⁻): 625.4586, found: 625.4568.

3-Hydroxy-2-(stearoyloxy)propyl (2-(trimethylammonio)ethyl) phosphate (**82**)



MSPC (20.0 mg, 27.3 μmol , 1.00 eq.) was dissolved in chloroform (1 mL) in a reaction vessel with lever lid. Enzyme solution (phospholipase A₁ from *Thermomyces lanuginosus*, 10 KLU/G, 80 μL) in bis-tris buffer (0.7 mL) was added and the mixture was vortexed for 15 min. The mixture was extracted with chloroform (3 \times 1.5 mL) and the combined organic layers were concentrated under reduced pressure. After extraction the pure product **82** (14.2 mg, 27.1 μmol , quant.) was obtained as white solid without further purification.

¹H-NMR (301 MHz, CHCl_3): δ [ppm] = 0.86 (t, J = 6.7 Hz, 3H, 18'-CH₃), 1.23 (s, 28 H, 14 \times CH₂), 1.57 (dd, J = 13.4, 6.3 Hz, 2H, 3'-CH₂), 2.27 (dd, J = 15.0, 7.4 Hz, 2H, 2'-CH₂), 3.27 (s, 9H, 3 \times CH_{3,PC}), 3.59–3.81 (m, 4H, 1-CH₂, 2''-CH₂), 3.88–4.14 (m, 3H, OH, 3-CH₂), 4.24–4.37 (m, 2H, 1''-CH₂), 4.86–4.95 (m, 1H, 2-CH).

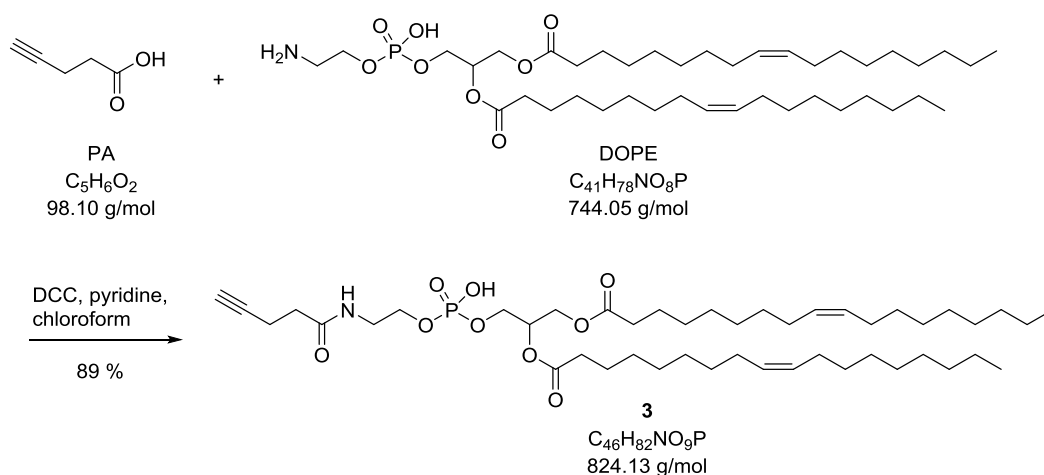
¹³C-NMR (76 MHz, CDCl_3): δ [ppm] = 14.09 (C-18'), 22.67 (C-17'), 24.84 (C-3'), 29.15, 29.30, 29.34, 29.48, 29.62, 29.65, 29.67, 29.69, 29.73 (C-4', C-5', C-6', C-7', C-8', C-9', C-10', C-11', C-12', C-13', C-14', C-15'), 31.91 (C-16'), 34.19 (C-2'), 54.40 (3 \times CH_{3,PC}), 59.38 (C-1'), 59.75 (C-1), 60.14 (C-3), 66.33 (C-2''), 72.96 (C-2), 173.36 (C-1').

ESI-MS (m/z): 524.4 [M+H]⁺, 546.4 [M+Na]⁺.

HR-MS (ESI): calculated for [C₂₆H₅₅NO₇P] ([M+H]⁺): 524.3711, found: 524.3706; calculated for [C₂₆H₅₄NO₇PNa] ([M+Na]⁺): 546.3530, found: 546.3527.

6.5.4 Synthesis of Ca^{2+} -sensitive Labelled Membrane Compartments

3-((Hydroxy(2-(pent-4-ynamido)ethoxy)phosphoryl)oxy)propane-1,2-diyl dioleate (3)



Pent-4-ynoic acid (PA, 10.8 mg, 110 μmol , 2.05 eq.) and DCC (16.1 mg, 78.0 μmol , 1.45 eq.) were dissolved in anhydrous chloroform (600 μL) and stirred at r.t. for 4 h. DOPE (40.0 mg, 53.8 μmol , 1.00 eq.) and pyridine (2.6 mL) were added and the reaction mixture was allowed to stir at 50 $^\circ\text{C}$ for 12 h. Solid compounds were filtered off and the filtrate was concentrated under reduced pressure. Flash column chromatography (RP silica gel, MeOH/ H_2O , 9:1) provided the pure product (**3**, 39.5 mg, 48.0 μmol , 89 %) as white solid.

TLC (*Alugram* RP-18, MeOH/ H_2O , 9:1): R_f = 0.53.

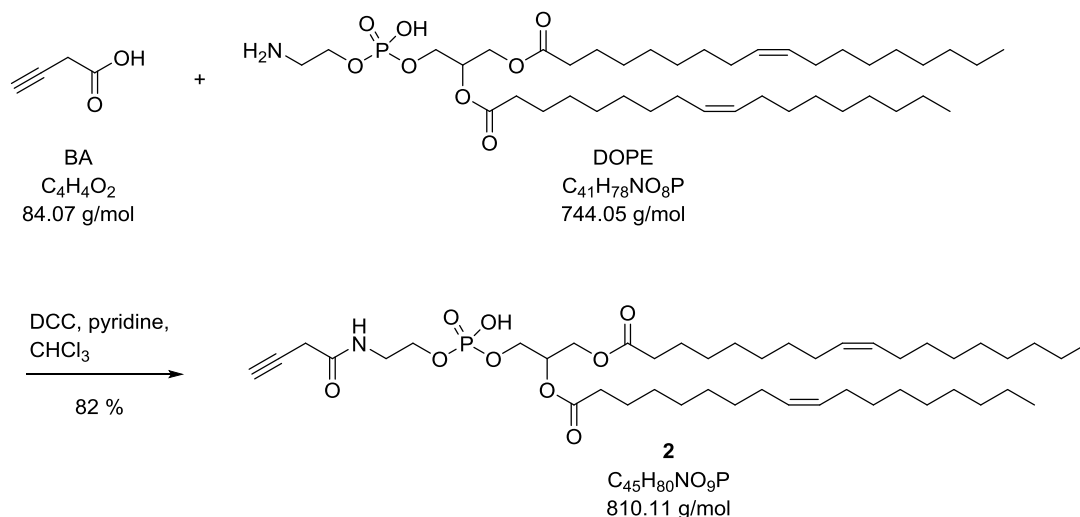
^1H -NMR (400 MHz, CDCl_3): δ [ppm] = 0.83 (t, J = 6.5 Hz, 6H, 18'- CH_3 , 18''- CH_3), 1.24 (d, J = 11.0 Hz, 40H, 20 \times CH_2), 1.55 (s, 4H, 3'- CH_2 , 3''- CH_2), 1.91–2.03 (m, 8H, 8'- CH_2 , 8''- CH_2 , 11'- CH_2 , 11''- CH_2), 2.39–2.54 (m, 8H, 2'- CH_2 , 2''- CH_2 , 5'''- CH_2 , 6'''- CH_2), 3.36 (t, J = 10.4 Hz, 1H, 8'''-CH), 3.48 (d, J = 4.1 Hz, 2H, 2'''- CH_2), 4.02 (dt, J = 9.2, 6.3 Hz, 4H, 1- CH_2 , 1'''- CH_2), 4.12 (dd, J = 12.2, 6.3 Hz, 1H, 3- $\text{CH}_{2,a}$), 4.33 (dd, J = 12.2, 3.3 Hz, 1H, $\text{CH}_{2,b}$), 5.21 (dt, J = 9.5, 5.2 Hz, 1H, 2-CH), 5.30 (s, 4H, 9'-CH, 10'-CH, 9''-CH, 10''-CH), 8.83 (sbr, 1H, NH).

^{13}C -NMR (101 MHz, CDCl_3): δ [ppm] = 14.09 (C-18', C-18''), 22.66, 24.85, 27.17, 27.21, 29.07, 29.10, 29.13, 29.20, 29.29, 29.50, 29.72, 29.75, 31.88, 33.33, 33.61, 34.03 (26 \times CH_2), 34.19, 35.04 (C-2', C-2''), 40.13 (C-2'''), 62.30 (C-1), 64.20 (C-3), 65.32 (C-1'''), 68.83 (C-8'''), 69.12 (C-2), 83.13 (C-7'''), 130.00 (C-9', C-10', C-9'', C-10''), 171.66 (C-4'''), 173.11 (C-1', C-1'').

^{31}P -NMR (203 MHz, CDCl_3): δ [ppm] = 0.16 (s, 1P, PO_4).

ESI-MS m/z : 824.6 $[\text{M}+\text{H}]^+$, 846.6 $[\text{M}+\text{Na}]^+$, 862.6 $[\text{M}+\text{K}]^+$, 822.6 $[\text{M}-\text{H}]^-$.

HR-MS (ESI): calculated for $[\text{C}_{46}\text{H}_{83}\text{NO}_9\text{P}]$ ($[\text{M}+\text{H}]^+$): 824.5800, found: 824.5809; calculated for $[\text{C}_{46}\text{H}_{82}\text{NO}_9\text{PNa}]$ ($[\text{M}+\text{Na}]^+$): 846.5619, found: 846.5626; calculated for $[\text{C}_{46}\text{H}_{81}\text{NO}_9\text{P}]$ ($[\text{M}-\text{H}]^-$): 822.5654, found: 822.5661.

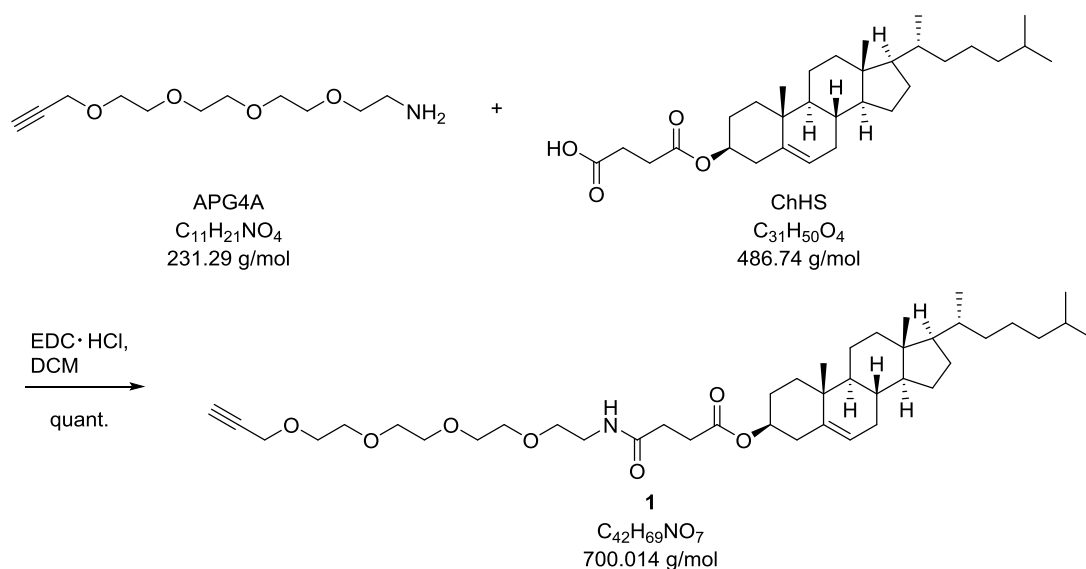
3-(((2-(But-3-ynamido)ethoxy)(hydroxy)phosphoryl)oxy)propane-1,2-diyl dioleate (**2**)

But-3-ynoic acid (BA, 6.95 mg, 82.7 μmol , 2.05 eq.) and DCC (12.1 mg, 58.5 μmol , 1.45 eq.) were dissolved in anhydrous chloroform (500 μL) and stirred at r.t. for 4 h. DOPE (30.0 mg, 40.3 μmol , 1.00 eq.) and pyridine (2 mL) were added and the reaction mixture was allowed to stir at 50 $^\circ\text{C}$ for 12 h. Solid compounds were filtered off and the filtrate was concentrated under reduced pressure. Flash column chromatography (RP silica gel, MeOH/ H_2O , 9:1) provided the pure product (**2**, 26.8 mg, 33.1 μmol , 82 %) as white solid.

TLC (*Alugram* RP-18, MeOH/ H_2O , 9:1): R_f = 0.46.

ESI-MS m/z : 932.6 $[\text{M}+\text{Na}]^+$, 848.5 $[\text{M}+\text{K}]^+$, 854.5 $[\text{M}+2\text{Na}]^+$, 808.6 $[\text{M}-\text{H}]^-$.

HR-MS (ESI): calculated for $[\text{C}_{45}\text{H}_{79}\text{NO}_9\text{P}]$ ($[\text{M}-\text{H}]^-$): 808.5498, found: 808.5473.

3 β -Hydroxy-1-(1-amino-PEG4-4-alkyne)-5-cholestene 3-hemisuccinate (1)

APG4A (12.5 mg, 54.1 μ mol, 1.00 eq.) and ChHS (26.3 mg, 54.1 μ mol, 1.00 eq.) were dissolved in anhydrous DCM (4 mL). EDC·HCl (15.5 mg, 81.1 μ mol, 1.50 eq.) was added and the reaction mixture was stirred at r.t. for 2 d. The organic solvent was removed under reduced pressure and the crude was purified via flash column chromatography (DCM/MeOH, 20:1). The isolated product **1** (37.8 mg, 54.0 μ mol, quant.) was obtained as white solid.

TLC (DCM/MeOH, 20:1): R_f = 0.39.

¹H-NMR (400 MHz, CDCl₃): δ [ppm] = 0.65 (s, 3H, CH₃), 0.84 (dd, J = 6.6, 1.8 Hz, 6H, 2 \times CH₃), 0.89 (d, J = 6.5 Hz, 3H, CH₃), 0.99 (s, 4H, CH₃, CH), 1.02–1.62 (m, 22H, 6 \times CH, 8 \times CH₂), 1.75–1.86 (m, 3H, CH₂, C \equiv CH), 1.88–2.02 (m, 2H, CH₂), 2.29 (d, J = 8.0 Hz, 2H, CH₂), 2.41 (t, J = 2.4 Hz, 1H, CH), 2.46 (t, J = 6.9 Hz, 2H, CH₂), 2.61 (t, J = 6.8 Hz, 2H, CH₂), 3.39–3.46 (m, 2H, CH_{2,PEG}-NH), 3.53 (t, J = 5.0 Hz, 2H, CH_{2,PEG}), 3.57–3.70 (m, 12H, 6 \times CH_{2,PEG}), 4.18 (d, J = 2.4 Hz, 1H, O-CH₂-C \equiv C), 4.52–4.63 (m, 1H, O-CH), 5.34 (d, J = 4.3 Hz, 1H, C=CH), 6.28 (s_{br}, 1H, NH).

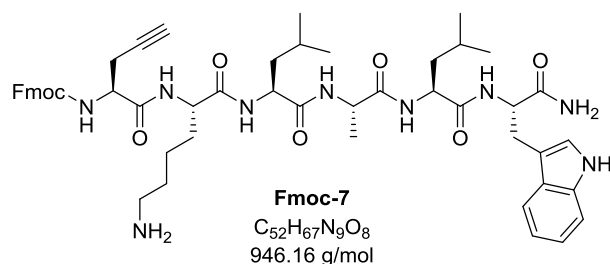
¹³C-NMR (101 MHz, CDCl₃): δ [ppm] = 11.86 (CH₃), 18.72 (CH₃), 19.31 (CH₃), 21.03 (CH₂), 22.56, 22.82, 23.83, 24.28, 27.75, 28.01, 28.23, 29.90, 30.99, 31.86, 31.91, 35.79, 36.19, 36.60, 36.98, 38.09, 39.36, 39.52, 39.74, 42.32 (CH₂-NH), 50.03 (CH), 56.14, 56.70 (2 \times CH), 58.41 (CH₂-C \equiv C), 69.12, 69.84 (2 \times CH_{2,PEG}), 70.28, 70.41, 70.54, 70.62 (5 \times CH_{2,PEG}), 74.26 (O-CH), 74.59 (C \equiv CH), 79.60 (C \equiv CH), 122.63 (C_q=CH), 139.67 (C_q=CH), 171.52 (C(O)O), 172.31 (C(O)N).

ESI-MS m/z : 700.5 [M+H]⁺, 717.5 [M+NH₄]⁺, 722.5 [M+Na]⁺.

HR-MS (ESI): calculated for $[\text{C}_{42}\text{H}_{70}\text{NO}_7]$ ($[\text{M}+\text{H}]^+$): 700.5147, found: 700.5156; calculated for $[\text{C}_{42}\text{H}_{73}\text{N}_2\text{O}_7]$ ($[\text{M}+\text{NH}_4]^+$): 717.5412, found: 717.5392; calculated for $[\text{C}_{42}\text{H}_{69}\text{NO}_7]$ ($[\text{M}+\text{Na}]^+$): 722.4966, found: 722.4965.

Alkyne peptides synthesised by applying SPPS:

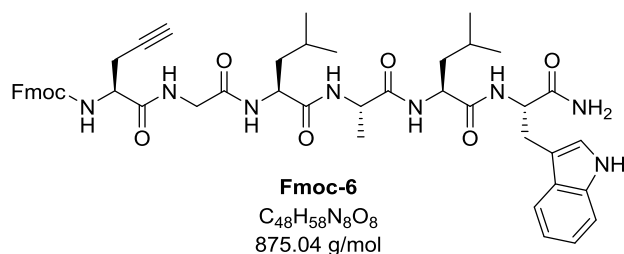
Peptides shorter than ten amino acids were synthesised using the protocol **GP1.1**.



HPLC (MN Nucleodur 100 column, RP-C18, 250×10.0 mm, 5 μ m, gradient: 10–80 % **V2** in 30 min): t_R = 24.3 min.

ESI-MS m/z : 946.5 $[M+H]^+$, 968.5 $[M+Na]^+$, 484.8 $[M+H+Na]^{2+}$

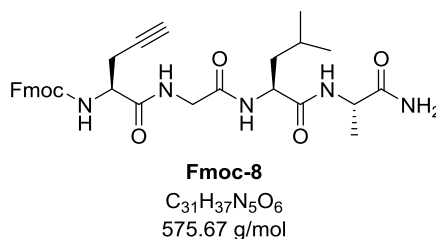
HR-MS (ESI): calculated for $[C_{52}H_{68}N_9O_8]$ ($[M+H]^+$): 946.5185, found: 946.5174.



HPLC (MN Nucleodur 100 column, RP-C18, 250×10.0 mm, 5 μ m, gradient: 10–80 % **V2** in 30 min): t_R = 22.4 min.

ESI-MS m/z : 897.4 $[M+Na]^+$, 460.2 $[M+2Na]^{2+}$.

HR-MS (ESI): calculated for $[C_{48}H_{58}N_8O_8Na]$ ($[M+H]^+$): 897.4270, found: 897.4256.

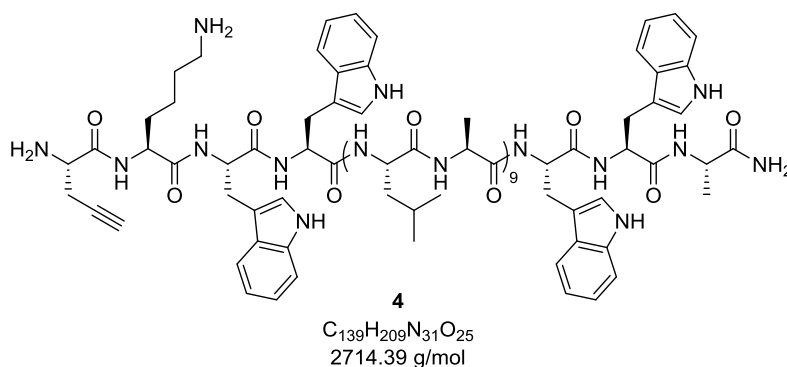


HPLC (ACE Excel 100A column, RP-C18, 10×2.1 mm, 2 μ m, gradient: 10–80 % **V3** in 15 min): t_R = 13.4 min.

ESI-MS m/z : 307.5 $[M+H+K]^{2+}$, 576.3 $[M+H]^+$, 598.1 $[M+Na]^+$, 614.2 $[M+K]^+$, 1173.4 $[2M+Na]^+$.

HR-MS (ESI): calculated for $[C_{31}H_{38}N_5O_6]$ ($[M+H]^+$): 576.2817, found: 576.2815; calculated for $[C_{31}H_{37}N_5O_6Na]$ ($[M+Na]^+$): 598.2636, found: 598.2637; calculated for $[C_{31}H_{37}N_5O_6K]$ ($[M+K]^+$): 614.2375, found: 614.2366.

Synthesis of the transmembrane peptide **WALP25 4** was performed using the protocol **GP1.2** for the first 24 amino acids and the protocol **GP1.1** for the N-terminal unnatural amino acid propargyl glycine.



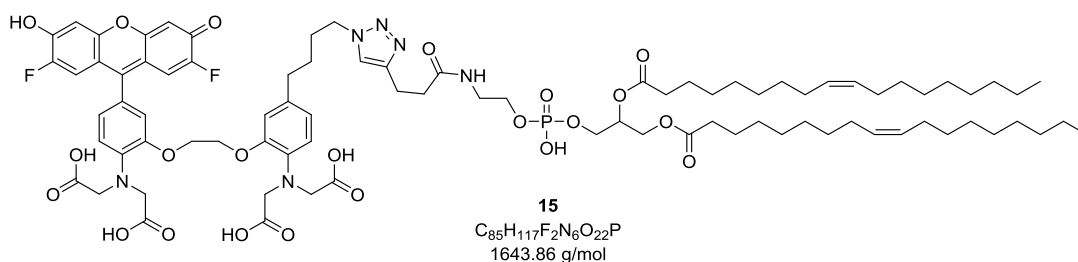
HPLC (MN Nucleodur 100 column, RP-C18, 250×10.0 mm, 5 μ m, gradient: 80–100 % **V1** in 30 min): t_R = 24.4 min.

ESI-MS m/z : 905.2 $[M+3H]^{3+}$, 912.9 $[M+2H+Na]^{3+}$, 1357.8 $[M+2H]^{2+}$, 1368.3 $[M+H+Na]^{2+}$, 5426.1 $[2M+H]^+$

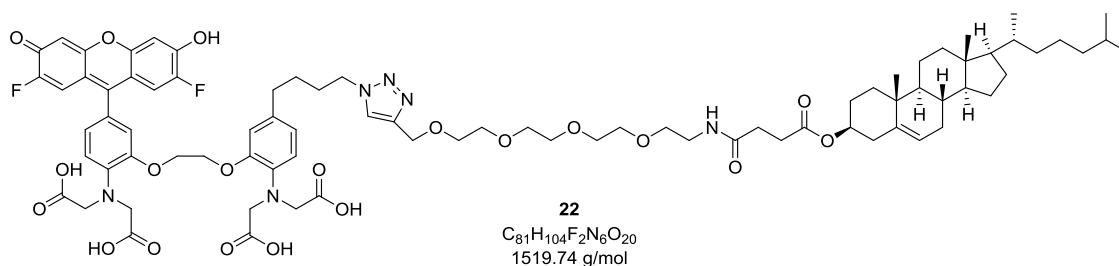
HR-MS (ESI): calculated for $[C_{139}H_{211}N_{31}O_{25}Na]$ ($[M+2H+Na]^{3+}$): 912.5358, found: 912.5339; calculated for $[C_{139}H_{211}N_{31}O_{25}]$ ($[M+2H]^{2+}$): 1357.3091, found: 1357.3064.

General procedure for attachment of sensors:

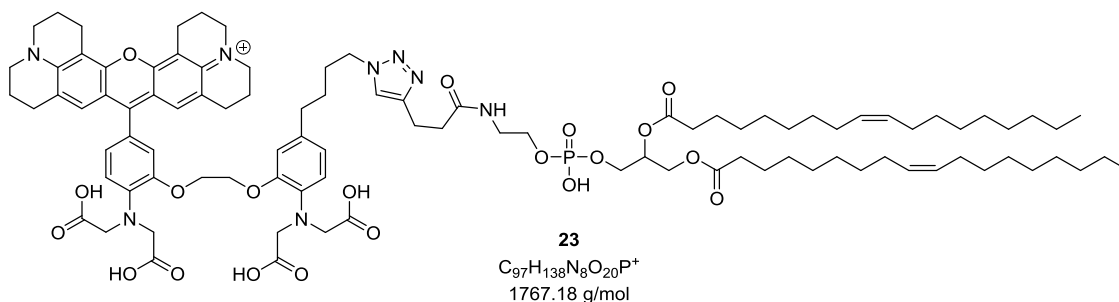
The respective sensor azide (1.00 eq.) and lipid alkyne (1.00 eq.) were added into a micro test tube. Then, the organic solvent (MeOH) in the stored stock solutions was removed under a gentle stream of nitrogen before usage. Afterwards, copper wire (700 mg per 100 nmol sensor) formed to a spiral was placed in the reaction vessel and DMF (500 μ L per 100 nmol sensor) was added. The tube was agitated for 17–24 h under light exclusion at 50 °C. The reaction mixture was allowed to cool down to r.t., the copper spiral was removed, the mixture was diluted with water and MeCN (1:1) and the product isolated via HPLC.



HPLC (ACE Excel 100A column, RP-C18, 10×2.1 mm, 2 μ m, gradient: 10–80 % **V3** in 15 min): t_R = 7.4 min.



HPLC (ACE Excel 100A column, RP-C18, 10×2.1 mm, 2 μ m, gradient: 10–80 % **V3** in 15 min): t_R = 7.2 min.



HPLC (*ACE Excel* 100A column, RP-C18, 10×2.1 mm, 2 μm, gradient: 50–80 % **V3** in 15 min): t_R = 18.5 min.

7 Abbreviations

| | |
|-------------------|---|
| Å | Ångström |
| δ | chemical shift |
| ε | extinction coefficient |
| °C | degree Celsius |
| AcOH | acetic acid |
| aq. | aqueous |
| BA | but-3-ynoic acid |
| BD | <i>Becton Dickinson</i> |
| Boc | tert-butoxycarbonyl |
| BuLi | butyl lithium |
| CaM | calmodulin |
| Cbz | carboxybenzyl |
| CD | circular dichroism |
| ChHS | cholesteryl hemisuccinate |
| COSY | correlation spectroscopy |
| d | dublett |
| DCM | dichloromethane |
| DIC | diisopropylcarbodiimide |
| DIPEA | diisopropylethylamine |
| DMAP | 4-dimethylaminopyridine |
| DMF | dimethylformamide |
| DMSO | dimethylsulfoxide |
| DOPE | 1,2-dioleoyl- <i>sn</i> -glycero-3-phosphoethanolamine |
| DOSY | diffusion-ordered spectroscopy |
| DSPC | 1,2-distearoyl- <i>sn</i> -glycero-3-phosphocholine |
| e.g. | <i>exempli gratia</i> ; for example |
| EDC·HCl | 1-(3-dimethylaminopropyl)-3-ethylcarbodiimide hydrochloride |
| eq. | equivalent |
| ER | endoplasmic reticulum |
| ESI | electron spray ionisation |
| EtOAc | ethyl acetate |
| EtOH | ethanol |
| Et ₂ O | diethyl ether |
| FC | flash column chromatography |
| Fmoc | fluorenylmethyloxycarbonyl |
| g | gram |

| | |
|------------------|--|
| <i>gem</i> | geminal |
| h | hour |
| HBTU | 2-(1H-benzotriazole-1-yl)-1,1,3,3-tetramethyluronium hexafluorophosphate |
| HEPES | 4-(2-hydroxyethyl)-1-piperazineethansulfonic acid |
| HMBC | heteronuclear multiple bond correlation |
| HOBt | 1-hydroxybenzotriazole |
| HPLC | high performance liquid chromatography |
| HR-MS | high resolution mass spectrometry |
| HSQC | heteronuclear single quantum coherence |
| Hz | hertz |
| <i>i.a.</i> | <i>inter alia</i> ; amongst other things |
| m | multiplett |
| M | molar |
| M | molar mass |
| <i>m/z</i> | mass to charge |
| MBHA | 4-methylbenzhydramine |
| Me | methyl |
| MeCN | acetonitrile |
| MeOH | methanol |
| min | minute |
| mL | millilitre |
| MOPS | 3-morpholinopropane-1-sulfonic acid |
| MS | mass spectrometry |
| MTBE | methyl tert-butyl ether |
| <i>m/z</i> | mass to charge |
| NBS | <i>N</i> -bromosuccinimide |
| NEt ₃ | triethylamine |
| NHS | <i>N</i> -hydroxysuccinimide |
| NMP | <i>N</i> -methylpyrrolidine |
| NMR | nuclear magnetic resonance |
| PA | pent-3-ynoic acid |
| PEG | polyethylene glycol |
| pH | <i>pondus hydrogenii</i> ; decimal logarithm of the reciprocal of hydrogen ion activity |
| PLC | preparative thin layer chromatography |
| PM | plasma membrane |
| PMB | <i>para</i> -methoxybenzyl |
| ppm | parts per million |
| q | quartett |

| | |
|--------|---|
| r.t. | room temperature |
| r_f | retention factor |
| Rhod- | <i>N</i> -(lyssamine rhodamine B sulfonyl)-1,2-dioleoyl-sn-3- |
| DOPE | phosphatidylehanolamine |
| RP | reverse phase |
| RPC | reverse phase column chromatography |
| rpm | rounds per minute |
| RyR | ryanodine receptor |
| s | singlett |
| SNARE | soluble <i>N</i> -ethylmaleimide-sensitive-factor attachment protein receptor |
| SPPS | solid phase peptide synthesis |
| SR | sarcoplasmic reticulum |
| Syb | synaptobrevin |
| Sx | syntaxin |
| t | triplett |
| TBAF | tert-butylammonium fluoride |
| TBSCl | tert-butyldimethylsilyl chloride |
| TES | triethylsilane |
| TESCl | triethylsilyl chloride |
| TFA | trifluoroacetic acid |
| TFE | trifluorethanol |
| THF | tetrahydrofurane |
| TIPSCl | triisopropylsilyl chloride |
| TIS | triisopropylsilane |
| TLC | thin layer chromatography |
| t_R | retention time |
| TRIS | tris(hydroxymethyl)aminomethane |
| UV | ultraviolet |
| Vis | visible |
| W | Watt |

8 Bibliography

- [1] W. Wildgen, *The Evolution of Human Language: Scenarios, Principles, and Cultural Dynamics*, John Benjamins Publishing Company, Amsterdam/Philadelphia, **2004**.
- [2] C. Wasternack, I. Stenzel, B. Hause, G. Hause, C. Kutter, H. Maucher, J. Neumerkel, I. Feussner, O. Miersch, *J. Plant Physiol.* **2006**, *163*, 297–306.
- [3] A. Andreou, I. Feussner, *Phytochemistry* **2009**, *70*, 1504–1510.
- [4] J. Newie, A. Andreou, P. Neumann, O. Einsle, I. Feussner, R. Ficner, *J. Lipid Res.* **2016**, *57*, 276–287.
- [5] A. Campbell, *Intracellular Calcium*, Wiley, **2015**.
- [6] B. Alberts, A. Johnson, J. Lewis, D. Morgan, M. Raff, K. Roberts, P. Walter, *Molekularbiologie Der Zelle*, Wiley-VCH, Weinheim, **2017**.
- [7] K. Cammann, U. Lemke, A. Rohen, J. Sander, H. Wilken, B. Winter, *Angew. Chemie Int. Ed.* **1991**, *30*, 516–539.
- [8] M. Schäferling, *Angew. Chemie - Int. Ed.* **2012**, *51*, 3532–3554.
- [9] R. M. Paredes, J. C. Etzler, L. T. Watts, W. Zheng, J. D. Lechleiter, *Methods* **2008**, *46*, 143–151.
- [10] R. Y. Tsien, *Biochemistry* **1980**, *19*, 2396–2404.
- [11] M. Oheim, M. van 't Hoff, A. Feltz, A. Zamaleeva, J. M. Mallet, M. Collot, *Biochim. Biophys. Acta - Mol. Cell Res.* **2014**, *1843*, 2284–2306.
- [12] A. I. Zamaleeva, G. Despras, C. Luccardini, M. Collot, M. De Waard, M. Oheim, J. M. Mallet, A. Feltz, *Sensors* **2015**, *15*, 24662–24680.
- [13] J. Graf, *Synthese von Fluoreszierenden Calcium- Sensoren Und Biomolekülen Zur Untersuchung Physiologischer Prozesse*, Georg-August-University Göttingen, **2016**.
- [14] S. McLaughlin, D. Murray, *Nature* **2005**, *438*, 605–11.
- [15] M. J. Berridge, *Nature* **1993**, *361*, 315–325.
- [16] G. van den Bogaart, K. Meyenberg, H. J. Risselada, H. Amin, K. I. Willig, B. E. Hubrich, M. Dier, S. W. Hell, H. Grubmüller, U. Diederichsen, et al., *Nature* **2011**, *479*, 552–555.
- [17] J. Bai, W. C. Tucker, E. R. Chapman, *Nat Struct Mol Biol* **2004**, *11*, 36–44.
- [18] A. V. Smirnov, D. S. English, R. L. Rich, J. Lane, L. Teyton, a. W. Schwabacher,

- S. Luo, R. W. Thornburg, J. W. Petrich, *J. Phys. Chem. B* **1997**, 101, 2758–2769.
- [19] K. Ingham, M. A. El-Bayoumi, *J. Am. Chem. Soc.* **1974**, 96, 1674–1682.
- [20] C. F. Chapman, M. Maroncelli, *J. Phys. Chem.* **1992**, 96, 8430–8441.
- [21] M. Negrerie, S. M. Bellefeuille, S. Whitham, J. W. Petrich, R. W. Thornburg, *J. Am. Chem. Soc.* **1990**, 112, 7419–7421.
- [22] A. Mosblech, I. Feussner, I. Heilmann, *Plant Physiol. Biochem.* **2009**, 47, 511–517.
- [23] I. Feussner, H. Kühn, C. Wasternack, *Trends Plant Sci.* **2001**, 6, 268–273.
- [24] A. Liavonchanka, I. Feussner, *J. Plant Physiol.* **2006**, 163, 348–357.
- [25] M. J. Berridge, M. D. Bootman, P. Lipp, *Nature* **1998**, 395, 645–648.
- [26] R. H. Scheller, *Nat. Med.* **2013**, 19, 1232–5.
- [27] T. Egawa, K. Hirabayashi, Y. Koide, C. Kobayashi, N. Takahashi, T. Mineno, T. Terai, T. Ueno, T. Komatsu, Y. Ikegaya, et al., *Angew. Chemie Int. Ed.* **2013**, 52, 3874–3877.
- [28] A. Matsui, K. Umezawa, Y. Shindo, T. Fujii, D. Citterio, K. Oka, K. Suzuki, *Chem. Commun.* **2011**, 47, 10407.
- [29] D. Bruns, R. Jahn, *Nature* **1995**, 377, 62–65.
- [30] H. Ai, K. L. Hazelwood, M. W. Davidson, R. E. Campbell, *Nat. Methods* **2008**, 5, 401–403.
- [31] W. Tomosugi, T. Matsuda, T. Tani, T. Nemoto, I. Kotera, K. Saito, K. Horikawa, T. Nagai, *Nat. Methods* **2009**, 6, 351–353.
- [32] D. A. Rusakov, A. Fine, *Neuron* **2003**, 37, 287–297.
- [33] G. J. Augustine, *Curr. Opin. Neurobiol.* **2001**, 11, 320–326.
- [34] Z. P. Pang, T. C. Südhof, *Curr. Opin. Cell Biol.* **2010**, 22, 496–505.
- [35] A. Jeremic, M. Kelly, J. A. Cho, S. J. Cho, J. K. H. Horber, B. P. Jena, *Cell Biol. Int.* **2004**, 28, 19–31.
- [36] T. C. Südhof, *Cold Spring Harb. Perspect. Biol.* **2012**, 4, 1–16.
- [37] E. Carafoli, *Nat. Rev. Mol. Cell Biol.* **2003**, 4, 326–332.
- [38] D. E. Clapham, *Cell* **2007**, 131, 1047–1058.
- [39] P. Uhlén, N. Fritz, *Biochem. Biophys. Res. Commun.* **2010**, 396, 28–32.
- [40] S. E. Webb, A. L. Miller, *Nat. Rev. Mol. Cell Biol.* **2003**, 4, 539–51.
- [41] T. H. E. Heart, B. Y. Sydney, *J. Physiol.* **1883**, 4, 29–42.

- [42] S. A. Stricker, V. E. Centonze, S. W. Paddock, G. Schatten, *Dev. Biol.* **1992**, 149, 370–380.
- [43] J. Ferreira-Martins, C. Rondon-Clavo, D. Tugal, J. A. Korn, R. Rizzi, M. E. Padin-Iruegas, S. Ottolenghi, A. De Angelis, K. Urbanek, N. Ide-Iwata, et al., *Circ. Res.* **2009**, 105, 764–774.
- [44] P. Uhlen, P. M. Burch, C. I. Zito, M. Estrada, B. E. Ehrlich, A. M. Bennett, *PNAS* **2006**, 103, 2160–2165.
- [45] M. Colella, F. Grisan, V. Robert, J. D. Turner, A. P. Thomas, T. Pozzan, *PNAS* **2008**, 105, 2859–2864.
- [46] M. J. Berridge, M. D. Bootman, H. L. Roderick, *Nat. Rev. Mol. Cell Biol.* **2003**, 4, 517–529.
- [47] M. D. Bootman, T. J. Collins, C. M. Peppiatt, L. S. Prothero, L. MacKenzie, P. De Smet, M. Travers, S. C. Tovey, J. T. Seo, M. J. Berridge, et al., *Cell Dev. Biol.* **2001**, 12, 3–10.
- [48] J. R. Slupsky, M. Ohnishi, M. R. Carpenter, R. a Reithmeier, *Biochemistry* **1987**, 26, 6539–44.
- [49] A. P. Arruda, M. Nigro, G. M. Oliveira, L. de Meis, *Biochim. Biophys. Acta - Biomembr.* **2007**, 1768, 1498–1505.
- [50] T. P. Jensen, L. E. Buckby, R. M. Empson, *Dev. Brain Res.* **2004**, 152, 129–136.
- [51] S. Nakayama, R. Kretsinger, *Annu. Rev. Biophys. Biomol. Struct.* **1994**, 23, 473–507.
- [52] S. W. Vetter, E. Leclerc, *Eur. J. Biochem.* **2003**, 270, 404–414.
- [53] D. Chin, A. R. Means, *Trends Cell Biol.* **2000**, 10, 322–328.
- [54] Y. Nishizawa, Y. Okui, S. Okuno, T. Miki, Y. Watanabe, H. Morii, *J. Clin. Investig.* **1988**, 82, 1165–1172.
- [55] M. G. Tansey, K. Luby-Phelps, K. E. Kamm, J. T. Stull, *J. Biol. Chem.* **1994**, 269, 9912–9920.
- [56] H. Hanser, “Calcium-Calmodulin-abhängige Proteinkinase II,” **1999**.
- [57] S. L. Hamilton, I. Serysheva, G. M. Strasburg, *News Physiol. Sci.* **2000**, 15, 281–284.
- [58] B. Katz, R. Miledi, *Nature* **1967**, 215, 651.
- [59] W. Wickner, R. Schekman, *Nat. Struct. Mol. Biol.* **2008**, 15, 658–664.
- [60] L. V. Chernomordik, J. Zimmerberg, M. M. Kozlov, *J. Cell Biol.* **2006**, 175, 201–207.

- [61] R. Jahn, D. Fasshauer, *Nature* **2012**, 490, 201–207.
- [62] D. Fasshauer, R. B. Sutton, A. T. Brunger, R. Jahn, *Proc. Natl. Acad. Sci. U. S. A.* **1998**, 95, 15781–6.
- [63] E. R. Chapman, S. An, N. Barton, R. Jahn, *J. Biol. Chem.* **1994**, 269, 27427–27432.
- [64] J. M. Hernandez, A. Stein, E. Behrmann, D. Riedel, A. Cypionka, Z. Farsi, P. J. Walla, S. Raunser, R. Jahn, *Science (80-.)*. **2012**, 336, 1581–1584.
- [65] P. Zhou, Z. P. Pang, X. Yang, Y. Zhang, C. Rosenmund, T. Bacaj, T. C. Südhof, *EMBO J.* **2013**, 32, 159–71.
- [66] P. I. R. Hanson R. Morisaki, H., Jahn, R. and Heuser, J. E., *Cell* **1997**, 90, 523–535.
- [67] R. B. Sutton, D. Fasshauer, R. Jahn, A. T. Brunger, *Nature* **1998**, 395, 347–353.
- [68] A. M. Walter, K. Wiederhold, D. Bruns, D. Fasshauer, J. B. Sørensen, *J. Cell Biol.* **2010**, 188, 401–413.
- [69] K. Wiederhold, T. H. Kloepper, A. M. Walter, A. Stein, N. Kienle, J. B. Sørensen, D. Fasshauer, *J. Biol. Chem.* **2010**, 285, 21549–21559.
- [70] P. Kumar, S. Guha, U. Diederichsen, *J. Pept. Sci.* **2015**, 21, 621–629.
- [71] R. Jahn, R. H. Scheller, *Nat. Rev. Mol. Cell Biol.* **2006**, 7, 631–643.
- [72] T. C. Südhof, *Nat. Med.* **2013**, 19, 1227–1231.
- [73] J. B. Sorensen, K. Wiederhold, E. M. Muller, I. Milosevic, G. Nagy, B. L. de Groot, H. Grubmuller, D. Fasshauer, *EMBO J.* **2006**, 25, 955–966.
- [74] J. Di Giovanni, C. C. Iborra, Y. Maulet, C. Lévêque, O. El Far, M. Seagar, *J. Biol. Chem.* **2010**, 285, 23665–23675.
- [75] H. R. Marsden, I. Tomatsu, A. Kros, *Chem. Soc. Rev.* **2011**, 40, 1572–1585.
- [76] M. Ma, D. Bong, *Acc. Chem. Res.* **2013**, 46, 2988–2997.
- [77] C. M. Paleos, D. Tsiourvas, Z. Sideratou, *ChemBioChem* **2011**, 12, 510–521.
- [78] A. S. Lygina, K. Meyenberg, R. Jahn, U. Diederichsen, *Angew. Chemie Int. Ed.* **2011**, 50, 8597–8601.
- [79] G. Stengel, L. Simonsson, R. A. Campbell, F. Höök, *J. Phys. Chem. B* **2008**, 112, 8264–8274.
- [80] H. R. Marsden, A. Kros, *Angew. Chemie Int. Ed.* **2010**, 49, 2988–3005.
- [81] H. Robson Marsden, A. V. Korobko, T. Zheng, J. Voskuhl, A. Kros, *Biomater. Sci.* **2013**, 1, 1046–1054.
- [82] A. Kashiwada, M. Tsuboi, K. Matsuda, *Chem. Commun.* **2009**, 695–697.

- [83] L. Simonsson, P. Jönsson, G. Stengel, F. Höök, *ChemPhysChem* **2010**, *11*, 1011–1017.
- [84] G. Stengel, R. Zahn, F. Höök, *J. Am. Chem. Soc.* **2007**, *129*, 9584–9585.
- [85] Y.-H. M. Chan, B. van Lengerich, S. G. Boxer, *Biointerphases* **2008**, *3*, FA17-FA21.
- [86] T. Zheng, J. Voskuhl, F. Versluis, H. R. Zope, I. Tomatsu, H. R. Marsden, A. Kros, *Chem. Commun.* **2013**, *49*, 3649–51.
- [87] Y. Gong, Y. Luo, D. Bong, *J. Am. Chem. Soc.* **2006**, *128*, 14430–14431.
- [88] S. Guha, J. Graf, B. Göricke, U. Diederichsen, *J. Pept. Sci.* **2013**, *19*, 415–422.
- [89] J.-D. Wehland, A. S. Lygina, P. Kumar, S. Guha, B. E. Hubrich, R. Jahn, U. Diederichsen, A. T. Brunger, K. Weninger, M. Bowen, et al., *Mol. BioSyst.* **2016**, *12*, 2770–2776.
- [90] F. Crick, *Nature* **1952**, *170*, 882–883.
- [91] J. R. Litowski, R. S. Hodges, *J. Biol. Chem.* **2002**, *277*, 37272–37279.
- [92] A. Lygina, Design , Synthesis and Fusion Activity of PNA/Peptide Hybrids as SNARE-Protein Models, **2011**.
- [93] P. E. Nielsen, M. Egholm, R. H. Berg, O. Buchardt, *Science (80-.)*. **1991**, *254*, 1497–1500.
- [94] B. Hyrup, P. Nielsen, *Bioorganic Med. Chem.* **1996**, *4*, 5–23.
- [95] R. Y. Tsien, T. Pozzan, T. J. Rink, *J. Cell Biol.* **1982**, *94*, 325–334.
- [96] R. Y. Tsien, *Calcium as a Cellular Regulator*, Oxford University Press New York, **1999**.
- [97] H. A. Behanna, S. I. Stupp, *Chem. Commun.* **2005**, 4845–4847.
- [98] G. Grynkiewicz, M. Poenie, R. Y. Tsien, *J. Biol. Chem.* **1985**, *260*, 3440–3450.
- [99] A. Minta, J. P. Y. Kao, R. Y. Tsien, *J. Biol. Chem.* **1989**, *14*, 8171–8178.
- [100] M. S. Islam, *Calcium Signalling*, Springer, Dordrecht, **2012**.
- [101] V. Ramamurthy, *Organic and Inorganic Photochemistry*, New York, **1998**.
- [102] L.-J. Fan, W. E. Jones Jr., *J. Phys. Chem. B* **2006**, *110*, 7777–7782.
- [103] K. R. Gee, K. A. Brown, W.-N. U. Chen, J. Bishop-Stewart, D. Gray, I. Johnson, *Cell Calcium* **2000**, *27*, 97–106.
- [104] M. W. Roe, J. J. Lemasters, B. Herman, *Cell Calcium* **1990**, *11*, 63–73.
- [105] M. Whitaker, *Physiol. Rev.* **2006**, *86*, 25–88.

- [106] G. Xia, Z. An, Y. Wang, C. Zhao, M. Li, Z. Li, J. Ma, *Chem. Pharm. Bull. (Tokyo)*. **2013**, *61*, 390–398.
- [107] M. Eberhard, P. Erne, *Biochem. Biophys. Res. Commun.* **1991**, *180*, 209–215.
- [108] V. K. Tiwari, B. B. Mishra, K. B. Mishra, N. Mishra, A. S. Singh, X. Chen, *Chem. Rev.* **2016**, *116*, 3086–3240.
- [109] W. Tang, M. L. Becker, *Chem. Soc. Rev.* **2014**, *43*, 7013–7039.
- [110] C. O. Kappe, E. Van der Eycken, *Chem. Soc. Rev.* **2010**, *39*, 1280–1290.
- [111] W. H. Binder, R. Sachsenhofer, *Macromol. Rapid Commun.* **2008**, *29*, 952–981.
- [112] A. A. Ali, M. Konwar, M. Chetia, D. Sarma, *Tetrahedron Lett.* **2016**, *57*, 5661–5665.
- [113] M. Collot, C. Loukou, A. V. Yakovlev, C. D. Wilms, D. Li, A. Evrard, L. Bourdieu, J.-F. Léger, N. Ropert, J. Eilers, et al., *J. Am. Chem. Soc.* **2012**, *134*, 14923–14931.
- [114] S. L. Presolski, V. P. Hong, M. G. Finn, *Curr. Protoc. Chem. Biol.* **2011**, *3*, 153–162.
- [115] S. Li, H. Cai, J. He, H. Chen, S. Lam, T. Cai, Z. Zhu, S. J. Bark, C. Cai, *Bioconjug. Chem.* **2016**, *27*, 2315–2322.
- [116] V. Castro, H. Rodríguez, F. Albericio, *ACS Comb. Sci.* **2016**, *18*, 1–14.
- [117] H. Li, R. Aneja, I. Chaiken, *Molecules* **2013**, *18*, 9797–9817.
- [118] C. Bouillon, A. Meyer, S. Vidal, A. Jochum, Y. Chevolot, J. Cloarec, J. Praly, J. Vasseur, F. Morvan, *J. Org. Chem.* **2006**, *71*, 4700–4702.
- [119] R. MacDonald, G. Swift, A. Przybyla, J. Chirgwin, *Methods Enzymol.* **1987**, *152*, 219–227.
- [120] I. Géci, V. V. Filichev, E. B. Pedersen, *Chem. - A Eur. J.* **2007**, *13*, 6379–6386.
- [121] V. Fagan, I. Toth, P. Simerska, *Beilstein J. Org. Chem.* **2014**, *10*, 1741–1748.
- [122] T. A. M. Bharat, J. Malsam, W. J. H. Hagen, A. Scheutzow, T. H. Söllner, J. A. G. Briggs, *EMBO Rep.* **2014**, *15*, 308–314.
- [123] G. J. Augustine, M. P. Charlton, S. J. Smith, *Annu. Rev. Neurosci.* **1987**, *10*, 633–693.
- [124] P. Heo, Y. Yang, K. Y. Han, B. Kong, J. H. Shin, Y. Jung, C. Jeong, J. Shin, Y. K. Shin, T. Ha, et al., *J. Am. Chem. Soc.* **2016**, *138*, 4512–4521.
- [125] T. Dittmar, K. S. Zänker, Eds. , *Cell Fusion in Health and Disease*, Springer, Dordrecht, **2011**.
- [126] Y. Gong, M. Ma, Y. Luo, D. Bong, *J. Am. Chem. Soc.* **2008**, *130*, 6196–6205.

- [127] M. F. Hanzal-Bayer, J. F. Hancock, *FEBS Lett.* **2007**, 581, 2098–2104.
- [128] S. J. Singer, G. L. Nicolson, *Science* (80-.). **1972**, 175, 720–731.
- [129] J. Malinsky, M. Opekarová, G. Grossmann, W. Tanner, *Annu. Rev. Plant Biol.* **2013**, 64, 501–529.
- [130] K. Simons, W. L. C. Vaz, *Annu. Rev. Biophys. Biomol. Struct.* **2004**, 33, 269–295.
- [131] E. London, *Biochim. Biophys. Acta - Mol. Cell Res.* **2005**, 1746, 203–220.
- [132] L. Bagatolli, P. B. Sunil Kumar, *Soft Matter* **2009**, 5, 3234–3248.
- [133] D. Marsh, *Handbook of Lipid Bilayers*, CRC Press, **2013**.
- [134] L. K. Tamm, in *Protein-Lipid Interact. From Membr. Domains to Cell. Networks*, Wiley-VCH Verlag GmbH & Co. KGaA, Weinheim, **2005**, pp. 337–365.
- [135] D. Lingwood, K. Simons, *Science* (80-.). **2010**, 327, 46–50.
- [136] K. Simons, E. Ikonen, *Nature* **1997**, 387, 569–572.
- [137] S. L. Regen, *Curr. Opin. Chem. Biol.* **2002**, 6, 729–735.
- [138] L. J. Pike, *J. Lipid Res.* **2006**, 47, 1597–1598.
- [139] D. L. Nelson, M. M. Cox, *Lehninger Principles of Biochemistry*, W. H. Freeman, **2004**.
- [140] L. Qiao, Y. Hu, F. Nan, G. Powis, A. P. Kozikowski, *Org. Lett.* **2000**, 2, 115–117.
- [141] Y. Nishizuka, *Nature* **1988**, 334, 661–665.
- [142] M. Leslie, *Science* (80-.). **2011**, 334, 1046–1047.
- [143] A. Kyrychenko, *Methods Appl. Fluoresc.* **2015**, 3, 42003.
- [144] S. W. Hell, *Science* (80-.). **2007**, 316, 1153–1158.
- [145] C. Eggeling, C. Ringemann, R. Medda, G. Schwarzmann, K. Sandhoff, S. Polyakova, V. N. Belov, B. Hein, C. von Middendorff, A. Schönle, et al., *Nature* **2009**, 457, 1159–62.
- [146] A. S. Shaw, *Nat. Immunol.* **2006**, 7, 1139–1142.
- [147] M. E. McClellan, M. H. Elliott, *Methods Mol. Biol.* **2017**, 1609, 185–194.
- [148] M. Edidin, *Nat. Rev. Mol. Cell Biol.* **2003**, 4, 414–418.
- [149] A. G. Szabo, D. M. Rayner, *J. Am. Chem. Soc.* **1980**, 102, 554–563.
- [150] J. W. Petrich, M. C. Chang, D. B. McDonald, G. R. Fleming, *J. Am. Chem. Soc.* **1983**, 105, 3824–3832.

- [151] A. J. B. Ross, K. W. Rousslang, L. Band, *Biochemistry* **1981**, 20, 4361–4369.
- [152] L. X.-. Q. Chen, J. W. Petrich, G. R. Fleming, *Chem. Phys. Lett.* **1987**, 139, 55–61.
- [153] J. W. Young, Z. D. Pozun, K. D. Jordan, D. W. Pratt, *J. Phys. Chem. B* **2013**, 117, 15695–15700.
- [154] J. M. Goldberg, L. C. Speight, M. W. Fegley, E. J. Petersson, *J. Am. Chem. Soc.* **2012**, 134, 6088–6091.
- [155] M. Negrerie, F. Gai, S. M. Bellefeuille, J. W. Petrich, *J. Phys. Chem.* **1991**, 95, 8663–8670.
- [156] J. Guharay, P. K. Sengupta, *Biochem. Biophys. Res. Commun.* **1996**, 219, 388–92.
- [157] O.-H. Kwon, A. H. Zewail, *Proc. Natl. Acad. Sci.* **2007**, 104, 8703–8708.
- [158] J. Catalan, P. Perez, J. C. del Valle, J. L. G. de Paz, M. Kasha, *Proc. Natl. Acad. Sci.* **2004**, 101, 419–422.
- [159] C. Al Taylor, M. A. El-Bayoumi, M. Kasha, *Proc. Natl. Acad. Sci.* **1969**, 63, 253–260.
- [160] D. E. Folmer, E. S. Wisniewski, A. W. Castleman, *Chem. Phys. Lett.* **2000**, 318, 637–643.
- [161] S. Takeuchi, T. Tahara, *Proc. Natl. Acad. Sci.* **2007**, 104, 5285–5290.
- [162] P. Pe, J. Carlos, J. L. G. De Paz, M. Kasha, *PNAS* **2002**, 99, 5793–5798.
- [163] M. M. Robison, B. L. Robison, *J. Am. Chem. Soc.* **1956**, 78, 1247–1251.
- [164] L. T. Pierce, M. M. Cahill, F. O. McCarthy, *Tetrahedron* **2011**, 67, 4601–4611.
- [165] M. Bandini, A. Eichholzer, *Angew. Chemie - Int. Ed.* **2009**, 48, 9533–9537.
- [166] J. Chen, A. A. Profit, G. D. Prestwich, *J. Org. Chem.* **1996**, 61, 6305–6312.
- [167] U. Näser, A. J. Pierik, R. Scott, I. Çinkaya, W. Buckel, B. T. Golding, *Bioorg. Chem.* **2005**, 33, 53–66.
- [168] G. Halperin, E. Kovalevski-Ishai, *US 8,569,529 B2*, **2013**.
- [169] E. Kovalevski-Ishai, Z. Ziniuk, G. Halperin, I. Mendel, *WO 2010/052718 A9*, **2010**.
- [170] A. Fürstner, K. Langemann, *J. Org. Chem.* **1996**, 61, 3942–3943.
- [171] P. D. Wadhavane, M. Á. Izquierdo, D. Lutters, M. I. Burguete, M. J. Marín, D. A. Russell, F. Galindo, S. V Luis, *Org. Biomol. Chem.* **2014**, 12, 823–831.
- [172] C. Baldoli, L. Falciola, E. Licandro, S. Maiorana, P. Mussini, P. Ramani, C. Rigamonti, G. Zinzalla, *J. Organomet. Chem.* **2004**, 689, 4791–4802.

- [173] B. Juma, M. Adeel, A. Villinger, H. Reinke, A. Spannenberg, C. Fischer, P. Langer, *Adv. Synth. Catal.* **2009**, 351, 1073–1079.
- [174] I. Johnson, M. Spence, *The Molecular Probes Handbook. A Guide to Fluorescent Probes and Labeling Technologies*, **2010**.
- [175] Z. Zhang, Z. Yang, H. Wong, J. Zhu, N. A. Meanwell, J. F. Kadow, T. Wang, *J. Org. Chem.* **2002**, 67, 6226–6227.
- [176] S. Aldous, M. Fennie, J. Jiang, S. John, WO 2008/121670 A1, **2008**.
- [177] H. Raistrick, R. Robinson, A. R. Todd, *J. Chem. Soc.* **1937**, 80.
- [178] R. C. Larock, E. K. Yum, *J. Am. Chem. Soc.* **1991**, 113, 6689–6690.
- [179] E. T. Nades, A. Lazareva, O. Daugulis, *J. Org. Chem.* **2011**, 76, 471–483.
- [180] R. C. Larock, E. K. Yum, M. D. Refvik, *J. Org. Chem.* **1998**, 63, 7652–7662.
- [181] L. S. Hegedus, *Angew. Chemie Int. Ed.* **1988**, 27, 1113–1126.
- [182] G. W. Gray, A. Mosley, *Mol. Cryst. Liq. Cryst.* **1978**, 48, 233–242.
- [183] A. Schulze, A. Giannis, *Synthesis (Stuttg.)*. **2006**, 257–260.
- [184] G. Jiang, Y. Xu, G. D. Prestwich, *J. Org. Chem.* **2006**, 71, 934–939.
- [185] T. Kano, M. Takeda, R. Sakamoto, K. Maruoka, *J. Org. Chem.* **2014**, 79, 4240–4244.
- [186] M. Bollinger, F. Manzenrieder, R. Kolb, A. Bochen, S. Neubauer, L. Marinelli, V. Limongelli, E. Novellino, G. Moessmer, R. Pell, et al., *J. Med. Chem.* **2012**, 55, 871–882.
- [187] S. F. Martin, J. A. Josey, *Tetrahedron Lett.* **1988**, 29, 3631–3634.
- [188] J. A. Rojas Stütz, C. Richert, *Tetrahedron Lett.* **2004**, 45, 509–513.
- [189] C. L. Branch, G. Burton, S. F. Moss, *Synth. Commun.* **1999**, 29, 2639–2644.
- [190] U. T. Bornscheuer, *Eur. J. Lipid Sci. Technol.* **2014**, 116, 1322–1331.
- [191] P. Adlercreutz, A. M. Lyberg, D. Adlercreutz, *Eur. J. Lipid Sci. Technol.* **2003**, 105, 638–645.
- [192] K. Clausen, *Eur. J. Lipid Sci. Technol.* **2001**, 103, 333–340.
- [193] W. W. Christie, X. Han, *Lipid Analysis*, Woodhead Publishing, Cambridge, **2012**.
- [194] H.-Y. Lin, B. B. Snider, *J. Org. Chem.* **2012**, 77, 4832–4836.
- [195] D. D. Vachhani, H. H. Butani, N. Sharma, U. C. Bhoya, A. K. Shah, E. V Van der Eycken, *Chem. Commun.* **2015**, 51, 1–82.
- [196] K. Inoue, H. Arai, J. Aoki, *Lipases Phospholipases Drug Dev.* **2005**, 1, 23–39.

- [197] I. H. Kim, H. S. Garcia, C. G. Hill, *J. Am. Oil Chem. Soc.* **2010**, *87*, 1293–1299.
- [198] X. Li, J. F. Chen, B. Yang, D. M. Li, Y. H. Wang, W. F. Wang, *Int. J. Mol. Sci.* **2014**, *15*, 15244–15258.
- [199] U. Rost, *Organisation and Recognition of Artificial Transmembrane Peptides*, **2016**.
- [200] A. Holt, L. Rougier, V. Réat, F. Jolibois, O. Saurel, J. Czaplicki, J. Antoinette Killian, A. Milon, *Biophys. J.* **2010**, *98*, 1864–1872.
- [201] T. M. Weiss, P. C. A. van der Wel, J. A. Killian, R. E. Koeppe, H. W. Huang, *Biophys. J.* **2003**, *84*, 379–385.
- [202] I. Feussner, C. Wasternack, *Annu. Rev. Plant Biol.* **2002**, *53*, 275–297.
- [203] G. Coffa, C. Schneider, A. R. Brash, *Biochem. Biophys. Res. Commun.* **2005**, *338*, 87–92.
- [204] M. Hamberg, B. Samuelsson, *Proc. Natl. Acad. Sci. U. S. A.* **1974**, *71*, 3400–3404.
- [205] G. Burr, M. Burr, *J. Biol. Chem.* **1929**, *82*, 345–367.
- [206] W.-H. Kunau, *Angew. Chemie* **1976**, *97*, 97–130.
- [207] P. Pohl, H. Wagner, *Fette, Seifen, Anstrichm.* **1972**, *74*, 424–435.
- [208] B. Samuelsson, S. Dahlen, J. A. N. A. Lindgren, C. A. Rouzer, C. N. Serhan, *Science (80-.)*. **1987**, *237*, 1171–1176.
- [209] A. R. Brash, *J. Biol. Chem.* **1999**, *274*, 23679–23682.
- [210] C. May, M. Höhne, P. Gnau, K. Schwennesen, H. Kindl, *Eur. J. Biochem.* **2000**, *267*, 1100–1109.
- [211] S. A. Tatulian, J. Steczko, W. Minor, *Biochemistry* **1998**, *37*, 15481–15490.
- [212] J. N. Siedow, *Annu. Rev. Plant Physiol. Plant Mol. Biol.* **1991**, *42*, 145–188.
- [213] C. Schneider, D. A. Pratt, N. A. Porter, A. R. Brash, *Chem. Biol.* **2007**, *14*, 473–488.
- [214] M. Hamberg, B. Samuelsson, *J. Biol. Chem.* **1967**, *242*, 5329–5325.
- [215] E. J. Corey, P. T. J. Landsbury, *J. Am. Chem. Soc.* **1983**, *105*, 4093–4094.
- [216] M. F. Browner, S. A. Gillmor, R. Fletterick, *Nat. Struct. Biol.* **1998**, *5*, 197.
- [217] H. W. Gardner, *Biochim. Biophys. Acta (BBA)/Lipids Lipid Metab.* **1989**, *1001*, 274–281.
- [218] S. Xu, T. C. Mueser, L. J. Marnett, M. O. Funk, *Structure* **2012**, *20*, 1490–1497.
- [219] S. Prévost, T. Ayad, P. Phansavath, V. Ratovelomanana-Vidal, *Adv. Synth. Catal.*

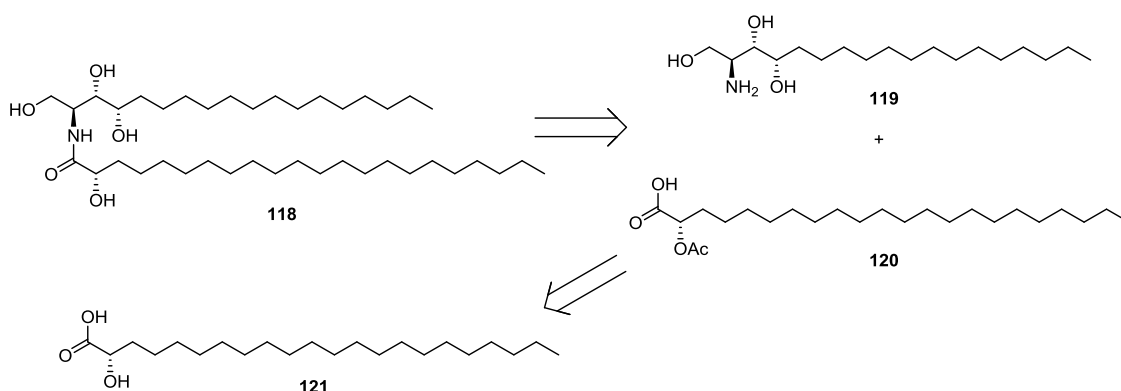
- 2011**, 353, 3213–3226.
- [220] V. Sharma, H. Batra, S. Tuladhar, *Method of Producing Berapost*, **2012**, US20120323025 A1.
- [221] S. G. Davies, A. M. Fletcher, E. M. Foster, J. A. Lee, P. M. Roberts, J. E. Thomson, *J. Org. Chem.* **2013**, 78, 2500–2510.
- [222] R. E. Synthesis, C. Structures, P. Properties, Y. Sawada, S. Furumi, A. Takai, M. Takeuchi, K. Noguchi, *J. Am. Chem. Soc.* **2012**, 1–4.
- [223] T. Imamoto, T. Kusumoto, Y. Tawarayama, Y. Sugiura, T. Mita, Y. Hatanaka, M. Yokoyama, *J. Org. Chem.* **1984**, 49, 3904–3912.
- [224] A. V. Bekish, *Tetrahedron Lett.* **2012**, 53, 3082–3085.
- [225] G. Tojo, M. Fernández, *Oxidation of Alcohols to Aldehydes and Ketones*, Springer, New York, **2006**.
- [226] N. P. Bowling, N. J. Burrmann, R. J. Halter, J. A. Hodges, R. J. McMahon, *J. Org. Chem.* **2010**, 75, 6382–6390.
- [227] J. E. Sieser, R. A. Singer, *Process for Preparing Fused Pyrazoles and Imidazoles via Cyclization of Amino Acids*, **2007**.
- [228] C. A. Urbina-Blanco, M. Skibiński, D. O'Hagan, S. P. Nolan, *Chem. Commun.* **2013**, 49, 7201.
- [229] A. Nasr El Dine, D. Grée, T. Roisnel, E. Caytan, A. Hachem, R. Grée, *European J. Org. Chem.* **2016**, 2016, 556–561.
- [230] P. Lakshmikapthi, C. Crevisy, R. Gree, *J. Comb. Chem.* **2002**, 4, 612–621.
- [231] P. Y. Kwok, F. W. Muellner, C. K. Chen, J. Fried, *J. Am. Chem. Soc.* **1987**, 109, 3684–3692.
- [232] B. Xu, M. Mae, J. A. Hong, Y. Li, G. B. Hammond, *Synthesis (Stuttg.)*. **2006**, 2006, 803–806.
- [233] I. Rico, D. Cantacuzene, C. Wakselman, *J. Chem. Soc. Perkin I* **1982**, 6–8.
- [234] C. Nadler, **2013**.
- [235] S. Djurdjevic, F. Yang, J. R. Green, *J. Org. Chem.* **2010**, 75, 8241–8251.
- [236] Z.-Q. Yang, S. J. Danishefsky, *J. Am. Chem. Soc.* **2003**, 125, 9602–9603.
- [237] M. Terada, Y. Ota, F. Li, Y. Toda, A. Kondoh, *J. Am. Chem. Soc.* **2016**, 138, 11038–11043.
- [238] B. Xu, G. B. Hammond, *Angew. Chemie - Int. Ed.* **2005**, 44, 7404–7407.
- [239] G. B. Hammond, *J. Fluor. Chem.* **2006**, 127, 476–488.

- [240] H. Hofmeister, K. Annen, H. Laurent, R. Wiechert, *Angew. Chemie Int. Ed. English* **1984**, 23, 727–729.
- [241] A. K. Ghosh, L. A. Kassekert, *Org. Lett.* **2016**, 18, 3274–3277.
- [242] S. M. Graham, G. D. Prestwich, *J. Org. Chem.* **1994**, 59, 2956–2966.
- [243] S. C. Gill, P. H. von Hippel, *Anal. Biochem.* **1989**, 182, 319–326.
- [244] R. C. MacDonald, R. I. MacDonald, B. P. M. Menco, K. Takeshita, N. K. Subbarao, L. R. Hu, *Biochim. Biophys. Acta - Biomembr.* **1991**, 1061, 297–303.
- [245] N. Asai, N. Fusetani, S. Matsunaga, J. Sasaki, *J. Nat. Prod.* **2001**, 64, 1210–1215.
- [246] B. Youn, G. E. Sellhorn, R. J. Mirchel, B. J. Gaffney, H. D. Grimes, C. Kang, *Proteins Struct. Funktion, Bioinforma.* **2006**, 65, 1008–1020.

9 Appendix

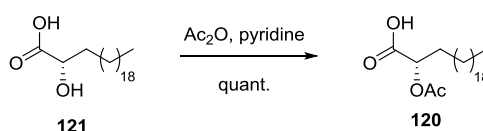
9.1 Ceramide 118

A protocol for the synthesis of ceramides starting from D-galactose was developed by ASAI *et al.*^[245] showing the examples of the total synthesis of ceramides proposed as sex pheromones of the hair crab *Erimacrus isenbeckii*. With the commercial available compounds of 2-hydroxydocosanoic acid (**121**) and phytosphinganine (**119**) the entire total synthesis can be reduced to a two-step procedure (**Scheme 9.1**). This short synthetic route consists of a protection step followed by a coupling reaction of sphinganine and fatty acid.



Scheme 9.1 Retrosynthesis of ceramide **118**.

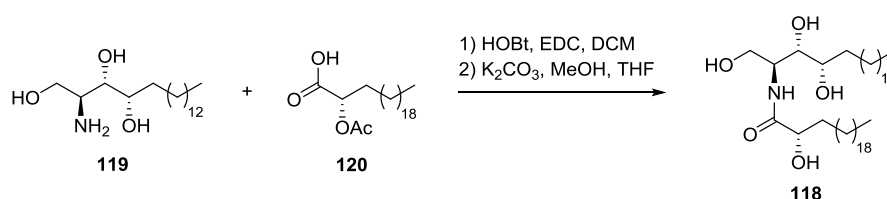
The first step included the protection of the secondary alcohol moiety of 2-hydroxydocosanoic acid (**121**) via acetylation (**Scheme 9.2**). To achieve this, the fatty acid (**121**) was dissolved in pyridine and treated with acetic anhydride. The reaction mixture was stirred at room temperature for 13 h which yielded the protected fatty acid **120**. It is crucial for this reaction to use fresh acetic anhydride. Utilisation of anhydride from bottles open for longer than approximately one month led to no product formation.



Scheme 9.2 Protection of the secondary hydroxy group by acetic anhydride-treatment.

Following the procedure of ASAI *et al.*, in the second step the sphinganine **119** and the acetylated fatty acid **120** were diluted in benzene along with the coupling reagent *N*-hydroxybenzotriazole (HOBt). The organic solvent was then removed under

reduced pressure and lyophilised to remove any traces of present water. Afterwards, the mixture was dissolved in anhydrous dichloromethane (DCM), 1-ethyl-3-(3-dimethyl-aminopropyl)carbodiimide (EDC) as a second coupling reagent was added and the reaction mixture stirred for 20 h. However, following this procedure with the compounds shown in **Scheme 9.3** product formation could not be observed. Therefore, the strategy was altered. Instead of diluting the starting materials together with HOBt in benzene and then removing solvent and water traces, phytosphinganine and **120** as well as HOBt and EDC were directly dissolved in anhydrous DCM and stirred at room temperature for 20 h under argon atmosphere. After standard workup procedure the coupling product was dissolved in methanol/tetrahydrofuran (MeOH/THF, 3:1) without preceding purification. After stirring for 2.5 h at room temperature in the presence of potassium carbonate (K_2CO_3) the acetyl group was cleaved off to yield the product **118**.

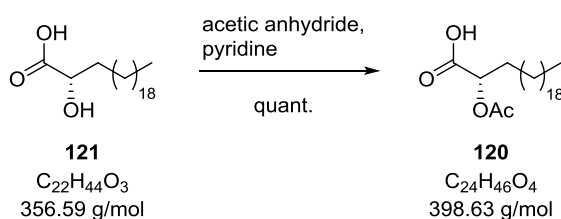


Scheme 9.3 Coupling step using HOBt and EDC followed by deprotection under basic conditions.

Isolation of **118** was not possible since the released urea derivative after EDC activation appeared to be inseparable from **118**. The crude product was handed over to Prof. Dr. I. FEÜßNER for further purification with subsequent analysis of the mode of action of **118** during apoptosis.

9.1.1 Synthesis of Ceramide 118

(S)-2-Acetoxydocosanoic acid (**120**)

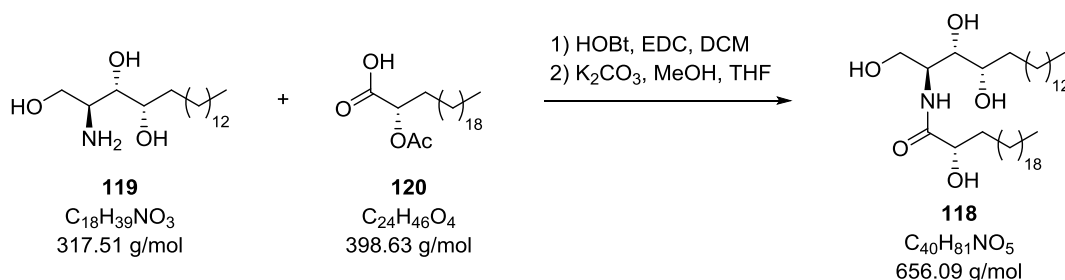


To a solution of (S)-2-hydroxydocosanoic acid (**121**, 8.60 mg, 28.0 μ mol, 1.00 eq.) in pyridine (550 μ L) acetic anhydride (550 μ L) was added. The mixture was stirred for 13 h at r.t. and then diluted with ice water. The solvent was evaporated under reduced pressure and the pure product **120** (9.31 mg, 23.4 μ mol, 83 %) was obtained as white solid.

ESI-MS m/z : 399.3 [M+H]⁺, 421.3 [M+Na]⁺, 819.7 [2M+Na]⁺.

HR-MS (ESI): calculated for [C₂₄H₄₇O₄] ([M+H]⁺): 399.3469, found: 399.3464; calculated for [C₂₄H₄₅O₄] ([M-H]⁻): 397.3323, found: 397.3311.

(S)-2-Hydroxy-N-((2S,3S,4R)-1,3,4-trihydroxyoctadecan-2-yl)-docosan-amide (**119**)



(S)-2-Acetoxydocosanoic acid (**120**, 2.72 mg, 6.82 μ mol, 1.00 eq.) and 4-hydroxy sphinganine (**119**, 2.36 mg, 7.43 μ mol, 1.09 eq.) were dissolved in dry DCM (240 μ L) under argon atmosphere together with HOBt (1.47 mg, 10.9 μ mol, 1.60 eq.). To the mixture EDC (2.16 mg, 11.3 μ mol, 1.65 eq.) was added. The mixture was allowed to stir for 24 h at r.t. and diluted with CHCl₃. The solution was washed with water, dried over MgSO₄ and concentrated. The residue was redissolved in THF (120 μ L) and methanol (350 μ L), K₂CO₃ (33.0 mg) was added and the mixture was stirred for 2.5 h. Removal of the solvents yielded the crude product **118** as white solid.

ESI-MS m/z : 678.7 [M+Na]⁺, 654.6 [M-H]⁻.

HR-MS (ESI): calculated for $[\text{C}_{40}\text{H}_{81}\text{NO}_5]$ ($[\text{M}-\text{H}]^-$): 654.6042, found: 654.6025.

10 Acknowledgement/Danksagung

Mein besonderer Dank gilt Prof. Dr. ULF DIEDERICHSEN für die Möglichkeit an interessanten Themenstellungen innerhalb seiner Gruppe zu arbeiten, sowie für die uneingeschränkte Unterstützung, Betreuung und die gewährte wissenschaftliche Freiheit während der gesamten Promotionszeit.

Prof. Dr. IVO FEUßNER danke ich für die Übernahme des Koreferats, die Betreuung und Diskussionsbereitschaft. Weiterhin bedanke ich mich für die Möglichkeit Experimente in seinen Laboren mit Unterstützung der Mitarbeiter durchführen zu dürfen.

Prof. Dr. EBBE NORDLANDER danke ich für die bereitwillige Übernahme des zweiten Koreferats im Rahmen des *Biometals* Promotionsprogramms.

Bei Prof. Dr. HARTMUT LAATSCH, Prof. Dr. MANUEL ALCARAZO, Prof. Dr. KONRAD KOSZINOWSKI und Dr. FRANZISKA THOMAS bedanke ich mich herzlich für die Teilnahme an meiner Prüfungskommission.

Dem gesamten Team der Massenabteilung sowie der NMR-Abteilung danke ich für das Messen unzähliger Proben und die freundliche Hilfe bei Fragen und Problemen.

Weiterhin danke ich dem gesamten Arbeitskreis DIEDERICHSEN für die gute Arbeitsatmosphäre und stetige Hilfsbereitschaft. Vielen Dank an die ehemaligen und aktuellen Laborkollegen aus Labor 130 für die schöne Zeit, wobei ich mich besonders bei SWANTJE NAWRATIL und HARITA RAO bedanken möchte. Insbesondere danke ich auch AOIFE NEVILLE und ANGELA HEINEMANN für die organisatorische Unterstützung sowie DANIEL FRANK für die technische Hilfestellung.

Dr. FRANZISKA THOMAS, WOLF MATHIS RINK und BARBARA HUBRICH möchte ich herzlich für ihre Hilfestellung in Rat und Tat danken.

Meiner Bachelorstudentin Isabel Großhennig danke ich für ihr engagiertes Arbeiten.

Für das Korrekturlesen dieser Arbeit bedanke ich mich bei Dr. SELDA KABATAS, Dr. MEIKE JUNIUS, Dr. JULIA GRAF, Dr. DENNIS HÜBNER, ANNA VERA LÜBBEN, SWANTJE NAWRATIL, BARBARA HUBRICH und meiner Schwester ANNE HANSEN.

Mein größter Dank gilt meiner Familie und meinen Freunden, die mir das Studium ermöglicht und mich besonders in anstrengenden und belastenden Phasen immer wieder aufgebaut und mir Kraft gegeben haben. Thorsten, dir danke ich für die schöne gemeinsame Zeit, dein Verständnis und deine Fähigkeit mich immer wieder zum lachen zu bringen. Danke, dass du immer für mich da bist.

Curriculum Vitae

Personal Information

| | |
|-------------------------|-----------------------|
| Name | Christine Hansen |
| E-Mail | chr-hansen@web.de |
| Date and Place of Birth | 18.06.1987 in Niebüll |
| Nationality | deutsch |

Education

| | |
|-------------------|--|
| 09.10.2017 | Doctoral examination for obtaining the degree " <i>Doctor rerum naturalium</i> " |
| 05.2013 – 10.2017 | PhD thesis: <i>Synthesis of Modified and Labelled Lipids for Analysis of Enzyme Mechanisms and Membrane Interactions</i> in the framework of the IRTG1422 "Metal Sites in Biomolecules" Research group of Prof. Dr. U. DIEDERICHSEN, Institute for Organic and Biomolecular Chemistry |
| 10.2010 – 03.2013 | Master of Science in Chemistry, Faculty of Chemistry, Georg-August-University Göttingen Master thesis: <i>Entwicklung eines photolabilen Auxiliars für die Ligation von Peptiden und Proteinen</i> Research group of Prof. Dr. U. DIEDERICHSEN, Institute for Organic and Biomolecular Chemistry |
| 10.2011 – 03.2012 | Erasmus exchange in Trondheim, Norway, Norwegian University of Science and Technology Research group of Prof. Dr. ODD R. GAUTUN Project: <i>Rational Drug Design: Studies towards the Synthesis of potential selective Inhibitors of Tyrosine Kinase 2</i> |
| 10.2007 – 08.2010 | Bachelor of Science in Chemistry, Faculty of Chemistry, Georg-August-University Göttingen Bachelor thesis: <i>Synthese von Nukleotidderivaten für die Umsetzung mit der Orotidin-5'-monophosphat Decarboxylase</i> Research group of Prof. Dr. U. DIEDERICHSEN, Institute for Organic and Biomolecular Chemistry |
| 06. 2007 | Abitur, Friedrich-Paulsen Schule, Niebüll |

Teaching Experience

| | |
|---------------|---|
| 01. – 02.2014 | <i>Chemie für Mediziner</i> , Supervision of Seminars and Practical Courses |
| 06. – 07.2014 | <i>Chemie für Mediziner</i> , Supervision of Seminars and Practical Courses |
| 01. – 02.2015 | <i>Chemie für Mediziner</i> , Supervision of Seminars and Practical Courses |
| 01. – 02.2016 | <i>Chemie für Mediziner</i> , Supervision of Seminars and Practical Courses |
| 06. – 07.2016 | <i>Chemie für Mediziner</i> , Supervision of Seminars and Practical Courses |

Language Skills

| | |
|-----------|-----------------|
| German | First language |
| English | Business fluent |
| Norwegian | Basic knowledge |